# SECTION III: SEDIMENTOLOGY

## CHAPTER 4: INTRODUCTION, SEDIMENTOLOGICAL FRAMEWORK

### 4.1. Introduction

#### 4.1.1. Previous work

Most previous work on the Cambrian shelf strata of Peary Land has been concerned primarily with regional mapping and stratigraphy, the sole exception being the work of O'Connor (1979) on the Portfjeld Formation. Some pertinent observations were made, however, in the course of reconnaisance mapping. Troelsen (1956) observed 'large-scale diagonal bedding' in the J.P. Koch Fjord - Henson Gletscher region indicating 'transport of material in a northerly direction'. Jepsen (1971) noted the rhythmic interbedding of sandstones and shales in the upper levels of the Buen Formation and in subsequent reviews, the formation has been referred to as a turbidite succession (Dawes 1976a). The dolomite breccias of the Brønlund Fjord Group in the Børglum Elv region were initially described as intraformational conglomerates (Troelsen 1956) but in a more detailed description of these rocks, Christie & Peel (1977) attributed breccia formation to 'large-scale slumping of alternating competent and incompetent, often mottled, thin dolomite beds.'

Preliminary results of this and associated studies were given by Ineson (1980) and Frykman (1980), and incorporated in recent stratigraphic reviews (Peel 1982b) and regional overviews (Hurst & Surlyk 1983).

4.1.2. Organization

The term facies was introduced by Gressly (1838) and the facies concept has been reviewed more recently by Teichert (1958) and Reading (1978). Following Reading (1978), a lithofacies is used here to refer to an objectively described 'body of rock with specified characteristics', which ideally reflects a particular depositional process or environment.

Twenty-five lithofacies are recognized in this study; four of these are further subdivided into subfacies. The succession is highly variable and could be further subdivided, but the number of lithofacies has been restricted as far as possible to avoid confusion.

Secondary dolomitization complicates the definition and interpretation of lithofacies. In most cases, the dolomites retain sufficient relict primary structure to enable a depositional interpretation to be made, albeit generalized where preservation is poor. Where equivalent limestones and dolomites are recognized, they are included and described in the same lithofacies.

Following Collinson (1969), a facies association is defined as a group of lithofacies which are genetically and spatially related, and together have some environmental significance. Study of the common vertical and lateral relationships of the lithofacies has led to recognition of four facies associations, each of which is considered to represent a particular environment. The associations and their constituent lithofacies are described separately (Chapters 5-7); lithofacies that occur in more than one association show slight but significant differences and are redescribed in each association.

The associations are interpreted in terms of the broad depositional framework. Facies association B, representing the outer shelf-slope, is described by means of two sub-associations, B1 and B2, that represent carbonate and siliciclastic sedimentation respectively. This split does not indicate a markedly different environmental setting, but resulted purely from variation in the composition of sediment supplied to the outer shelf. The subdivision is made purely for convenience, particularly as the siliciclastic rocks are not spread through the succession but form a distinct unit at the Early - Middle Cambrian boundary.

Associations B and C are further subdivided into assemblages, recurrent groups of facies that, in contrast to the lithological subdivision described above, represent distinct sub-environments within the broad environmental setting.

In Chapter 8, the lateral and vertical relationships of these associations and their constituent assemblages is described, and a model is developed for shelf sedimentation during Cambrian times.

## 4.2. Environmental Framework

Shelf sedimentation in the Peary Land region during the Cambrian resulted in a varied succession of clastic and carbonate rocks (Portfjeld and Buen Formations, Brønlund Fjord and Tavsens Iskappe Groups, Fig. 3.2.). These are unconformably succeeded by a uniform, laterally persistent sequence of Ordovician carbonates (Wandel Valley Formation). Brief descriptions and interpretations of the Portfjeld, Buen and Wandel Valley Formations are given here, in order to outline the pattern of shelf sedimentation prior to and after deposition of the Brønlund Fjord and Tavsens Iskappe Groups, which are the subjects of subsequent chapters.

4.2.1. Portfjeld Formation

The Portfjeld Formation is a widespread and varied succession of dolomites with subordinate terrigenous sandstone intervals. Its stratigraphy has been described previously (3.3.1., 3.4.1.); important points are:

(i) it rests unconformably on Proterozoic rocks,

(ii) it thins towards the south-east, and is not recognized south of southern Valdemar Glückstadt Land or east of Danmark Fjord,

(iii) it thickens towards the north, and shows its maximum development in the G.B. Schley Fjord region, north-east Peary Land (Fig. 2.2.).

The Portfjeld Formation typically comprises cross-bedded oolitic and intraclastic dolomites, flat pebble conglomerates and algal-laminated dolomites displaying planar, crinkly, domal, digitate and columnar stromatolites. Dark grey, bituminous dolomites rich in black chert form a distinctive laterally-persistent unit near the base of the formation in southern Peary Land (Fig. 4.1.; O'Connor 1979). Oncolites and pisolites are common at certain horizons; desiccation cracks, shallow channels and brecciated horizons are of more restricted occurrence. A typical section is shown in Fig. 4.1.

The Portfjeld Formation exhibits features typical of sediments deposited in modern and ancient inferred shallow-water carbonate platform environments (Bathurst 1971; Wilson 1975). O'Connor (1979) concluded that the depositional environment was "undoubtedly ...... shallow water, near shore", the presence of desiccation cracks indicating intermittent

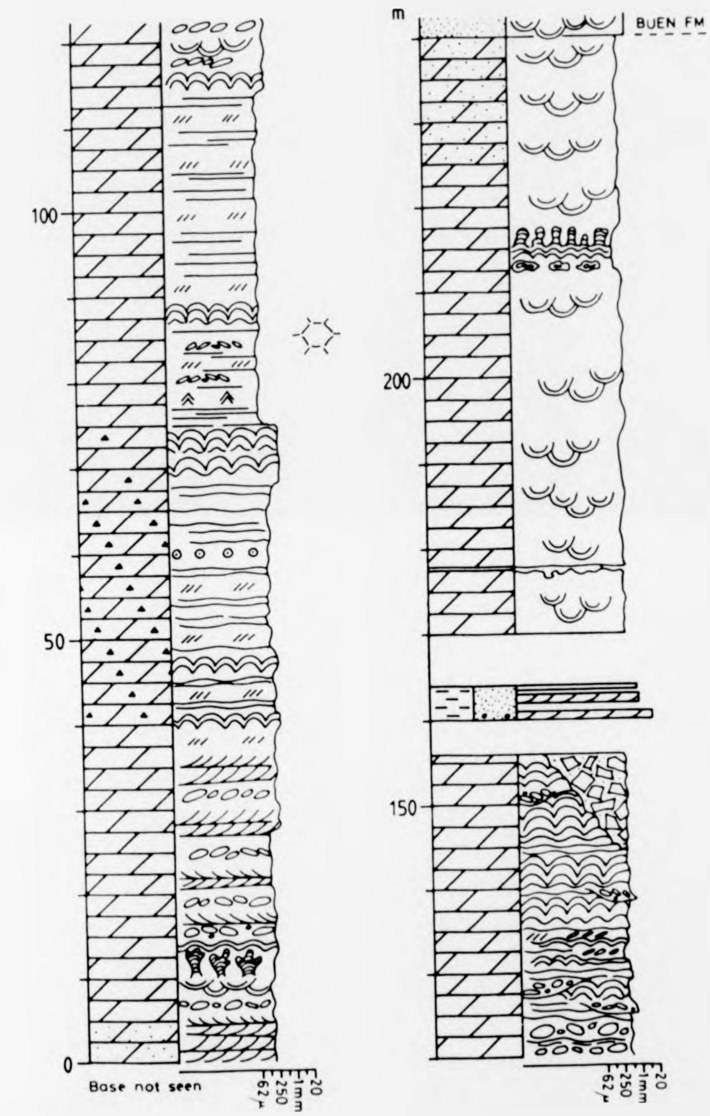


Figure 4.1. Representative section through the Portfjeld Formation on the north side of Nedre Midsommersø. Discordant sandy breccia at 150m and irregular surface at 178m are probably karstic solution features.

subaerial exposure. He reported the occurrence of herringbone cross-bedding, indicative of tidal processes, with a dominant flow direction towards the north-west.

Following O'Connor (1979) and Hurst & Surlyk (1983), the Portfjeld Formation is considered to represent deposition in shallow-subtidal and intertidal environments on a marine carbonate platform. Ooid and intraclast grainstones were deposited on subaqueous carbonate sand banks in shallow turbulent water, while fetid and algal-laminated carbonate muds and silts accumulated in protected shallow-subtidal and low - to moderate-energy intertidal environments. Hurst & Surlyk (1983) compared the Portfjeld Formation to the cyclic peritidal facies described by Markello & Read (1982), formed by repeated rapid submergence and subsequent progradation of shallow-subtidal and intertidal facies; cyclic repetition of facies has not been demonstrated, however, and in the absence of detailed sections such a comparison is highly conjectural.

The accumulation of a thick pile of shallow-water platform carbonates, particularly in north-eastern Peary Land, indicates steady uniform subsidence of a stable shelf following the initial transgression over Proterozoic basement. The northerly increase in the thickness of the formation probably reflects differential shelf subsidence towards the incipient trough (Hurst & Surlyk 1983). The occurrence of brecciated horizons that may have resulted from evaporite solution and/or karstic solution (see also Hurst & Surlyk 1983) and rare palaeokarstic surfaces in southern Peary Land indicate periodic emergence of southern, near shore zones. Localized terrigenous incursions probably record northward progradation of shoreface environments during such regressive episodes (O'Connor 1979; Hurst & Surlyk 1983).

4.2.2. Buen Formation

The Portfjeld Formation is conformably overlain by the siliciclastic Buen Formation (Fig. 3.2), which is composed of a lower sandstone-dominated member and an upper mudstone-dominated member. This subdivision is recognizable throughout southern Peary Land and in north-east Peary land where the mudstone member is equivalent to the Schley Fjord Shale of Troelsen (1956). The lower sandstone member is dominant in central southern Peary Land (Fig. 4.2) but thins to the north and west, forming less than half of the formation in the J.P. Koch Fjord area (Peel 1979). The formation achieves its maximum known thickness of more than 500m to the west-south-west, in southern Wulff Land, where the lower sandstone member is dominant (Peel 1980a).

The sandstone member is a varied succession of fine-to very coarse-grained pebbly sandstones with subordinate conglomerate, laminated siltstone and silty mudstone interbeds (Fig. 4.2). Discrete units (10-20m thick) of cross-bedded, medium to coarse-grained pebbly sandstone form prominent rusty red-brown weathering ledges in southern Peary Land (Fig. 4.2; Peel 1979). Within any one such unit, there is commonly an upward increase in grain size and set thickness (Fig. 4.2). Trough and tabular cross-sets range from 0.05 to 1.5m in thickness, the larger sets tending to show a tabular morphology (Fig. 4.3); herringbone cross-bedding is observed locally.

The remainder of the sandstone-dominated member comprises medium- to small-scale, tabular and trough cross-bedded, fine-to coarse-grained sandstones interbedded with bioturbated sandstones and mudstones and discrete erosively-based beds (0.05 - 0.5m) of fine to medium-grained sandstone. The latter are sometimes graded and commonly show parallel lamination and

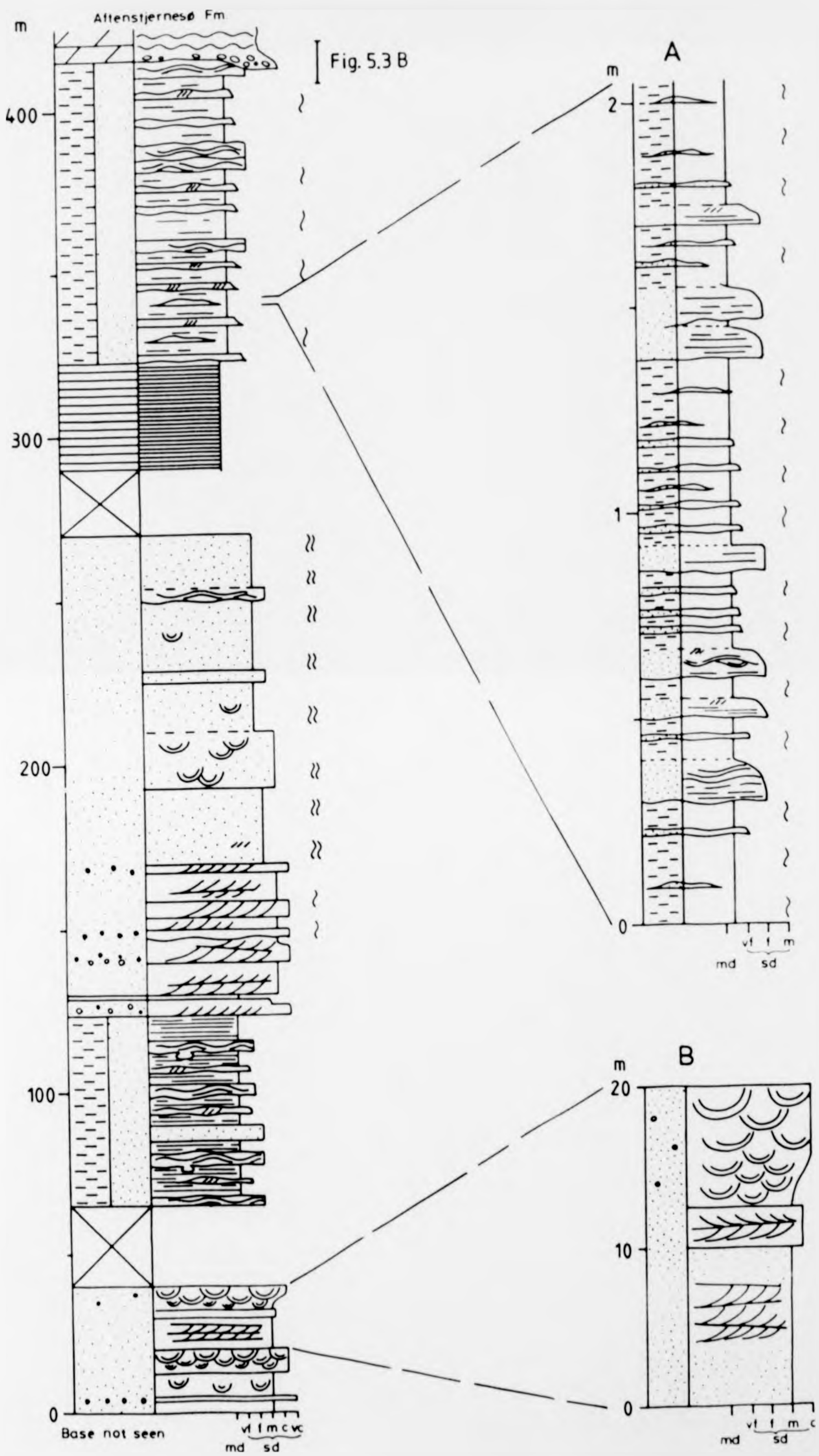


Figure 4.2. Buen Formation at its type locality on the south side of Buen. Detailed section through the upper beds was measured at the south-east corner of Buen (locality 21).

Figure 4.3. Large-scale tabular cross-bedding in the lower Buen Formation. About 4km north of Slusen, south central Peary Land.

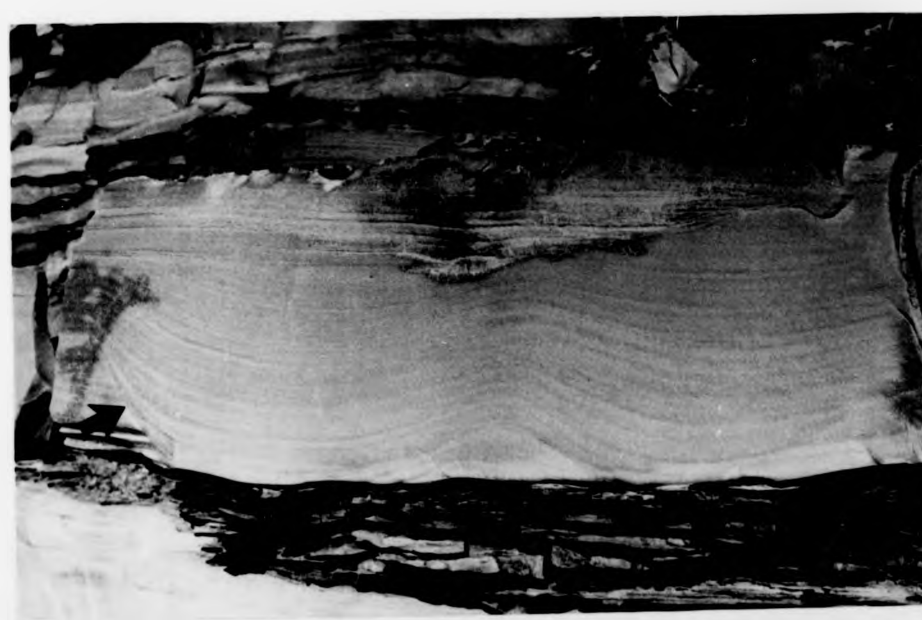

Figure 4.4. A variant of hummocky cross-stratification? Note the sharp, gently undulating base of the sand sheet and the internal erosion surface (arrow). Individual laminae thicken into the scour and the oblique lamination grades up into parallel lamination. Note also the symmetry of the peaked bedform and its vertical, accretionary growth pattern suggesting oscillatory flow and rapid sedimentation. Upper Buen Formation, locality 21, central Peary Land.

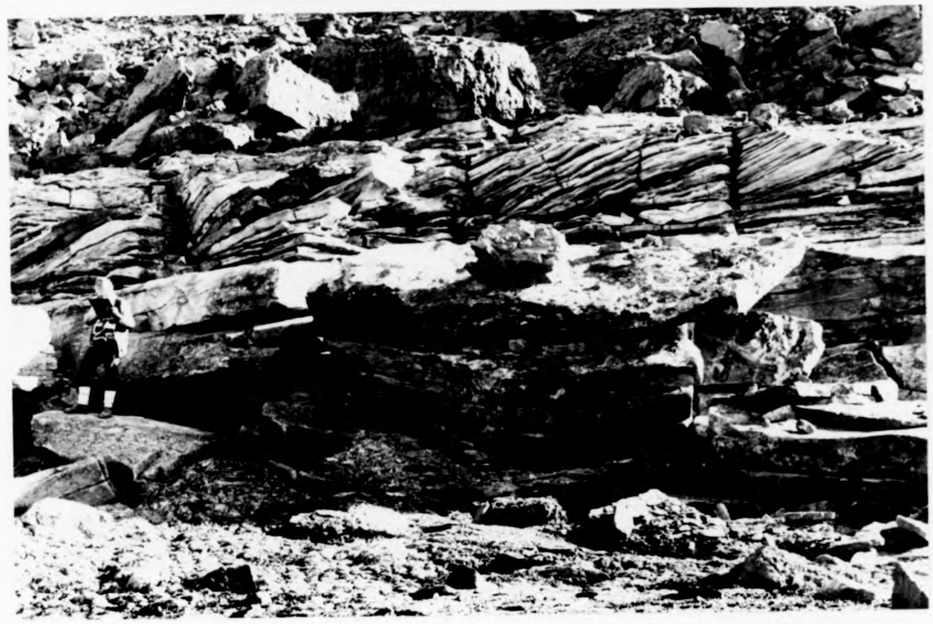

Figure 4.3. Large-scale tabular cross-bedding in the lower Buen Formation. About 4km north of Slusen, south central Peary Land.

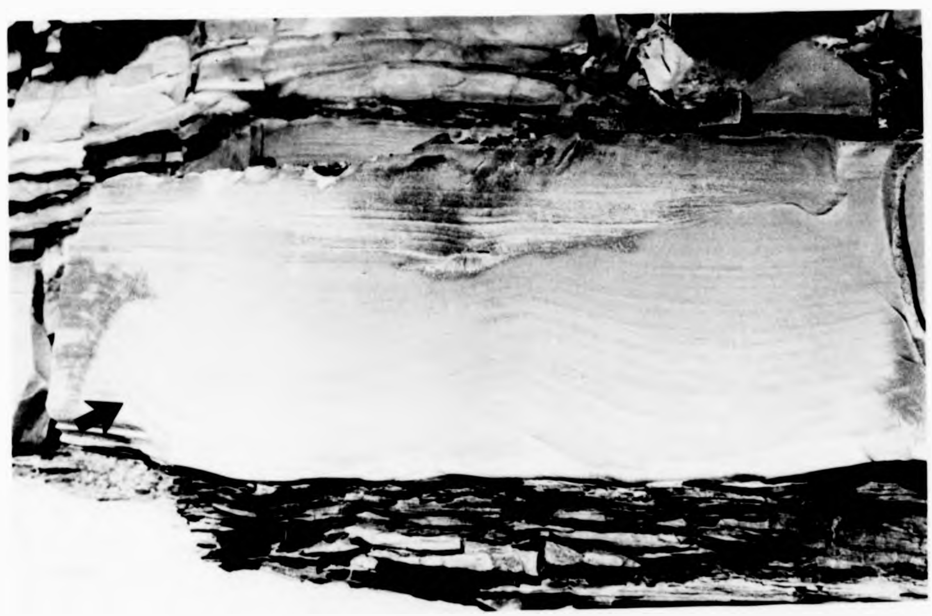

Figure 4.4. A variant of hummocky cross-stratification? Note the sharp, gently undulating base of the sand sheet and the internal erosion surface (arrow). Individual laminae thicken into the scour and the oblique lamination grades up into parallel lamination. Note also the symmetry of the peaked bedform and its vertical, accretionary growth pattern suggesting oscillatory flow and rapid sedimentation. Upper Buen Formation, locality 21, central Peary Land.

low-angle hummocky cross-stratification. Symmetrical wave ripples are present locally, and glauconite is abundant. Bioturbation is common, particularly towards the top of the sandstone member, where *Skolithus*, *Arenicolites*, *Diplocraterion* and *Cruziana* were recorded.

The upper member is composed mainly of parallel-laminated or bioturbated grey-green silty mudstones interbedded locally with thin-bedded fine-to medium-grained sandstones. The latter are particularly conspicuous towards the south-east (Frykman 1980). In places the mudstones yield rich faunas of olenellid trilobites, hyolithids, ostracods brachiopods and molluscs (Palmer & Peel 1979).

In the type area, in central southern Peary Land, the proportion of sandstone in the upper member increases markedly in the upper 90 m of the formation, which comprises an interbedded succession of bioturbated silty mudstones and thin-to medium-bedded, very fine to medium-grained sandstones (Fig. 4.2.). Thin sandstone beds (0.02 - 0.15 m) have sharp locally erosive bases, pinch and swell laterally and commonly exhibit grading, parallel-lamination and ripple cross-lamination in a fashion reminiscent of the Bouma turbidite abc divisions (Bouma 1962). Current ripple cross-lamination indicates flow towards the north or north-west. Thicker sandstone beds (0.2 - 0.5 m) display parallel lamination and low-angle cross-stratification (Fig. 4.4.) comparable to the hummocky cross-stratification of Harms *et al.* (1975). Some beds display wave-rippled tops (Fig. 5.3.). Bioturbation is common; non-specific, sub-horizontal sand-stuffed burrows are abundant and identifiable ichnogenera are *Planolites*, *Rusophycus* and '*Diplichnites*'.

A marine environment is indicated for the Buen Formation by the open marine fauna, the trace fossil assemblage and the presence of glauconite. The lower sandstone-dominated interval is considered to represent deposition in a moderate-to high-energy inner shelf environment. Herringbone cross-bedding is generally considered to be indicative of bidirectional tidal currents (Johnson 1978). Coarsening-upward sequences have been described from a number of ancient shallow marine clastic successions (Brenner & Davies 1974; Berg 1975; Spearing 1975) and reflect the lateral migration of sand sheets, waves, bars or shoals under the influence of storm waves or wind-forced currents, tidal or oceanic currents. Following these workers, the coarsening-and thickening-upward sequences are considered to represent subtidal sand bars or sheets that migrated over 'interbar' rippled and bioturbated sands and silts. The dominance of an ichnofauna interpreted to be due to suspension-feeders supports the interpretation of a mobile shifting substrate (Rhoads 1967). This sandstone member has only been studied in a reconnaissance fashion, and the relative importance of wave and tidal processes is unknown; the occurrence of hummocky cross-stratification (Harms *et al.* 1975; Dott & Bourgeois 1982) and herringbone cross-bedding suggests that both processes were operative.

The mudstone-dominated member was deposited in a low-energy marine environment in which the accumulation of mud, silt and fine sand from suspension was the dominant depositional process. Deposition was below normal wave base; the preservation of primary lamination at some levels indicates periodic restricted circulation and poor oxygenation of bottom waters. The dominance of deposit-feeding traces in bioturbated intervals supports the interpretation of a low-energy environment (Rhoads 1967).

The thin-bedded sandstones resemble turbidites, but the presence of wave ripples and the association with hummocky cross-stratified sandstones indicates deposition from waning storm-induced currents, as described from modern and ancient clastic shelves (Goldring & Bridges 1973; Cant 1980; Nelson 1982). The thicker sandstone beds showing hummocky cross-bedding record the passage of storm-induced geostrophic currents (Swift *et al.* 1983).

Deposition of the Buen Formation thus records, firstly, an abrupt change from carbonate to clastic sedimentation throughout Peary Land. Following Hurst & Surlyk (1983), it is considered unlikely that this change represents progradation of deltaic/shoreface facies across a carbonate platform due to a relative fall in sea level (*cf.* Kendall & Schlager 1981). Rather, the swamping of the carbonate platform by clastic detritus reflects uplift and rejuvenation of cratonic source terrains, possibly associated with shelf tilting (Hurst & Surlyk 1983).

Secondly, the formation records a gradual relative rise in sea level, probably due to increased subsidence of the shelf. This is reflected in the upward transition from sand-dominated inner shelf to fine-grained outer shelf facies, both in southern and north-eastern Peary Land. The distribution of facies and the limited palaeocurrent data indicate a stable, low-relief shelf, deepening towards the north-west. Inner shelf environments were characterized by an interplay of storm and tidal processes, while high-energy events in the outer shelf environment were predominantly the result of storm-induced currents and waves. A comparable model of shelf sedimentation has been developed by Anderton (1976) for the Jura Quartzite in the Precambrian of Scotland.

The Buen Formation in Peary Land is overlain by the carbonate-dominated Brønlund Fjord Group. The significance of this distinct facies change and the subsequent evolution of the Cambrian shelf is covered in Chapters 5-8.

4.2.3. Wandel Valley Formation

The Wandel Valley Formation (late Early-early Middle Ordovician), which lies above the Brønlund Fjord and Tavsens Iskappe Groups, is the basal formation in a thick succession of Ordovician-Silurian platform carbonates (Peel 1982b; 2.2.). It rests unconformably on underlying, mainly Cambrian and Proterozoic sedimentary rocks, overstepping onto progressively older rocks from west Peary Land to Kronprins Christian Land (Fig. 2.3.; Peel 1979, 1980c, 1982b). The unconformity is planar, and the basal beds of the formation are of approximately similar age throughout eastern North Greenland (J.S. Peel, pers. comm. 1983).

In central southern Peary Land, the Wandel Valley Formation is composed wholly of dolomite and is readily divisable into three members; a dark grey or brown-weathering middle member sandwiched between two pale grey-weathering dolomite members (Christie & Peel 1977). The latter include flat-pebble conglomerates, cross-stratified silty or ooidal dolomites and planar or domal algal laminates. Small channels and desiccation cracks are occasionally observed. Dark dolomites occur inter-bedded with the pale facies in the lower member as well as forming much of the middle member. They display intense burrow mottling and locally contain rich silicified faunas dominated by gastropods (Yochelson & Peel 1975; Christie & Peel 1977). In western and north-eastern Peary Land, the formation contains subordinate, lime mud-dominated limestone beds

(Peel 1979; Christie & Ineson 1979).

By analogy with modern carbonate environments (Kendall & Skipwith 1969; Bathurst 1971; Logan *et al.* 1974) and ancient inferred shallow-water carbonate successions (Wilson 1975), the Wandel Valley Formation is considered to represent sedimentation in restricted, shallow-subtidal (lagoonal?) and intertidal environments on an extensive, shallow-water carbonate platform. The low diversity and restricted nature of the fauna in these carbonates probably reflects elevated salinities as suggested by Christie & Peel (1977). Evaporitic deposits are unknown from this formation in Peary Land, but anhydrite is common at this stratigraphic level in Warming Land to the west (the Cape Webster Formation; Peel 1980a). In their review of the Lower Palaeozoic shelf deposits of eastern North Greenland, Hurst & Surlyk (1983) inferred that the Wandel Valley Formation formed in a peritidal carbonate platform environment. They recognized a cyclic alternation of subtidal and intertidal carbonate facies, considered to record episodic rapid submergence followed by progradation of shallow subtidal and intertidal facies.

In Kronprins Christian Land, algal-laminated and mudcracked pale dolomites are subordinate to a thick succession (200 m) of dark grey burrowed dolomitic lime mudstones and wackestones, with thin skeletal intraclast lime grainstone interbeds (the Amdrup Member; Peel *et al.* 1981). The dominance of micritic limestones over dolomites and the presence of a more diverse open-marine fauna (trilobites, ostracods, gastropods) in this area suggests deposition in a predominantly low-energy subtidal environment with near normal salinities. This perhaps reflects a more offshore position on the carbonate platform than that of central southern Peary Land, at least in the late Early Ordovician (Peel *et al.* 1981).

The Wandel Valley Formation thus records a regional marine transgression in late Early Ordovician times over a vast area of the eastern and central North Greenland shelf. Following the transgression, carbonate sedimentation in shallow-subtidal and peritidal platform environments (Armstrong & Lane 1981) continued without recognizable breaks until at least the late Llandovery (Christie & Peel 1977; Mabillard 1980) indicating protracted steady subsidence of a stable shelf.

# CHAPTER 5 OUTER SHELF - ASSOCIATION A

## 5.1. Outer shelf - introduction

Rocks assigned to the outer shelf form nearly two-thirds of the Brønlund Fjord and Tavsens Iskappe Groups. They typically comprise dark-coloured, fine-grained, thin-bedded argillaceous and bituminous carbonates interbedded with graded carbonate grainstones and carbonate breccia beds. Carbonates dominate, but a distinctive, laterally persistent terrigenous interval occurs near the Lower - Middle Cambrian boundary (Fig. 3.2; Henson Gletscher and Sæterdal Formations). Over 70% of the carbonates are dolomitized. The distribution of dolomite is crudely facies-controlled and is typical of sequences dominated by thick breccia beds and graded beds, and carbonates adjacent to the pervasively dolomitized platform margin facies. Uniformly thin-bedded, argillaceous, fine-grained carbonate sequences are undolomitized or only partially dolomitized. The latter are commonly richly fossiliferous, yielding trilobites, brachiopods, pelmatozoans, sponge spicules, hyolithids and assorted molluscs (Peel 1979; Palmer & Peel 1979).

Thirteen lithofacies are recognized, and are grouped into two associations - Associations A and B,which are interpreted as representing an incipient carbonate ramp and an outer shelf-slope respectively. The carbonate lithofacies are ordered roughly according to grain size from lime mudstones (Lithofacies 1-4) to carbonate breccias (Lithofacies 9).

The stratigraphic relationships between these associations

# CHAPTER 5 OUTER SHELF - ASSOCIATION A

## 5.1. Outer shelf - introduction

Rocks assigned to the outer shelf form nearly two-thirds of the Brønlund Fjord and Tavsens Iskappe Groups. They typically comprise dark-coloured, fine-grained, thin-bedded argillaceous and bituminous carbonates interbedded with graded carbonate grainstones and carbonate breccia beds. Carbonates dominate, but a distinctive, laterally persistent terrigenous interval occurs near the Lower - Middle Cambrian boundary (Fig. 3.2; Henson Gletscher and Sæterdal Formations). Over 70% of the carbonates are dolomitized. The distribution of dolomite is crudely facies-controlled and is typical of sequences dominated by thick breccia beds and graded beds, and carbonates adjacent to the pervasively dolomitized platform margin facies. Uniformly thin-bedded, argillaceous, fine-grained carbonate sequences are undolomitized or only partially dolomitized. The latter are commonly richly fossiliferous, yielding trilobites, brachiopods, pelmatozoans, sponge spicules, hyolithids and assorted molluscs (Peel 1979; Palmer & Peel 1979).

Thirteen lithofacies are recognized, and are grouped into two associations - Associations A and B,which are interpreted as representing an incipient carbonate ramp and an outer shelf-slope respectively. The carbonate lithofacies are ordered roughly according to grain size from lime mudstones (Lithofacies 1-4) to carbonate breccias (Lithofacies 9).

The stratigraphic relationships between these associations and associations C and D are shown schematically on Fig. 5.1. Association A forms the basal unit of the succession and is overlain by Association B. Associations C and D cap the succession. The relationships between the associations are discussed in Chapter 8.

## 5.2 Association A : Incipient carbonate ramp

This association is confined to the basal beds of the Aftenstjernesø Formation. The transition from the siliciclastic Buen Formation to the carbonate-dominated Brønlund Fjord Group is abrupt and forms a readily recognizable lithostratigraphic boundary. It is marked by a distinctive phosphorite-glauconite-carbonate assemblage at the base of the carbonate succession which forms a persistent 2-7m thick unit throughout Peary Land (Frykman 1980). This interval (Member A of the Brønlund Fjord Formation of previous usage; see Christie & Peel 1977) has been the subject of a sedimentological and diagenetic study by Frykman (1980, 1981). It is characterized by pale grey or buff-brown weathering, glauconitic and phosphoritic skeletål carbonates which yield a rich diverse fauna of late Early Cambrian age including trilobites *(Bonnia, Calodiscus, Olenellus* and *Wanneria)*, pelagiellids, *Fordilla troyensis, Chancelloria*, hyolithids, *Hyolithellus, Linnarssonia* and other inarticulate brachiopods (Christie & Peel 1977; Palmer & Peel 1979).

Similar rocks occur within the outer shelf-slope association; collectively they are assigned to Lithofacies 6 (phosphoritic glauconitic skeletal carbonates). Those occurring within Association B are described separately in Chapter 6.

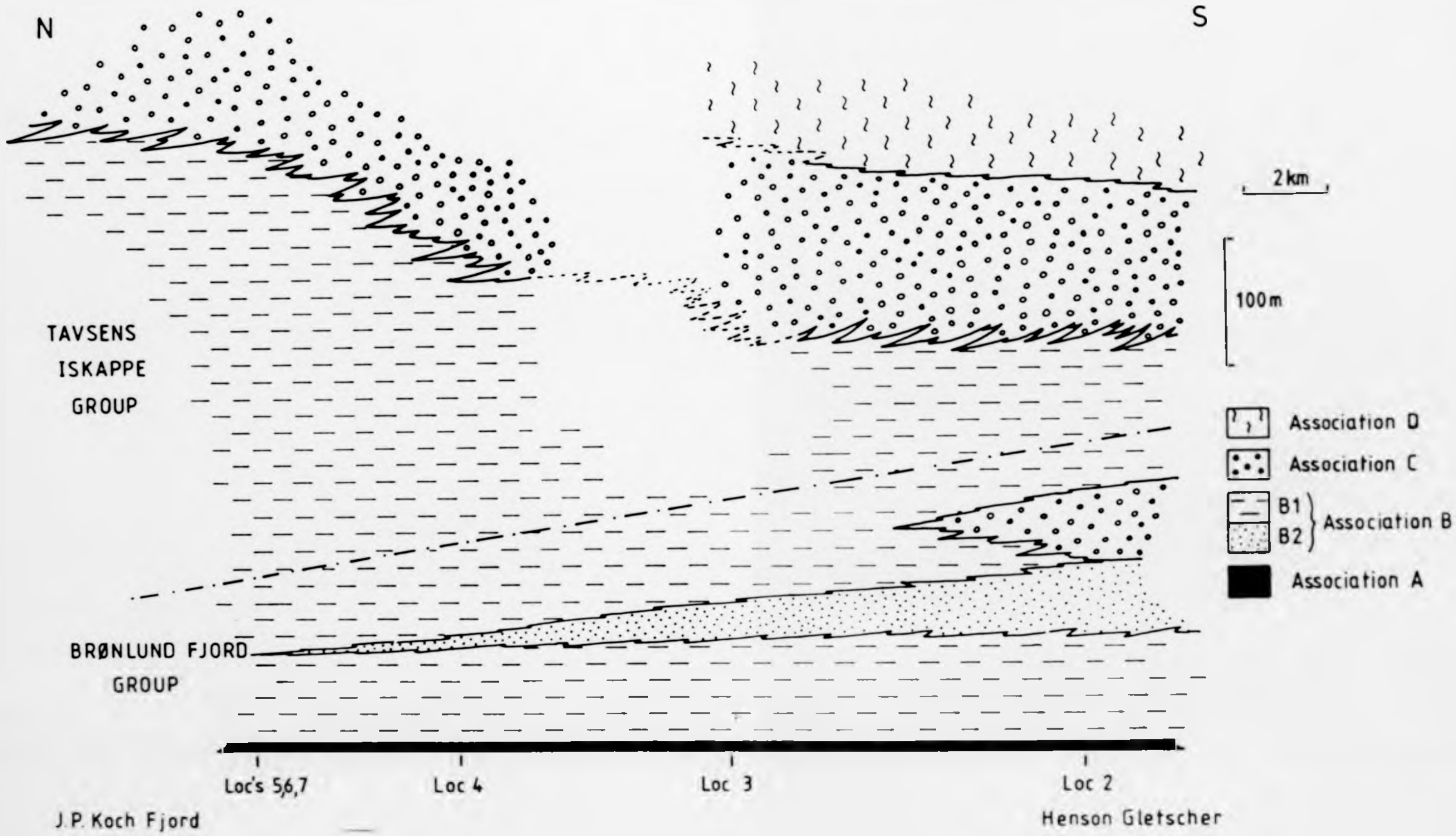


Figure 5.1. Relationship between Associations A,B, C and D in the north-south transect between J.P. Koch Fjord and Henson Gletscher.

5.2.1 Lithofacies 6 ; Phosphoritic, glauconitic skeletal carbonates

The basal beds of the Aftenstjernesø Formation are composed of dolomite in most sections. At two localities adjacent to Hans Tavsens Iskappe (Løndal and eastern Fimbuldal) however, primary limestone fabrics are preserved, and the following facies description relies heavily on analogies drawn between these limestones and the more typical dolomites. In undolomitized sections, Lithofacies 6 comprises interbedded skeletal lime wackestones (subfacies 6a) and skeletal, intraclastic packstones and grainstones (subfacies 6b). Black to dark-brown phosphorite occurs within both subfacies, forming isolated nodules, stringers and persistent seams within lime mud-dominated intervals and intraclasts within fragmental packstone and grainstone beds (Frykman 1980).

5.2.1.1 Subfacies 6a

The lime wackestones display wavy nodular bedding (Fig. 5.2) with common terrigenous mudstone flasers, partings and rare interbeds up to 0.2m thick (Fig. 5.3). In dolomitized sections, mid-pale grey medium to fine crystalline dolomites contain a scattering of 'ghost' carbonate shell fragments, together with phosphatic bioclasts, glauconite pellets and fine-grained quartz sand or coarse silt. The terrigenous mudstones locally display a wispy lamination but are commonly bioturbated. In terrigenous mudstone-rich intervals the associated carbonate is generally ferroan.

Partially or non-dolomitized examples comprise heavily bioturbated skeletal wackestone containing bioclasts (trilobite,

Figure 5.2. Dark argillite flasers and discontinuous beds within glauconitic skeletal dolomites. Argillaceous wisps and flasers commonly pass laterally into irregular stylolitic seams (arrow). Aftenstjernesø Formation, locality 20, central Peary Land.


Figure 5.4. Photomicrograph (PPL) of bioturbated skeletal wackestone (LF.6). Note random orientation of bioclasts (mainly trilobite (T), subordinate pelmatozoan (P)) and geopetal/spar fills of burrows (arrowed). Dark patch (upper right) is pyrite. Scale bar = 1mm. GGU 197577, Aftenstjernesø Formation, locality 10, west Peary Land.

Figure 5.2. Dark argillite flasers and discontinuous beds within glauconitic skeletal dolomites. Argillaceous wisps and flasers commonly pass laterally into irregular stylolitic seams (arrow). Aftenstjernesø Formation, locality 20, central Peary Land.


Figure 5.4. Photomicrograph (PPL) of bioturbated skeletal wackestone (LF.6). Note random orientation of bioclasts (mainly trilobite (T), subordinate pelmatozoan (P)) and geopetal/spar fills of burrows (arrowed). Dark patch (upper right) is pyrite. Scale bar = 1mm. GGU 197577, Aftenstjernesø Formation, locality 10, west Peary Land.

Figure 5.2. Dark argillite flasers and discontinuous beds within glauconitic skeletal dolomites. Argillaceous wisps and flasers commonly pass laterally into irregular stylolitic seams (arrow). Aftenstjernesø Formation, locality 20, central Peary Land.


Figure 5.4. Photomicrograph (PPL) of bioturbated skeletal wackestone (LF.6). Note random orientation of bioclasts (mainly trilobite (T), subordinate pelmatozoan (P)) and geopetal/spar fills of burrows (arrowed). Dark patch (upper right) is pyrite. Scale bar = 1mm. GGU 197577, Aftenstjernesø Formation, locality 10, west Peary Land.

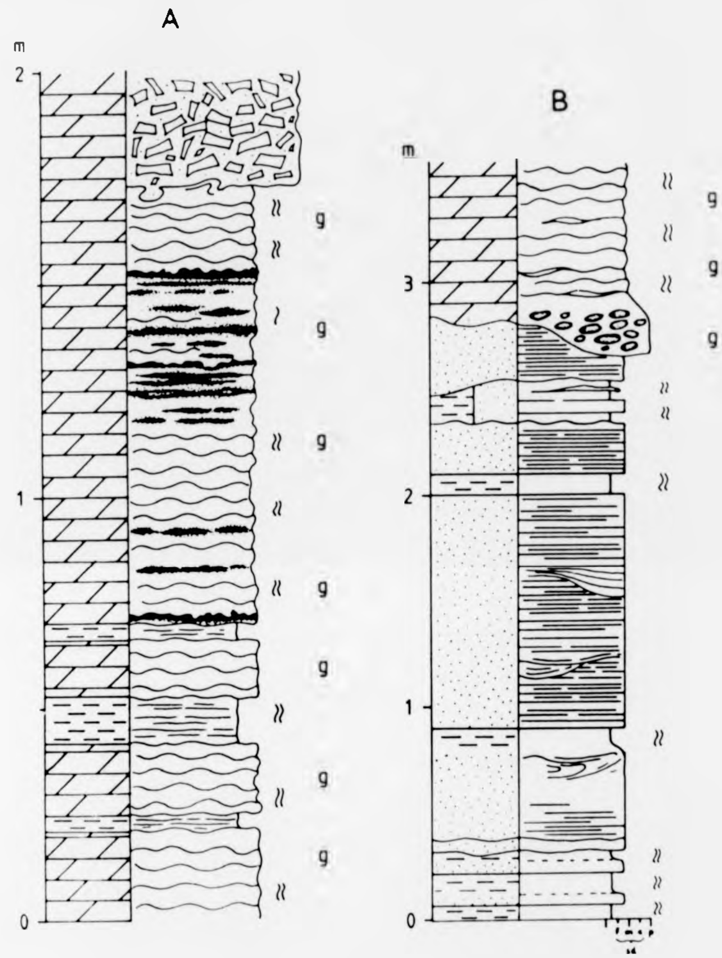


Figure 5.3. A. Section through phosphoritic, glauconitic dolomites at the base of the Aftenstjernesø Formation in its type section. Phosphorite (dense stipple) occurs both as irregular nodules and as discrete horizons with sharp tops. Locality 1, east Freuchen Land. B. Sharp erosional contact between sandstones of the Buen Formation and glauconitic phosphoritic dolomites of the Aftenstjernesø Formation. Locality 21, central Peary Land.

pelmatozoan and inarticulate brachiopod), glauconite and rare peloids in a matrix of neomorphic microspar (Fig. 5.4). Intense bioturbation is indicated by the lack of primary sedimentary structures and the random orientation of bioclasts (Fig. 5.4). Burrow-mottling is locally defined by dolomite patches (5-10mm diameter) devoid of bioclasts with a weak concentric array of bioclasts in the surrounding wackestone. Discrete subhorizontal or oblique branching burrows (2-5mm diameter) are locally abundant, and closely resemble *Chondrites* burrow systems. They are filled with geopetal lime mud or silt and calcite spar cement and transect the 'churned' burrowed fabric (Fig. 5.4) indicating protracted biogenic reworking of the sediment.

Disseminated and framboidal pyrite is common; it locally fills *Chondrites* burrows and partially replaces calcite bioclasts. Glauconite occurs mainly as bright green, structureless pellets (100-150μm diameter) which are sub-rounded to well-rounded except where secondary dolomite rhombs encroach on the pellet margins. Rarely, glauconite occurs as a replacement of skeletal grains or as skeletal moulds and Frykman (1981) recorded glauconite impregnation of a cemented hardground surface.

Bioclasts are disarticulated and fragmentary, although not substantially abraded; they are strewn in a fine-grained matrix of 5-15μm equigranular microspar. Skeletal grains are commonly rimmed by calcite spar; single crystal pelmatozoan grains have syntaxial overgrowths, whereas trilobite fragments commonly display a bladed isopacheous fringe, 50-200μm thick. Frykman (1981) suggested that the spar represents early diagenetic cement that formed prior to biogenic mixing with lime mud.

Nodular bedding is well-developed, particularly in argillaceous intervals where discontinuous pale green, silt partings and flasers drape and outline carbonate-rich nodules (Fig. 5.2). Flattened burrows and fractured bioclasts within silt flasers and internodular carbonate suggest that compaction around early diagenetic, cemented zones was responsible, at least in part, for the nodular structure (*cf.* Garrison & Kennedy 1977). Subsequent modification and enhancement of the nodular fabric by pressure solution is indicated by stylolites that truncate skeletal grains at nodule margins and by the concentration of insoluble components (silt, clay, glauconite, phosphatic detritus) along internodular zones. The development of nodular carbonate is further discussed in Chapter 6.

Phosphorite occurs mainly as nodules, stringers and semi-continuous laminae in this subfacies. Where primary fabrics are recognizable, it is clear that the phosphorite preferentially replaced fine-grained carbonate (lime mud). Skeletal grains generally retain their carbonate mineralogy, resulting in phosphorite internal and external moulds. Erosion of such indurated, shelly phosphorite-impregnated mud would yield skeletal internal moulds, as observed within associated skeletal grainstone beds (subfacies 6b, see below). Comparable shell moulds formed by selective phosphatization of indurated micrite within shells have been described from the Cretaceous of south-east England (Kennedy & Garrison 1975a). The good preservation of skeletal structure in phosphorite moulds suggests that phosphorite impregnation preceded dolomitization; bioclasts in phosphorite-free beds are poorly preserved and are defined solely by slight colour variation within the dolomite mosaic.

The phosphorite itself is structureless or faintly mottled and grades into non-phosphoritic carbonate. Locally, however, discrete phosphorite laminae or thin beds (1-10mm thick) grade downwards into unphosphatized carbonate but have sharp, irregular upper surfaces (Figs 5.3A, 5.5 & 5.6). These surfaces display pedestals, overhangs and scoured hollows with a relief of up to several centimetres and are typically overlain by dolomitized skeletal grainstones containing angular phosphorite intraclasts and worn internal moulds (Fig. 5.5). Complex multiple phosphorite seams are produced by vertical and lateral coalescence of nodules and bands (Fig. 5.5). A detailed example of one such complex phosphorite surface of Middle Cambrian age is given in Chapter 6.

5.2.1.2 Subfacies 6b

Lime packstone and grainstone beds commonly have sharp, erosive bases (Figs 3.13, 5.3B & 5.5); this is particularly evident where they overlie black phosphorite horizons (Fig. 5.5). Beds are up to 0.2m thick and are commonly lenticular. In dolomitized sections they comprise medium to coarse crystalline, glauconitic, pale grey dolomite with a relict grainstone or packstone fabric. In partially dolomitized or undolomitized sections they are composed of fragmented, abraded skeletal elements (50-80%; trilobite, pelmatozoan hyolithid, *Salterella* and sponge spicules), glauconite (5-15%) and a variable proportion of intraclastic and lithoclastic detritus (Figs 5.7 &5.8). Shell fragments are often densely packed or imbricated; cross-lamination and current ripples occur locally. Although lime mud (neomorphosed to microspar) commonly forms up to 30% of the rock, umbrella and bridging fabrics demonstrate the

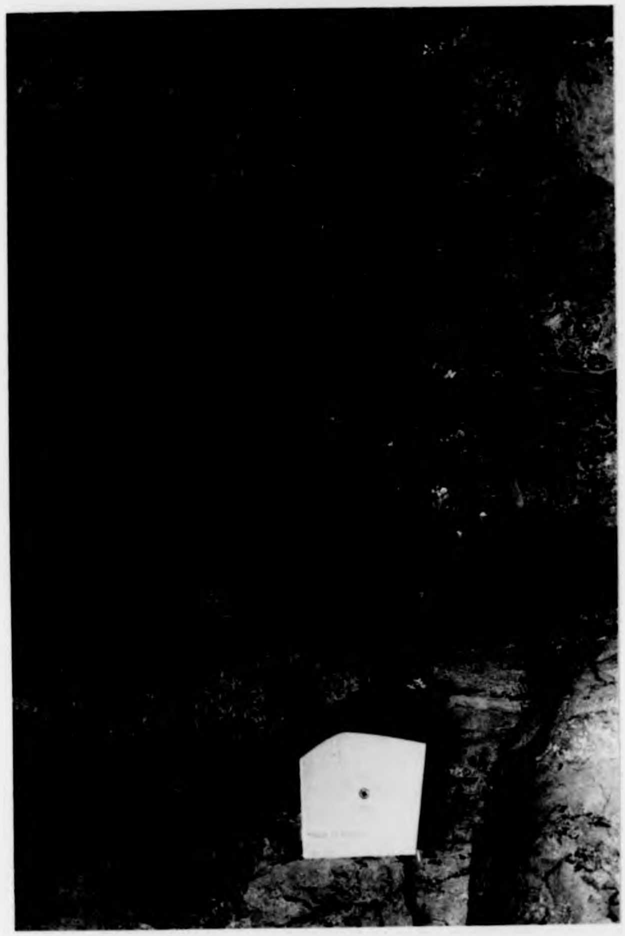

Figure 5.5. Glauconitic skeletal dolomite with black phosphorite nodules (A) and bands with sharp, irregular upper surfaces (B). Note scatter of phosphoritie intraclasts above surface B. Aftenstjernesø Formation, locality 1, east Freuchen Land.

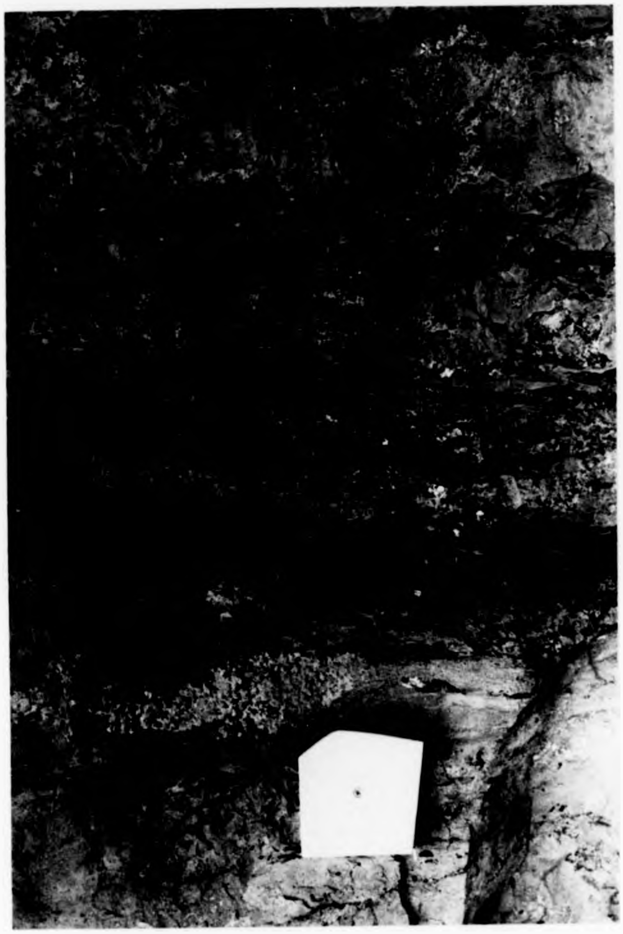

Figure 5.5. Glauconitic skeletal dolomite with black phosphorite nodules (A) and bands with sharp, irregular upper surfaces (B). Note scatter of phosphoritie intraclasts above surface B. Aftenstjernesø Formation, locality 1, east Freuchen Land.

Figure 5.6. Argillaceous dolomitic limestones with an irregular phosphorite-impregnated surface (arrowed). Aftenstjernesø Formation, eastern Fimbuldal, west Peary Land.

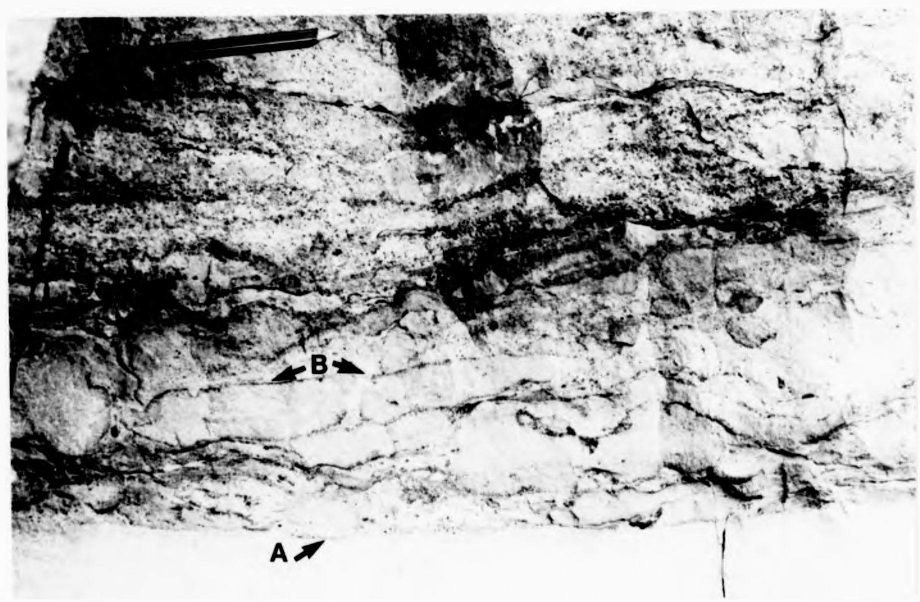


Figure 5.7. Sharp erosional contact (A) between Buen Formation sandstones and glauconitic, phosphoritic dolomites of the Aftenstjernesø Formation (see also Figs 3.13 & 5.3B). Note the lag of phosphorite-rimmed sandstone pebbles (B) derived from the underlying Buen Formation. Black specks are predominantly glauconite. Locality 21, central Peary Land.

Figure 5.6. Argillaceous dolomitic limestones with an irregular phosphorite-impregnated surface (arrowed). Aftenstjernesø Formation, eastern Fimbuldal, west Peary Land.

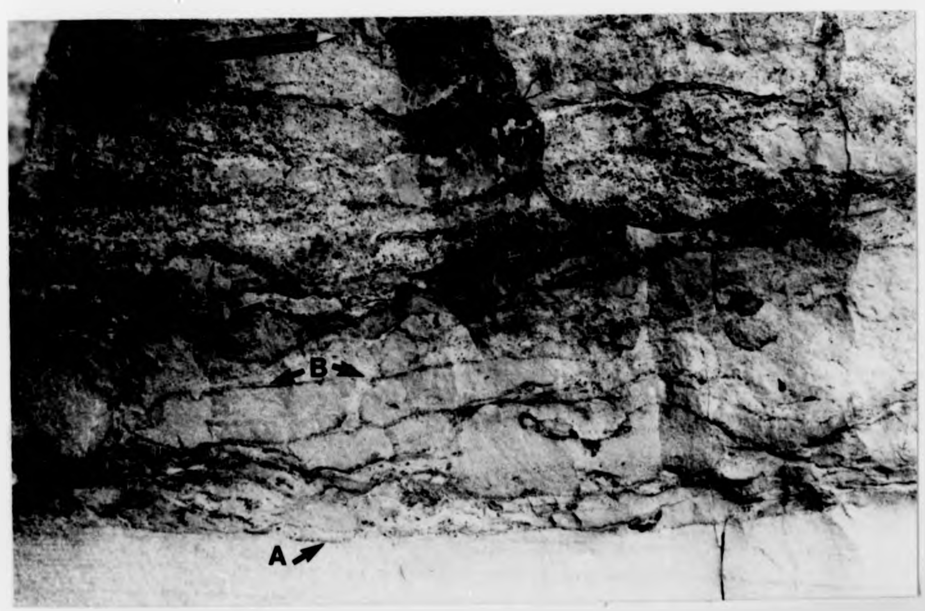


Figure 5.7. Sharp erosional contact (A) between Buen Formation sandstones and glauconitic, phosphoritic dolomites of the Aftenstjernesø Formation (see also Figs 3.13 & 5.3B). Note the lag of phosphorite-rimmed sandstone pebbles (B) derived from the underlying Buen Formation. Black specks are predominantly glauconite. Locality 21, central Peary Land.

Figure 5.8. Photomicrograph (PPL) of dolomitic skeletal grainstone (LF.6) composed mainly of trilobite (T) and nested hyolithid cones (H). D : dolomite; P : pyrite; G : glauconite. Scale bar = 1mm. GGU 197578, Aftenstjernesø Formation, locality 10, west Peary Land.

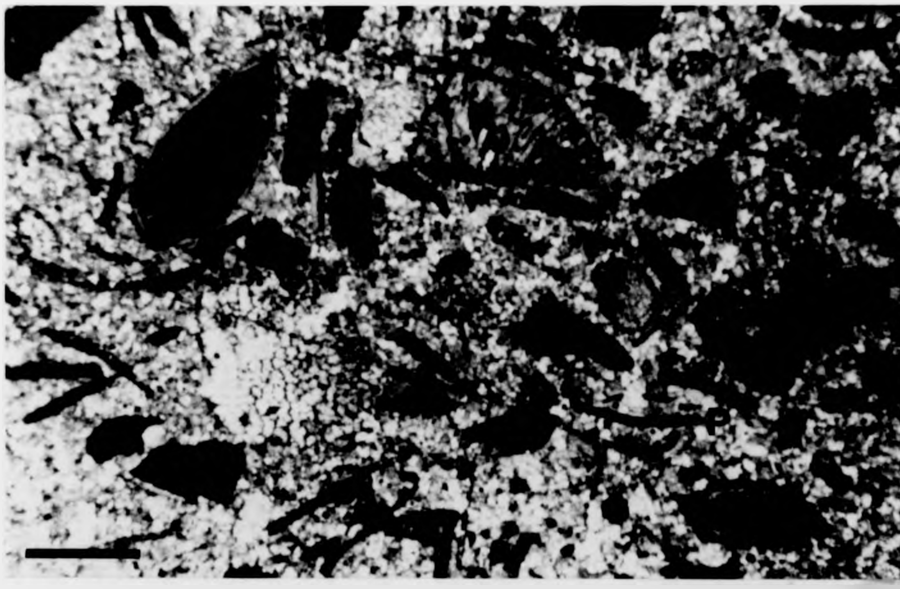

Figure 5.9. Photomicrograph (PPL) of dolomitized intraclastic, skeletal grainstone (LF.6). Dark phosphorite occurs as angular intraclasts, primary phosphatic shell fragments (P) and internal moulds (top left). Note weakly phosphoritized pelmatozoan grains (N). Scale bar = 1mm. GGU 218504, Aftenstjernesø Formation, locality 1, east Freuchen Land.


Figure 5.8. Photomicrograph (PPL) of dolomitic skeletal grainstone (LF.6) composed mainly of trilobite (T) and nested hyolithid cones (H). D : dolomite; P : pyrite; G : glauconite. Scale bar = 1mm. GGU 197578, Aftenstjernesø Formation, locality 10, west Peary Land.

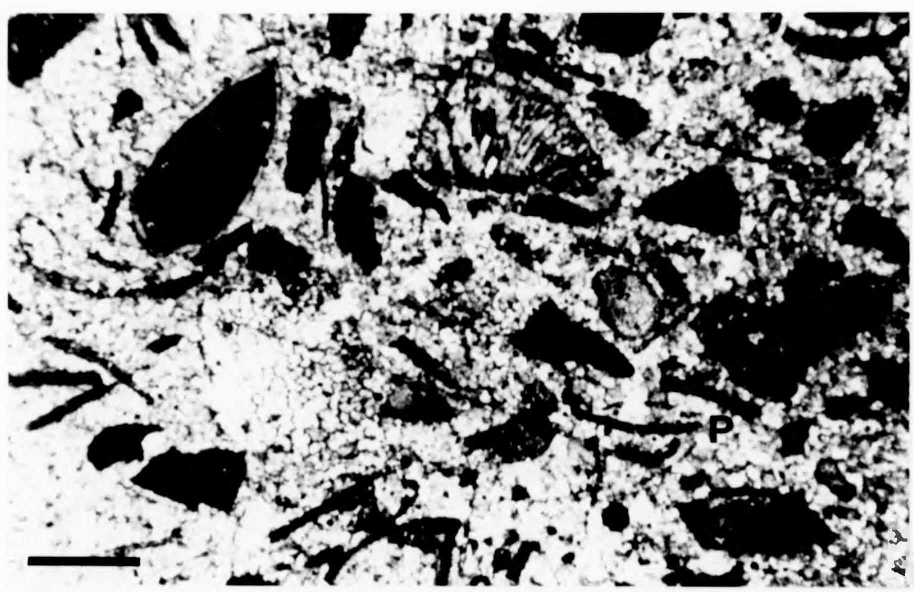


Figure 5.9. Photomicrograph (PPL) of dolomitized intraclastic, skeletal grainstone (LF.6). Dark phosphorite occurs as angular intraclasts, primary phosphatic shell fragments (P) and internal moulds (top left). Note weakly phosphoritized pelmatozoan grains (N). Scale bar = 1mm. GGU 218504, Aftenstjernesø Formation, locality 1, east Freuchen Land.

primary grain support (*cf*. Bowman 1979). Lime mud commonly occurs in skeletal traps (i.e. beneath trilobite doublures or within hyolithid cones) in an otherwise mud-free grainstone which suggests reworking of bioclasts from a primary muddy, shelly sediment.

These rocks are cemented by coarse bladed calcite radiating from bioclasts, by syntaxial overgrowths on pelmatozoan fragments and by blocky calcite spar.

Phosphorite occurs mainly as detrital fragments in this subfacies. They comprise primary phosphatic skeletal elements (e.g. inarticulate brachiopods) and phosphorite intraclasts, peloids, shell internal moulds and partially phosphatized lithoclasts (Figs 5.5, 5.7 and 5.9). Phosphorite intraclasts (1-50mm) are angular or irregular in outline and often contain carbonate skeletal grains. The intraclasts are common in grainstone and packstone beds that overlie phosphorite surfaces (see subfacies 6a); clearly, this reflects erosion of indurated phosphorite.

#### 5.2.1.3 Interpretation

a) General

The rich, diverse fauna and the presence of glauconite indicate an open marine environment. Heavily bioturbated nodular lime wackestones (subfacies 6a) record the slow accumulation of lime mud from suspension in a low-energy but well-oxygenated environment that supported a diverse benthic shelly fauna and burrowing infauna. Thorough bioturbation and early diagenetic nodular cementation suggest a slow rate of sediment accumulation (Jones *et al*. 1979; Mullins *et al*. 1980).

primary grain support (*cf.* Bowman 1979). Lime mud commonly occurs in skeletal traps (i.e. beneath trilobite doublures or within hyolithid cones) in an otherwise mud-free grainstone which suggests reworking of bioclasts from a primary muddy, shelly sediment.

These rocks are cemented by coarse bladed calcite radiating from bioclasts, by syntaxial overgrowths on pelmatozoan fragments and by blocky calcite spar.

Phosphorite occurs mainly as detrital fragments in this subfacies. They comprise primary phosphatic skeletal elements (e.g. inarticulate brachiopods) and phosphorite intraclasts, peloids, shell internal moulds and partially phosphatized lithoclasts (Figs 5.5, 5.7 and 5.9). Phosphorite intraclasts (1-50mm) are angular or irregular in outline and often contain carbonate skeletal grains. The intraclasts are common in grainstone and packstone beds that overlie phosphorite surfaces (see subfacies 6a); clearly, this reflects erosion of indurated phosphorite.

5.2.1.3 Interpretation

a) General

The rich, diverse fauna and the presence of glauconite indicate an open marine environment. Heavily bioturbated nodular lime wackestones (subfacies 6a) record the slow accumulation of lime mud from suspension in a low-energy but well-oxygenated environment that supported a diverse benthic shelly fauna and burrowing infauna. Thorough bioturbation and early diagenetic nodular cementation suggest a slow rate of sediment accumulation (Jones *et al.* 1979; Mullins *et al.* 1980).

Interbedded terrigenous mudstones are commonly both bioturbated and glauconitic and suggest similar bottom conditions during periods of reduced carbonate input.

The skeletal grainstone and packstone beds (subfacies 6b) reflect periodic winnowing and reworking of shelly lime muds by tractional bottom currents or wave action. Shell imbrication and rippling indicate entrainment and active migration of skeletal sands. The scoured surfaces lined with shelly intraformational conglomerate lags (Figs 5.5 & 5.7) indicate episodic erosion and reworking of indurated sediment. The morphology of the low-angle erosion surface illustrated in Fig. 3.13 is comparable to surfaces described by Anderton (1976) from the Dalradian of Scotland, which he ascribed to erosion by episodic high-energy storm-surge currents.

The alternation of mud-rich and mud-poor skeletal carbonates in this lithofacies suggests fluctuating energy levels - winnowing and local transport of shelly sands followed by the accumulation of lime mud and silt from suspension.

b) Phosphorite and glauconite

Studies of modern occurrences of phosphorite and glauconitic. have established the environmental conditions that favour their genesis. Present-day marine phosphorites are known to be forming in two main areas - the Namibian continental shelf at depths of 60-120m (Baturin *et al.* 1970) and the continental slope off the Peru and Chile coast in water depths of 200-400m (Burnett *et al.* 1980). The association between phosphorites and oceanic upwelling has been known for some time (Kazakov 1937). Organic-rich sediment is essential for phosphorite genesis and recent work has shown that the role of upwelling is to provide a sustained flow of nutrient-rich waters to the photic zone where biological productivity is high and the accumulation of organic-enriched sediment is favoured. A further consequence of upwelling and high organic productivity is the formation of a discrete oxygen deficient layer (the oxygen minimum zone; Thiede & Van Andel 1977); clearly, preservation of organic matter on the seabed and the formation of phosphorite is favoured within this oxygen-depleted zone. It is significant, however, that phosphorites forming presently on the Peru-Chile continental slope occur preferentially at the upper (100m depth) and lower (400m) boundaries of the oxygen minimum zone rather than throughout the oxygen-deficient layer (Burnett *et al.* 1980). A further requirement for the formation of phosphorites is a low rate of sediment accumulation, either due to winnowing and phosphorite concentration or to reduced sediment supply (Jarvis 1980; Baturin 1982).

Glauconite is commonly associated with phosphorites in ancient and Recent deposits (Odin & Letolle 1980) which suggests similar environmental requirements. It occurs over a wide range of latitudes in marine waters ranging from 60 to 350m in depth (Odin & Letolle *op. cit.*). It is generally regarded as forming by degradation of sheet silicates (McRae 1972) although numerous examples of glauconite replacement of carbonate have been documented (e.g. Kennedy & Garrison 1975b). Reduced rates of sedimentation and a mildly reducing environment are considered necessary for glauconite formation (McRae 1972; Odin & Letolle 1980).

By analogy with modern occurrences, therefore, the presence genesis and recent work has shown that the role of upwelling is to provide a sustained flow of nutrient-rich waters to the photic zone where biological productivity is high and the accumulation of organic-enriched sediment is favoured. A further consequence of upwelling and high organic productivity is the formation of a discrete oxygen deficient layer (the oxygen minimum zone; Thiede & Van Andel 1977); clearly, preservation of organic matter on the seabed and the formation of phosphorite is favoured within this oxygen-depleted zone. It is significant, however, that phosphorites forming presently on the Peru-Chile continental slope occur preferentially at the upper (100m depth) and lower (400m) boundaries of the oxygen minimum zone rather than throughout the oxygen-deficient layer (Burnett *et al.* 1980). A further requirement for the formation of phosphorites is a low rate of sediment accumulation, either due to winnowing and phosphorite concentration or to reduced sediment supply (Jarvis 1980; Baturin 1982).

Glauconite is commonly associated with phosphorites in ancient and Recent deposits (Odin & Letolle 1980) which suggests similar environmental requirements. It occurs over a wide range of latitudes in marine waters ranging from 60 to 350m in depth (Odin & Letolle *op. cit.*). It is generally regarded as forming by degradation of sheet silicates (McRae 1972) although numerous examples of glauconite replacement of carbonate have been documented (e.g. Kennedy & Garrison 1975b). Reduced rates of sedimentation and a mildly reducing environment are considered necessary for glauconite formation (McRae 1972; Odin & Letolle 1980).

By analogy with modern occurrences, therefore, the presence of glauconite and phosphorite indicates deposition in a sediment-starved, subtidal environment. Organic productivity in oxygenated surface waters was high, possibly due to oceanic upwelling; phosphorite and glauconite formed in organic-rich sediment under mildly reducing, dysaerobic conditions. Water depth is poorly constrained and deposition may have occurred under several tens or several hundreds of metres of water.

The nodular phosphorite probably formed by replacement of fine-grained carbonate at shallow depths below the sediment surface, as observed today (Baturin 1982). The irregular phosphorite surfaces, however, are comparable to mineralized hardgrounds described from ancient carbonate sequences (Bromley 1967; Kennedy & Garrison 1975b; Jarvis 1980). A number of features suggest that these surfaces represent true submarine hardgrounds, formed by the exhumation of a cemented, phosphatized carbonate layer:-

1. Frykman (1981) demonstrated that fibrous or bladed calcite cements are locally reworked and, in one instance, are draped by glauconite at an impregnated surface.

2. Many surfaces are highly irregular and scalloped; fragile arches, overhangs and caverns are commonly preserved.

3. Angular phosphorite intraclasts are common in associated skeletal lags.

Several phosphorite layers show evidence of phosphorite impregnation at the sediment surface (Fig. 5.6), a process which is commonly inferred for ancient mineralized hardgrounds (Bromley 1967; Kennedy & Garrison 1975b), but is unknown today (Bentor 1980). Further description and discussion of phosphorite surfaces is included in Chapter 6.

### 5.2.2 Lithological variation

The sedimentary logs shown on Figs 3.13 and 5.3 illustrate the vertical and lateral variation observed within the association. In most sections there is a gradual upward decrease in the proportion of terrigenous detritus within the basal 0.1-1m of the carbonate succession. At Buen (locality 21, Fig.3.3; Figs 5.3B & 3.13), however, the clastic - carbonate boundary is sharp and erosional; phosphorite-rimmed sandstone pebbles, derived from the underlying Buen Formation, occur within the basal shelly glauconitic lag deposit (0.1-0.5m thick; Fig. 5.7).

The upper boundary of the association may be abrupt. At locality 1, for example, the glauconitic, phosphoritic carbonates are overlain by a massive carbonate breccia bed (Figs 3.9 & 5.3A). Typically, however, the association grades upwards into dark, nodular or laminated carbonates (Lithofacies 1, 7).

Whereas glauconite is present in these beds at all localities studied, non-skeletal phosphorite is less widely distributed. It is best developed in the most north-westerly section (Locality 1, Fig. 5.3A) but becomes scarce towards the south and south-east (e.g. at Koch Væg and in Løndal). Phosphorite seams were recorded at most localities along Wandel Dal between Øvre Midsommersø and Børglum Elv (Fig. 3.3), but they are typically thin and discontinuous in this area and form a minor part of the section.

The relative proportion of grainstones and packstones (subfacies 6b) to wackestones and mudstones (subfacies 6a) over the outcrop area is not accurately known, since positive identification of the subfacies is often difficult in unfavourably weathered dolomitized sections. In general, however, a south or south-easterly increase in energy is suggested by the apparent southward increase in winnowed skeletal carbonates relative to burrowed, phosphoritic mud-dominated carbonates with discrete terrigenous mudstone interbeds (compare Fig. 5.3A with Figs 5.3B and 3.9B).

### 5.2.3 Environmental interpretation

This basal unit of the carbonate succession is clearly condensed, as suggested by Frykman (1980, 1981) and Hurst & Surlyk (1983). It reflects slow sediment accumulation with frequent erosional and non-depositional events which are represented locally by incipient and mature hardgrounds (Frykman 1980). Inferred processes include deposition from suspension and tractional bottom currents and there is no evidence of the gravity flow processes that typify the succeeding outer shelf-slope sediments.

The environment is envisaged as an extensive, low-relief subtidal marine shelf, with depositional slopes of insufficient magnitude to promote sediment failure and gravity flow. The sediments were deposited at or below normal wave base, but were periodically reworked by storm waves or storm-induced currents. Sedimentation rates were low, due to siliciclastic starvation, repeated winnowing of fines and the embryonic nature of the carbonate shelf. A gradual shallowing towards the south or south-east is suggested by the distribution of phosphorite and mud-rich skeletal carbonates. The marked offshore increase in the proportion of phosphorite may reflect the impingement of the upper levels of an oxygen-depleted layer that developed beneath well-oxygenated, agitated surface waters. As observed in modern environments, phosphorite genesis is favoured at this boundary between oxic and anoxic waters (Burnett *et al.* 1980).

Although contemporaneous inshore deposits are not preserved, the lack of evidence for appreciable depositional slopes and the gradual southward increase in depositional energy suggest a comparison with the carbonate ramp model of Ahr (1973) and inferred ancient carbonate ramps (e.g. Read 1980).

The transition from clastic to carbonate deposition represents a significant change in sedimentation over a vast area of the shelf in North Greenland, probably due to siliciclastic starvation and consequent onset of carbonate production in the less turbid shelf waters. Siliciclastic starvation probably resulted from drowning of the clastic shelf and the suppression of terrigenous distributory systems as suggested by Hurst & Surlyk (1983). As carbonate sedimentation became established, the development of inshore high-energy carbonate shoals would further inhibit offshore dispersal of land-derived detritus. Smith (1977) described a clastic to carbonate transition in the Mississipian of Montana which shows many of the features described here. Shallow-water siliciclastic sediments are abruptly overlain by a thin, widespread, glauconitic interval comprising bioclastic wackestones, packstones and grainstones. He suggested that this unit represented a relatively rapid transgression which resulted in mantling of terrigenous sediment sources and termination of clastic influx.

Hurst & Surlyk (1983) proposed that this transgressive event was probably of tectonic origin, resulting from tilting and subsidence of the Peary Land shelf. It is significant, however, that this condensed interval at the transition from clastic to carbonate facies is present at this stratigraphic level throughout North Greenland. In Washington Land, west North Greenland (Fig 1.1), the transition from terrigenous clastics (Humboldt Formation) to dolomites (Kastrup Elv Formation) is marked by a 1m thick unit of burrowed, glauconitic sandstones and siltstones with thin conglomerate interbeds that locally contain a diverse fauna and phosphatic intraclasts (Henriksen & Peel 1976; J.S. Peel, pers. comm. 1984). Clearly, the transgression was of regional extent, suggesting a eustatic mechanism.

Association A, interpreted here as an incipient carbonate ramp, is restricted to the thin basal unit of the carbonate sequence. The shelf rapidly became differentiated into an inshore, shallow-water carbonate platform and an outer shelf-slope environment.

# CHAPTER 6 : OUTER SHELF - ASSOCIATION B

## Association B; Outer shelf - slope.

The outer shelf - slope association is dominated by carbonates, but includes a distinctive terrigenous wedge at around the Lower-Middle Cambrian boundary. The facies of this association are thus subdivided into two groups:- carbonates (B1) and siliciclastics (B2).

## 6.1. B1. Carbonates.

This sub-association comprises nine facies.

### 6.1.1. Lithofacies 1; Bituminous laminated carbonate.

Limestones (51%), dolomitic limestones (9%) and dolomites (40%) of this lithofacies are dark grey or black, weather mid-grey to sooty black, and commonly form recessive, dark weathering outcrops (e.g. Figs 3.6 & 3.8). They form units a few centimetres to tens of metres thick and are characteristic of the Henson Gletscher Formation, although also occurring widely elsewhere in the succession (Figs 3.16 & 3.38).

In undolomitized sections, the lithofacies comprises bituminous lime mudstones with occasional micropeloidal or skeletal wackestone laminae. A well-developed, laterally persistent parallel lamination is ubiquitous and produces a platy or friable, shaly weathered surface (Figs 6.1 & 3.18). The fine lamination (0.1-5mm thick) is defined by compositional (organic content, quartz silt) or subtle grain size differences and clearly represents a primary, depositional structure. Lamination within early diagenetic concretions is more diffuse, however, which suggests that

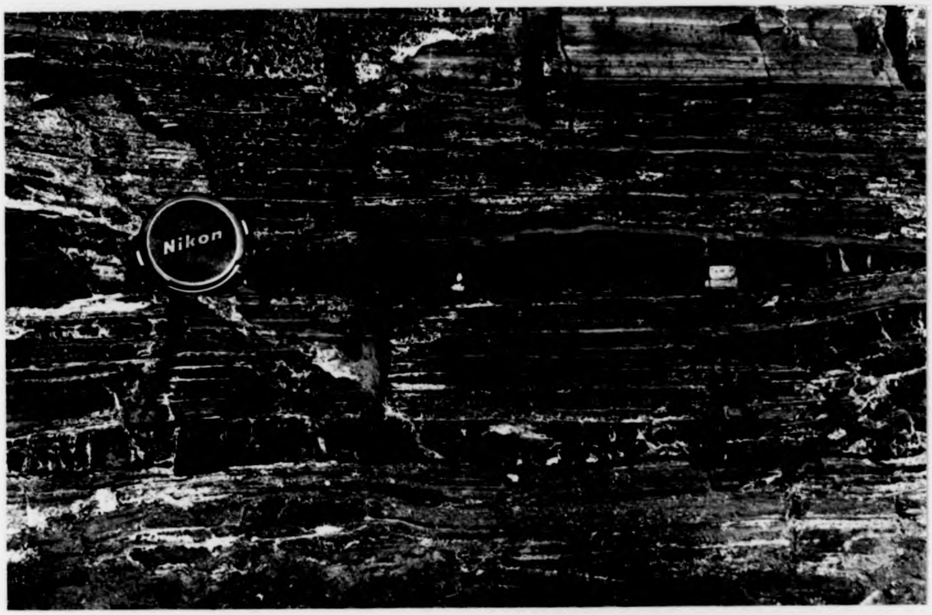


Figure 6.1. Laminated bituminous dolomite (LF.1) with lenticular black chert nodules. Note the continuity of laminae across carbonate-chert contacts (centre right) and the lack of significant differential compaction suggesting post-compactional development of chert nodules (compare with Fig. 6.2). Henson Gletscher Formation, locality 1, east Freuchen Land.


Figure 6.2. Laminated bituminous dolomite (LF.1) with carbonate concretion. Note the deflection of lamination from concretion to 'host' rock, indicating early diagenetic, pre- and syncompactional growth. Henson Gletscher Formation, locality 1, east Freuchen Land.

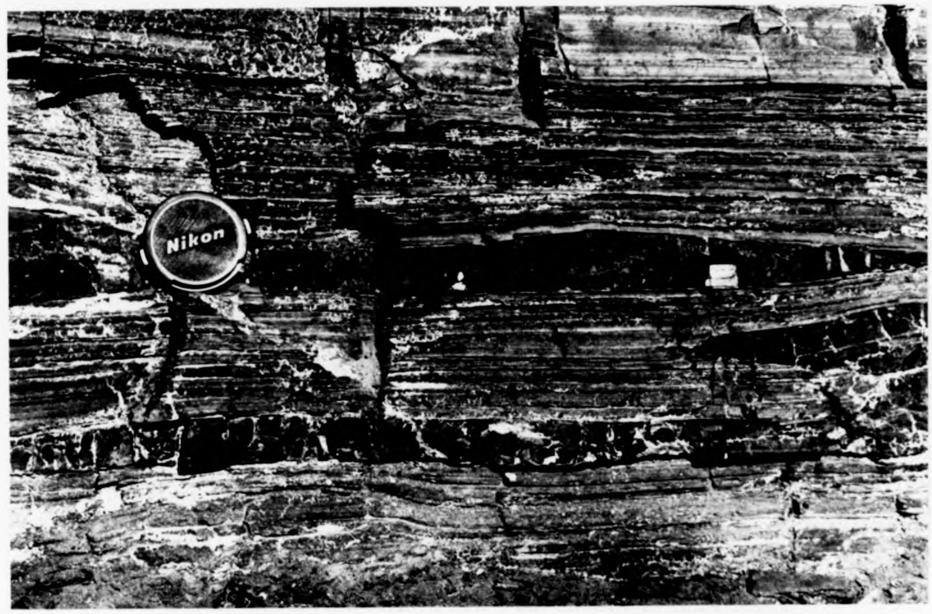


Figure 6.1. Laminated bituminous dolomite (LF.1) with lenticular black chert nodules. Note the continuity of laminae across carbonate-chert contacts (centre right) and the lack of significant differential compaction suggesting post-compactional development of chert nodules (compare with Fig. 6.2). Henson Gletscher Formation, locality 1, east Freuchen Land.

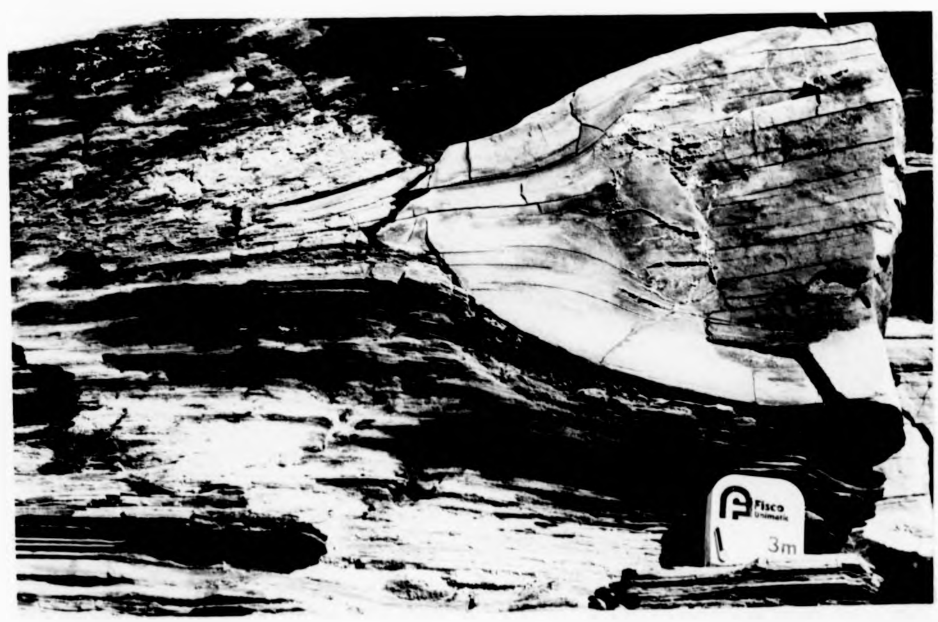


Figure 6.2. Laminated bituminous dolomite (LF.1) with carbonate concretion. Note the deflection of lamination from concretion to 'host' rock, indicating early diagenetic, pre- and syncompactional growth. Henson Gletscher Formation, locality 1, east Freuchen Land.

compaction and associated diagenetic processes have enhanced a less differentiated primary lamination (Fig. 6.2). Some wackestone or packstone laminae (1-5mm thick) show micrograding of coarse to fine silt-sized micritic peloids that are locally replaced, partially or wholly, by dark brown or black phosphorite (Fig. 6.3). Rarely, these laminae are internally cross-laminated and have sharp, scoured bases.

Sponge spicules and agnostoid trilobites are typical of this facies; individual laminae are locally extremely rich in complete trilobites. Preservation is excellent and delicate, unbroken quadrate sponge spicules are common. Most spicules are composed of clear sparry calcite (Fig. 6.3), but the presence of a relict axial canal and the occurrence of partially replaced siliceous spicules indicates an original silica composition (*cf.* Meyers 1977). Bioturbation is rare. In the Henson Gletscher Formation, however, laminated bituminous dolomites locally grade upwards into massive, bioturbated dolomites (Lithofacies 2; Fig. 6.4).

Early diagenetic, ellipsoidal carbonate concretions are common and range up to a metre across (Figs 3.18 & 6.2). The deflection of primary lamination at the margin of concretions indicates pre- and syn-compactional development (Fig. 6.2; Raiswell 1971) and gives a crude measure of the magnitude of conpaction of these rocks; values between 40% and 60% are typical (maximum 85%). Black chert is locally abundant (Figs 3.18 & 6.1). It forms elongate lenses, stringers and discontinuous bands up to 0.2m thick. Its secondary origin is indicated by the lenticular, nodular habit, by the gradational margins and by the persistence of primary laminae across chert-carbonate contacts (Fig. 6.1).

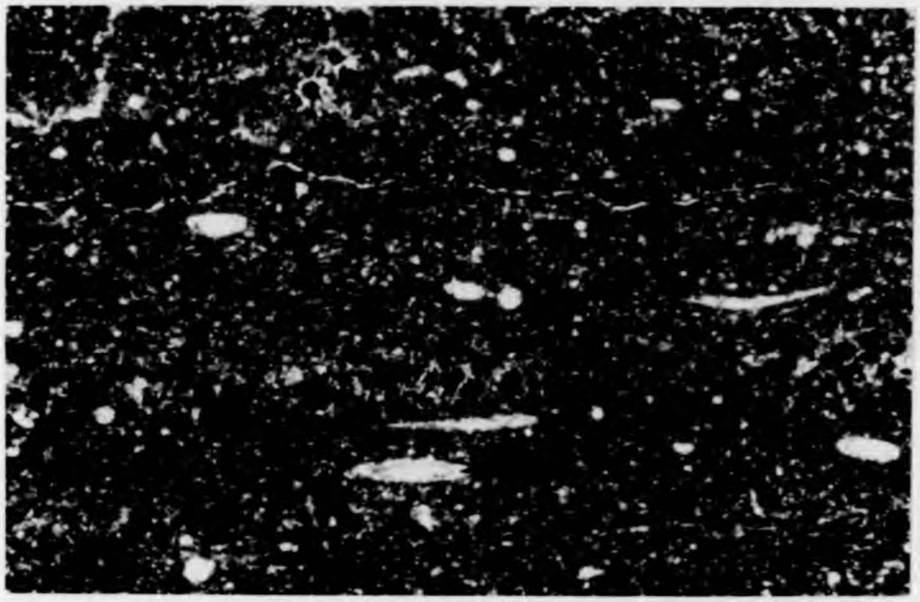

Figure 6.3. Photomicrograph (PPL) of spicular lime mudstone (LF.1), mainly neomorphosed to microspar. Sponge spicules show relict axial canals (arrow) indicating a primary siliceous composition. Vague lamination defined by phosphoritic pellets (black). Scale bar = 1mm. GGU 218533, Henson Gletscher Formation, locality 1, east Freuchen Land.

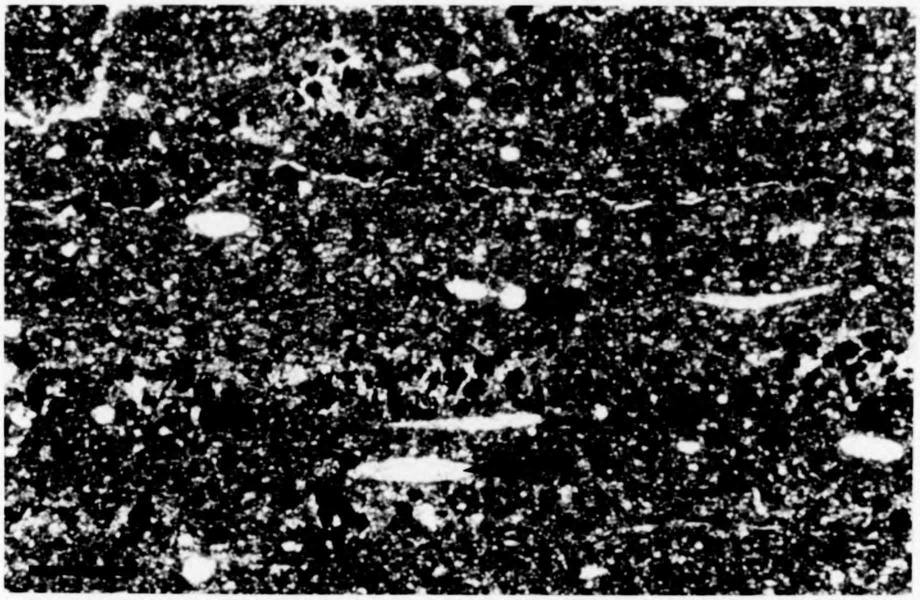

Figure 6.3. Photomicrograph (PPL) of spicular lime mudstone (LF.1), mainly neomorphosed to microspar. Sponge spicules show relict axial canals (arrow) indicating a primary siliceous composition. Vague lamination defined by phosphoritic pellets (black). Scale bar = 1mm. GGU 218533, Henson Gletscher Formation, locality 1, east Freuchen Land.

The abundant evidence for calcite replacement of siliceous sponge spicules indicates that biogenic spicular silica was the dominant source for the secondary chert (*cf.* Meyers 1977). Compactional effects are less obvious adjacent to chert nodules than their carbonate counterparts (compare Figs 6.1 & 6.2), and syn- to post-compactional development is indicated.

These laminated carbonates are highly bituminous and locally pyritic; they emit a fetid smell on fracturing and contain a total organic carbon content of up to 1·2% ( Rolle + Wrang 1981). Lime mudstones are commonly neomorphosed to microspar (20-50$\mu$m) and occasionally to pseudospar showing a relict fibrous, spherulitic habit. Dolomitized representatives of this lithofacies comprise fine to medium crystalline dolomite; relict sedimentary lamination (defined by bituminous microstylolitic seams), 'ghost' fossils and partially dolomitized lime mudstones testify to the secondary nature of the dolomite.

Interpretation.

The finely-laminated nature of these pyritic, bituminous fine-grained carbonates indicates deposition in stagnant anoxic conditions. Preservation of delicate sedimentary structures is regarded as the most reliable evidence of anoxia, particularly when associated with a high organic carbon content (Waples 1983). Evidence of current activity is rare, and deposition from suspension is the favoured mechanism. Micro-graded lime silt laminae resulted from episodic supply of coarser sediment to the water column, possibly due to offshore storm currents (*cf.* Neumann & Land 1975). The rare erosively-based, cross-stratified laminae attest to the infrequent action of weak geostrophic bottom currents or low-density, muddy turbidity currents (*cf.* Stow & Shanmugam 1980).

The trilobite-spicule fauna indicates an open marine environment, but is clearly an allochthonous, transported assemblage; the sponge spicules are disaggregated and the trilobite faunas are dominated by agnostoids which are generally regarded as planktic forms (Robison 1972). Benthic faunas are absent and bioturbation is rare, supporting the idea of a poorly oxygenated environment incapable of supporting either an infauna or a benthic shelly fauna (the anaerobic biofacies of Byers 1977). The concentration of fossils, particularly trilobites, along certain bedding planes may reflect mass mortality (Wilson 1975) or reduced sediment supply and consequent concentration of planktic faunal elements. The presence of pyrite and phosphorite also suggests slow sedimentation rates and poorly oxygenated bottom conditions (Read 1980; Baturin 1982).

This lithofacies compares closely with the 'laminated lime mudstone' facies of Wilson (1969, 1975) which he considered to indicate deposition in low-energy, deep-water marine environments. Similar bituminous, laminated lime mudstones have been described fron throughout the stratigraphical record in inferred 'basinal' or 'deeper water' successions (e.g. Cook & Taylor 1977; Keith & Friedman 1977; Read 1980); settling of suspended lime mud is generally considered to be the dominant process with a subordinate contribution from contour currents, nepheloid layers or dilute turbidity currents. Comparable hemipelagic deposits flanking modern shallow-water carbonate banks were termed 'peri-platform ooze' by Schlager & James (1978).

6.1.2. Lithofacies 2; Dark bioturbated dolomite.

Dark grey dolomites of this lithofacies show mid-grey to pale fawn-grey weathering colours and typically form pale stripes within sequences dominated by dark laminated carbonates (Figs 3.14 & 6.4). They are only recognized in the Henson Gletscher and Sæ terdal Formations (Figs 3.16 & 3.17) where they form units 0.05-2m thick and display thin to thick stylolitic bedding. Equivalent limestones are not recognized.

In the field, faint mottling, discontinuous wispy lamination and small spar-filled burrows characterize the facies, but a pale, weathered patina commonly obscures finer detail. Polished slabs and thin sections reveal intense bioturbation; mottling and fine burrowing is defined by pale dolomite patches, pyrite or geopetal burrow fills (Figs 6.5 & 6.6). The bioturbation generally resulted in a mottled, churned, heterogeneous texture and discrete, well-defined burrows are rare. Where present, individual cylindrical burrows are 0.3-2mm in diameter, sub-horizontal or oblique, locally branched and have structureless pale sediment or geopetal sediment and spar fills (Fig. 6.6); these burrows are assigned to *Chondrites*. Recognizable dolomitized skeletal grains are rare; where present, disarticulated trilobite fragments are randomly oriented with respect to bedding.

In thin section these rocks comprise a mosaic of pale fawn to dark brown, anhedral dolomite crystals (15-50μm); intercrystalline bituminous matter is common and burrow fills are defined by patches of clear or pale fawn dolomite (Fig. 6.6).

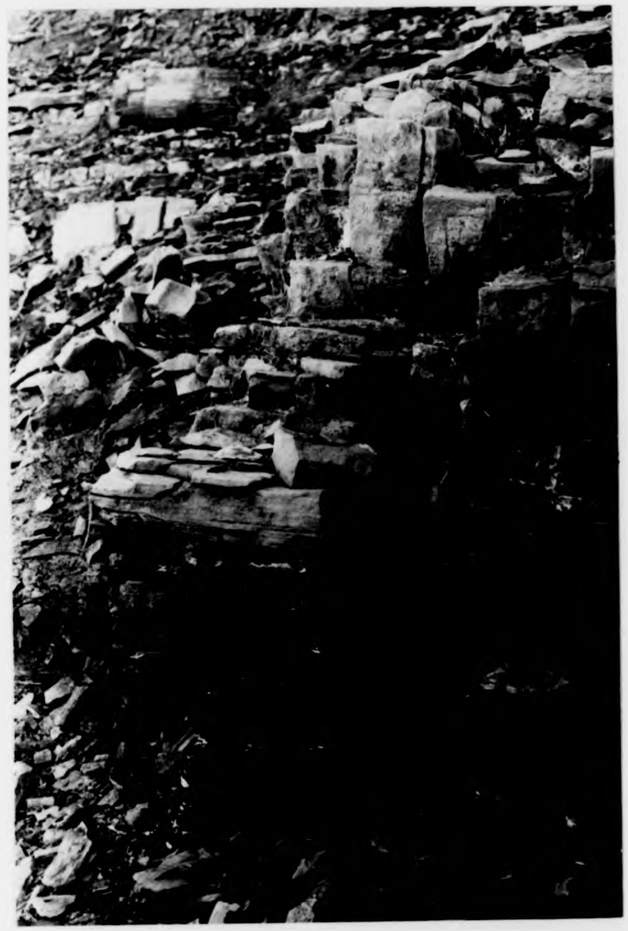

Figure 6.4. Vertical transition from shaly, parallel-laminated bituminous dolomite (LF.1) into massive, bioturbated, pale-weathering dolomite (LF.2). Hammer (centre right) for scale. Henson Gletscher Formation, locality 1, east Freuchen Land.

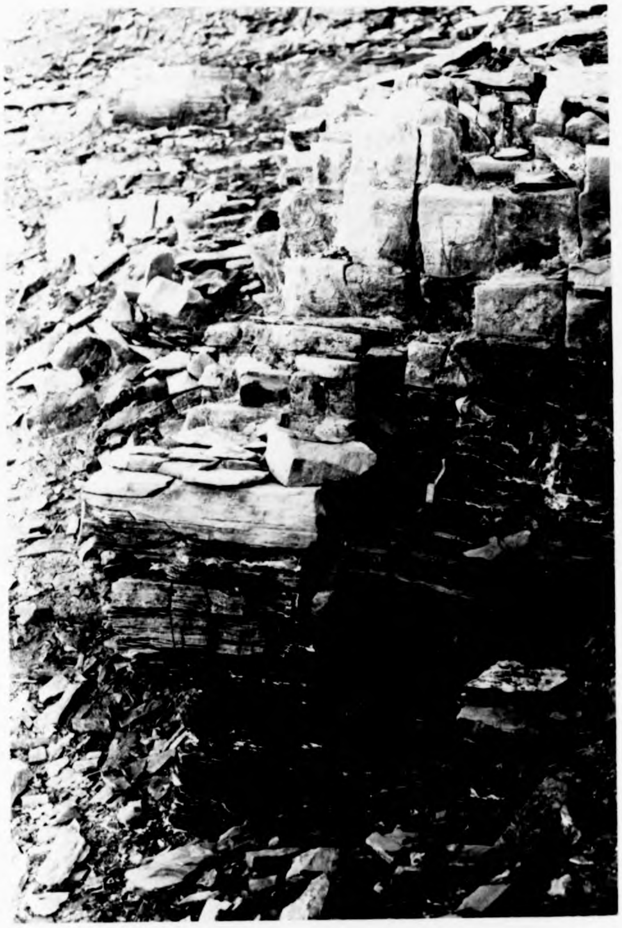

Figure 6.4. Vertical transition from shaly, parallel-laminated bituminous dolomite (LF.1) into massive, bioturbated, pale-weathering dolomite (LF.2). Hammer (centre right) for scale. Henson Gletscher Formation, locality 1, east Freuchen Land.


Figure 6.5. Polished surface, cut normal to bedding, of heavily bioturbated dolomite (LF.2). GGU 218515, Henson Gletscher Formation, locality 1, east Freuchen Land.


Figure 6.5. Polished surface, cut normal to bedding, of heavily bioturbated dolomite (LF.2). GGU 218515, Henson Gletscher Formation, locality 1, east Freuchen Land.

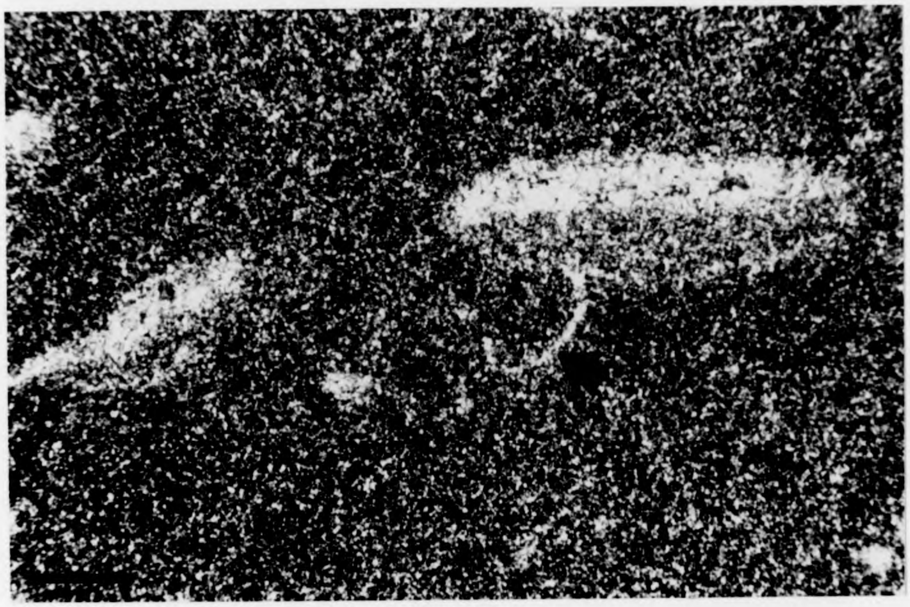

Figure 6.6. Photomicrograph (PPL) of fine crystalline, bioturbated dolomite (LF.2). Obvious burrows (?*Chondrites*) have geopetal sediment and spar cement fills. Note 'ghosted' skeletal grain (arrow). Scale bar = 1mm. GGU 218517, Henson Gletscher Formation, locality 1, east Freuchen Land.

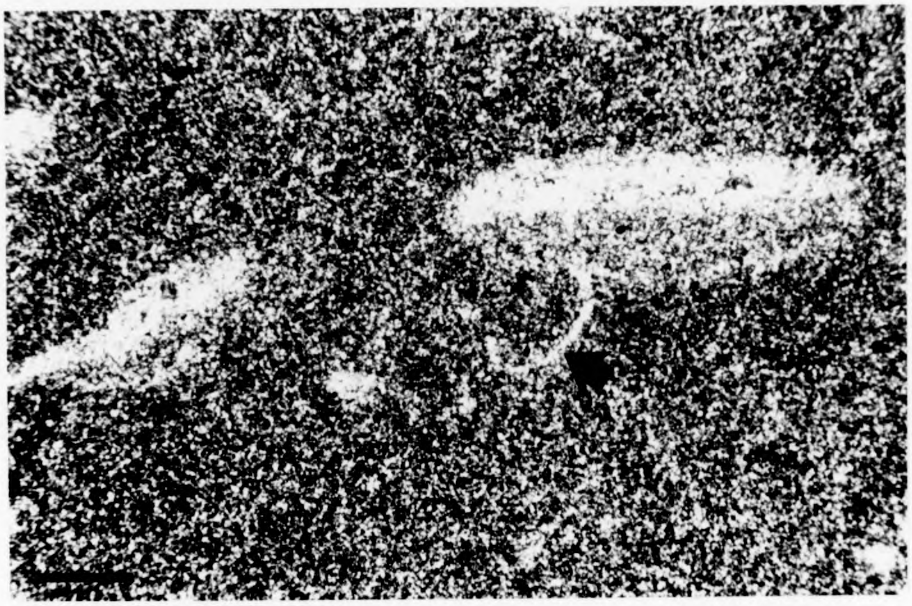

Figure 6.6. Photomicrograph (PPL) of fine crystalline, bioturbated dolomite (LF.2). Obvious burrows (?*Chondrites*) have geopetal sediment and spar cement fills. Note 'ghosted' skeletal grain (arrow). Scale bar = 1mm. GGU 218517, Henson Gletscher Formation, locality 1, east Freuchen Land.

Interpretation.

Interpretation of this lithofacies is inhibited by the lack of a limestone equivalent. However, the gross features (dark, bituminous carbonate, bioturbated fabric, paucity of 'ghost' allochems) suggest a primary, organic-rich, fine-grained precursor. Thus, these rocks probably represent dolomitized lime muds and silts that were deposited mainly from suspension in a low-energy marine environment below wave base. This interpretation is supported by the common transition between this lithofacies and bituminous, laminated, spicular carbonates (Lithofacies 1; see Fig. 6.4).

Despite the evidence of an active infauna, these rocks are commonly bituminous and apparently lack a benthic shelly fauna. This suggests that the level of oxygenation was sufficient to support a soft-bodied infauna, but not a benthic shelly fauna (the dysaerobic biofacies of Byers 1977). *Chondrites* has been recognized from all marine environments, littoral to deep-sea (Häntzchel 1975, pp W49-52), but it is significant that the *Chondrites* - producing organism appears to show a greater tolerance to reduced oxygen levels than other burrowing organisms (Kelts & Arthur 1981).

The alternation between anoxic and weakly oxygenated bottom conditions, reflected by the alternation of Lithofacies 1 and 2, may have resulted from a periodic improvement in circulation within the water column or from a reduction in the supply of organic matter; both mechanisms would lead to an increase in available oxygen at the sediment surface (Waples 1983). The former is more likely, particularly in the coarsening-upward sequences described later (6.2.3, Fig. 6.81), where the evidence of increased oxygenation of bottom waters is accompanied by evidence of sediment reworking by currents.

### 6.1.3. Lithofacies 3; Argillaceous lime mudstones.

This lithofacies comprises thin-bedded, dark grey carbonates interbedded with grey or greenish-grey weathering calcareous terrigenous mudstones (Figs 3.26 & 3.44). Over 80% of the carbonate beds are composed of lime mudstone; lime wackestones, packstones, grainstones and dolomites make up the remainder. Dark argillaceous medium to fine crystalline dolomites form only 12% of the lithofacies. These thin-bedded limestones are typical of the Ekspedition Bræ, Holm Dal and Erlandsen Land Formations where they form monotonous sequences up to 80m thick, weathering mid-grey or fawn-grey (Figs 3.25, 3.42, 3.60 & 3.61).

The limestones form thin (typically 20-40mm), parallel-sided beds that alternate with partings or interbeds (up to 0.5m thick) of terrigenous silty mudstone (Figs 3.63 & 6.7). Individual beds are laterally persistent and the limestone and argillite components are generally well segregated (Figs 3.63 & 6.7); the boundaries may be sharp or gradational over a few millimetres. Bedding is sometimes wavy in lime-rich intervals (Fig. 3.26) where silty mudstone partings are wispy and discontinuous. The terrigenous mudstones range from silty claystones to coarse siltstones, display a fissile, shaly bedding

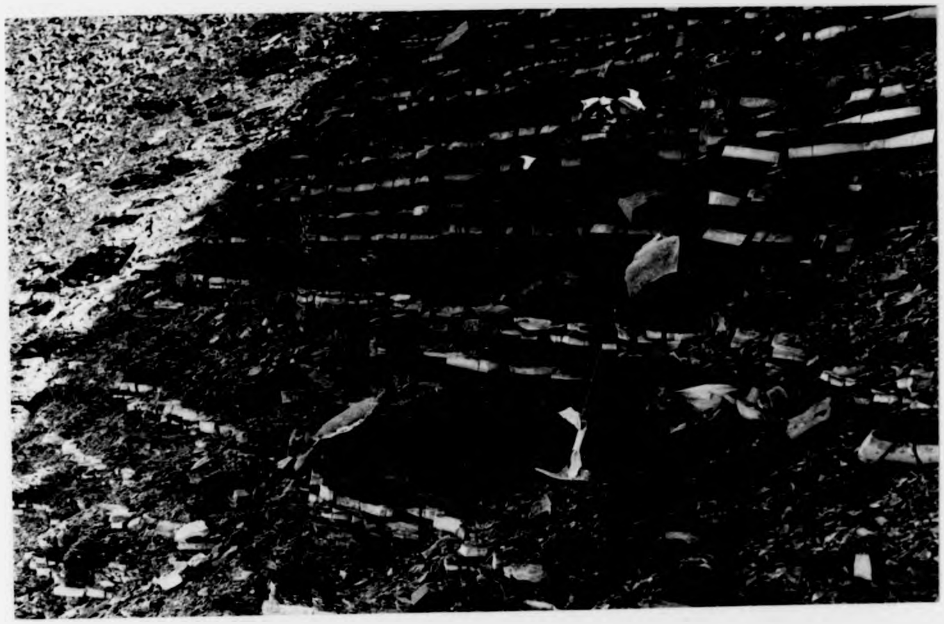

Figure 6.7. Thin-bedded, argillaceous lime mudstones (LF.3). The limestone beds are typically laterally persistent although locally pinching and swelling. Ekspedition Bræ Formation, locality 1, east Freuchen Land.

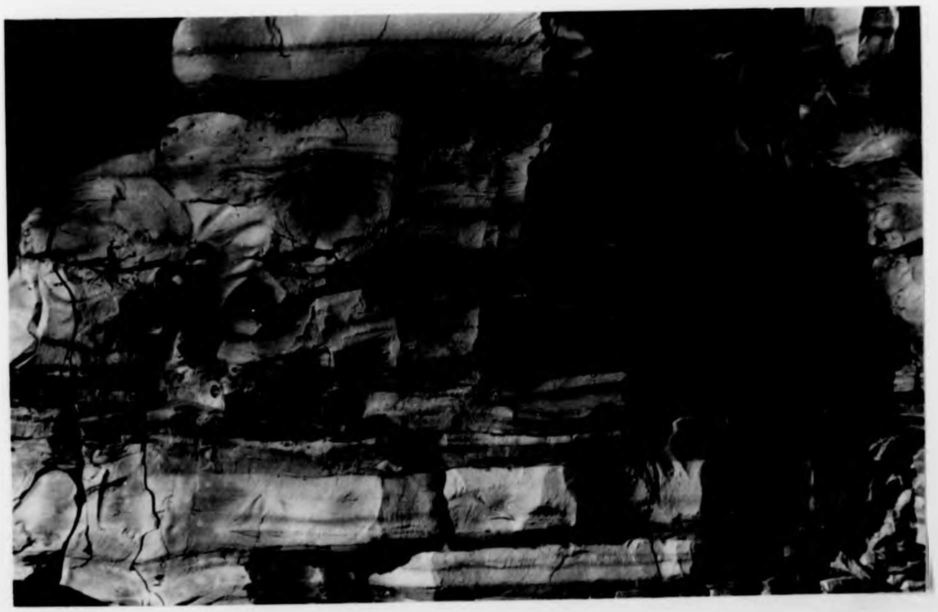

Figure 6.8. Spar-filled burrows with pale nodular rims (arrows) in argillaceous lime mudstones (LF.3). Erlandsen Land Formation, locality 11, central Peary Land.

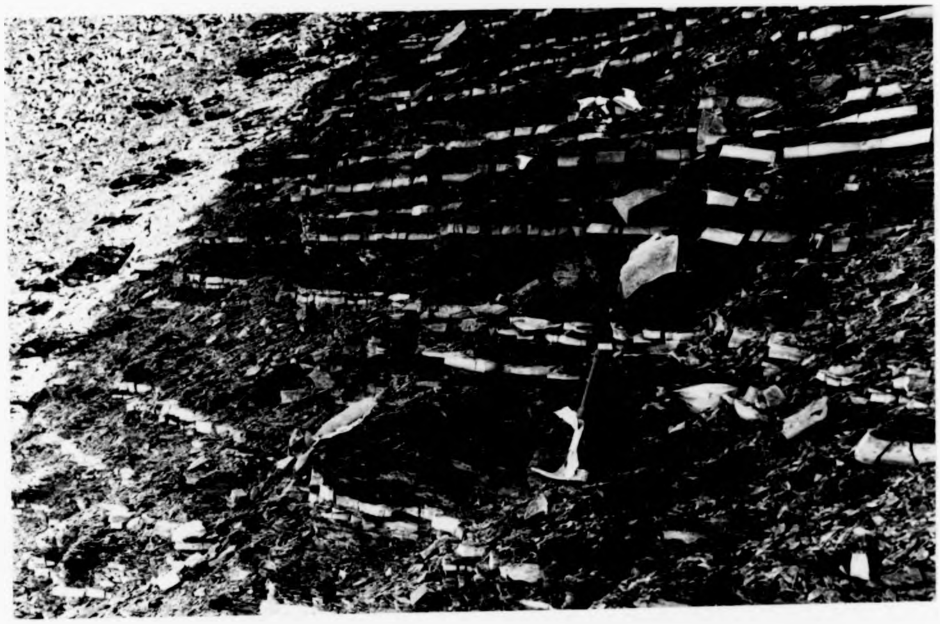

Figure 6.7. Thin-bedded, argillaceous lime mudstones (LF.3). The limestone beds are typically laterally persistent although locally pinching and swelling. Ekspedition Bræ Formation, locality 1, east Freuchen Land.

Figure 6.8. Spar-filled burrows with pale nodular rims (arrows) in argillaceous lime mudstones (LF.3). Erlandsen Land Formation, locality 11, central Peary Land.

and contain flattened, poorly preserved trilobites and sponge spicules.

Bioturbation is scarce overall, but is locally important within individual limestone beds which show irregular, knobbly bedding surfaces. *Chondrites* burrow systems occur in the Ekspedition Bræ Formation where they are often picked out by pyrite. In the Erlandsen Land Formation, isolated spar-filled burrows (2-5mm diameter) have pale nodular haloes (Fig. 6.8) and apparently acted as nuclei during early diagenetic, differential cementation.

Three variants are recognized within the lime mud-dominated, thin carbonate beds:- massive, laminated and graded beds. The latter are rare; massive and laminated beds together form over 90% of the lithofacies.

*Massive* beds comprise structureless or weakly laminated lime mudstones. Weak parallel lamination is defined by diffuse colour streaks reflecting variation in organic and/or argillite content. A scatter of angular quartz silt grains (< 1%) is present in some beds. Well preserved, articulated trilobites and sponge spicules are common and typically lie parallel to bedding.

The *laminated* beds comprise interlaminated lime mudstone and peloidal, skeletal lime packstone or grainstone (Fig. 6.9). The coarser laminae range from 0.1 to 4mm in thickness and have gradational or sharp bases and gradational tops. Small-scale loading is locally present at basal contacts but neither erosive boundaries nor tractional sedimentary

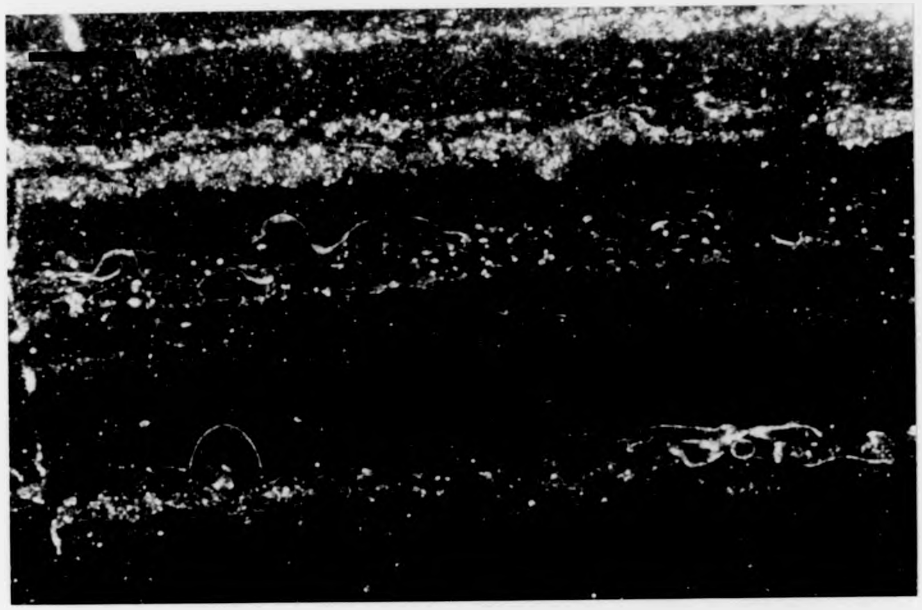

Figure 6.9. Photomicrograph (PPL) of laminated lime mudstone (LF.3) with thin silty, peloidal skeletal packstone or grainstone laminae. Skeletal grains are mainly trilobite fragments (characteristic cross-section lower left). Scale bar = 1mm. GGU 218652, Holm Dal Formation, locality 7, west Peary Land.

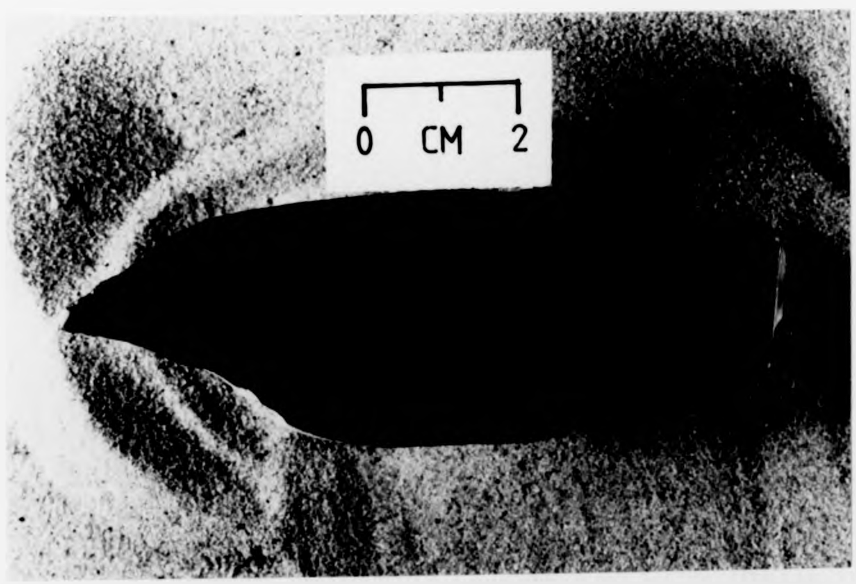


Figure 6.10. Polished surface, cut normal to bedding, of weakly graded limestone (LF.3). Note scoured base and upward transition from skeletal, peloidal wackestone (shell fragments arrowed) into laminated, dark lime mudstone, which is locally burrowed in the upper cm. GGU 218502, Ekspedition Bræ Formation, locality 1, east Freuchen Land.

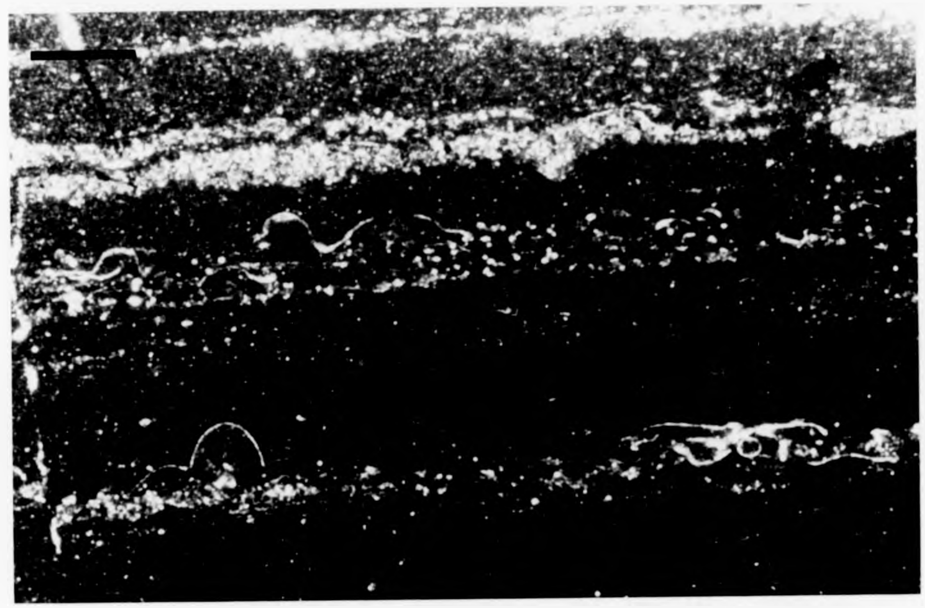

Figure 6.9. Photomicrograph (PPL) of laminated lime mudstone (LF.3) with thin silty, peloidal skeletal packstone or grainstone laminae. Skeletal grains are mainly trilobite fragments (characteristic cross-section lower left). Scale bar = 1mm. GGU 218652, Holm Dal Formation, locality 7, west Peary Land.

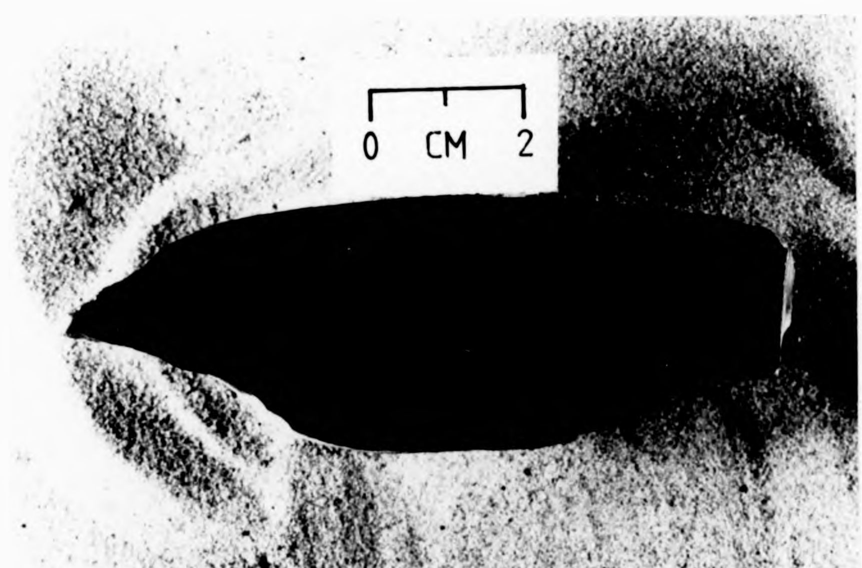


Figure 6.10. Polished surface, cut normal to bedding, of weakly graded limestone (LF.3). Note scoured base and upward transition from skeletal, peloidal wackestone (shell fragments arrowed) into laminated, dark lime mudstone, which is locally burrowed in the upper cm. GGU 218502, Ekspedition Bræ Formation, locality 1, east Freuchen Land.

structures are observed. The intervening lime mudstone laminae range from less than a millimetre to several centimetres in thickness and are lithologically identical to the massive limestone beds described above. The coarser laminae are composed of structureless micritic peloids (40-100μm diameter) and skeletal elements (trilobite, brachiopod, spicules, pelmatozoan) which are commonly disarticulated but not extensively abraded. Terrigenous silt is common, particularly in the Holm Dal Formation where angular coarse silt and very fine sand (mainly quartz with minor plagioclase and microcline feldspar, muscovite mica) forms up to 30% of some laminae.

The *graded* beds are 10-30mm thick, have sharp, locally erosional bases (Fig. 6.10) and show weak normal grading from peloidal, skeletal lime packstone or wackestone into structureless or laminated lime mudstone. Upper surfaces are occasionally bioturbated and some lime packstone beds show ripple cross-lamination.

Neomorphic recrystallization is a common feature of these rocks - fabrics range from homogeneous micrite to microspar mosaics. Lime grainstone laminae display blocky spar cements that are composed of ferroan calcite in argillite-rich sequences. Oldershaw & Scoffin (1967) documented a similar relationship between ferroan carbonate and argillite content; they suggested that clays may be an important contributor of iron during carbonate diagenesis.

Interpretation

These thin-bedded, argillaceous, dark limestones are closely comparable to the 'deeper-water' or 'basinal' limestones described by

Wilson (1969,1975), Cook & Taylor (1977) and others (see Cook & Enos 1977). The fine grain size, parallel lamination, scarcity of bioturbation and absence of shallow-water features indicate deposition in a low-energy, poorly oxygenated marine environment below storm wave-base.

Comparable sequences of interbedded limestones and marls have been interpreted as either the deposits of dilute density currents (Davies 1977) or hemipelagic sediments deposited from suspension (Cook & Taylor 1977). Those favouring the former interpretation generally regard the limestones as the deposits of mud-rich turbidity currents and the interbedded marls as the hemipelagic interval (Thomson & Thomasson 1969; Davies 1977; Yurewicz 1977 ). The massive and laminated beds (> 90% of the lithofacies) rarely show evidence of current action and are ungraded on the scale of individual beds. Furthermore, discrete limestone beds commonly contain a number of micrograded packstone or grainstone laminae and thus do not represent single depositional events. Following Cook & Taylor (1977) the laminated and massive mudstones are interpreted as hemipelagic sediments (*cf.* Lithofacies 1) that accumulated from suspension. A similar mechanism is envisaged for the intercalated terrigenous silty mudstones. The micrograded coarser laminae within the laminated beds record episodic introduction of silt and sand-sized detritus to the water column.

In contrast, the subordinate graded limestones show erosional bases and rare cross-lamination and probably represent the deposits of low-density, mud-rich turbidity currents (*cf.* Davies 1977).

The parallel, laterally persistent nature of bedding and the occurrence of discrete graded beds suggests that the segregation of lime and terrigenous mud is essentially a primary, depositional feature. The origin of such rhythmic interbedding of lime-rich and lime-poor sediment in basinal or deep-water carbonate sequences is poorly understood (Keith & Friedman 1977). Since production of lime sediment during the Early Palaeozoic was restricted to shallow-water settings (James & Mountjoy 1983) it is probable that the limestone-argillite alternation described here results from episodic offshire dispersal of lime sediment from the shallow-water platform within background sedimentation of terrigenous muds. A similar mechanism was invoked for Middle Cambrian argillaceous lime mudstones in Utah (Brady & Keopnick 1979). It is not clear, however, whether the periodicity of lime sediment supply was solely a function of the episodic nature of the dispersal processes (storm currents or density currents; Davies 1977) or was related to variation in the rate of carbonate production (i.e. a seasonal climatic control; Wilson 1969; Williams 1983).

### 6.1.4. Lithofacies 4; Platy, nodular carbonates.

Very thin-bedded nodular carbonates are a characteristic and often spectacular component of the outer shelf-slope association. The facies includes microsparitic limestones (53%), dolomitic limestones (11%), and dolomites (36%). They are commonly bituminous, locally cherty or argillaceous (notably in the Fimbuldal Formation) and despite the thin platy nature of bedding they generally form prominent weathering features

(Fig. 3.22). In some sections they are interbedded with graded or laminated carbonate but more commonly they occur in discrete units, up to 50m thick (Fig. 3.38). This lithofacies is characteristic of the Sydpasset and Fimbuldal Formations (Figs 3.17B & 3.38) and occurs locally in the Aftenstjernesø Formation.

In undolomitized sections, the lithofacies is typified by pale grey microspar sheets and lenses, 2-20mm in thickness (commonly 5-10mm) interbedded with and enveloped by darker, more bituminous microspar (Figs 3.23, 6.11). In the following description and discussion, the pale sheets and lenses are referred to as 'nodules', the dark, laminated carbonate as 'matrix'. The separation of the nodules is commonly 5-10mm but can range from a bituminous stylolitic parting to an interval of dark laminated microspar, 0.2m thick. Brittle deformation of the nodular structure is common and ranges from minor pull-aparts or buckles to extensive brecciation. Fossils were rarely observed in the field, but sponge spicules, trilobites, brachiopods and *Girvanella* tubules were recognized in thin section. Bioclasts are uncompacted within nodules, but are commonly flattened or fractured within matrix zones.

Nodules.

Platy, sheet-like or lenticular nodules are the dominant form (Figs 3.23 & 6.11). In the Sydpasset Formation spherical or oval nodules are common (Fig. 6.12) and often produce a spectacular 'pseudo-conglomerate', particular in deformed brecciated intervals (Fig. 6.16). The spherical, oval forms are typically 5-30mm in diameter, but where associated with fibrous calcite (see below) may be up to 0.2m across (Fig. 3.24). In the Aftenstjernesø Formation tubular or cylindrical


Figure 6.11. Platy nodular limestones (LF.4). The thin nodular sheets pinch out abruptly (A) and are locally fractured (lower centre), pulled apart or brecciated (centre). Sydpasset Formation, locality 10, west Peary Land.

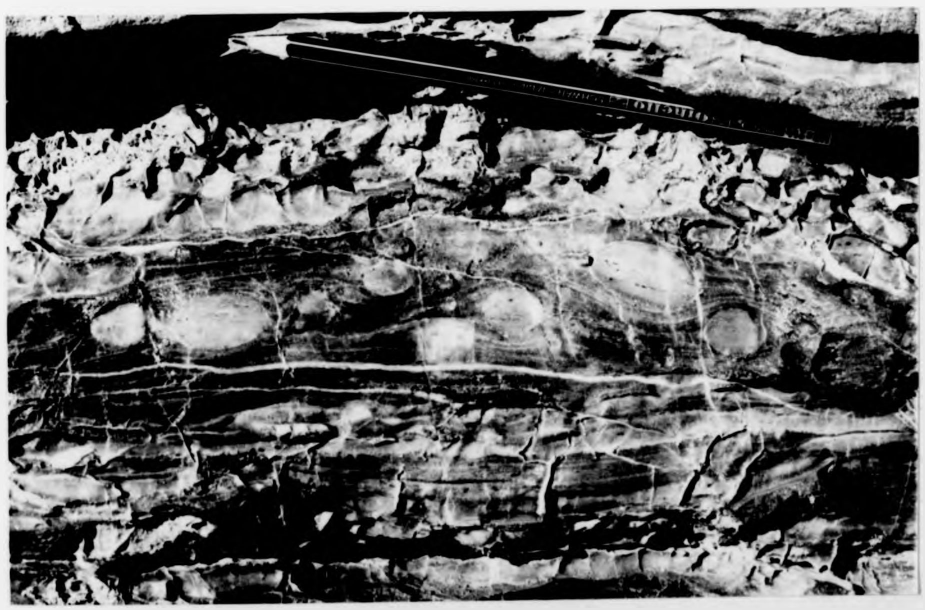

Figure 6.12. Limestone showing oval and spherical nodular forms (LF.4). Note the faint parallel lamination within nodules passing laterally into the well-laminated darker 'matrix'. Warping of matrix lamination suggests early diagenetic, precompactional nodule development. Sydpasset Formation, locality 10, west Peary Land.


Figure 6.11. Platy nodular limestones (LF.4). The thin nodular sheets pinch out abruptly (A) and are locally fractured (lower centre), pulled apart or brecciated (centre). Sydpasset Formation, locality 10, west Peary Land.

Figure 6.12. Limestone showing oval and spherical nodular forms (LF.4). Note the faint parallel lamination within nodules passing laterally into the well-laminated darker 'matrix'. Warping of matrix lamination suggests early diagenetic, precompactional nodule development. Sydpasset Formation, locality 10, west Peary Land.

nodules (5-15mm diameter) occur with their long axes parallel to bedding. They delineate simple, gently winding or straight, unbranched and branched horizontal burrows that are tentatively referred to *Planolites*. Clearly the nodule diameter may vastly exceed the dimensions of the original burrow (e.g. Fig. 6.8) and caution should be exercised in the rigid classification of trace fossils preserved in this fashion.

Nodule-matrix boundaries appear sharp at outcrop (Fig. 6.11) and may be outlined by stylolites, but in thin section they are commonly gradational over 50-150μm (Fig. 6.13). The contact is generally planar or smoothly curved with localised pinch and swell or knobbly irregularities (Figs 3.23 & 6.11). Laterally, platy nodules may be persistent for up to 4m, but they invariably pinch out and are enveloped by the dark matrix. Faint parallel lamination within nodules is defined by bituminous blebs and wisps, or relict micrite clots (Fig. 6.14). In undeformed zones, this lamination can occasionally be traced laterally across nodule-matrix boundaries, and is continuous with the well-developed matrix lamination (Fig. 6.14).

The nodules typically comprise an equigranular polygonal mosaic of clear microspar (10-30μm crystals; Fig. 6.13). Clots of relict micrite (or fine microspar; 5-10μm) display abrupt and gradational boundaries and locally define the diffuse lamination. Some nodules have a finer grained (5-15μm) microspar rim, coarsening inwards to the typical 20-30μm polygonal mosaic.

nodules (5-15mm diameter) occur with their long axes parallel to bedding. They delineate simple, gently winding or straight, unbranched and branched horizontal burrows that are tentatively referred to *Planolites*. Clearly the nodule diameter may vastly exceed the dimensions of the original burrow (e.g. Fig. 6.8) and caution should be exercised in the rigid classification of trace fossils preserved in this fashion.

Nodule-matrix boundaries appear sharp at outcrop (Fig. 6.11) and may be outlined by stylolites, but in thin section they are commonly gradational over 50-150μm (Fig. 6.13). The contact is generally planar or smoothly curved with localised pinch and swell or knobbly irregularities (Figs 3.23 & 6.11). Laterally, platy nodules may be persistent for up to 4m, but they invariably pinch out and are enveloped by the dark matrix. Faint parallel lamination within nodules is defined by bituminous blebs and wisps, or relict micrite clots (Fig. 6.14). In undeformed zones, this lamination can occasionally be traced laterally across nodule-matrix boundaries, and is continuous with the well-developed matrix lamination (Fig. 6.14).

The nodules typically comprise an equigranular polygonal mosaic of clear microspar (10-30μm crystals; Fig. 6.13). Clots of relict micrite (or fine microspar; 5-10μm) display abrupt and gradational boundaries and locally define the diffuse lamination. Some nodules have a finer grained (5-15μm) microspar rim, coarsening inwards to the typical 20-30μm polygonal mosaic.

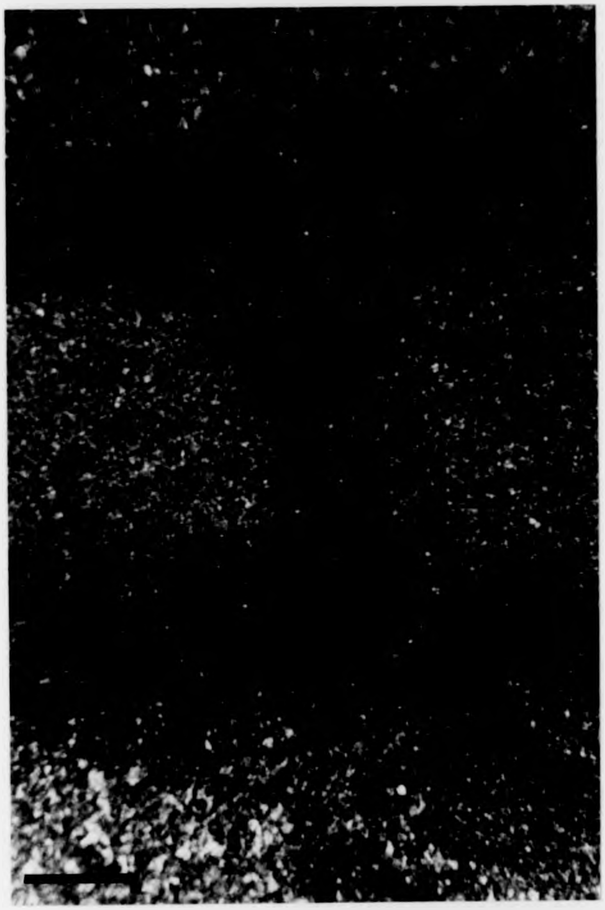

Figure 6.13. Photomicrograph (PPL) of platy nodular limestone (LF.4) showing two stages of nodule growth, the early (pale) phase pulled apart and healed by secondary growth. Note the uniform microspar of the nodule in contrast to the microspar-pseudospar fabric of the matrix. Scale bar = 1mm. GGU 218617, Fimbuldal Formation, locality 4, west Peary Land.

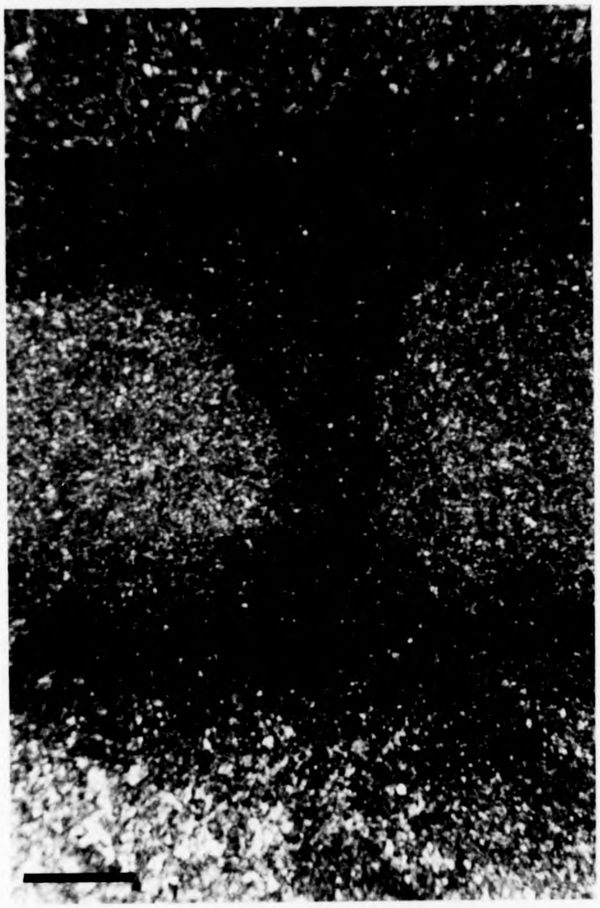

Figure 6.13. Photomicrograph (PPL) of platy nodular limestone (LF.4) showing two stages of nodule growth, the early (pale) phase pulled apart and healed by secondary growth. Note the uniform microspar of the nodule in contrast to the microspar-pseudospar fabric of the matrix. Scale bar = lmm. GGU 218617, Fimbuldal Formation, locality 4, west Peary Land.


Figure 6.14. Polished surface, cut normal to bedding, of platy nodular limestone (LF.4). Faint lamination within the pale nodules is traceable laterally into the well-laminated matrix (e.g. centre left). Light blotchy areas (F) within matrix are coarse fibrous calcite; note the persistence of dark laminae through these areas indicating a post-compactional, replacive origin. Fibrous calcite is mainly restricted to matrix zones, although fibrous calcite at centre left radiates from a pale nodule. Late diagenetic stylolite (S) separates partially dolomitized zone (D) from limestone beneath. Width of view = 6.5cm. GGU 271810, Sydpasset Formation, locality 10, west Peary Land.

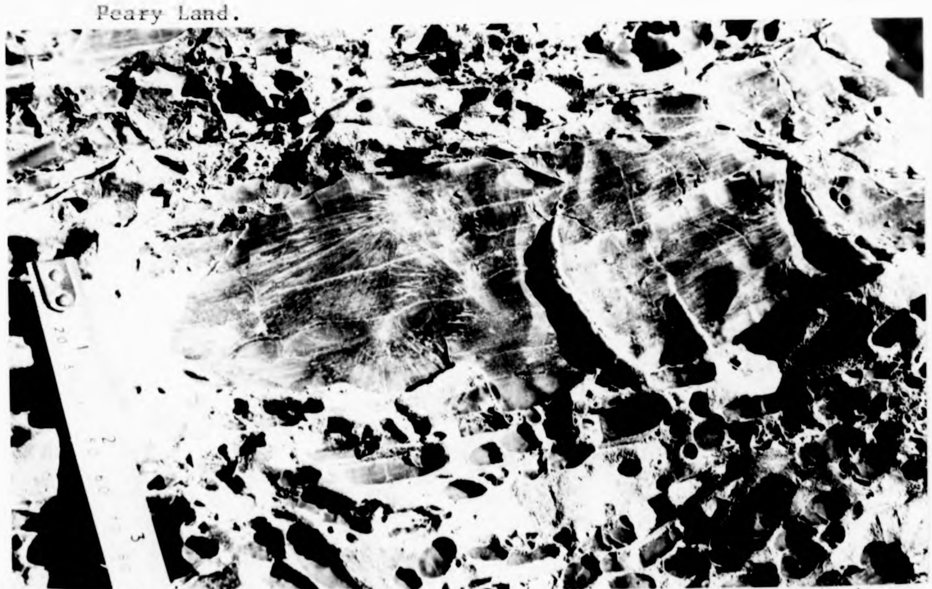

Figure 6.15. Dolomitic nodular limestones (LF.4) (normal to bedding), showing a zone of irregular fibrous calcite development. Weathering picks out the prominent, paler dolomite in the surrounding nodular limestones. Note the preferential dolomitization of matrix and the apparent resistance of nodules and fibrous calcite to replacement. Sydpasset Formation, locality 10, west Peary Land.

Figure 6.14. Polished surface, cut normal to bedding, of platy nodular limestone (LF.4). Faint lamination within the pale nodules is traceable laterally into the well-laminated matrix (e.g. centre left). Light blotchy areas (F) within matrix are coarse fibrous calcite; note the persistence of dark laminae through these areas indicating a post-compactional, replacive origin. Fibrous calcite is mainly restricted to matrix zones, although fibrous calcite at centre left radiates from a pale nodule. Late diagenetic stylolite (S) separates partially dolomitized zone (D) from limestone beneath. Width of view = 6.5cm. GGU 271810, Sydpasset Formation, locality 10, west Peary Land.

Figure 6.15. Dolomitic nodular limestones (LF.4) (normal to bedding), showing a zone of irregular fibrous calcite development. Weathering picks out the prominent, paler dolomite in the surrounding nodular limestones. Note the preferential dolomitization of matrix and the apparent resistance of nodules and fibrous calcite to replacement. Sydpasset Formation, locality 10, west Peary Land.

Matrix.

The dark, grey or grey-brown matrix has a bituminous or argillaceous, microstylolitic lamination which drapes around and in places passes into the pale nodules (Figs 3.23, 6.12 & 6.14). The crystalline fabric is highly variable, ranging from homogeneous pseudospar (50-400μm, generally 50-150μm) to a patchy or sublaminar mosaic of micrite, microspar and pseudospar. Calcite crystals are brown and cloudy, intercrystalline bitumen is common and crystal boundaries are often irregular and sutured. The lamination is mainly defined by intercrystalline organic matter or argillite streaks and wisps, 10-20μm thick and up to 3000μm long, which commonly have an irregular stylolitic form. Less commonly, the lamination is picked out by size variation in the neomorphic crystal fabric.

Fibrous calcite.

In the Sydpasset Formation, this lithofacies contains abundant fibrous calcite that forms spectacular spherical, oval and irregular fan-shaped structures (Figs 3.24, 6.14 & 6.15). The fibrous calcite commonly occurs as stellate fringes radiating from pale microspar nodules; composite concretions are observed locally (Fig. 3.24). Fibrous calcite also forms irregular interfering fans that generally emanate from microspar nodules and radiate out within the dark laminated matrix (Figs 6.14 & 6.15). Although originating at diffuse nodular nuclei (Fig. 6.16), the fibrous spar terminates abruptly at the margin of adjacent nodules and isolated spherical microspar nodules may be totally enveloped in coarse fibrous calcite (Fig. 6.17). The bituminous matrix lamination is faithfully preserved within fibrous calcite rays (Fig. 6.14) indicating a replacive, neomorphic origin. Field observations indicate that individual crystals may be up to 100mm long and 3mm thick; fibres 0.2-1mm x 1-10mm are typical in thin section. Compromise boundaries between fibres

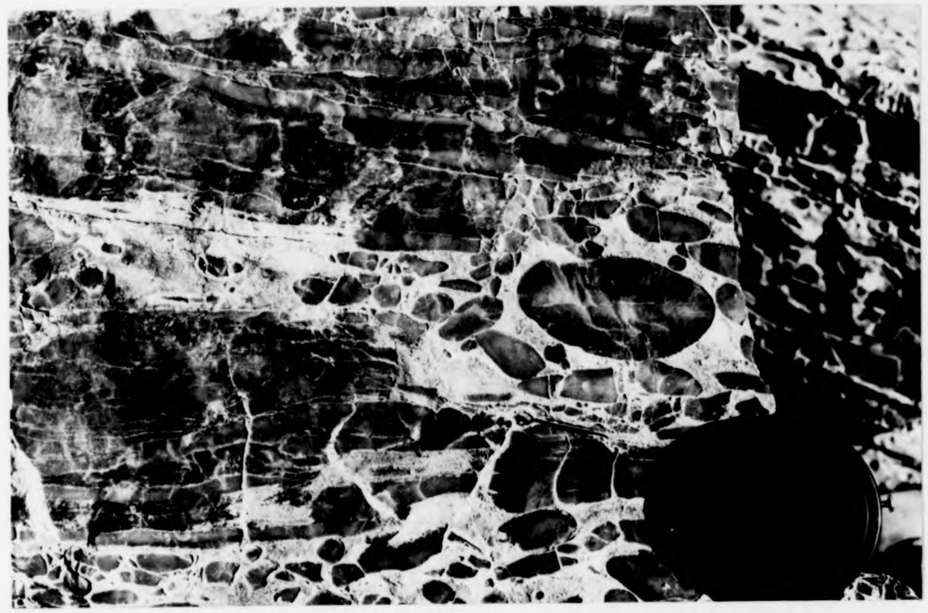

Figure 6.16. Fibrous calcite forming a fringe around an elongate pale nodule (centre right) within an impersistent, discordant brecciated zone, picked out by dolomite (pale). LF,4, Sydpasset Formation, locality 10, west Peary Land.

Figure 6.17. Fibrous calcite emanating from a spherical nodule but enveloping, rather than replacing, adjacent pale nodules (arrowed). LF.4, Sydpasset Formation, locality 1, east Freuchen Land.

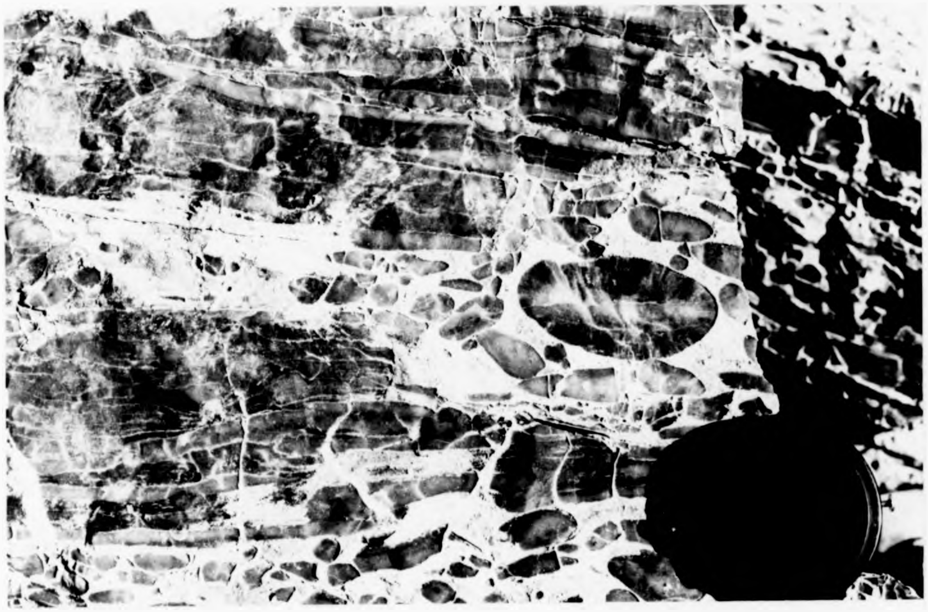

Figure 6.16. Fibrous calcite forming a fringe around an elongate pale nodule (centre right) within an impersistent, discordant brecciated zone, picked out by dolomite (pale). LF,4, Sydpasset Formation, locality 10, west Peary Land.

Figure 6.17. Fibrous calcite emanating from a spherical nodule but enveloping, rather than replacing, adjacent pale nodules (arrowed). LF.4, Sydpasset Formation, locality 1, east Freuchen Land.

are planar or locally irregular where microspar crystals intervene (Fig. 6.18); where individual fibres are separated by a polygonal microspar mosaic, the crystals show triangular cross-sections (Fig. 6.19). A transition is commonly evident from polygonal, equigranular microspar (20-30μm) at the nodule core into the radiating fibrous fringe (Fig. 6.18).

Deformation structures.

A characteristic feature of this lithofacies is the widespread disruption of bedding, ranging from minor fractures to extensive brecciation. A complete gradation is observed from small-scale pull-aparts and buckles involving a few adjacent nodular layers (Figs 6.11 & 6.20) through discrete, thin (0.2-0.15m) brecciated horizons (Figs 6.20 & 6.21) to intensely brecciated intervals with wavy, undulatory bedding (Figs 3.40, 6.22). In all cases the nodules and matrix show a differing response to deformation. The nodules (both microspar and fibrous pseudospar varieties) reacted in a brittle fashion whereas the dark matrix responded in a more ductile, plastic fashion. In pull-aparts and crumples the nodules generally show sharp, angular breaks and the matrix is introduced to fractures from beneath and above (Fig. 6.23). Where displacement is small, lamination within the adjacent matrix may be preserved. On bedding-planes the fractured nodular layers show a superficial resemblance to desiccation cracks (Fig. 6.24). Where brecciation is more intense, the matrix surrounding fragmented nodules is structureless. Where undisturbed strata pass laterally or vertically into a brecciated zone, a sharp contact is commonly observed between the laminated internodular carbonate

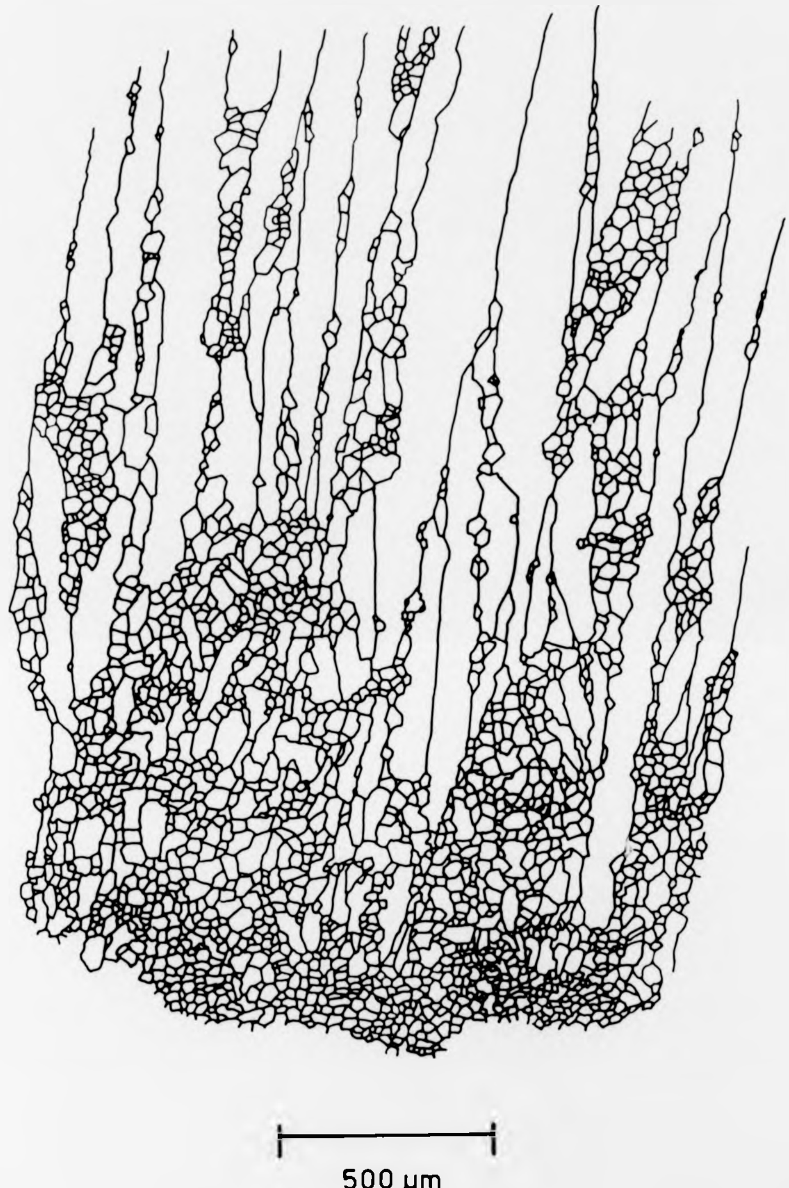


Figure 6.18. Diagram showing the transition from equigranular microspar to coarse fibrous calcite. Drawn from acetate peel. GGU 271807, LF.4, Sydpasset Formation, locality 10, west Peary Land.

Figure 6.19. Photomicrograph (XP) of fibrous calcite (LF.4) showing the triangular cross-sectional form of individual fibres. Scale bar = 1mm. GGU 271807, Sydpasset Formation, locality 10, west Peary Land.

Figure 6.20. Platy nodular limestones (LF.4), normal to bedding, showing extensional fractures and pull-aparts (P), compressional buckles (lower centre) and discrete brecciated horizons (top). Sydpasset Formation, locality 1, east Freuchen Land.

Figure 6.19. Photomicrograph (XP) of fibrous calcite (LF.4) showing the triangular cross-sectional form of individual fibres. Scale bar = 1mm. GGU 271807, Sydpasset Formation, locality 10, west Peary Land.

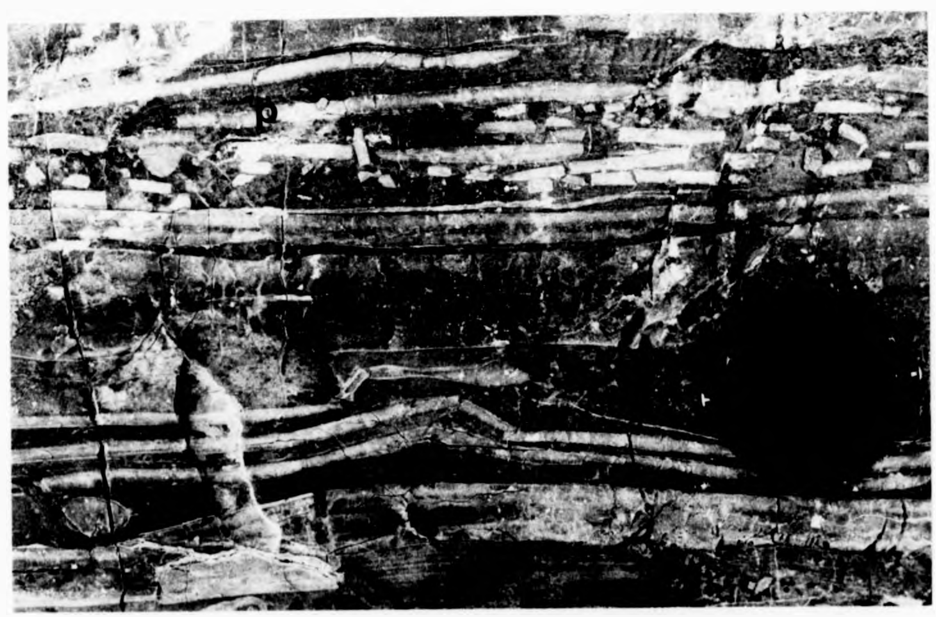

Figure 6.20. Platy nodular limestones (LF.4), normal to bedding, showing extensional fractures and pull-aparts (P), compressional buckles (lower centre) and discrete brecciated horizons (top). Sydpasset Formation, locality 1, east Freuchen Land.

Figure 6.21. Nodular dolomites (LF.4) with a thin brecciated horizon. Note gradational upper boundary indicating an interstratal, sub-surface brecciation process. Aftenstjernesø Formation, locality 19, central Peary Land.

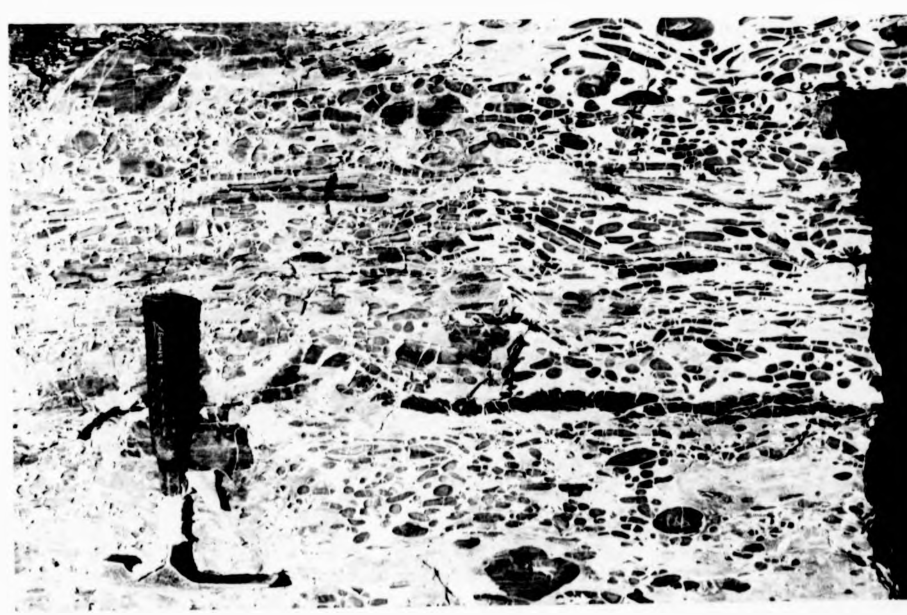

Figure 6.22. Pseudo-conglomeratic appearance of brecciated nodular dolomitic limestones (LF.4). Dolomite is the pale, prominent weathering component. Sydpasset Formation, locality 10, west Peary Land.

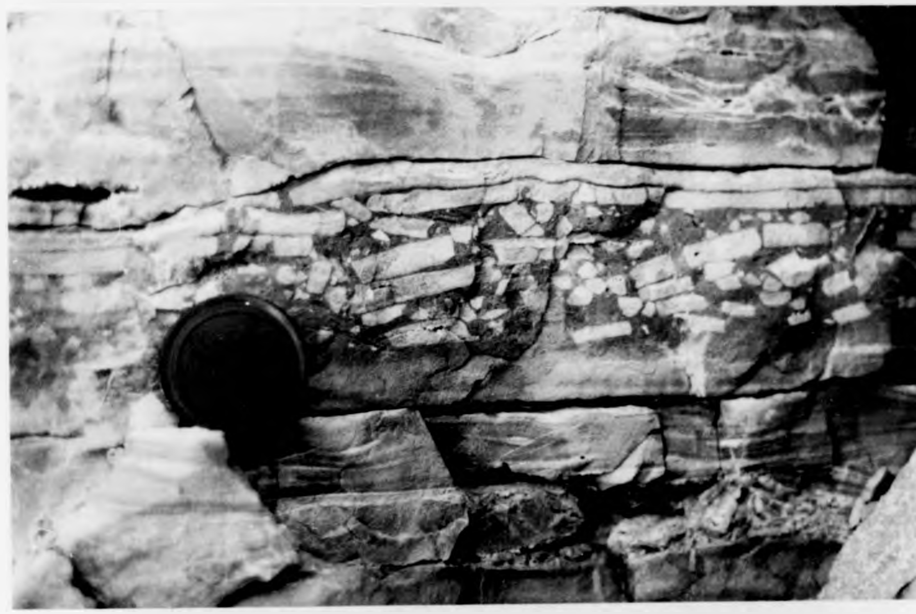

Figure 6.21. Nodular dolomites (LF.4) with a thin brecciated horizon. Note gradational upper boundary indicating an interstratal, sub-surface brecciation process. Aftenstjernesø Formation, locality 19, central Peary Land.

Figure 6.22. Pseudo-conglomeratic appearance of brecciated nodular dolomitic limestones (LF.4). Dolomite is the pale, prominent weathering component. Sydpasset Formation, locality 10, west Peary Land.

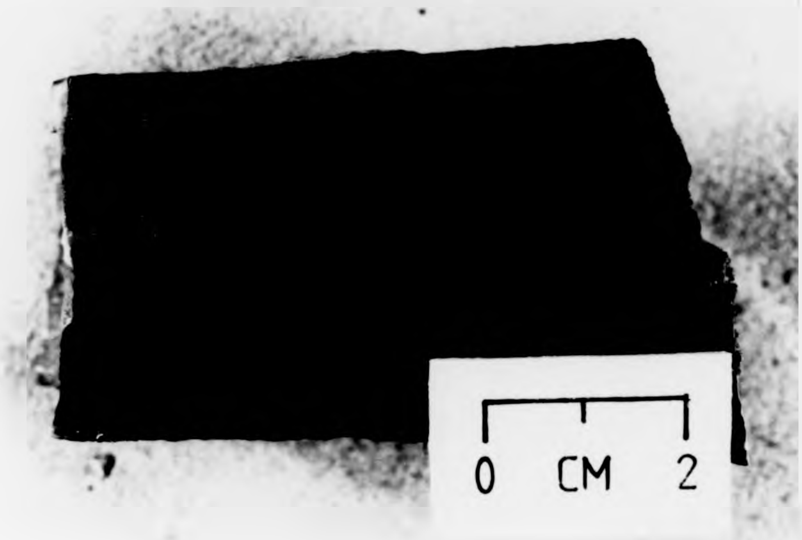


Figure 6.23. Polished surface, cut normal to bedding showing a pulled-apart nodule. Note the angular nature of the fracture, the gap being filled by the surrounding matrix. GGU 218535, LF.4, Sydpasset Formation, locality 1, east Freuchen Land.

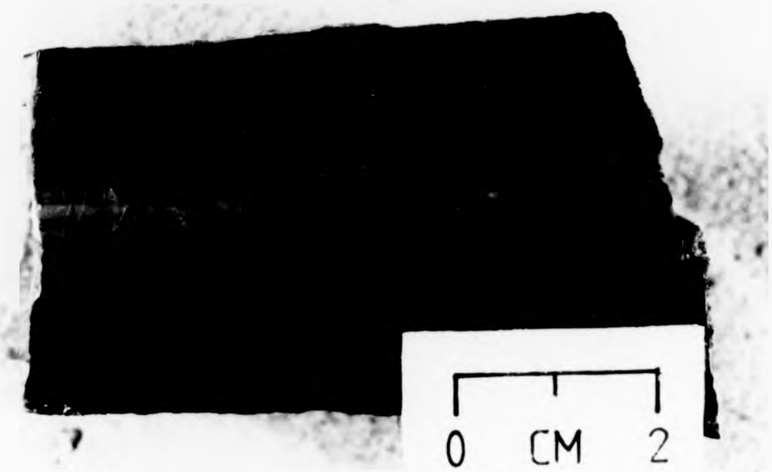


Figure 6.23. Polished surface, cut normal to bedding showing a pulled-apart nodule. Note the angular nature of the fracture, the gap being filled by the surrounding matrix. GGU 218535, LF.4, Sydpasset Formation, locality 1, east Freuchen Land.

Figure 6.24. Bedding plane view of brecciated horizon within platy-nodular dolomites (LF.4). Note occasional elongate nodules (N) which probably nucleated on horizontal burrows. Aftenstjernesø Formation, locality 10, west Peary Land.

Figure 6.25. A discordant brecciated zone. Note the sharp contact (arrowed) between the undeformed, laminated dark matrix and the structureless dark carbonate within the disturbed zone. LF.4, Sydpasset Formation, locality 1, east Freuchen Land.


Figure 6.24. Bedding plane view of brecciated horizon within platy-nodular dolomites (LF.4). Note occasional elongate nodules (N) which probably nucleated on horizontal burrows. Aftenstjernesø Formation, locality 10, west Peary Land.

Figure 6.25. A discordant brecciated zone. Note the sharp contact (arrowed) between the undeformed, laminated dark matrix and the structureless dark carbonate within the disturbed zone. LF.4, Sydpasset Formation, locality 1, east Freuchen Land.

and the structureless, homogeneous matrix of the brecciated zone (Fig. 6.25). Discrete brecciated intervals within parallel-bedded carbonates commonly have gradational upper and lower boundaries (Figs 6.20 & 6.21).

Where disruption is more widespread, horizontal and oblique brecciated zones coalesce and isolate irregular areas of relatively undeformed strata (Figs 6.16 & 6.26). In the Sydpasset Formation islands of undeformed nodular limestone commonly show extensive fibrous calcite development (Figs 6.15 & 6.26); the coarse calcite spar clearly proved resistant to brecciation.

The matrix within brecciated zones is composed mainly of bituminous microspar (or its dolomitized equivalent), but sparry calcite and dolomite cements locally occupy cavities between and beneath brecciated nodules.

Measured sections through this facies commonly demonstrate an upward increase in the intensity of deformation. For example, in the Sydpasset Formation at Ekspedition Bræ and in Løndal (Figs 3.17B & 6.26) the lower levels are dominated by essentially undeformed, parallel-bedded platy nodular limestones with isolated pull-aparts and crumples and rare thin discontinuous brecciated horizons. Upwards, the brecciated intervals become thicker and more frequent and finally coalesce to form a heterogeneous brecciated complex (Figs 6.22 & 6.26).

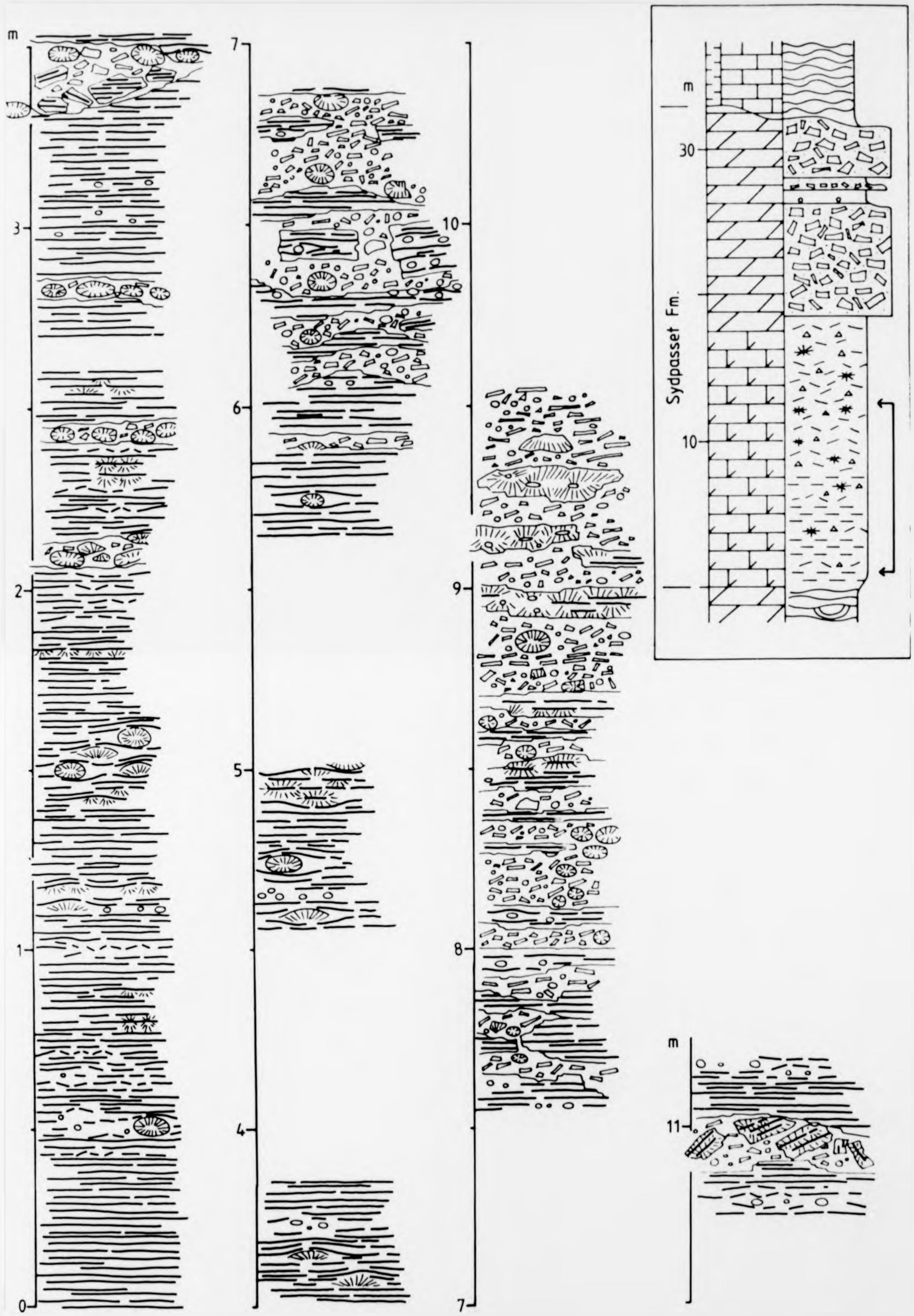


Figure 6.26. Detailed measured section through platy nodular dolomitic limestones of the Sydpasset Formation at locality 10, Løndal, west Peary Land. Inset shows position of detailed section within the formation. Note the upward increase in frequency and intensity of deformation.

Bedding is commonly irregular or wavy in these highly deformed zones and locally discrete 'ruck' folds are recognizable (Fig. 6.27). The contact between the folded beds in Fig. 6.27 and the underlying parallel-bedded strata is sharp and represents a detachment plane. The fold style is parallel and slightly asymmetrical; the amplitude decreases while the wavelength increases up the section until the structure peters out in irregular-bedded, brecciated nodular carbonates.

Dolomite.

Medium to coarse crystalline dolomites assigned to this lithofacies show all the gross lithological characteristics of the platy nodular limestones but the detailed definition of nodule-matrix boundaries is generally obscured. This 'blurring' of structures, together with the common occurrence of partially dolomitized limestones, demonstrates the secondary nature of the dolomite.

Equigranular, anhedral mosaics are typical, with crystal dimensions from 50μm to 400μm (commonly 100-150μm). Nodule cores commonly comprise euhedral to subhedral rhombic dolomite crystals with up to 30% intercrystalline porosity. In places, dolomitized nodules have open vuggy centres.

In partially dolomitized sections, dolomite occurs preferentially within brecciated zones, in the dark internodular matrix and along nodule margins. Microspar nodules and fibrous calcite fans are commonly preserved as calcareous islands within a sea of dolomite (Figs 6.15 & 6.22).

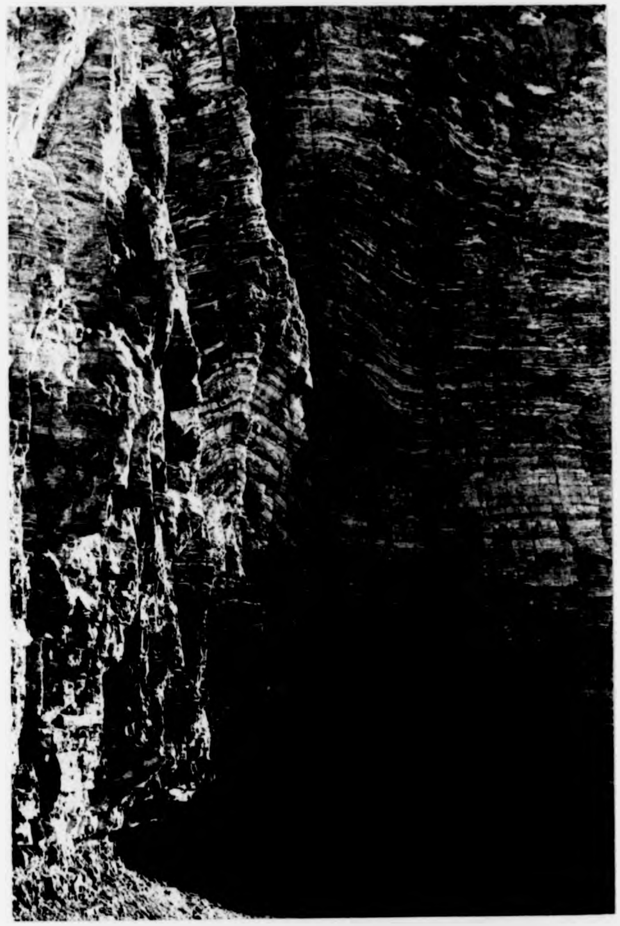

Figure 6.27. Isolated 'ruck' fold within platy nodular dolomitic limestones (LF.4). Note the sharp, horizontal lower boundary of the folded zone (arrowed). Vertical field of view is about 10m. Sydpasset Formation, locality 1, east Freuchen Land.

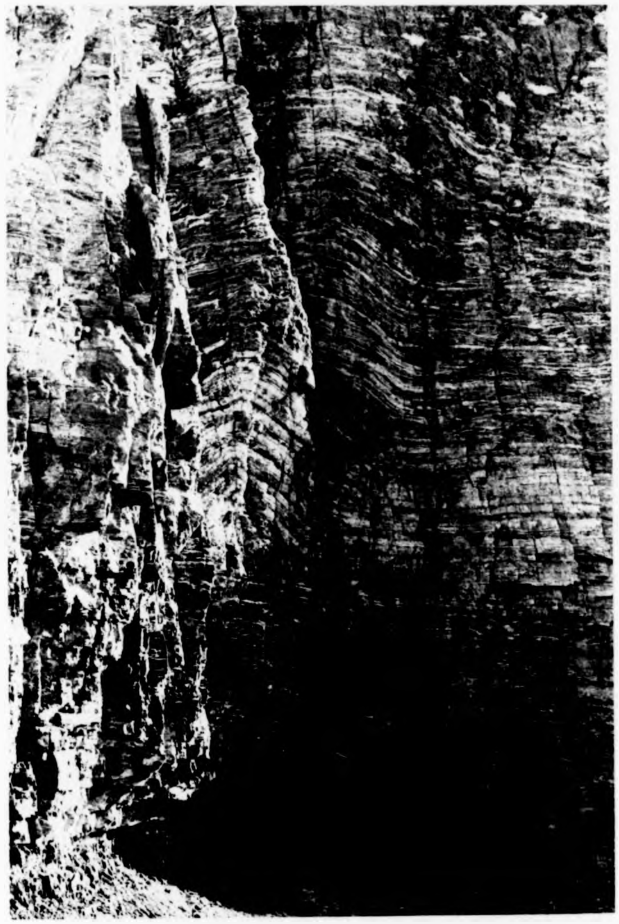

Figure 6.27. Isolated 'ruck' fold within platy nodular dolomitic limestones (LF.4). Note the sharp, horizontal lower boundary of the folded zone (arrowed). Vertical field of view is about 10m. Sydpasset Formation, locality 1, east Freuchen Land.

Clearly the nodular structures were less susceptible to dolomitization, probably due to reduced permeability and increased crystalline stability resulting from early diagenetic lithification and neomorphism. The distribution of dolomite suggests a strong permeability control, perhaps reflecting dolomitization of a differentially lithified sediment. In places, however, partially dolomitized calcite-cemented fractures cut laminated internodular matrix, which suggests that dolomitization postdated at least partial lithification of the matrix carbonate.

Interpretation.

The discontinuous, lenticular nature of the pale nodules and the evidence of primary parallel lamination passing laterally from nodule to matrix indicates that this distinctive structure is the result of secondary diagenetic processes rather than being a primary depositional feature. Nodular limestones are represented in carbonate sequences of all ages and from a range of depositional environemtns (Jenkyns 1974; Noble & Howells 1974; Wilson & Jordan 1983) but closely comparable facies are rare in the literature. Morphologically similar cherty dolomite limestones were illustrated by Hurst (1980, p.47) who assigned them to a starved basinal environment. Silurian carbonates of grossly similar aspect in Arctic Canada were described by Sodero & Hobson (1979) and interpreted as the deposits of restricted inter-island bays.

The following features indicate a primary fine-grained lime-mud dominated sediment:-

1. Relict micrite clots within a microspar-pseudospar neomorphic fabric.

2. Bituminous, argillaceous carbonate showing a diffuse parallel lamination.

3. Gradational vertical transition into bituminous, argillaceous lime mudstones (Lithofacies 1 & 3).

The presence of spicules and trilobite fragments indicates an open marine environment. In the absence of shallow-water indicators or evidence of current action, this lithofacies is considered to represent bituminous, argillaceous lime muds that accumulated from suspension in a low-energy, poorly oxygenated environment, below storm wave-base.

Further insight into the depositional environment is provided by the early diagenetic history of these rocks. The following discussion is based primarily on study of the Sydpasset Formation but is applicable elsewhere. A basic diagenetic sequence is evident (Fig. 6.28) although many of the processes overlapped substantially.

a) Differential lithification of platy, lenticular and spherical nodules.

It is not clear whether this process enhanced a primary compositional or grain size heterogeneity within the fine-grained sediment. The regular banding is suggestive of a varve-like depositional interbedding but no evidence remains of such a primary structure. Dickson & Barber (1976) related the growth of early diagenetic concretions to the distribution of organic matter (see also Raiswell & White 1978); other workers have proposed that differential cementation may be centred on burrows (Fürsich 1973), coarse

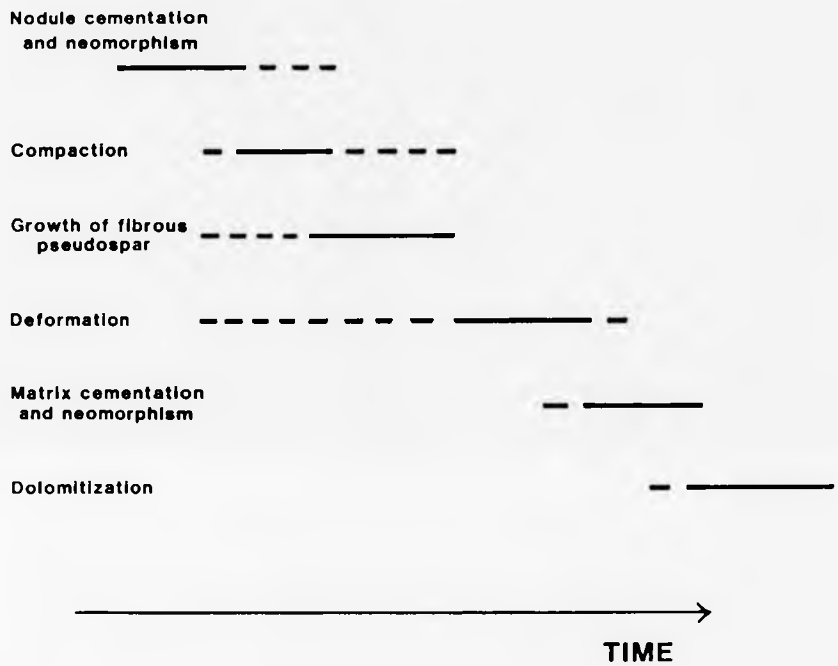


Figure 6.28. Schematic representation of the inferred diagenetic sequence for the platy nodular carbonates (LF.4) of the Sydnasset Formation.

skeletal or intraclastic calcite grains (Jenkyns 1974). The latter is unlikely to be an important factor here as allochems are rare. Similarly, nucleation of nodules around burrows may be locally important but is not generally applicable. These rocks are commonly bituminous, however, and the distribution of organic matter may have been an important factor during early diagenesis. Preferential cementation around organic-rich laminae or clots would result in platy spheroidal and lenticular nodules.

Alternatively, the nodular structure may reflect a primary alternation of lime-rich and lime-poor laminae - the result of episodic supply of lime sediment to the water column. Preferential cementation of lime mud-rich laminae would produce persistent sheets, isolated lenses or spherical nodules, depending on the spacing of nucleation sites.

b) Compaction and growth of radial fibrous spar.

Matrix lamination passes laterally into and is deflected around nodules, indicating significant volume reduction. The relative importance of compaction and pressure solution in producing such features has provoked much debate (see Garrison & Kennedy 1977; Wanless 1979, 1982; Pratt 1982). The persistence of laminae across nodule-matrix boundaries suggests that the matrix lamination, though enhanced and modified, is a primary feature and is not solely the result of concentration of insoluble components due to pressure solution, as suggested by Wanless (1982). The plastic response of the laminated matrix to deformation suggests a poorly lithified or unlithified sediment, particularly where deformation results in the complete destruction of lamination (Fig. 6.25). Such a plastic, poorly lithified sediment is unlikely to undergo appreciable pressure solution. The volume reduction and enhanced lamination in the inter-nodular matrix is considered to be mainly the result of simple compaction. Organic-rich seams have been produced experimentally by the compaction of lithified muddy carbonate sediment (Shinn *et al.* 1977). Further modification and enhancement of the lamination by pressure solution occurred at a later stage in diagenesis.

The fibrous calcite in the Sydpasset Formation compares favourably with the stellate masses of radial fibrous spar described by Bathurst (1971) from the Dinantian of Britain. He recognized a transition from an equigranular microspar core of decimicron size into radially arranged, elongate pseudospar crystals. These structures were considered to be clearly replacive since they "transect the once continuous fabric of carbonate detritus" (Bathurst 1971, p. 494). Preservation of lamination within the fibrous calcite described here indicates a similar neomorphic origin. According to Bathurst, neomorphism within a microspar clot reaches a critical stage when radial outward growth of marginal microspar crystals at the expense of the surrounding carbonate is favoured over lateral enlargement at the expense of adjacent microspar crystals. This results ultimately in radially arranged pseudospar crystals that taper towards the microspar core (Fig. 6.18). It is interesting to note that although calcite fibres radiate from microspar nuclei, further growth is inhibited by the impingement of adjacent pale nodules (Fig. 6.17). Thus, the most spectacular fibrous structures occur in horizons with relatively few pale nodules and, conversely, fibrous calcite is of minor importance in intervals of extensive platy nodule development. This supports the suggestion by Bathurst (1971) that neomorphism proceeds by cannibalization of mineralogically heterogeneous, unstable carbonate crystals and ceases when stable neomorphic crystals impinge to form a continuous mosaic. Hence the degree of neomorphic enlargement possible, given optimum conditions, is dependant on the density of nucleation sites.

The fibrous calcite commonly overgrows the compacted, laminated matrix, indicating post-compactional growth. Locally, however, features indicating pre- and syn-compactional growth are observed and it appears likely that the processes of nodule lithification, neomorphism and compaction overlapped substantially, both within any one area and vertically and laterally within the sediment column.

c) Deformation.

The complete spectrum of structures from isolated pull-aparts to extensively brecciated carbonate indicates that all these features are the result of common process. The gradational boundaries and local diachroneity of breccia horizons argues for a subsurface interstratal process and the contrasting behaviour of nodules and matrix suggests that deformation occurred during early diagenesis when much of the internodular carbonate was poorly lithified or unlithified. Indeed in places pull-aparts are healed by further nodule growth (Fig. 6.13) and localized boudinage and folding of nodules indicates a semi-plastic state. Thus, in some areas, deformation occurred prior to complete lithification of the nodular component.

Subsurface interstratal fracturing and brecciation is generally attributed to solution of a soluble component (evaporite) with resultant collapse and brecciation of adjacent strata (e.g. Goldstein & Collins 1984). In the absence of relict evaporites or evidence of the former presence of evaporite minerals (e.g. Folk & Pittman 1971) such a mechanism is considered unlikely, particularly in the light of common evidence of lateral movement rather than vertical foundering. Lateral movement is particularly well illustrated by the small-scale features - fractures, pull-aparts and buckles. Similar pull-aparts in Cambrian slope carbonates of Virginia, U.S.A. were interpreted as tension cracks due to creep on the sea bottom, possibly related to downslope movement (Pfeil & Read 1980; see also Keith & Friedman 1977). Following this reasoning, the formation of thin brecciated horizons with gradational boundaries is readily explained by lateral slip along a discrete horizon. Thin (3-5cm) breccia beds with gradational margins were described by Reinhardt (1977) from the Appalachians. He interpreted them as 'intraformational slump breccias' but did not elaborate further; a similar origin is probable.

The pervasively brecciated zones with irregular wavy bedding are conceptually more difficult but probably record a protracted period of minor interstratal slip along closely spaced horizons resulting in almost complete destruction of the parallel nodular bedding. Lateral movement is locally demonstrated by discrete 'ruck' folds where the brecciated, folded strata slipped along a basal plane of décollement. The depth below the sediment surface at which interstratal creep and sliding occurred is generally unknown although in the example illustrated in Fig. 6.27 slippage occurred under at least 10m of sediment. In other facies similar structures can be shown to have formed within the upper 1-2m of the differentially lithified sediment (see Lithofacies 5). At greater depths below the sediment surface, compaction of differentially lithified carbonate may have resulted in high pore-fluid pressures between impermeable nodular sheets and contributed to loss of cohesion and ultimate failure.

Summary.

To summarize, this lithofacies represents argillaceous bituminous lime muds that accumulated from suspension in a poorly oxygenated marine environment below storm wave base. Sedimentation rates were low, as indicated by the ubiquitous evidence of early diagenetic nodular cementation and extensive neomorphism (Bathurst 1971; Müller & Fabricus 1974; Noble & Howells 1974; Mullins *et al.* 1980). Interstratal creep and sliding reflect deposition on an unstable slope.

### 6.1.5 Lithofacies 5; Thin-bedded skeletal carbonates.

This lithofacies includes a wide variety of thin- to medium-bedded, mid-dark grey carbonates (lime wackestones, packstones, grainstones and equivalent dolomites) that are grouped together on their gross apsect, common association and ubiquitous skeletal content. Limestones and dolomites are equally represented and the facies is widespread through both stratigraphic groups forming units up to 90m thick. Wavy-bedded skeletal wackestones dominate but in places they are interbedded with laminated or cross-stratified, thin-bedded skeletal grainstones and packstones.

The skeletal pelleted wackestones, and equivalent medium to fine crystalline dolomites, are dark grey and commonly argillaceous. Bedding is generally thin (0.01-0.05m), wavy, irregular or lumpy, particularly in argillaceous sequences where silty terrigenous mudstone partings and discontinuous wisps are common (Fig. 6.29). In argillite-poor intervals, bedding is less pronounced, resulting in structureless or faintly mottled carbonate with impersistent stylolitic bedding planes. Bioturbation is ubiquitous in both limestones and dolomites. Mottling locally delineates horizontal unbranched straight or gently curving burrows (*Planolites*) and '*Diplichnites*' was recorded from the upper beds of the Holm Dal Formation. A homogenized, churned and faintly mottled structure is evident on polished slabs and in thin section; primary lamination is rarely observed. Peloids and bioclasts form up to 50% of the rock, supported in a fine-grained micritic matrix that is locally neomorphosed to microspar.

Lime packstones and grainstones, and equivalent medium crystalline dolomites, generally form discontinuous laminae and thin (0.01-0.03m) lenticular beds. Thicker (0.05-0.1m) grainstone beds occur locally and have sharp, erosional bases and show ripple cross-lamination or small-scale trough cross-bedding (Fig. 6.30). Skeletal grains and peloids dominate (48-95% of allochems; Fig. 6.31); the remainder comprises in-

Figure 6.29. Wavy-bedded, argillaceous lime mudstones and skeletal wackestones (LF.5). Hammer (lower centre) for scale. Ekspedition Bræ Formation, locality 10, west Peary Land.

Figure 6.30. Skeletal dolomites (LF.5) showing parallel lamination and small-scale cross-bedding. Sydpasset Formation, locality 12, central Peary Land.

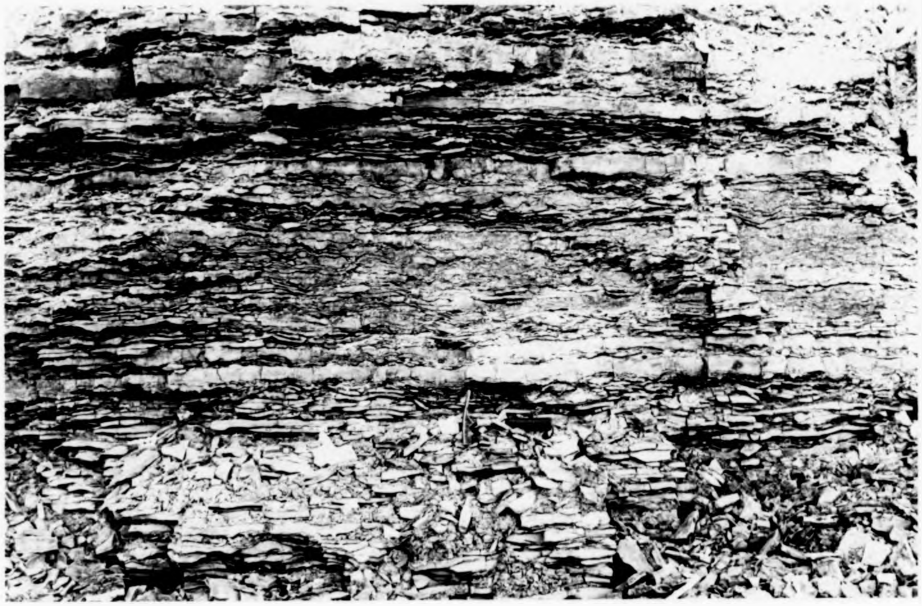

Figure 6.29. Wavy-bedded, argillaceous lime mudstones and skeletal wackestones (LF.5). Hammer (lower centre) for scale. Ekspedition Bræ Formation, locality 10, west Peary Land.

Figure 6.30. Skeletal dolomites (LF.5) showing parallel lamination and small-scale cross-bedding. Sydpasset Formation, locality 12, central Peary Land.

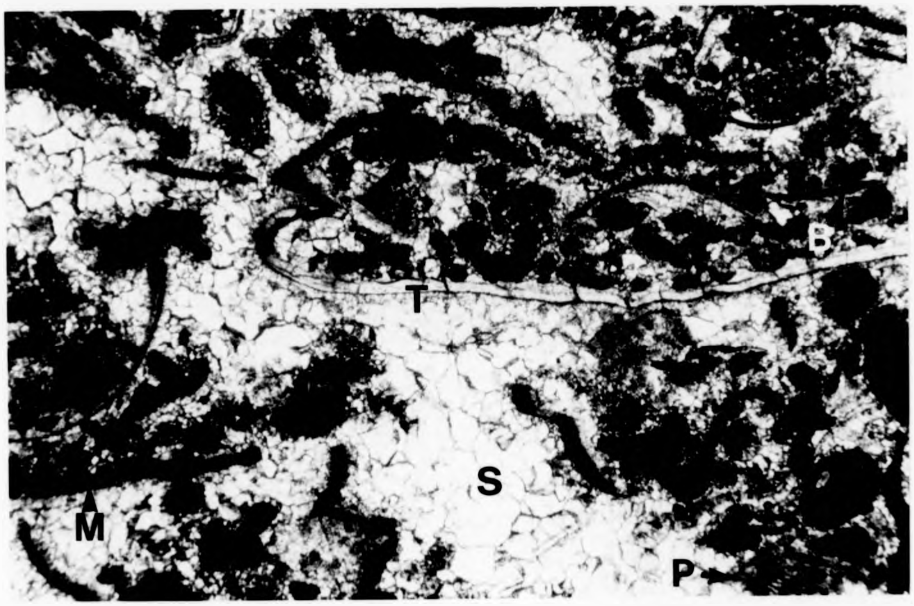


Figure 6.31. Photomicrograph (PPL) of peloidal, skeletal packstone (LF.5) composed mainly of dark micritic peloids, micritized skeletal grains (M), phosphatic brachiopod (B), pelmatozoan (P), and trilobite (T) grains. Note cement fringe on skeletal grains (e.g. trilobite T) and coarse blocky spar cement (S). Scale bar = 1mm. GGU 218592, Ekspedition Bræ Formation, locality 2, west Peary Land.

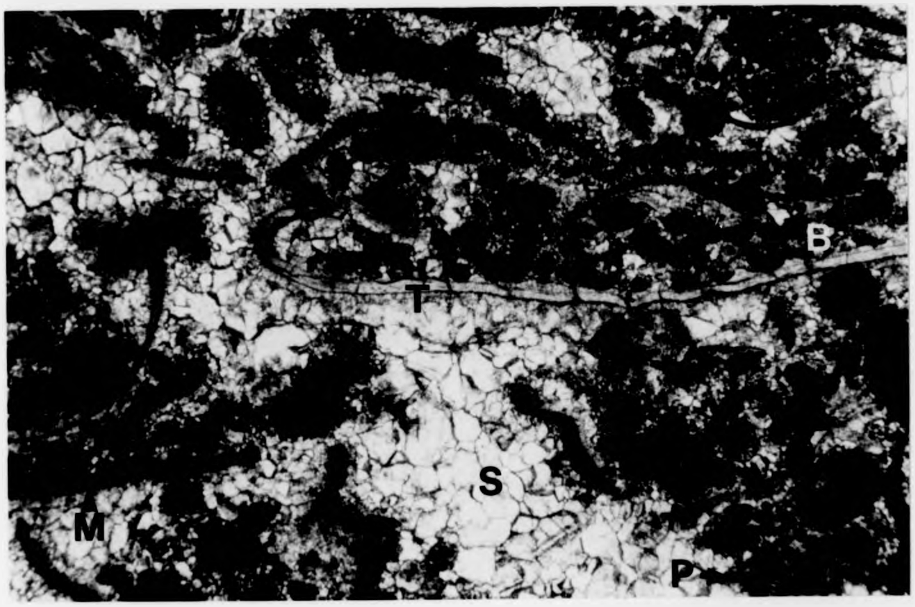


Figure 6.31. Photomicrograph (PPL) of peloidal, skeletal packstone (LF.5) composed mainly of dark micritic peloids, micritized skeletal grains (M), phosphatic brachiopod (B), pelmatozoan (P), and trilobite (T) grains. Note cement fringe on skeletal grains (e.g. trilobite T) and coarse blocky spar cement (S). Scale bar = 1mm. GGU 218592, Ekspedition Bræ Formation, locality 2, west Peary Land.

traclasts, quartz sand and silt, interstitial lime mud and rare ooids.

The fauna is rich and diverse. Trilobites, brachiopods, sponge spicules and varied molluscs are abundant; archaeocyathids and *Salterella* are important in some Lower Cambrian exposures. *Girvanella* tubules occur in a few samples. In wackestone beds, skeletal grains are disarticulated though not abraded, and are randomly oriented relative to bedding. Bioclasts in skeletal packstone and grainstone beds are fragmented and commonly worn.

In a few sections through the Sydpasset, Henson Gletscher and Paralleldal Formations, thin-bedded skeletal dolomites show a secondary nodular banding (Fig. 6.32). Locally these rocks are brecciated (Fig. 6.33) or show pull-aparts, boudinage and microfaults (Fig. 6.32). The pale nodular bands are fractured or stretched whereas the internodular component clearly acted in a ductile fashion, filling fractures and breccia interstices. Such breccias (0.01-0.15m thick) are laterally impersistent and have gradational boundaries; they are strongly reminiscent of the interstratal creep breccias of Lithofacies 4.

In the Paralleldal Formation at its type section deformed nodular dolomites are draped and overlain by undeformed, parallel-bedded carbonates (Fig. 6.32). No evidence of subaerial exposure is evident at this level and submarine differential lithification and deformation is indicated at depths of less than 2m beneath the sediment surface.

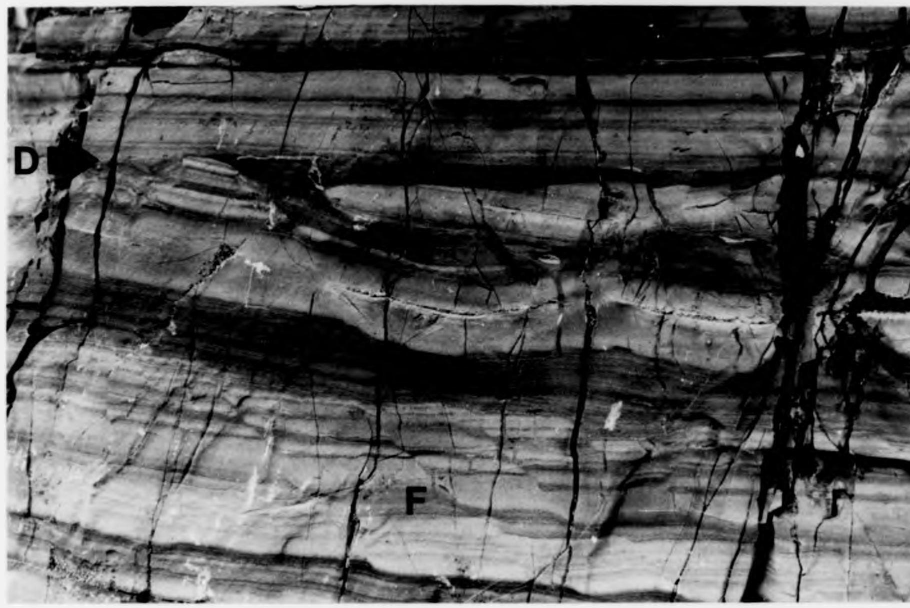


Figure 6.32. Synsedimentary deformation of nodular banding within laminated skeletal dolomites (LF.5). Note extensional pull-aparts (P) and normal microfaults (F); internodular carbonate fills pull-aparts indicating differential lithification. Deformed zone draped (D) by parallel bedded dolomite indicating that early diagenetic, differential lithification and deformation occurred close to the sediment surface. Paralleldal Formation, locality 15, central Peary Land.

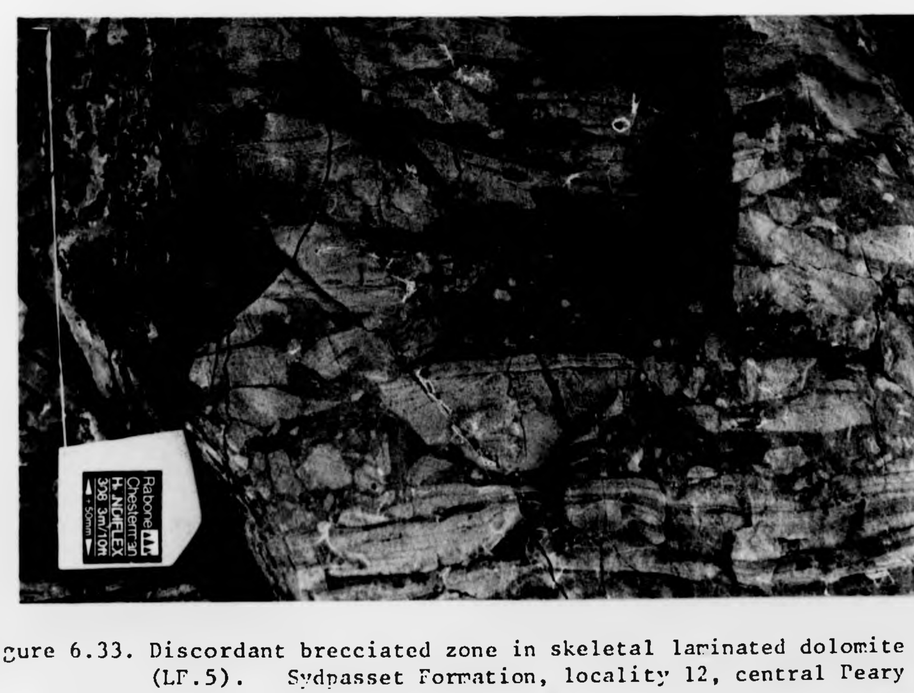

Figure 6.33. Discordant brecciated zone in skeletal laminated dolomite (LF.5). Sydpasset Formation, locality 12, central Peary Land.


Figure 6.32. Synsedimentary deformation of nodular banding within laminated skeletal dolomites (LF.5). Note extensional pull-aparts (P) and normal microfaults (F); internodular carbonate fills pull-aparts indicating differential lithification. Deformed zone draped (D) by parallel bedded dolomite indicating that early diagenetic, differential lithification and deformation occurred close to the sediment surface. Paralleldal Formation, locality 15, central Peary Land.

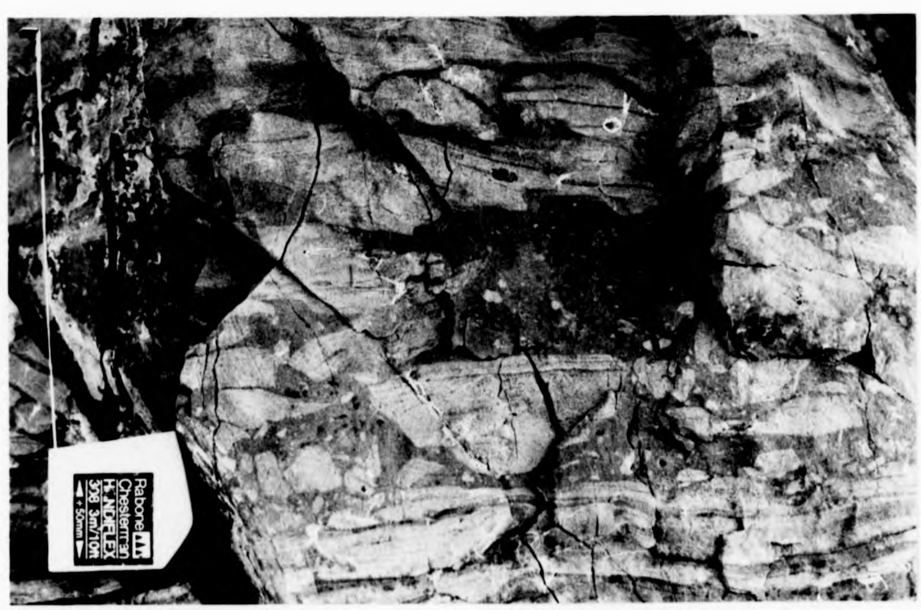


Figure 6.33. Discordant brecciated zone in skeletal laminated dolomite (LF.5). Sydpasset Formation, locality 12, central Peary Land.

Interpretation.

The rich, diverse fauna and intense bioturbation indicate deposition in an open marine, well-oxygenated environment (Wilson 1975; Byers 1977). The wavy-bedded skeletal wackestones that dominate the lithofacies are comparable to the idealized 'open shelf' facies of Wilson (1975). Accumulation of carbonate and siliciclastic mud suggests a non-turbulent, subtidal environment below normal wave base (Bowman 1979; Read 1980). Primary depositional structures were obliterated by bioturbation; early lithification combined with subsequent differential compaction and pressure solution produced the wavy, irregular bedding that is so typical of subtidal open shelf carbonates (Jones *et al.* 1979; Wilson & Jordan 1983). In wackestone-dominated successions, occasional thin skeletal packstone and grainstone interbeds record rare high energy conditions probably due to major storm events. Deposition at or above storm wave base is indicated (*cf.* Jones & Dixon 1976).

This interpretation provides little restriction on the water depth during deposition. Comparable lithologies have been assigned to shallow subtidal platform (Bowman 1979), deep ramp (Read 1980) deep shelf (Lohmann 1976) and slope environments (Brady & Koepnick 1979); Wilson (1975, p.25) suggested that this facies may accumulate in tens or hundreds of metres of water.

Intervals dominated by laminated and cross-bedded skeletal grainstones and packstones record higher energy levels and suggest deposition at or above normal wave base.

Syn-sedimentary microfaults, pull-aparts and boudinage are attributed to downslope creep of differentially lithified sediments. Discontinuous brecciated horizons are interpreted as the result of minor interstratal sliding (*cf.* Lithofacies 4). Comparable impersistent interstratal breccias in the Lower Palaeozoic succession of Newfoundland were figured by Cook & Mullins (Fig. 23, 1983).

6.1.6. Lithofacies 6; Phosphoritic, glauconitic skeletal carbonates.

Glauconite- and phosphorite-bearing carbonates are best developed within the basal unit of the Brønlund Fjord Group; this interval is assigned to Association A, the incipient ramp, and has been described earlier (5.2.1.). The lithofacies also occurs as thin, mainly pale-weathering units, 0.1-1.3m thick) within fine-grained, mud-dominated outer shelf sequences. Two distinct occurrences are recognized.

a) Thin, isolated phosphorite horizons.

Two such horizons were located within thin-bedded, argillaceous lime mudstone sequences of the Ekspedition Bræ and Holm Dal Formations. The latter example is poorly exposed but is common in float and scree blocks.

The phosphoritic horizon in the Ekspedition Bræ Formation comprises a laterally persistent bed, 0.07-0.1m thick, composed of laminated and bioturbated lime mudstone with discontinuous laminae and lenses of skeletal lime wackestone, packstone and grainstone (Fig. 6.34). Black

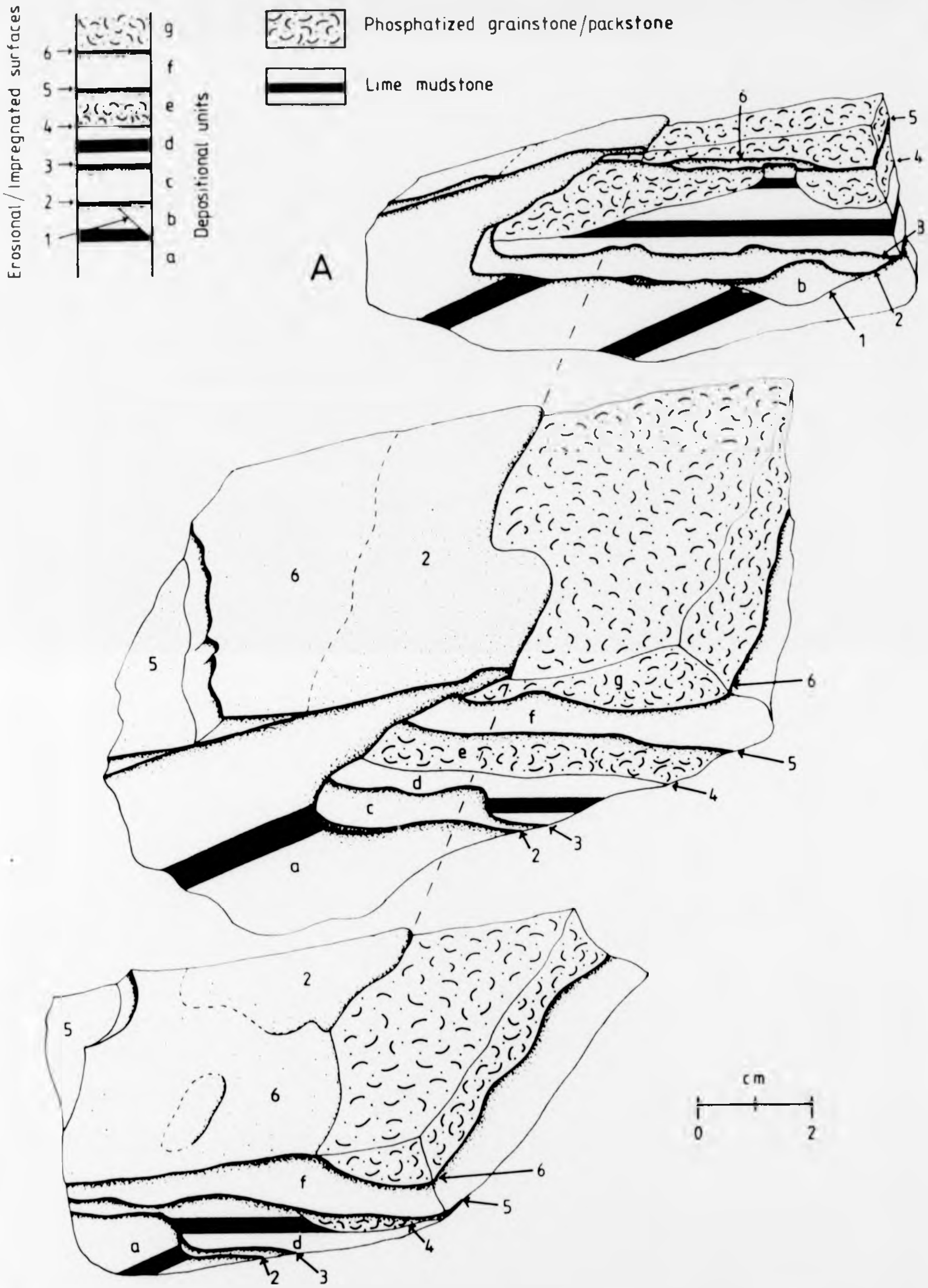


Figure 6.34. Diagram showing the complex three-dimensional morphology of a multiple phosphorite horizon (LF.6). Stipple represents phosphorite. Note that minor slumping and buckling of the basal interval (units a,b capped by phosphorite surface 2) preceded deposition and impregnation of succeeding units. Face A shown in Fig. 6.36. GGU 218546, Ekspedition Bræ Formation, locality 1, east Freuchen Land.

or dark brown phosphorite occurs as a complex, anastamosing array of thin impregnated surfaces, 0.2-1.5mm thick; the succession of phosphoritized surfaces and limestone facies reflects a complex history of deposition, winnowing, erosion and phosphorite impregnation. The phosphorite surfaces have diffuse gradational bases and sharp irregular tops (Fig. 6.35); overhangs, pedestals and scour hollows are common and individual surfaces show a relief of up to 0.05m. The irregularity commonly reflects differential erosion but some overhangs and ridges are the result of minor buckling and fracture of the phosphorite skin (Figs 6.34 & 6.36).

Skeletal grainstones and packstones form lenses and impersistent laminae that generally occupy depressions and overlie scoured, impregnated surfaces. Worn skeletal grains (trilobite, brachiopod and pelmatozoan fragments), peloids and intraclasts (locally with *Girvanella*) are commonly replaced partially or wholly by structureless brown phosphorite and some grains show finely laminated, accretionary phosphorite coatings (Fig. 6.37). The packstones and grainstones are cemented by blocky calcite spar; locally a fine inclusion pattern within this cement preserves the outline of an early botryoidal cement fringe, 50-150μm thick (Fig. 6.38). The gross morphology of this pseudomorphed early cement is similar to the submarine aragonite cements described by Ginsburg & James (1976; see also James & Ginsburg 1979) from Holocene reefs in Belize.

A detailed study of this phosphoritic interval reveals a complex history. In the sample depicted in Fig. 6.34, six erosion surfaces are present, four of which show phosphorite impregnation. The phosphorite occurs preferentially within lime mudstone and in partially replaced


Figure 6.35. Photomicrograph (PPL) of phosphorite surfaces (LF.6; surfaces 2 and 3 on Fig. 6.34). Bioturbated lime mudstone or peloidal wackestone darkens upwards, with progressive phosphorite replacement, to the sharp irregular phosphorite surface. Note the coalescence of individual phosphorite crusts (A,B,C) on the 'high'. Scale bar = 1mm. GGU 218546, Ekspedition Bræ Formation, locality 1, east Freuchen Land.

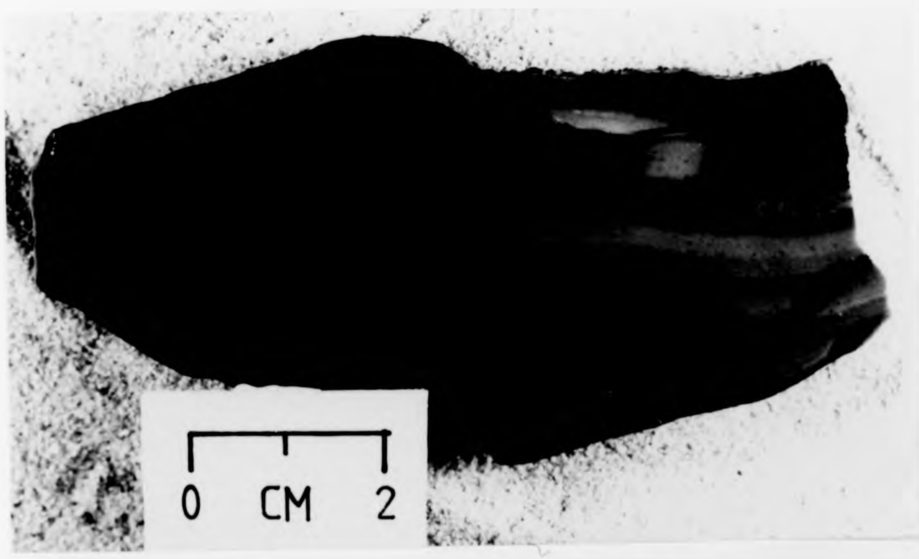


Figure 6.36. Polished surface, cut normal to bedding, showing irregular phosphoritized surfaces. Pale, banded sediment = weakly bioturbated lime mudstone; dark granular sediment = phosphoritic grainstone, packstone and wackestone. Surfaces 1-6, see Fig. 6.34. GGU 218546, Ekspedition Bræ Formation, locality 1, east Freuchen Land.


Figure 6.35. Photomicrograph (PPL) of phosphorite surfaces (LF.6; surfaces 2 and 3 on Fig. 6.34). Bioturbated lime mudstone or peloidal wackestone darkens upwards, with progressive phosphorite replacement, to the sharp irregular phosphorite surface. Note the coalescence of individual phosphorite crusts (A,B,C) on the 'high'. Scale bar = 1mm. GGU 218546, Ekspedition Bræ Formation, locality 1, east Freuchen Land.


Figure 6.36. Polished surface, cut normal to bedding, showing irregular phosphoritized surfaces. Pale, banded sediment = weakly bioturbated lime mudstone; dark granular sediment = phosphoritic grainstone, packstone and wackestone. Surfaces 1-6, see Fig. 6.34. GGU 218546, Ekspedition Bræ Formation, locality 1, east Freuchen Land.

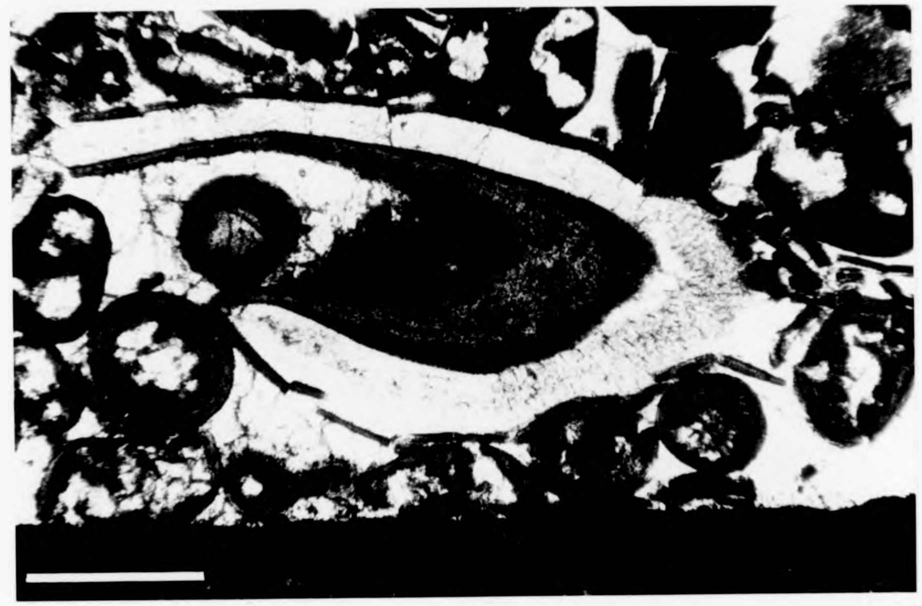

Figure 6.37. Photomicrograph (PPL) of phosphoritic skeletal, ooid grainstone (LF.6) resting on a phosphoritized lime mudstone surface (Fig. 6.34, unit g, surface 6). Large phosphorite-rimmed trilobite fragment occupies centre of view, in contact with structureless dark phosphorite pellets (upper right) and phosphorite ooids showing well-developed concentric structure. Note evidence of compaction against the phosphorite surface. Scale bar = 0.5mm. GGU 218546, Ekspedition Bræ Formation, locality 1, east Freuchen Land.

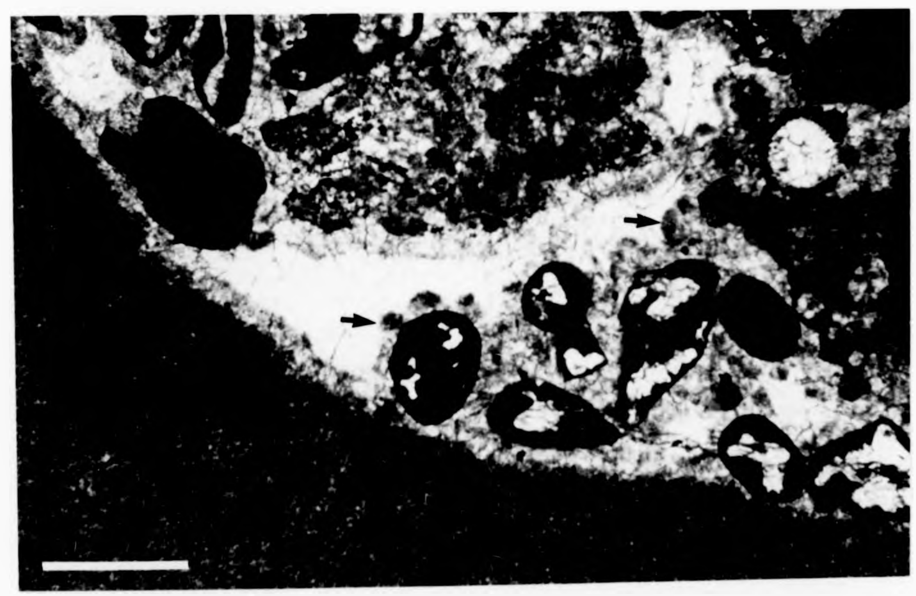

Figure 6.38. Photomicrograph (PPL) of phosphoritic peloidal intraclastic grainstone overlying weakly impregnated lime mudstone (LF.6; Fig 6.34, unit e, surface 4). Note the pseudomorphed early cement fringe (arrowed) showing a distinctive botryoidal form. Scale bar = 0.5mm. GGU 218546, Ekspedition Bræ Formation, locality 1, east Freuchen Land.

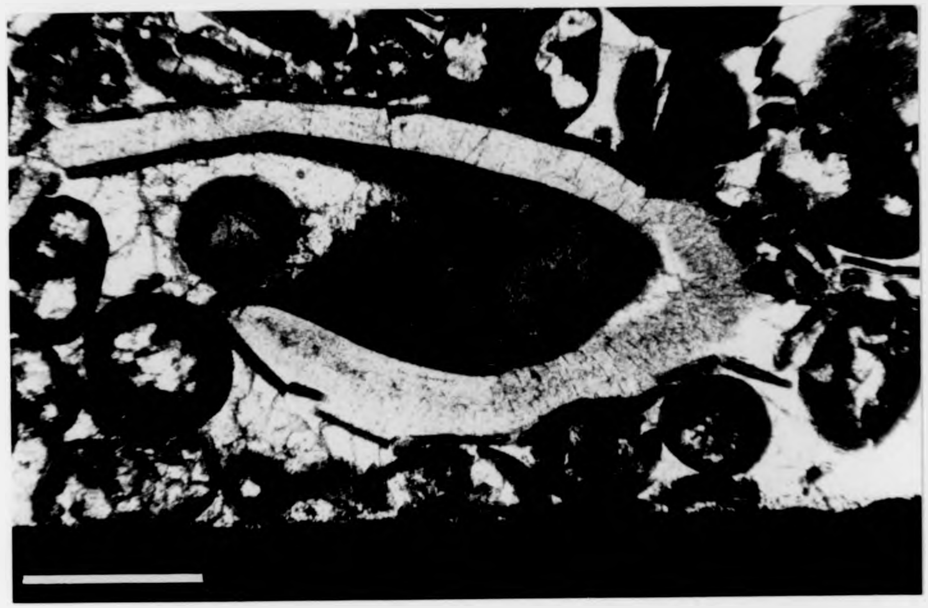

Figure 6.37. Photomicrograph (PPL) of phosphoritic skeletal, ooid grainstone (LF.6) resting on a phosphoritized lime mudstone surface (Fig. 6.34, unit g, surface 6). Large phosphorite-rimmed trilobite fragment occupies centre of view, in contact with structureless dark phosphorite pellets (upper right) and phosphorite ooids showing well-developed concentric structure. Note evidence of compaction against the phosphorite surface. Scale bar = 0.5mm. GGU 218546, Ekspedition Bræ Formation, locality 1, east Freuchen Land.

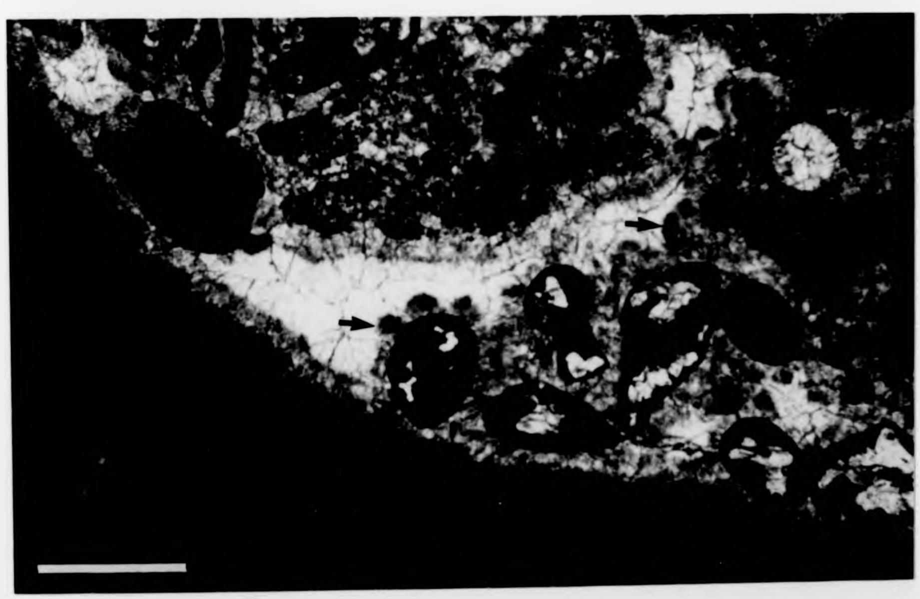

Figure 6.38. Photomicrograph (PPL) of phosphoritic peloidal intraclastic grainstone overlying weakly impregnated lime mudstone (LF.6; Fig 6.34, unit e, surface 4). Note the pseudomorphed early cement fringe (arrowed) showing a distinctive botryoidal form. Scale bar = 0.5mm. GGU 218546, Ekspedition Bræ Formation, locality 1, east Freuchen Land.

areas skeletal calcite remains unaltered. Pyrite is common at impregnated surfaces and locally forms crusts up to 1mm thick. The thickness of individual phosphorite laminae is commonly uniform despite the irregularity of the erosion surfaces; this suggests surficial impregnation rather than exhumation of subsurface phosphorite. In general, phosphorite layers coalesce on topographic 'highs' and bifurcate into hollows; this occurs on the scale of individual laminae and the whole laminated complex (Fig. 6.34), and reflects preferential accumulation of lime mud within protected hollows and crevices during impregnation while fine sediment was winnowed from exposed areas.

No evidence of boring or encrustation was observed in the example from the Ekspedition Bræ Formation. Near the base of the Holm Dal Formation, however, similar phosphorite surfaces show numerous circular rimmed craters (1-2mm diameter) that probably represent echinoderm holdfasts (pers. comm. J.S. Peel, 1985).

b) Glauconitic skeletal carbonates.

Near the base of the Henson Gletscher Formation and the laterally equivalent Sæterdal Formation, glauconitic skeletal carbonates form distinctive pale weathering ledges. In most sections they comprise glauconitic medium to coarse crystalline dolomites with a relict skeletal grainstone-packstone fabric but in Løndal (Fig. 3.3) these rocks are only locally dolomitized (Figs 3.17A & 6.81). They form the upper, coarse-grained portion (0.2-1.3m thick) of cyclic, coarsening-upward sequences (Fig. 6.81), the significance of which is discussed later (6.2.3). Thinly interbedded (2-30mm) skeletal peloidal packstones, grainstones and rare wackestones pass upward into skeletal grainstones that locally display shell imbrication and trough cross-bedding (Fig. 6.39). Trilobite fragments form over 70% of the skeletal grains; pelmatozoan and phosphatic brachiopod fragments account for the remainder. Much of the pelleted lime mud in packstone layers is perched on the upper surfaces of skeletal grains which suggests that the mud filtered into position after deposition of a mud-poor skeletal grainstone.

Green, well-rounded pellets of glauconite (100-200μm diameter) are particularly abundant in densely packed, skeletal grainstone layers. Cloudy, bladed calcite cement emanates from trilobite fragments whereas pelmatozoan grains show syntaxial cement overgrowths; the remaining pore space is occluded by clear blocky calcite cement.

Interpretation.

The presence of phosphorite and glauconite in sediments indicates deposition in a marine environment characterized by low sedimentation rates or non-deposition, high organic productivity and periodic reducing conditions at the sediment surface (see 5.2.1.3).

The multiple phosphorite horizons within argillaceous lime mud-stone sequences record a complex depositional history and clearly are highly condensed. They closely resemble mineralized hardgrounds described from younger carbonate sequences (Bromley 1967; Kennedy & Garrison 1975b; Jarvis 1980). Truncated cements and encrusted, bored hardground litho-clasts have not been identified however, and lithification to form a true submarine hardground cannot be proven. Partial lithification, at

Figure 6.39. Trough cross-bedded, glauconitic, skeletal lime grainstones (LF.6). Henson Gletscher Formation, locality 10, west Peary Land.

Figure 6.39. Trough cross-bedded, glauconitic, skeletal lime grainstones (LF.6). Henson Gletscher Formation, locality 10, west Peary Land.

least, is suggested by (a) the preservation of irregular surfaces with unsupported, fragile overhangs and caverns, (b) fractured phosphorite skins over minor slump folds (*cf.* Garrison & Fischer 1969) and (c) lcoal encrustation by echinoderms. Early diagenetic submarine cementation is indicated by the relict botryoidal rim cements, although exposure of these cements on the sea floor cannot be demonstrated. Early diagenetic cementation and the formation of probable hardgrounds further testify to reduced rates of sedimentation or non-deposition (Shinn 1969; Bathurst 1971; Kennedy & Garrison 1975b).

Phosphorite impregnation occurred at the sediment surface. Replacement of lime mud was the dominant process, but the concentrically laminated rims on bioclasts and peloids resemble the phosphatic ooids described by Swett & Crowder (1982) and are similarly interpreted as representing primary phosphorite accretion rather than diagenetic replacement of a carbonate precursor.

The glauconitic skeletal carbonates of the Henson Gletscher and Sæterdal Formations cap shelly coarsening-upward sequences. They record deposition in well-oxygenated turbulent waters at or above normal wave base, in an environment supporting a prolific benthic shelly fauna. Lime mud and silt accumulated during less turbulent periods, but winnowing of fines was common. Reworking of skeletal grains from muddy sediment is often indicated by residual lime mud trapped beneath trilobite doublures in otherwise mud-free grainstones. The worn, fragmented nature of skeletal grains in grainstone-dominated intervals and the presence of shell imbrication and cross-bedding testify to periodic high energy conditions when skeletal sands actively migrated and formed ripples and megaripples. The occurrence of glauconite and the evidence of winnowing, reworking and concentration of shell debris suggest slow rates of sediment accumulation.

The phosphorite horizons and the glauconitic shelly carbonates essentially represent similar depositional events. They are both condensed intervals recording winnowing and reworking of sediment in association with a high organic productivity. The differences between them probably result solely from their relative positions on the outer shelf. Glauconitic, mud-poor skeletal sands accumulated in turbulent water at or above wave-base while phosphoritic lime muds and muddy sands were deposited farther offshore, below normal wave base.

### 6.1.7. Lithofacies 7; Irregular nodular carbonates.

These carbonates are only recognized in the Aftenstjernesø Formation and over 95% of the lithofacies are dolomites. Dolomitic limestones occur only in Løndal and on the western margin of Hans Tavsens Iskappe. The lithofacies typically comprises grey or brown weathering dolomite differentiated into pale irregular, interlocking nodules and dark intervening matrix. The nodules are 0.02-0.05m thick normal to bedding and show a range of forms from isolated lensoid, oval or irregular amoeboid nodules to impersistent sheets (<0.1m thick) with irregular knobbly surfaces (Fig. 6.40). These nodular carbonates are commonly interbedded with graded carbonates (Lithofacies 8). The relative proportions


Figure 6.40. Irregular, nodular dolomitic limestones and dolomites (LF.7), interbedded with sharp-based, weakly graded limestones (A; LF.8). Dolomitic zones (D) weather mid-grey in contrast to the pale grey lime wackestone/mudstone nodules. Aftenstjernesø Formation, locality 10, west Peary Land.


Figure 6.40. Irregular, nodular dolomitic limestones and dolomites (LF.7), interbedded with sharp-based, weakly graded limestones (A; LF.8). Dolomitic zones (D) weather mid-grey in contrast to the pale grey lime wackestone/mudstone nodules. Aftenstjernesø Formation, locality 10, west Peary Land.

of the two facies is variable but a rhythmic interbedding is commonly developed (Fig. 6.40).

Sedimentary structures are rare within nodules; a discontinuous wispy bituminous lamination is locally present. Bioturbation is ubiquitous. *Chondrites* and *Planolites* burrows occur locally and indeterminate spar-filled burrows and vague burrow-mottling are common. Some cylindrical or tubular nodules delineate horizontal and oblique burrows. In partially dolomitized intervals, the internodular matrix and nodule margins are preferentially dolomitized (Fig. 6.40); nodule cores comprise bioturbated lime mudstone or wackestone with a neomorphic microspar fabric. Allochems form up to 10% of the rock and comprise trilobite and phosphatic brachiopod fragments and bituminous peloids (50-100μm diameter) of probable faecal origin. Skeletal grains are randomly oriented with respect to bedding. Dolomitized nodules comprise clear or pale brown, medium to coarse crystalline dolomite containing 'ghost' outlines of carbonate skeletal grains and peloids. Nodule cores often have a euhedral or subhedral dolomite fabric with up to 30% intercrystalline porosity; some nodules have open vuggy cores.

The internodular matrix is dark grey or black and is commonly bituminous or argillaceous. The nodules show a variable packing density; consequently the matrix ranges from millimetre-thick sutures between nodules to lenticular, discontinuous lenses and pods up to a few centimetres thick (Fig. 6.40). Matrix-nodule boundaries are typically sharp and stylolitic; burrows and bioclasts within nodules are often truncated at the contact. In places the boundary is gradational over a few millimetres. The dark lamination within the matrix comprises discontinuous bituminous microstylolite seams that swirl around and enwrap the nodules (Fig.6.41); in places the lamination is truncated at stylolitic nodule boundaries. Skeletal grains lie subparallel to the lamination and are commonly fractured. The internodular matrix is mainly dolomitized, comprising a medium crystalline dolomite mosaic, but locally patches of bituminous microspar (10-30μm crystals) are preserved.

At a few localities the nodules show angular fractures and pull-aparts and display evidence of rotation and brecciation (Fig. 6.42). The fractures are generally filled with the dark internodular matrix component, reflecting its plastic, poorly lithified nature during nodule disruption.

Interpretation.

The mud-rich primary fabric preserved in nodules suggests deposition in a low-energy marine environment beneath the level of wave-action or tidal currents. Moderate oxygenation of bottom waters is indicated by the evidence of an active infauna. The relative paucity of skeletal detritus may reflect high turbidity, an unfavourable 'soupy' substrate (*cf.* Kennedy & Garrison 1975) or insufficient oxygen for the establishment of a benthic shelly fauna. The argillaceous lime mud and silt probably represents mainly hemipelagic sediment, derived from adjacent

Figure 6.41. Polished surface, cut normal to bedding of irregular nodular dolomite (LF.7). Pale nodules are separated by dark, faintly laminated 'matrix' carbonate (left) or bituminous stylolites (centre right). Note randomly oriented, uncompacted skeletal grains within nodules (arrows). Scale bar = 2cm. GGU 197581, Aftenstjernesø Formation, locality 10, west Peary Land.

Figure 6.41. Polished surface, cut normal to bedding of irregular nodular dolomite (LF.7). Pale nodules are separated by dark, faintly laminated 'matrix' carbonate (left) or bituminous stylolites (centre right). Note randomly oriented, uncompacted skeletal grains within nodules (arrows). Scale bar = 2cm. GGU 197581, Aftenstjernesø Formation, locality 10, west Peary Land.

Figure 6.42. Fractured, locally brecciated nodules; fractures filled with dark internodular component. Pencil (lower left) for scale. LF.7, Aftenstjernesø Formation, locality 10, west Peary Land.

Figure 6.42. Fractured, locally brecciated nodules; fractures filled with dark internodular component. Pencil (lower left) for scale. LF.7, Aftenstjernesø Formation, locality 10, west Peary Land.

shallow-water carbonate environments. The association with fine-grained carbonate turbidites (Fig. 6.40), however, suggests that low-density turbidity currents may have contributed to the mud-dominated sediment pile. Bioturbation would obliterate the subtle diagnostic features of dilute turbidity current deposits (Stow & Shanmugam 1980).

Comparable nodular carbonates have been described from throughout the geological record (Garrison & Fischer 1969; Tucker 1974; Noble & Howells 1974; Kennedy & Garrison 1975b). The development of the nodular structure is generally considered to be a diagenetic, post-depositional process although examples of redeposition of nodules have been described by Hopkins (1977) and Kennedy & Garrison (1975b). General agreement on the timing and mechanism of development has not been reached. Theories range from sedimentary boudinage (Wobber 1967) through early diagenetic cementation combined with compaction and late diagenetic pressure solution (Noble & Howells 1974; Kennedy & Garrison 1975b) to pressure solution processes alone (Wanless 1979). That pressure solution played a significant role is generally undisputed but the relative importance of early diagenetic processes is the subject of much debate (e.g. Wanless 1979, 1982; Pratt 1982). The flaser nodular structure described from chalks of southern England is closely comparable to that described here (Garrison & Kennedy 1977) It was suggested that this resulted from burial pressure solution accentuating an early diagenetic cementation pattern. According to Wanless (1979) however, such a flaser nodular structure can be formed from a homogeneous or heterogeneous argillaceous carbonate precursor by pressure solution processes alone. Clearly then, diagenetic interpretation of these rocks depends on evidence of early nodular cementation in the shallow subsurface at insufficient burial depths for pressure solution.

Firstly, nodular cementation of modern carbonate sediments has been documented by Müller & Fabricus (1974) in the Mediterranean and Mullins *et al.* (1980) on carbonate slopes off the Bahamas. These workers suggested that high-Mg calcite cements are precipitated directly from sea water, and thus nodule formation is favoured by slow sedimentation and persistent irrigation.

Secondly, studies of ancient nodular carbonates commonly reveal evidence of early diagenetic cementation in submarine environments at shallow depths below the sediment surface. Kennedy & Garrison (1975b) described a range of structures from isolated, lithified nodules through irregular semi-continuous nodules (incipient hardgrounds) to mineralized, bored and encrusted hardgrounds. This, they suggested, represents stages in progressive lithification beginning with nodule formation below the sediment surface and ending with scour and exhumation of lithified hardgrounds. A similar process was envisaged by Bromley (1965) and Noble & Howells (1974).

Sufficient evidence exists therefore for early diagenetic patchy cementation at shallow depths below the sediment surface. Early, differential lithification is suggested in this study by:

a) the uncompacted nature of the nodules (cylindrical burrows; randomly oriented unfractured bioclasts) in contrast to the compacted fabric of the internodular matrix (lamination enwrapping nodules, fractured bioclasts parallel to lamination, flattened burrows)

b) fractured, brecciated nodules surrounded by dark 'matrix' carbonate.

The presence of amoeboid nodules as clasts in mass flow deposits (Fig. 6.62; *cf.* Hopkins 1977) further testifies to the early development of nodules, close to the sediment surface.

It is proposed that a primary interbedded lime-rich and lime-poor sediment suffered biogenic reworking, resulting in a patchy, irregular distribution of impure (argillaceous or bituminous) and pure lime sediment. Such a primary heterogeneity is indicated by the occurrence of dark 'matrix' burrow fills within pale carbonate (Fig. 6.45). Early diagenetic differential cementation produced a patchy incipient nodular structure around which the unlithified internodular carbonate was draped during compaction. Matrix compaction caused rotation and fracturing of bioclasts and the development of a weak lamination due to flattening of organic detritus and burrow fills (*cf.* Shinn *et al.* 1977). Subsequent pressure solution at nodule margins and within the matrix caused further differentiation and enhancement of the nodular structure, and accentuated the matrix lamination.

Localized fracturing and brecciation of nodules probably resulted from minor subsurface downslope creep of differentially lithified carbonates (see Lithofacies 4,5 & Tucker 1974).

### 6.1.8 Lithofacies 8; Graded carbonates

This lithofacies comprises thin- to medium-bedded, normally graded, peloidal skeletal and intraclastic limestones and equivalent cream or pale to mid-grey dolomites showing relict grain size grading. It also includes thin-bedded dolomites that show no recognizable primary grain fabrics but are included on the basis of similar bedding style, relict sedimentary structures and a vague colour grading. Limestones make up only 5% of the facies but offer the most complete record of primary depositional fabrics and structures. Graded carbonates are characteristic of the Aftenstjernesø Formation, where they form nearly 70% of the formation in some sections (Fig. 6.43). They also occur in the Sydpasset, Fimbuldal, Henson Gletscher, Ekspedition Bræ and Paralleldal Formations.

Beds are typically 0.01 to 0.1m thick (Fig. 6.44) but are often up to 0.3m thick and beds of 0.6m thickness occur locally in the Afternstjernesø Formation. In two detailed sections through this formation (170 beds) nearly three-quarters of the beds are less than 0.1m thick. These thinner beds have sharp, planar bases and individual beds are laterally persistent (Fig. 3.10). Small scours are sometimes present (3% of beds < 0.1m thick) but sole marks are generally scarce. Stylolitization of bed contacts is common, however, and the real abundance of sole marks is unknown. Upper contacts are commonly gradational, passing into dark laminated or nodular carbonate (Fig. 6.44 & 6.50). Bioturbation of the upper few centimetres is common, and some beds are completely disrupted by burrowing. Some graded limestones show *Chondrites* and *Teichichnus* burrow systems (Fig. 6.45). The former are oval or circular in cross-section, 0.1 - 1.5mm in diameter and have calcite cement, pyrite or geopetal lime mud and cement

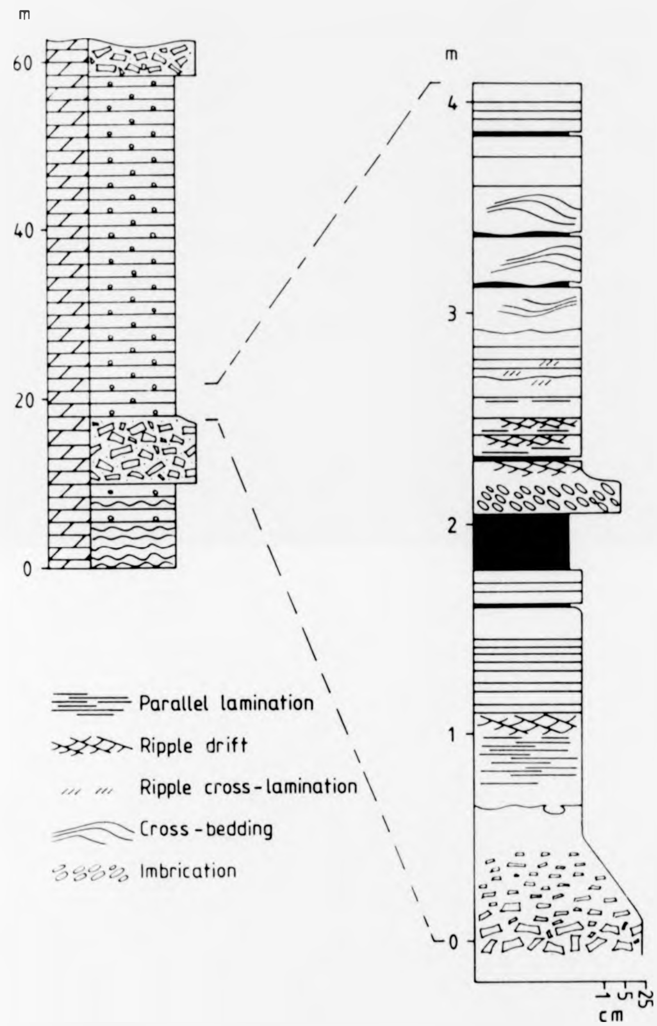


Figure 6.43. Detailed section through the lower beds of the Aftenstjernesø Formation at locality 4, west Peary Land.

Figure 6.44. Thin-bedded dolomites of the Aftenstjernesø Formation showing sharp, planar or locally erosional (arrow) bases and gradational tops; internally structureless. LF.8, locality 4, west Peary Land.

Figure 6.44. Thin-bedded dolomites of the Aftenstjernesø Formation showing sharp, planar or locally erosional (arrow) bases and gradational tops; internally structureless. LF.8, locality 4, west Peary Land.

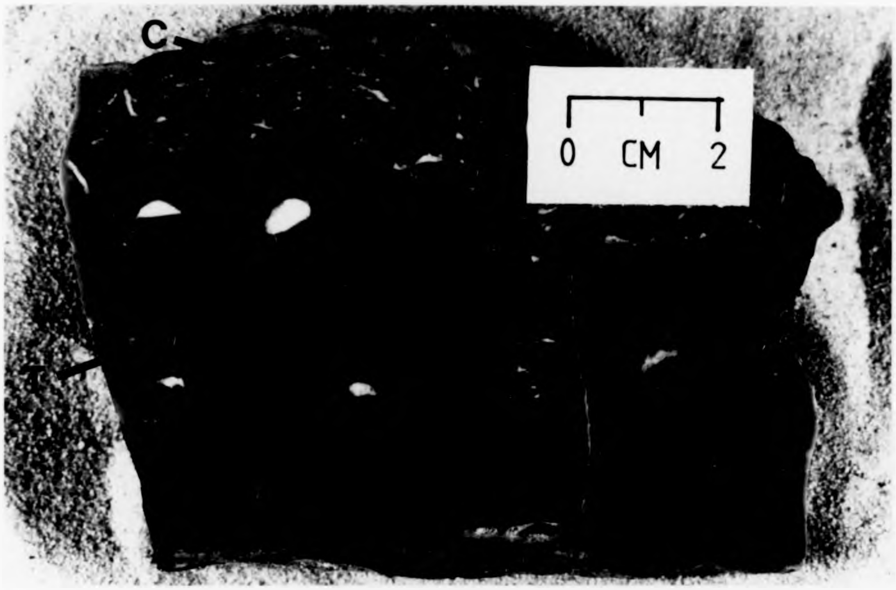


Figure 6.45. Polished surface, normal to bedding, showing weak normal grading from pale grey peloidal packstone (basal 2cm) into dark wackestone and mudstone. Note faint parallel lamination and bioturbated upper half. C: *Chondrites*; T: *Teichichnus*. GGU 218672, LF.8, Aftenstjernesø Formation, locality 10, west Peary Land.

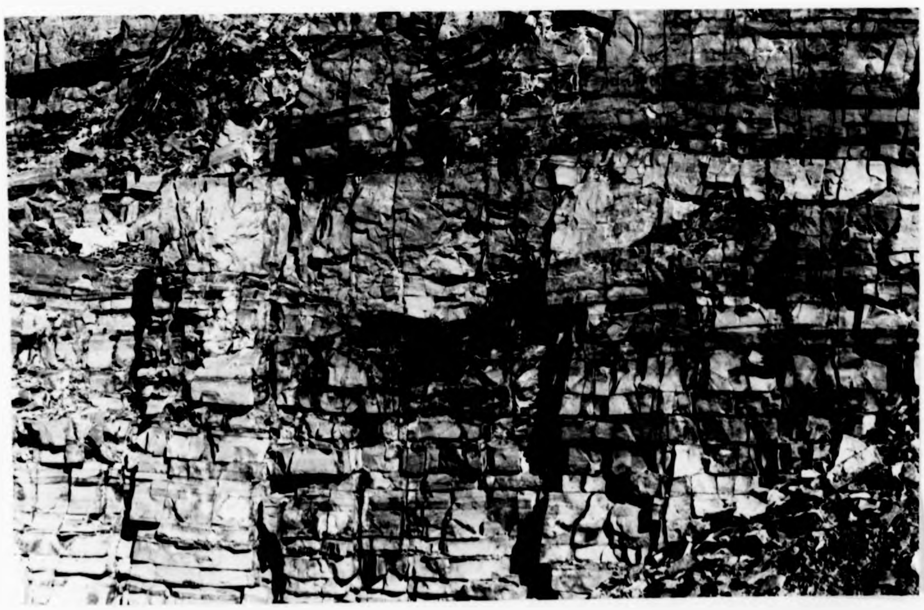

Figure 6.46. Massive pale dolomite bed (0.6m thick where arrowed) occupying a deep scour or channel cut into parallel-bedded dolomites. LF.8, Aftenstjernesø Formation, locality 1, east Freuchen Land.

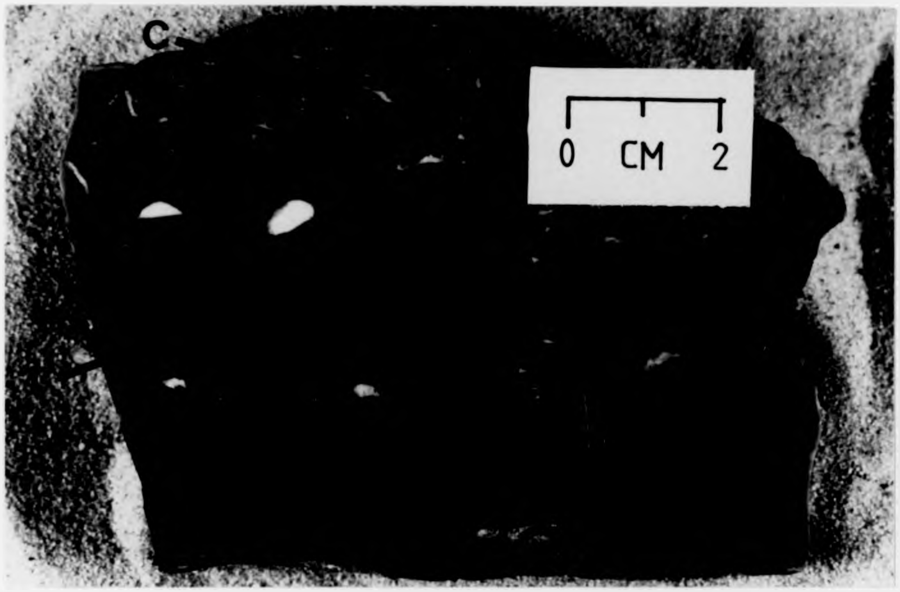


Figure 6.45. Polished surface, normal to bedding, showing weak normal grading from pale grey peloidal packstone (basal 2cm) into dark wackestone and mudstone. Note faint parallel lamination and bioturbated upper half. C: *Chondrites*; T: *Teichichnus*. GGU 218672, LF.8, Aftenstjernesø Formation, locality 10, west Peary Land.

Figure 6.46. Massive pale dolomite bed (0.6m thick where arrowed) occupying a deep scour or channel cut into parallel-bedded dolomites. LF.8, Aftenstjernesø Formation, locality 1, east Freuchen Land.

fills. Lime mud fills are commonly pelleted and may represent faecal detritus.

Beds over 0.1m thick typically have sharp, erosional and loaded bases and, in places, fill deep scours or channels (Fig. 6.46). Where bioturbation is absent, bed tops are sharp and planar although locally showing a gentle upward convexity (Fig. 3.10).

The limestones and the thicker dolomite beds commonly display normal size grading (Fig. 6.47) but grading is rarely demonstrable in dolomite beds less than 0.1m thick. Grading is often rapid, passing from a poorly-sorted, structureless basal interval (medium sand to coarse pebble) into parallel- or cross-laminated fine sand or coarse silt grade carbonate (Fig. 6.47). Pebbles are commonly imbricated and, where undolomitized, comprise 0.01 - 0.1m elongate or equidimensional clasts of lime mudstone or wackestone in a peloidal, skeletal packstone or grainstone matrix. One bed in the Aftenstjernesø Formation (Fig. 6.43) contains imbricated, well-rounded pebbles of cream, granular sucrosic dolomite, lithologically similar to dolomitized grainstones (Lithofacies 14) of the platform margin association. Grain size grading in the thin-bedded,fine-grained beds is generally obscured by either dolomitization or neomorphic recrystallization. The bed in Fig. 6.45, for example, is composed mainly of 10 - 30μm microspar but shows faint colour grading from a pale fawn base with weak parallel lamination into a darker, burrowed top. Similar 'colour grading' occurs in many dolomite beds that show no primary grain fabrics.

Diffuse to well-developed parallel lamination is the most common sedimentary structure, occurring in 15% of beds less than 0.1m

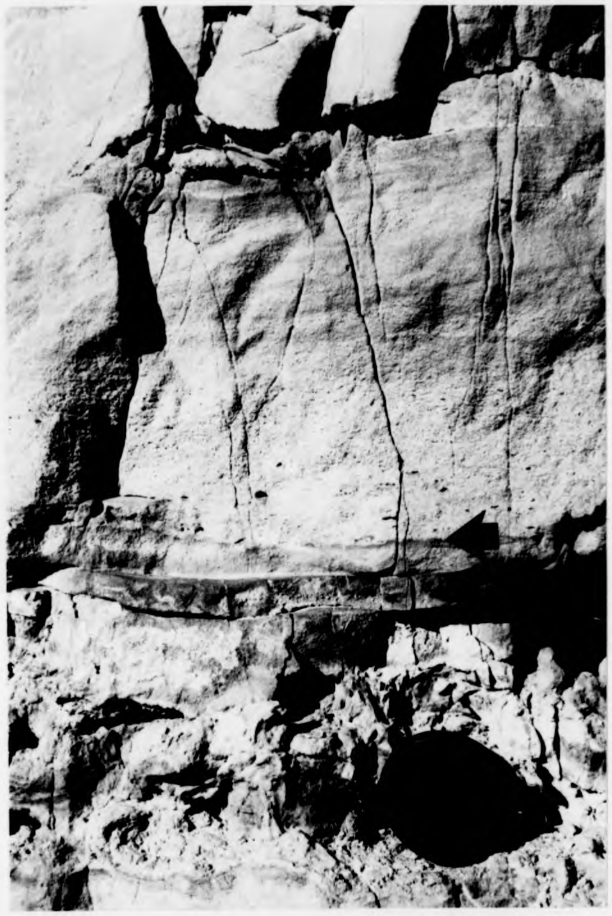

Figure 6.47. Intraclastic dolomite bed. Note sharp base (arrowed), lower graded, structureless division and upper stratified division. LF.8, Aftenstjernesø Formation, locality 10, west Peary Land.

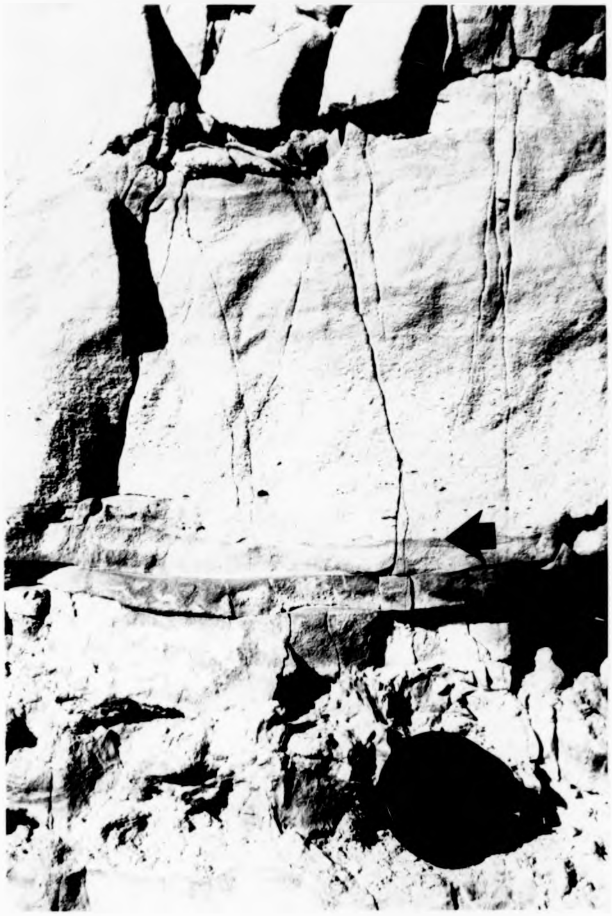

Figure 6.47. Intraclastic dolomite bed. Note sharp base (arrowed), lower graded, structureless division and upper stratified division. LF.8, Aftenstjernesø Formation, locality 10, west Peary Land.

thick and in 28% of beds over 0.1m thick. The majority of beds (72% of beds less than 0.1m and 52% of beds greater than 0.1m) are structureless, but preservation of sedimentary structures is poor at outcrop and slabbing and polishing often reveals structures that were not apparent in the field (e.g. Fig. 6.48). Hence the high proportion of structureless beds is probably partly a function of preservation. Beds over 0.1m thick commonly display parallel lamination, ripple cross-lamination and/or cross-bedding. Rarely a single bed has a basal structureless, graded division, passing upward through parallel- and cross-laminated carbonate into a parallel-laminated or burrowed fine-grained top (Fig. 6.48 & 3.11). More commonly, beds over 0.2m thick are mainly structureless with a thin laminated cap. In thinner beds, parallel lamination or ripple cross-lamination may occur throughout. Cross-lamination forms 0.01 - 0.03m sets; the climbing ripple-drift types 1 and 2 of Jopling & Walker (1968) are the common forms. Current ripples with amplitudes of 0.01 - 0.02m and wavelengths of 0.3 - 0.4m occur in the Aftenstjernesø Formation in Paralleldal (locality 19).

Cross-bedding occurs in 20% of beds over 0.1m thick. It takes the form of indistinct low-angle foresets (Fig. 6.47) or megaripple-scale climbing cross-stratification (Fig. 6.49). Sets are typically 0.05 - 0.1m thick but are locally up to 0.15m thick. The cross-bedding may occur directly above the bed base (Fig. 6.49) or overlie a basal graded or parallel-laminated interval (Fig. 6.47) and locally is itself overlain by ripple cross-laminated carbonate.

Graded limestones comprise intraclastic, peloidal and skeletal lime grainstone and packstone, and thin-bedded packstones, wackestones and mudstones. The intraclasts are mainly laminated or burrowed lime

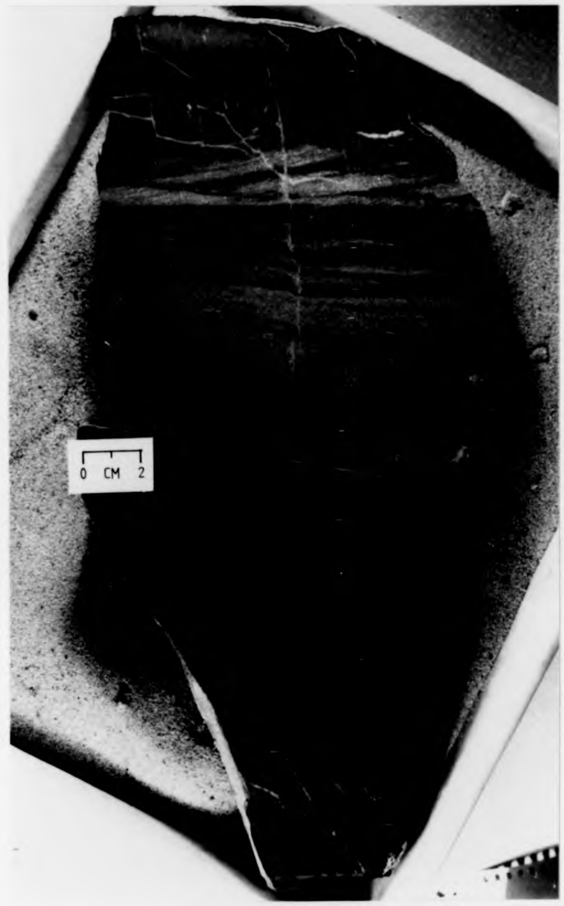


Figure 6.48. Polished surface, normal to bedding, of graded dolomite bed (LF.8) showing Bouma ABCD divisions. GGU 218510, Aftenstjernesø Formation, locality 1, east Freuchen Land.

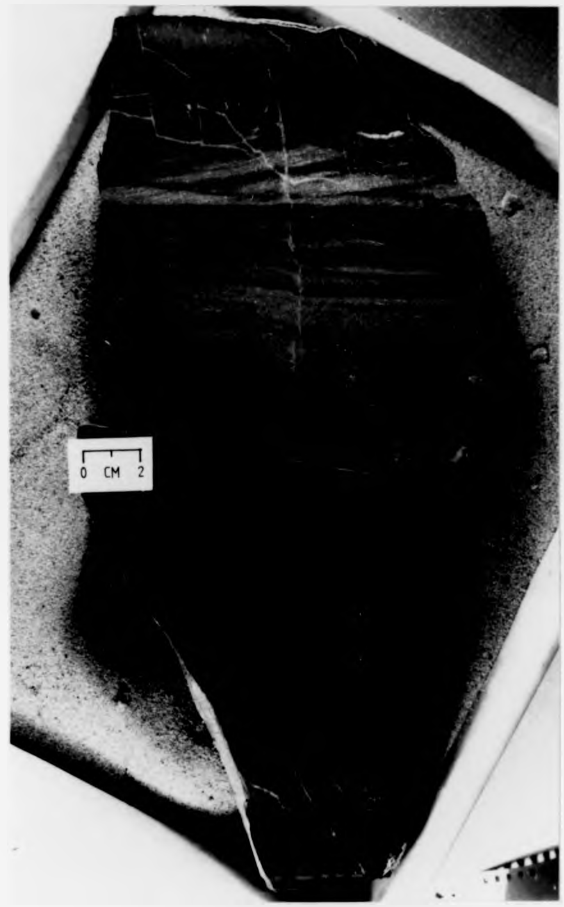


Figure 6.48. Polished surface, normal to bedding, of graded dolomite bed (LF.8) showing Bouma ABCD divisions. GGU 218510, Aftenstjernesø Formation, locality 1, east Freuchen Land.

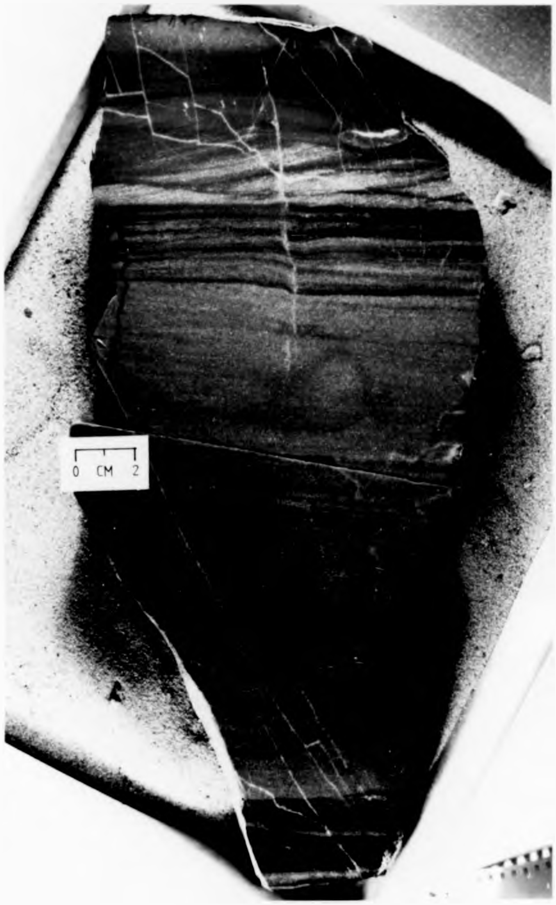


Figure 6.48. Polished surface, normal to bedding, of graded dolomite bed (LF.8) showing Bouma ABCD divisions. GGU 218510, Aftenstjernesø Formation, locality 1, east Freuchen Land.

Figure 6.49. Cross-bedded dolomite bed (LF.8). Note sharp planar base (arrowed) and low-angle climbing foresets. Aftenstjernesø Formation, locality 4, west Peary Land.

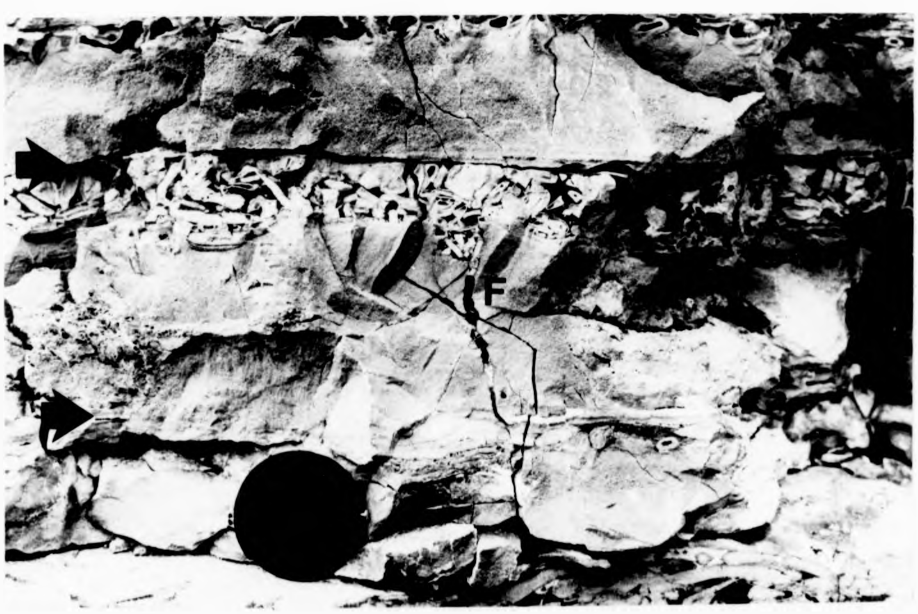


Figure 6.50. Sharp-based (arrows) graded beds (LF.8) interbedded with brecciated nodular dolomite (LF.4). Note the angular fracture (F) infilled with brecciated nodular carbonate. Aftenstjernesø Formation, locality 2, west Peary Land.

Figure 6.49. Cross-bedded dolomite bed (LF.8). Note sharp planar base (arrowed) and low-angle climbing foresets. Aftenstjernesø Formation, locality 4, west Peary Land.

Figure 6.50. Sharp-based (arrows) graded beds (LF.8) interbedded with brecciated nodular dolomite (LF.4). Note the angular fracture (F) infilled with brecciated nodular carbonate. Aftenstjernesø Formation, locality 2, west Peary Land.

mudstone or wackestone with up to 10% peloidal lime grainstone intraclasts. Structureless micrite (or microspar) peloids are dominant in the matrix grainstone with subordinate ooids and bioclasts (trilobite, pelmatozoan and brachiopod fragments). Blocky calcite cements are ferroan in argillaceous intervals in contrast to the non-ferroan calcite of the allochems.

Dolomite beds are composed of medium - coarse crystalline dolomite. Relict structures and grains are defined by slight colour differences or, less commonly, by variation in crystal size or intracrystalline porosity. In the upper half of the Aftenstjernesø Formation north of Øvre Midsommersø, pale graded dolomites contain a scatter of spherical moulds (0.5 - 1.5m diameter) that probably represent leached primary grains (ooids?).

Deformation structures are rare. Where graded beds are interbedded with nodular carbonate (Lithofacies 4, 7) the latter may show pull-aparts and extensive brecciation whereas the graded beds display rare brittle fractures (Fig. 6.51). Thinner beds (0.01 - 0.05m) locally exhibit extensive small-scale boudinage.

## Interpretation

The sharp erosional bases, normal grading and burrowed tops indicate deposition from episodic, waning, turbulent currents. The grading and sequence of structures in some thicker beds is comparable to that described by Bouma (1962) from siliciclastic turbidites (Fig. 6.51a). Similar features can be produced by waning storm-induced currents (Brenchley & Newall 1982; Nelson 1982) but the lack of wave ripples or hummocky cross-bedding and the lateral persistence of bedding

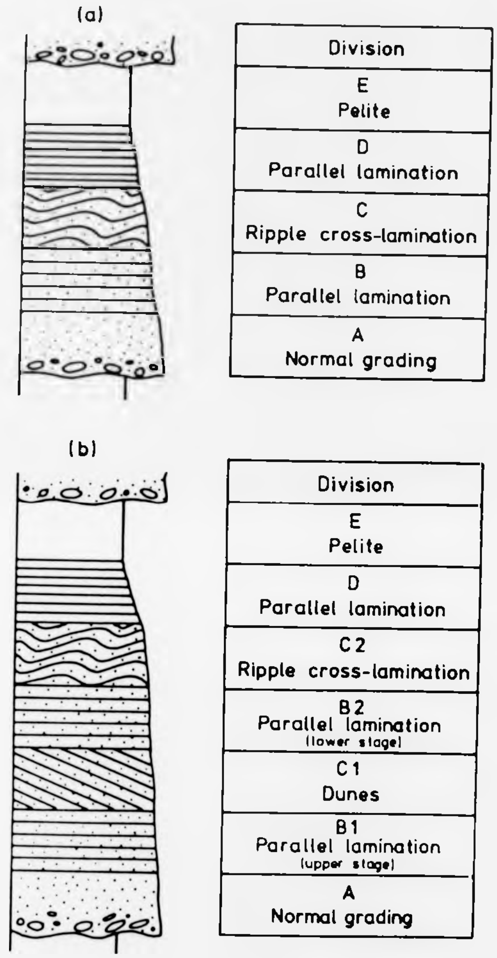


Figure 6.51. The sequence of sedimentary structures in turbidites (a) after Bouma (1962) (b) after Allen (1982).

argues against such an interpretation. Carbonate turbidites have been described from both Recent (Rusnak & Nesteroff 1964; Davies 1968; Crevello & Schlager 1980) and ancient deposits (Davies 1977; Pfeil & Read 1980). Typically, they have sharp, erosive bases and gradational or burrowed tops. Well-developed Bouma sequences may be rare (Bornhold & Pilkey 1971) or completely absent (Davies 1977).

By analogy with these examples, these rocks are interpreted as the deposits of lime mud-rich turbidity currents. An open marine source area is indicated by the bioclastic content. The varying degrees of bioturbation and the nature of the associated lithofacies suggest deposition in both aerobic and anaerobic environments. The trace fossils offer little environmental information. *Chondrites* is known from a wide range of marine environments (Häntzchel 1975) and although *Teichichnus* is often considered typical of muddy shelf environments (Baldwin 1977) it is not restricted to this environment and has been recorded from deep-sea sediments (Ekdale 1977).

Cross-bedding is rarely observed in siliciclastic sand turbidites. Its absence has been attributed to suppression of dune bedforms by fine-grained sediment load (Hubert 1966; Walton 1967), to the lack of suitably coarse-grained material (Walton 1967; Allen 1970) or to the rapid passage of the flow through the range of flow conditions necessary for dune development (Walker 1965). In contrast, cross-bedding has been described from several carbonate turbidite successions (Hubert 1966; Thomson & Thomasson 1969; Tucker 1969; Ricci-Lucchi & Valmori 1980) and its occurrence may reflect the greater range of grain sizes in carbonate turbidites (Allen 1982) or the different hydrodynamic properties of carbonate particles compared to silicate grains (Ricci-

Lucchi & Valmori 1980). In the examples described by Tucker (1969) and Hubert (1966) the cross-bedded division replaces or is directly overlain by the cross-laminated C division. Thomson & Thomasson (1969), however, described a dune cross-bedded interval that succeeded the basal, graded A division and was followed by parallel-laminated carbonate of the B division. Allen (1970, 1982) modified the ideal Bouma sequence to incorporate these data (Fig. 6.51). In this study A → C1 → C2, B1 → C1 → C2 and C1 → C2 sequences were recognized (Fig. 6.51).

### 6.1.9 Lithofacies 9; Breccia beds

This lithofacies encompasses all bedded breccias in the succession, thus excluding the discontinuous, discordant interstratal creep breccias (Lithofacies 4,5) and the karstic breccias that occur locally beneath the Wandel Valley Formation unconformity (see 8.4). In the outer shelf-slope association, the breccia beds are composed of carbonate, whereas in the foreslope assemblage of the platform margin, mixed carbonate-siliciclastic sandstone breccias are common (see 7.1.1).

#### Carbonate breccia beds

These massive beds produce prominent cliff-forming features and constitute 15 - 25% of the Brønlund Fjord Group and up to 35% of the Tavsens Iskappe Group. They exhibit a complete spectrum of compositions from limestone (13%) through dolomitic limestone (5%) to dolomite (82%). The calcareous beds weather mid-dark grey while the dolomites show pale weathering colours - brown, pale fawn-grey, cream and orange.

Thickness

Beds range in thickness from 0.2 to 45m, with about half measuring between 0.5 and 4m thick (Fig. 6.52). Recognition of multiple, amalgamated breccia sequences is hampered by the loss of textural detail in coarsely dolomitized carbonates; the maximum values should be treated with caution. Fig. 6.52 shows the breccia composition relative to bed thickness and clearly illustrates the overwhelming dominance of dolomite in beds over a metre thick.

Geometry and Boundaries

The breccia beds are sheet-like to broadly lenticular bodies with subparallel bounding surfaces (Fig. 6.53); channelling is rare. Pinch and swell is common, however, and discontinuous pod-like bodies are often observed in cliff sections (Fig. 3.47). Individual sheets can often be shown to have considerable lateral extent. In west Peary Land a prominent breccia bed (5 - 13m thick) in the Aftenstjernesø Formation can be confidently correlated over an area of 20km by 15km and its western limits have not been determined (Fig. 6.54). Around Buen in central Peary Land, a breccia bed with a distinctive hummocky upper surface can be traced for about 25km from east to west and 15km from south to north (Fig. 6.55). Its eastern limit is unknown but assuming an average thickness of 15m over the known area, the bed has a minimum volume of 3km$^3$. Thin breccia beds often show a smoothly tapering, lenticular cross section (Fig. 6.56).

Bed bases are typically sharp, planar and non-erosive with minor, localised irregularities (Fig. 6.57). In a survey of 77 beds, only 6% possess erosional, channelled bases (Fig. 3.45), the remainder being planar (75%) or gently undulating and locally irregular (19%).

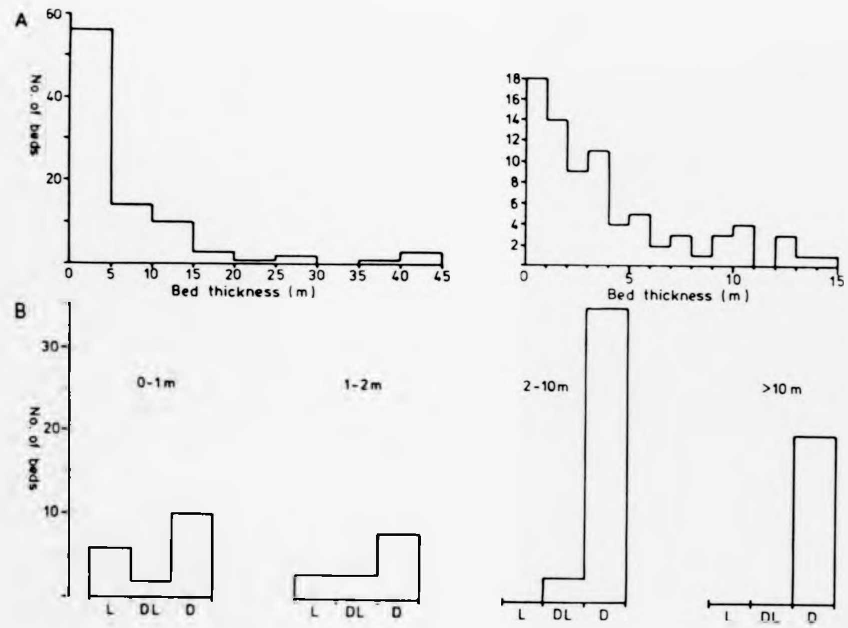


Figure 6.52. A. Histograms of breccia bed thickness. B. Histograms showing the relationship between lithology and bed thickness. L : limestone; DL : dolomitic limestone; D : dolomite.

Figure 6.53. Massive dolomite breccia bed (c. 10m thick) near the base of the Aftenstjernesø Formation; note flat, parallel boundaries (arrowed). LF.9, locality 2, west Peary Land.

Figure 6.56. Lenticular dolomite breccia bed (0.3m thick; base and top indicated) with a flat, non-erosional base and a convex top. LF.9, Løndal Formation, locality 10, west Peary Land.

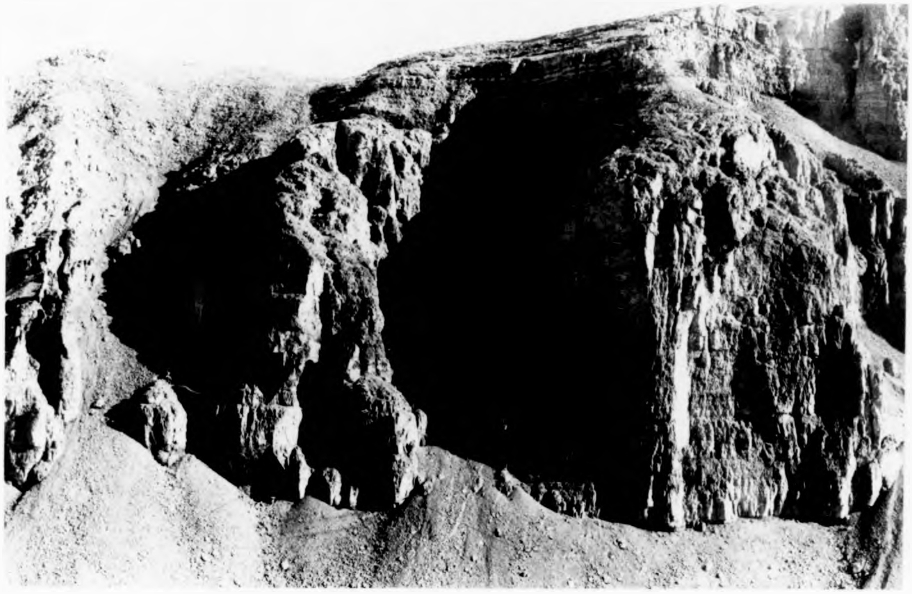

Figure 6.53. Massive dolomite breccia bed (c. 10m thick) near the base of the Aftenstjernesø Formation; note flat, parallel boundaries (arrowed). LF.9, locality 2, west Peary Land.

Figure 6.56. Lenticular dolomite breccia bed (0.3m thick; base and top indicated) with a flat, non-erosional base and a convex top. LF.9, Løndal Formation, locality 10, west Peary Land.

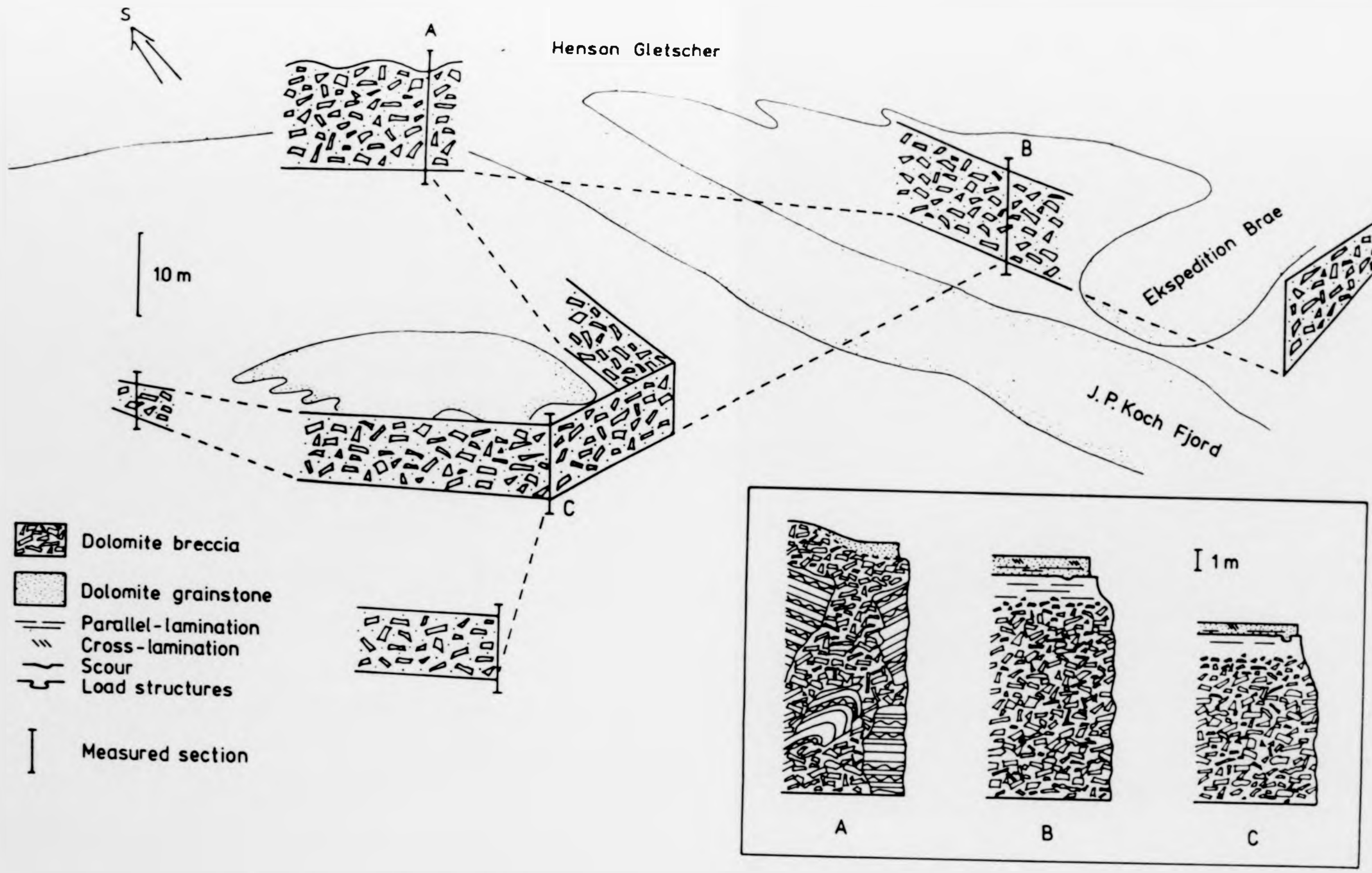


Figure 6.54. Diagram showing the lateral variation within a single breccia bed in the Aftenstjernesø Formation in west Peary Land. Sections A, B and C are at localities 2, 1 and 4 respectively.

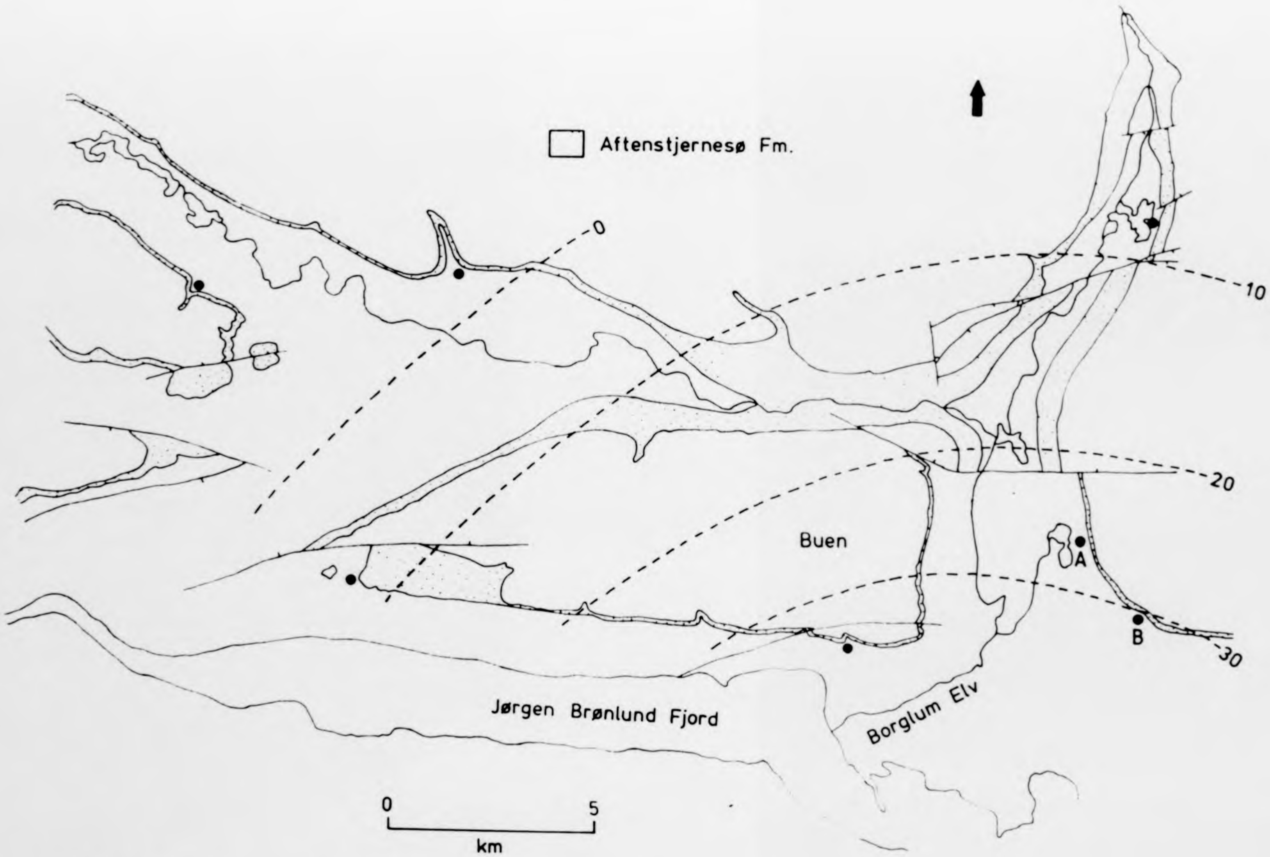


Figure 6.55. Isopach map of a breccia bed in the Aftenstjernesø Formation in the Jørgen Brønlund Fjord region. Contouring (in metres) is based on measured sections (black circles) and observations of cliff sections along the south and east side of Buen. Sections A and B measured by R.L. Christie and J.S. Peel.

Figure 6.57. Sharp planar base of dolomite breccia bed (LF.9). Clast-supported breccia composed mainly of tabular clasts which locally show apparent imbrication e.g. at A. Note, however, opposed clast stacking at B - the overall fabric is random. Aftenstjernesø Formation, locality 10, west Peary Land.

Figure 6.59. 10m thick dolomite breccia bed (LF.9) with a flat, non-erosional base and an irregular, hummocky top. Aftenstjerensø Formation, locality 2, west Peary Land.

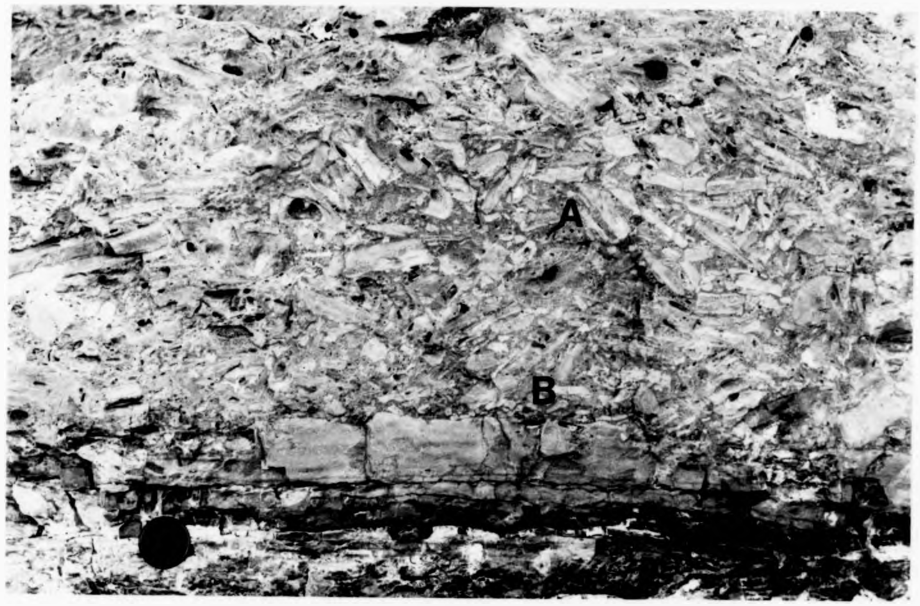


Figure 6.57. Sharp planar base of dolomite breccia bed (LF.9). Clast-supported breccia composed mainly of tabular clasts which locally show apparent imbrication e.g. at A. Note, however, opposed clast stacking at B - the overall fabric is random. Aftenstjernesø Formation, locality 10, west Peary Land.

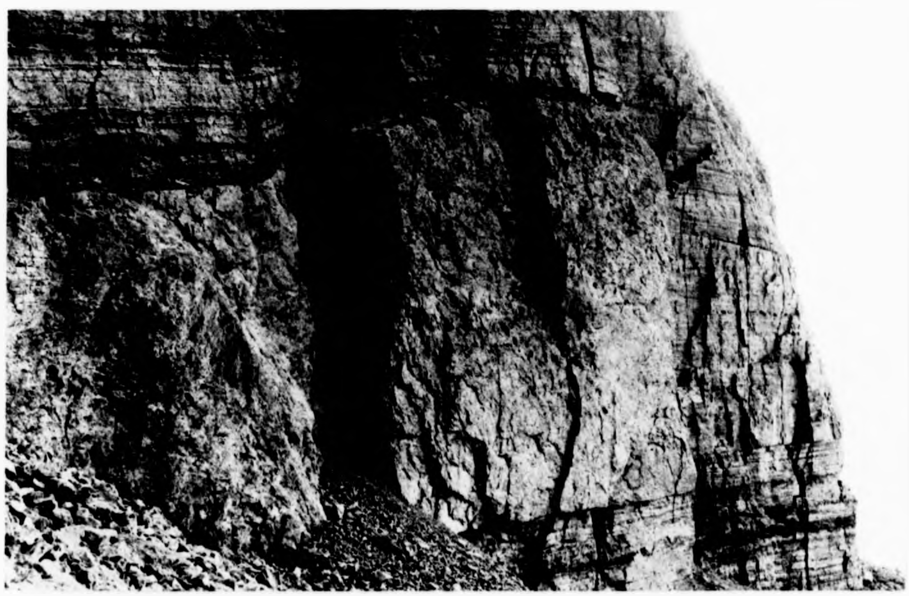

Figure 6.59. 10m thick dolomite breccia bed (LF.9) with a flat, non-erosional base and an irregular, hummocky top. Aftenstjerensø Formation, locality 2, west Peary Land.

Indeed, demonstrably lenticular beds commonly have planar, non-erosive bases and convex-upward tops rather than a channelled base (Fig. 6.56). Some beds have irregular, undulating basal contacts with a relief of up to 2m (Fig. 6.58). Significantly, where the lower boundary is irregular, corresponding irregularities are not observed at the upper surface (Fig. 6.58).

The upper surfaces of the breccia beds range from planar or gently undulating to hummocky and highly irregular (Figs 6.53, 6.59, 6.60 & 6.61); 65% of beds have flat, planar tops. The irregular upper surfaces are of two types:- (a) wavy, hummocky surfaces that are largely independent of clast size or internal fabric, and (b) irregular tops that result from the protrusion of large clasts above the general level of the breccia bed. In cross-section, type (a) describe roughly symmetrical gentle waves (Fig. 6.60) or irregular hummocks (Fig. 6.59) with a relief of up to several metres. In plan view, they form irregular mounds with no recognizable linear form. No relationship was observed between clast fabric within the breccias and the hummocky upper surfaces. In a few composite beds, the irregular hummocks are related to areas of superposed breccia phases (Fig. 6.72).

Type (b) occurs in 5% of measured beds and produces spectacular breccia beds. Pale, rectangular or equidimensional blocks of structureless or cross-bedded dolomite up to 100x30m in cross-section, locally project high above the surrounding breccia bed and are draped by overlying sediments (Fig. 6.61). In Løndal, a pale, cross-bedded block (30x35m) with sub-vertical bedding protrudes 15m above the surrounding breccia bed (Fig. 3.57). Other examples were recognized in cliffs at Buen and in Fimbuldal (Fig. 6.61). In such inaccessible cliff faces, these

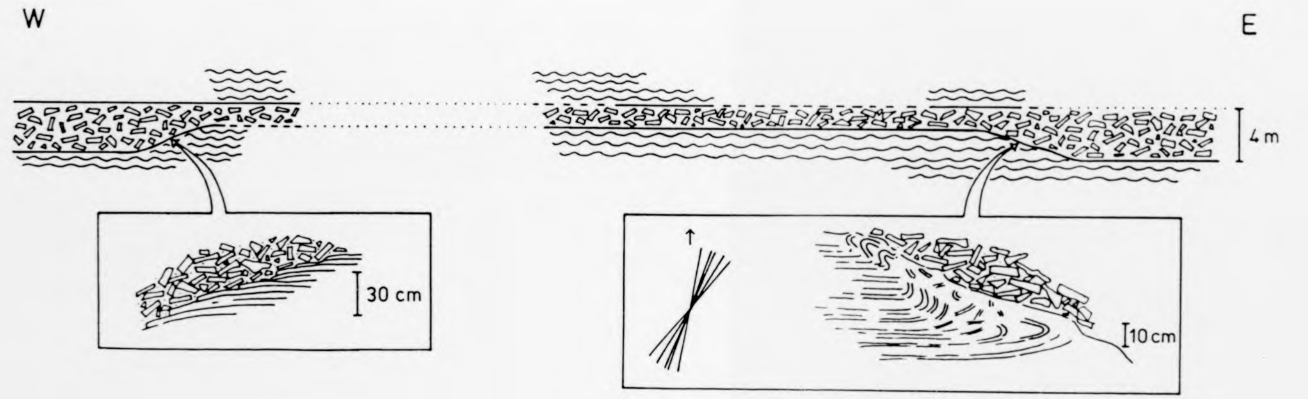


Figure 6.58. Sketch of a limestone breccia bed (LF.9) with an irregular base and a flat top. Insets show details of the irregular contacts. Drag fold axes are oriented NNE-SSW (see spoke diagram) and folds are overturned towards the west, indicating flow towards the WNW. Hence, although superficially resembling channel margins, the basal irregularities are not related to flow direction. Drawn from photographs and field sketches. Ekspedition Bræ Formation, locality 10, west Peary Land.

Figure 6.60. Pale breccia bed (arrowed) near the base of the Fimbuldal Formation, with a hummocky upper surface. Height of exposed cliff about 300m i.e. relief on breccia bed of up to 10m. Northside of Ekspedition Bræ , viewed towards the north, east Freuchen Land.

Figure 6.61. Pale breccia bed (LF 9; arrowed), about 10m thick containing large pale carbonate clasts. Block A is estimated to be 30 x 75m in cross-section. B: Brønlund Fjord Group, F: Fimbuldal Formation. South side of Fimbuldal, west Peary Land, viewed towards the south.

Figure 6.60. Pale breccia bed (arrowed) near the base of the Fimbuldal Formation, with a hummocky upper surface. Height of exposed cliff about 300m i.e. relief on breccia bed of up to 10m. Northside of Ekspedition Bræ , viewed towards the north, east Freuchen Land.


Figure 6.61. Pale breccia bed (LF 9; arrowed), about 10m thick containing large pale carbonate clasts. Block A is estimated to be 30 x 75m in cross-section. B: Brønlund Fjord Group, F: Fimbuldal Formation. South side of Fimbuldal, west Peary Land, viewed towards the south.

blocks show a gross resemblance to in situ reef carbonates, a problem recognized by Mountjoy *et al.* (1972).

Clasts

The breccias are composed of two distinct clast types. Over 75% of the beds are composed wholly of tabular or platy clasts of mid- or dark grey lime mudstone and skeletal, peloidal lime wackestone or their dolomitized equivalents - pale to dark grey, coarse crystalline dolomite. Rectangular or equidimensional blocks of pale, structureless or cross-stratified dolomite or lime grainstone are less significant volumetrically, occurring in only 22% of measured beds where they are subordinate to the tabular, fine-grained clasts.

The tabular clasts are mainly of medium pebble to coarse cobble size, with a mean length of 0.09m. Large slabs of thin-bedded carbonate up to 10x20m in cross-section occur locally and may show internal deformation and incipient disaggregation into elongate pebble- to cobble-sized clasts (*cf.* Cook & Taylor 1977). Rectangular outlines are typical but a wide variety of shapes are present, from angular tablets or platy sheets to irregular clasts with rounded margins (Figs 6.57 & 6.62). The low sphericity and irregular amoeboid outline of many of the latter clasts suggests that rounding was not the result of attrition but rather that the clast shape was inherited from an original nodular bedding structure. The occurrence of large slabs of partially disaggregated nodular carbonate within breccia beds supports this suggestion (Fig. 6.63). Some beds are composed wholly of thin (5 - 20mm thick) platy clasts that are closely comparable to the platy nodular carbonates (Lithofacies 4) of this association (Fig. 6.64).

Figure 6.62. Clast-supported dolomite breccia (LF.9) composed of pebble to cobble-sized clasts with a dark interstitial matrix. Note irregular, nodular-shaped clasts (arrowed) and the weak alignment of tabular clasts parallel to bedding. Aftenstjernesø Formation, locality 1, east Peary Land.

Figure 6.62. Clast-supported dolomite breccia (LF.9) composed of pebble to cobble-sized clasts with a dark interstitial matrix. Note irregular, nodular-shaped clasts (arrowed) and the weak alignment of tabular clasts parallel to bedding. Aftenstjernesø Formation, locality 1, east Peary Land.

Figure 6.63. Partially disaggregated slab of nodular dolomite within a dolomite breccia bed (LF.9). Note the similarity between the pale breccia clasts (lower left) and the disrupted pale nodules. Aftenstjernesø Formation, locality 21, central Peary Land.

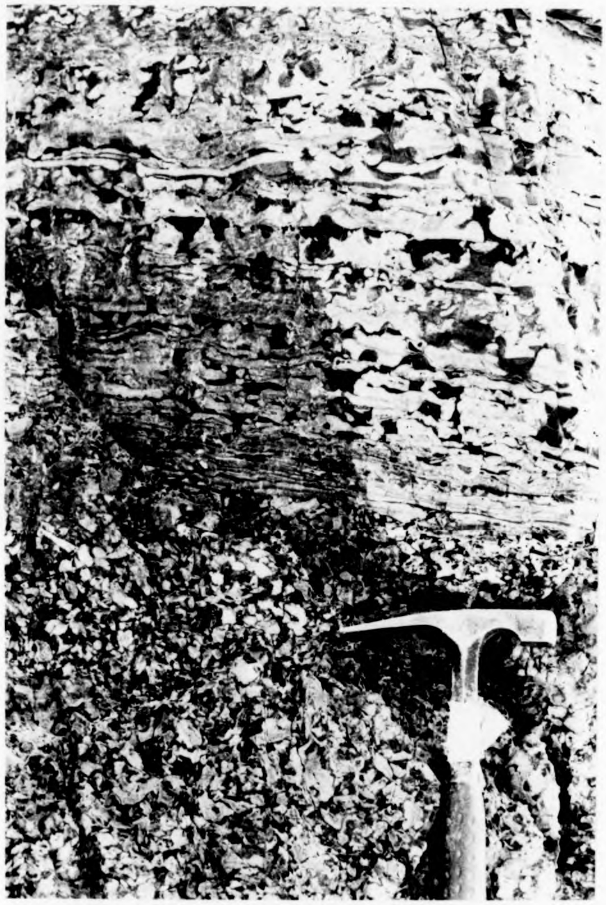

Figure 6.63. Partially disaggregated slab of nodular dolomite within a dolomite breccia bed (LF.9). Note the similarity between the pale breccia clasts (lower left) and the disrupted pale nodules. Aftenstjernesø Formation, locality 21, central Peary Land.

Figure 6.64. Clast-supported dolomite breccia (LF.9) composed mainly of thin platy clasts. Sydpasset Formation, locality 10, west Peary Land.

Figure 6.64. Clast-supported dolomite breccia (LF.9) composed mainly of thin platy clasts. Sydpasset Formation, locality 10, west Peary Land.

The pale lime grainstone and dolomitized grainstone clasts range from millimetre-sized chips to huge, house-sized, blocks (Fig. 6.61). They are white, pale yellow or cream coloured and are internally structureless or cross-bedded. Rectangular or equidimensional angular blocks dominate but sub-rounded clasts occur locally (Fig. 3.41). Grainstone clasts were only recognized in beds over 1m in thickness and consequently are mainly dolomitized (Fig. 6.52). Undolomitized grainstone blocks were recorded from a single bed (Fig. 3.41) where they comprise ooidal and peloidal, intraclastic grainstones; early diagenetic, isopachous calcite rim-cements are truncated at clast margins (Figs 6.65 & 6.66).

Matrix

The breccia beds have a pervasive grey or black carbonate matrix. In undolomitized beds, it comprises dark lime mudstone or peloidal, skeletal lime wackestone (Fig. 6.65). Dolomitized matrix comprises equigranular, medium crystalline dolomite.

The proportion of matrix ranges from 10% to 90%; matrix-free breccia beds are not observed. In a study of 85 beds, 80% are clast-supported (matrix < 30%; Clifton 1973), 7% are matrix-supported and insufficient detail is preserved in the remaining beds to estimate the relative proportions. 'Clasts' were generally taken to be larger than granule size (> 4mm), but in many cases the definition of a clast-supported framework based on an arbitrary grain-size division is artificial since large clasts may be supported in a sea of finer breccia that acts as matrix (Figs 6.67 & 3.41). The majority of beds however show a clear bimodal grain size population and have an undisputed clast-supported framework with an interstitial pervasive fine-grained matrix

Figure 6.65. Photomicrograph (PPL) of limestone breccia (LF.9) containing lime mudstone (M; commonly neomorphic microspar) and intraclastic, peloidal grainstone clasts (G) in a dark argillaceous lime mudstone matrix. Note sharp margin of grainstone clast, truncating grains and sparry cement (arrow). Dark stylolites common along clast boundaries. Scale bar = 1mm. GGU 218619, Fimbuldal Formation, locality 4, west Peary Land.

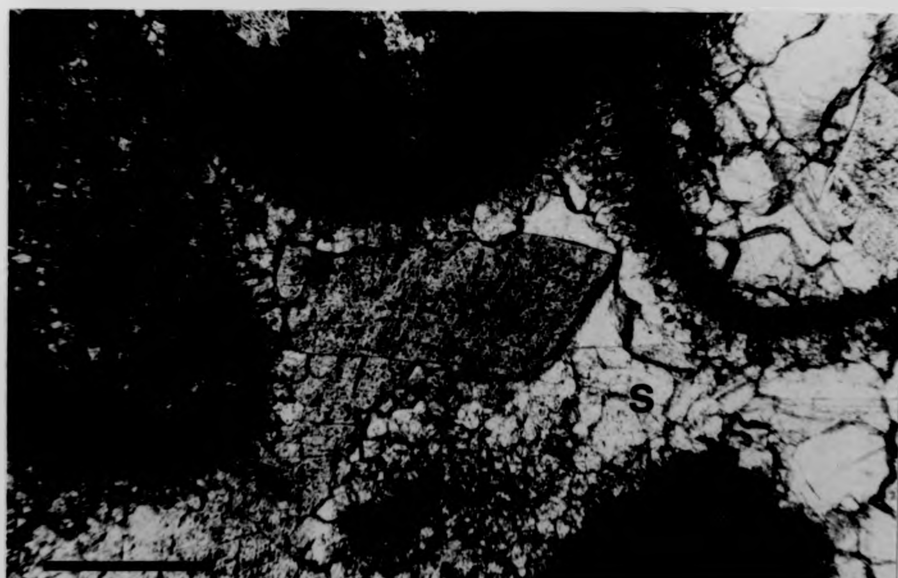


Figure 6.66. Photomicrograph (PPL) showing early fibrous rim cement (arrow) coating ooids and peloids in a lime grainstone clast from a limestone breccia bed (LF.9). S : blocky calcite spar cement; D : dolomite. Scale bar = 0.5mm. GGU 218618, Fimbuldal Formation, locality 4, west Peary Land.

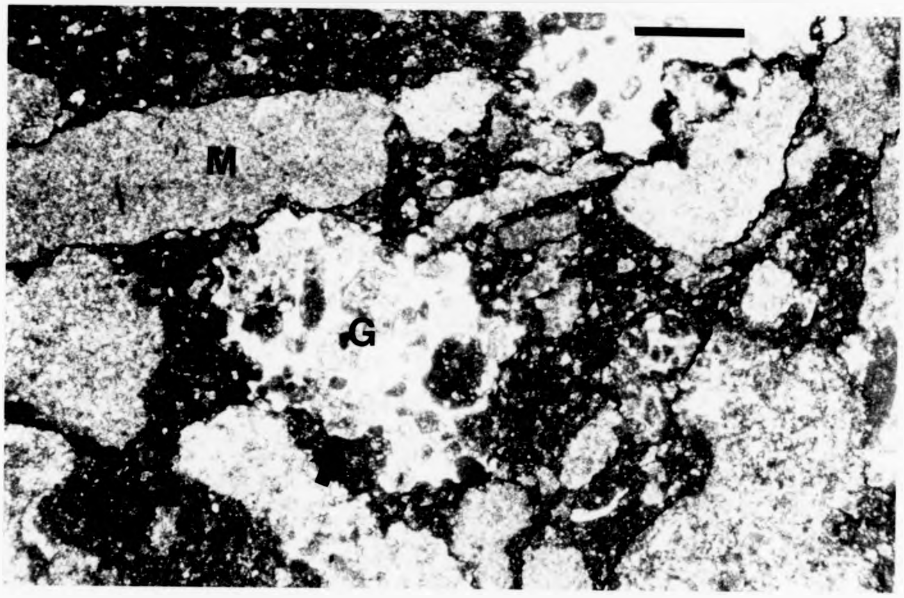


Figure 6.65. Photomicrograph (PPL) of limestone breccia (LF.9) containing lime mudstone (M; commonly neomorphic microspar) and intraclastic, peloidal grainstone clasts (G) in a dark argillaceous lime mudstone matrix. Note sharp margin of grainstone clast, truncating grains and sparry cement (arrow). Dark stylolites common along clast boundaries. Scale bar = 1mm. GGU 218619, Fimbuldal Formation, locality 4, west Peary Land.

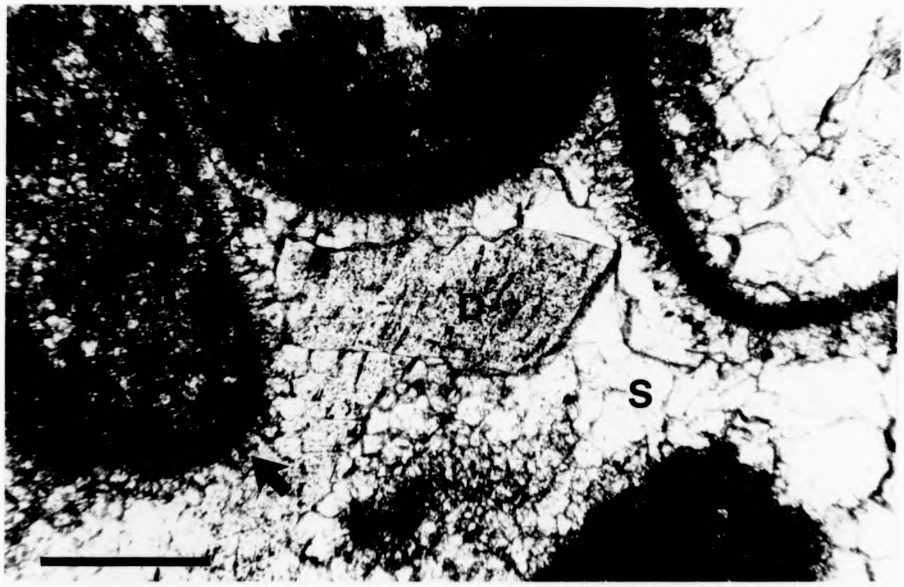


Figure 6.66. Photomicrograph (PPL) showing early fibrous rim cement (arrow) coating ooids and peloids in a lime grainstone clast from a limestone breccia bed (LF.9). S : blocky calcite spar cement; D : dolomite. Scale bar = 0.5mm. GGU 218618, Fimbuldal Formation, locality 4, west Peary Land.

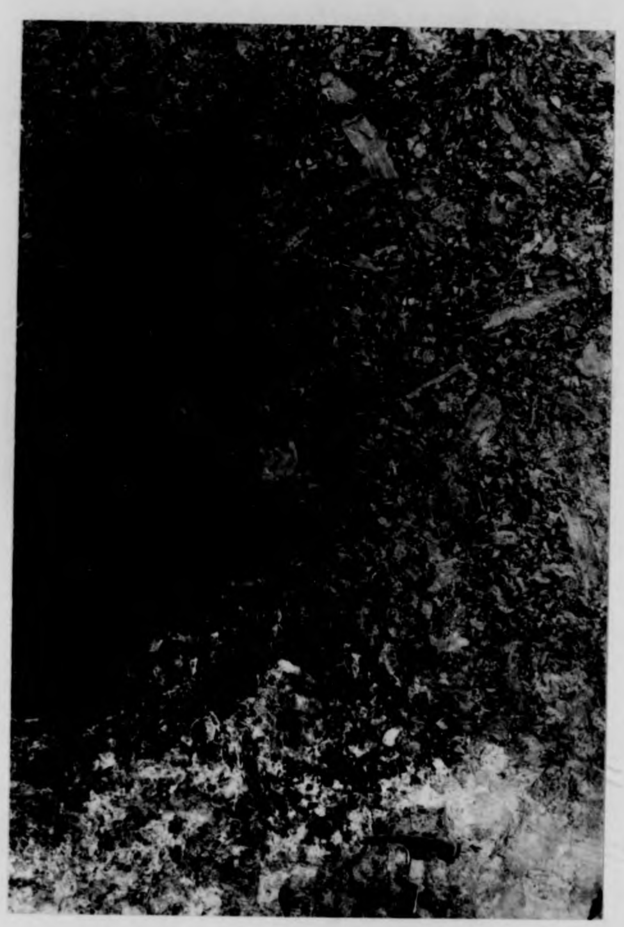

Figure 6.67. Dolomite breccia (LF.9) composed of randomly oriented cobble-sized clasts supported in a matrix of fine-grained breccia. Aftenstjernesø Formation, locality 21, central Peary Land.

Figure 6.67. Dolomite breccia (LF.9) composed of randomly oriented cobble-sized clasts supported in a matrix of fine-grained breccia. Aftenstjernesø Formation, locality 21, central Peary Land.

(Figs 6.57 & 6.62). In places, the clast-rich nature of these beds is exaggerated by stylolitization at clast contacts (Fig. 6.65).

## Grading and Fabric

The breccia beds are mainly massive and unstratified (Fig.6.53). They are very poorly sorted, comprising clasts from a few millimetres to tens of metres across with a pervasive fine-grained matrix (sand to clay grade). Some beds show moderate sorting of the coarse fraction (Fig. 6.62) although this is probably a feature inherited from the source material rather than sorting developed during transport (see Figs 6.63 & 6.68).

The breccia beds fall into three groups - ungraded beds (73%), partially graded beds (24%) showing normal coarse-tail grading in only the upper portion of the bed, and beds showing normal coarse-tail grading throughout (3%). Distribution grading and inverse grading are absent.

In the partially graded beds the bulk of the bed is poorly sorted and ungraded; normal coarse-tail grading is often restricted to the upper few tens of centimetres of the bed. The graded interval may form the upper half of the bed however (Fig. 6.54) and,where well-developed,clast-supported breccia grades upward into dark, structureless or vaguely stratified dolomite with rare, widely dispersed clasts (Figs 6.69 & 6.70).

Continuous normal coarse-tail grading is rare and was recognized in only two beds. In the clast-supported dolomite bed depicted in Fig. 6.71, the average clast size of the coarse fraction

Figure 6.68. Bedded slab within a dolomite breccia bed (LF.9) showing brecciation and partial disaggregation. Note that a breccia derived from this slab would show a bimodal clast distribution, determined by the lithology and state of differential lithification of the source rock. Note also that the coarse fraction would appear relatively well-sorted. Aftenstjernesø Formation, locality 10, west Peary Land.

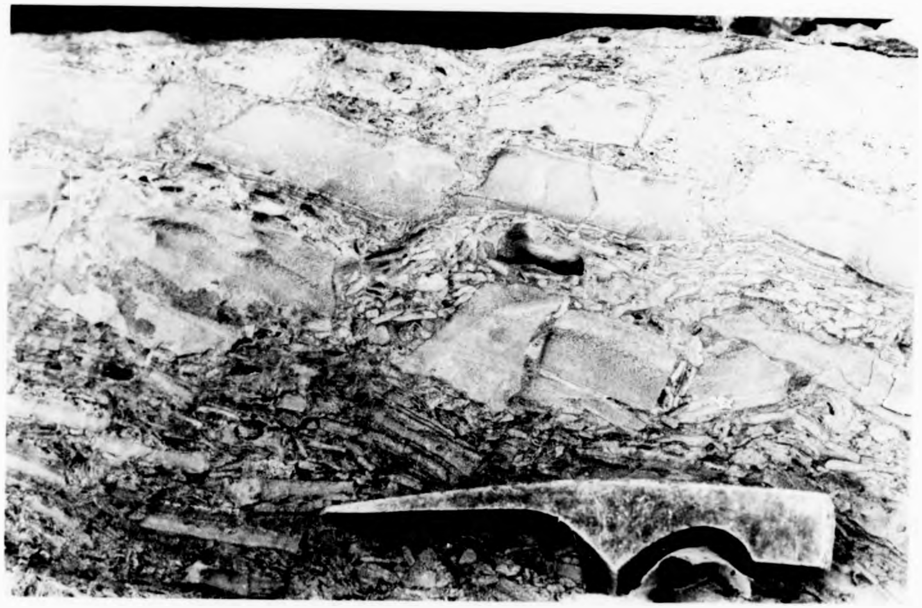

Figure 6.68. Bedded slab within a dolomite breccia bed (LF.9) showing brecciation and partial disaggregation. Note that a breccia derived from this slab would show a bimodal clast distribution, determined by the lithology and state of differential lithification of the source rock. Note also that the coarse fraction would appear relatively well-sorted. Aftenstjernesø Formation, locality 10, west Peary Land.

Figure 6.69. A 10m thick dolomite breccia bed (LF.9); approximate base and top arrowed. Hammer (small arrow) for scale. The lower two-thirds is ungraded clast-supported breccia showing a weak bedding-parallel clast fabric. Grades normally in upper third into structureless dark dolomite, overlain sharply by a pale dolomite cap. Aftenstjernesø Formation, locality 1, east Freuchen Land.

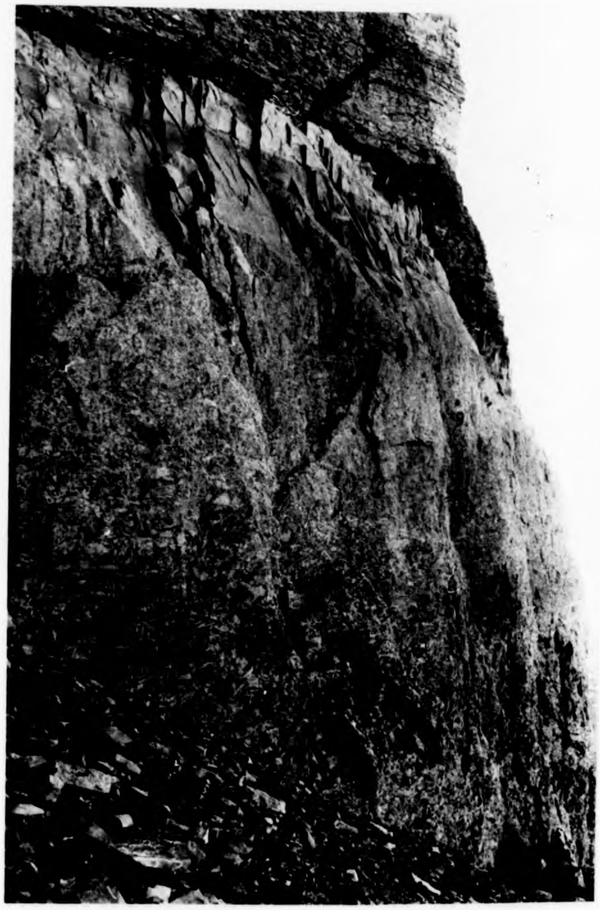

Figure 6.69. A 10m thick dolomite breccia bed (LF.9); approximate base and top arrowed. Hammer (small arrow) for scale. The lower two-thirds is ungraded clast-supported breccia showing a weak bedding-parallel clast fabric. Grades normally in upper third into structureless dark dolomite, overlain sharply by a pale dolomite cap. Aftenstjernesø Formation, locality 1, east Freuchen Land.

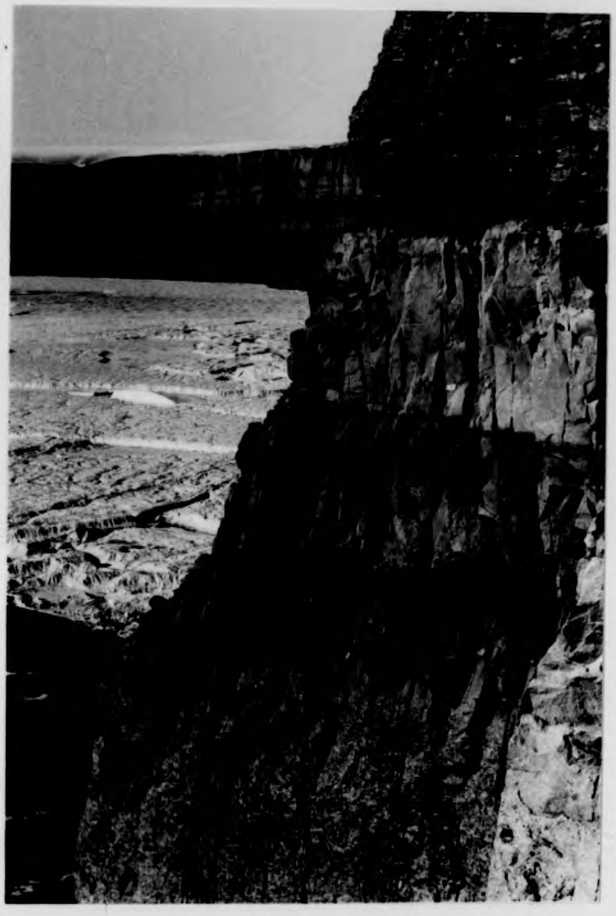

Figure 6.70. Upper levels of dolomite breccia bed (LF.9) shown in Fig. 6.69. Normally graded upper zone capped by a pale dolomite bed ('dolomite grainstone') with a sharp, planar base and top (90cm thick). Aftenstjernesø Formation, locality 1, east Freuchen Land.

Figure 6.70. Upper levels of dolomite breccia bed (LF.9) shown in Fig. 6.69. Normally graded upper zone capped by a pale dolomite bed ('dolomite grainstone') with a sharp, planar base and top (90cm thick). Aftenstjernesø Formation, locality 1, east Freuchen Land.


Figure 6.71. Dolomite breccia bed (LF.9) showing normal coarse-tail grading of equidimensional clasts. Note erosional base and floating tabular clasts in upper levels. Sydpasset Formation, locality 2, west Peary Land.

decreases from 0.1m at the base to 0.015m in the upper half of the bed. Interestingly, despite this normal coarse-tail grading of equidimensional clasts, large tabular rafts of thin-bedded carbonate occur at any level in the bed and are common within pebble-sized breccia near the top of the bed (Fig. 6.71).

No relationship has been recognized between matrix : clast ratio, bed thickness and presence or absence of grading, but graded beds generally have flat, planar tops. whereas ungraded beds show both planar and hummocky upper surfaces.

Elongate, tabular clasts are randomly oriented or show a preferred orientation subparallel to bedding. Disorganized, chaotic fabrics are dominant, accounting for well over half of the beds in which clasts are recognizable (Fig. 6.67). Clasts are locally stacked and define an apparent imbrication but adjacent areas within the same bed commonly show opposed stacking orientations and the overall fabric is random (Fig. 6.57). The scarcity of bedding-plane exposure and three-dimensional exposure of clasts precluded a detailed quantitative study of clast fabric but in vertical, two-dimensional exposures, no significant imbrication was recognized.

Bedding-parallel fabrics vary from weakly developed in which only large clasts (> 0.3m) are oriented within a chaotic, finer-grained breccia (Fig. 6.62), to well-developed, in which the majority of tabular, elongate clasts are oriented parallel to bedding.

<u>Composite beds</u>

Five composite beds were recognized. The term 'composite' is used here to describe individual breccia beds that can be subdivided into separate zones on the basis of clast density, orientation, lithology or shape. These zones are lenticular, pinch and swell laterally and are commonly impersistent and merge to form homogeneous breccia. Composite beds are thus distinguished from multiple breccia sequences formed of superposed, amalgamated discrete breccia beds (e.g. Fig. 3.64).

A well-exposed composite bed is depicted in Fig. 6.72. The lower zone, which locally forms the whole bed, is a clast-supported breccia composed of dark tabular clasts and large, thin-bedded slabs; pale sucrosic dolomite clasts are rare. The upper clast-supported breccia is composed mainly of blocky, equidimensional clasts of pale cream dolomite that locally show cross-bedding; dark tabular clasts and bedded slabs are scarce. The lower zone is persistent laterally but varies in thickness and is locally subordinate to the upper pale breccia. Where the upper zone is absent the breccia shows normal coarse-tail grading in its upper levels and is capped by a pale yellow, structureless or graded dolomite bed (see below). Passing laterally into the composite region, the bed thickens, the upper surface becomes irregular or hummocky and the pale capping bed is discontinuous, occurring preferentially within hollows on the irregular breccia surface (Fig. 6.72).

The contact between the two zones undulates markedly and, although locally sharp it is generally gradational over a few centimetres. It is delineated by a thin matrix-rich interval, 0.01 - 0.1m thick (Fig. 6.73); the lower zone grades rapidly into this interval and locally displays a weak alignment of clasts parallel to the boundary.

Grainstone caps.

43% of breccia beds have a capping bed of lime grainstone or

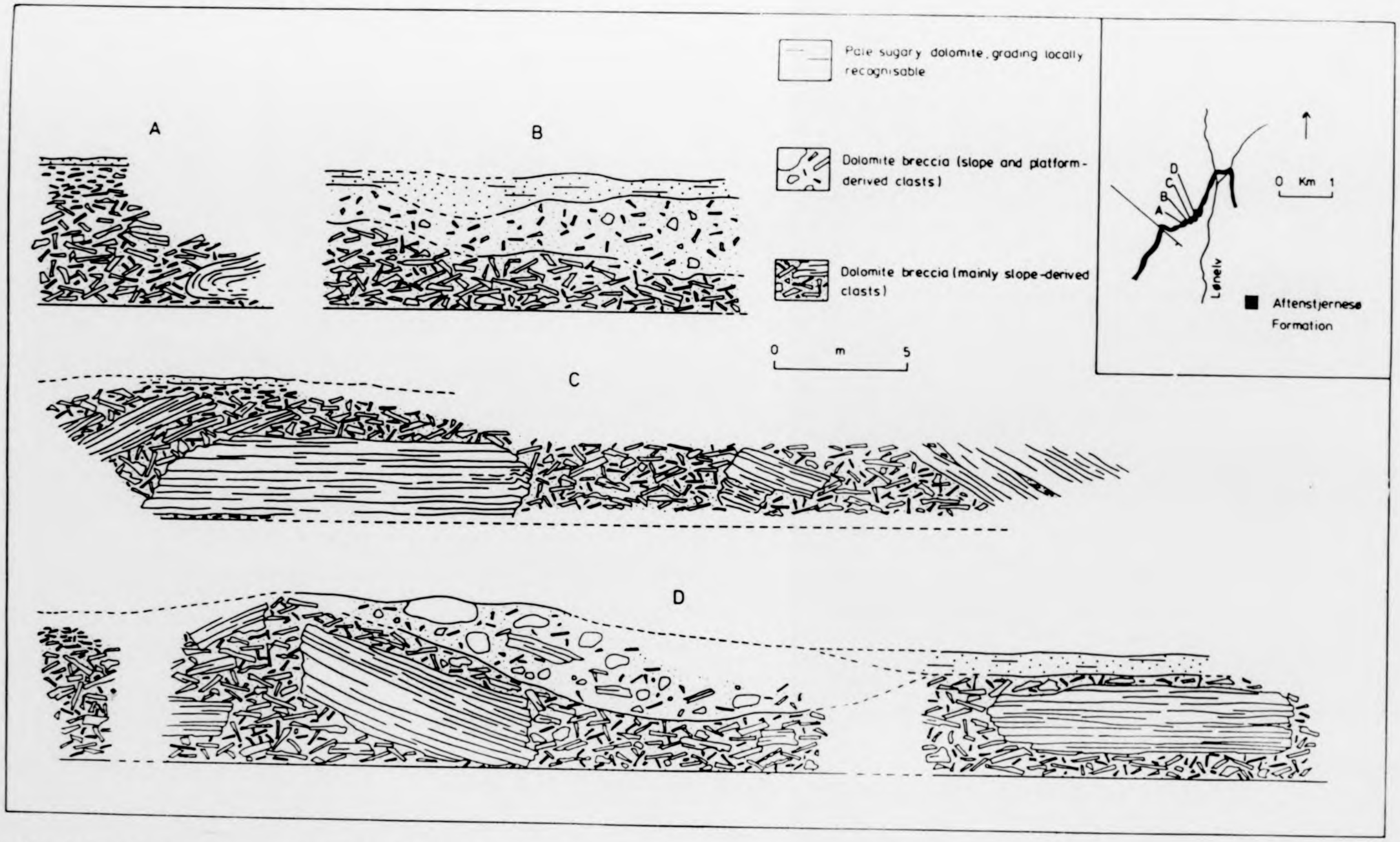


Figure 6.72. Lateral variation in a composite breccia bed (LF.9) in the Aftenstjernesø Formation, locality 10, west Peary Land.

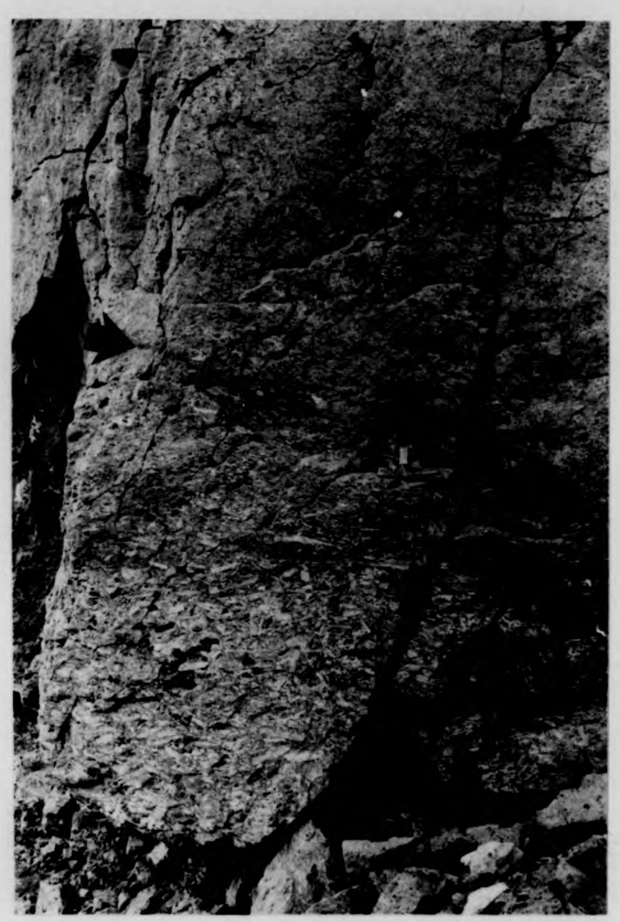

Figure 6.73. Contact (arrowed) between the two distinct zones of the composite dolomite breccia bed (LF.9) shown in Fig. 6.72 (section B). Junction between the lower, coarser-grained and upper vuggy breccias marked by a thin matrix-rich band.

Figure 6.73. Contact (arrowed) between the two distinct zones of the composite dolomite breccia bed (LF.9) shown in Fig. 6.72 (section B). Junction between the lower, coarser-grained and upper vuggy breccias marked by a thin matrix-rich band.

pale-coloured, medium to coarse crystalline dolomite. They range between 0.08 and 2 m in thickness with a mean of 0.6 m (Fig. 6.74). Over half of these beds form laterally continuous sheets capping parallel-bounded breccia beds. The lower breccia bed of the Aftenstjernesø Formation, for example, has a distinctive dolomite cap that can be traced in continuous exposure for at least 5km south of Ekspedition Bræ (Figs 6.54, 6.69 & 6.70). Capping beds may be absent or discontinuous on hummocky breccia beds; where present, they are often confined to depressions, pinching out or thinning over the hummocks (Figs 6.54 & 6.72). A plot of breccia bed thickness against cap thickness shows a positive linear relationship (significant at the 99.9% level), disregarding the beds capping composite breccia beds (Fig. 6.74). This suggests that the breccia beds and the succeeding grainstone caps are genetically related.

In undolomitized sections, capping beds comprise peloidal, intraclastic and skeletal lime grainstones and packstones, commonly exhibiting normal grading. Lime mudstone and wackestone intraclasts range from coarse pebble to sand grade and are angular to sub-rounded. Some beds are rich in abraded skeletal debris that includes trilobite and pelmatozoan fragments. Equivalent dolomite beds generally yield little relict textural information, although lithoclasts and vague peloidal 'ghosts' are sometimes recognizable. By analogy with the undolomitized beds however, the pale dolomite caps represent dolomitized grainstones or packstones (shortened to 'dolomite grainstone' on many figures).

Bed bases are typically sharp and may be planar (Fig. 6.70) or erosional, locally displaying scours and load structures (Figs 6.72

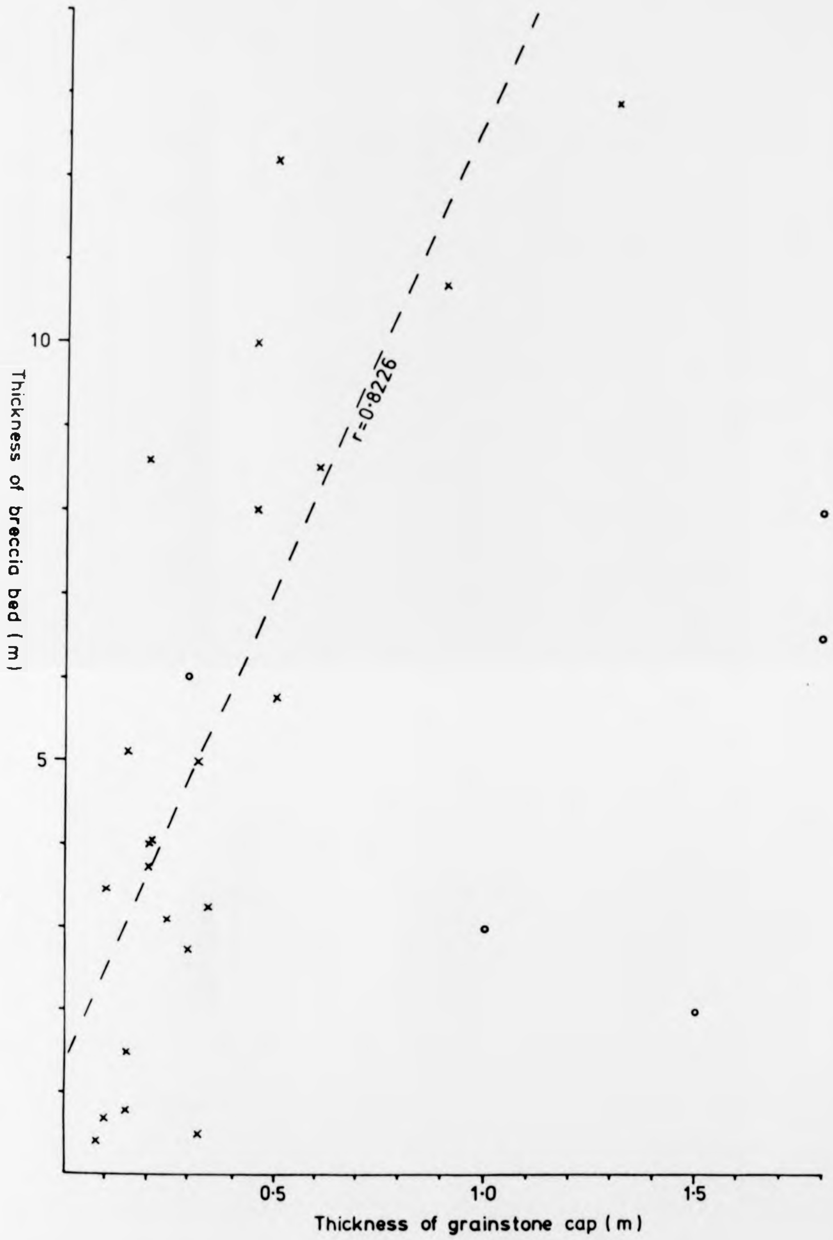


Figure 6.74. Plot of breccia bed thickness versus thickness of grainstone capping bed. Beds capping composite breccias denoted by open circles.

& 6.75). Protruding clasts in the underlying breccia bed are draped or flanked by the grainstone bed. Gradational contacts with the underlying breccia were observed rarely. Structureless beds predominate particularly where dolomitized (Fig. 6.70) but favourably weathered surfaces often show a graded or structureless basal interval, passing up into parallel-laminated and ripple cross-laminated carbonate (Figs 6.54 & 6.75). Bed tops are mainly sharp and planar or current rippled but are locally gradational where bioturbated. Four dolomite capping beds show a more complex multiple graded structure with one or more diffuse intraclastic horizons (0.05 - 0.15m thick) rich in small (5 - 20mm) angular clasts, interstratified with structureless pale dolomite. It is significant that three of these atypical beds overlie composite breccia beds.

Interpretation

Poor sorting, pervasive fine-grained matrix, lack of stratification and chaotic, disorganized clast fabrics are characteristic features of subaerial debris flow deposits (Johnson 1970; Pierson 1980), and comparable carbonate rudites from ancient and modern carbonate sequences have been interpreted as the deposits of submarine debris flows (e.g. Cook *et al.* 1972; Davies 1977; Crevello & Schlager 1980). In ideal debris flow however, clasts are supported during flow by buoyancy and the cohesive strength of the matrix (Middleton & Hampton 1973); consequently a matrix-supported framework is often considered to be a prerequisite for inferring a debris flow origin (Nardin *et al.* 1979). Theoretical studies (Middleton & Hampton 1973) and observations of natural subaerial debris flows (Johnson 1970) have demonstrated that plastic flows of this type may contain less than 10% fine-grained matrix and ancient clast-rich deposits are commonly included under the debris

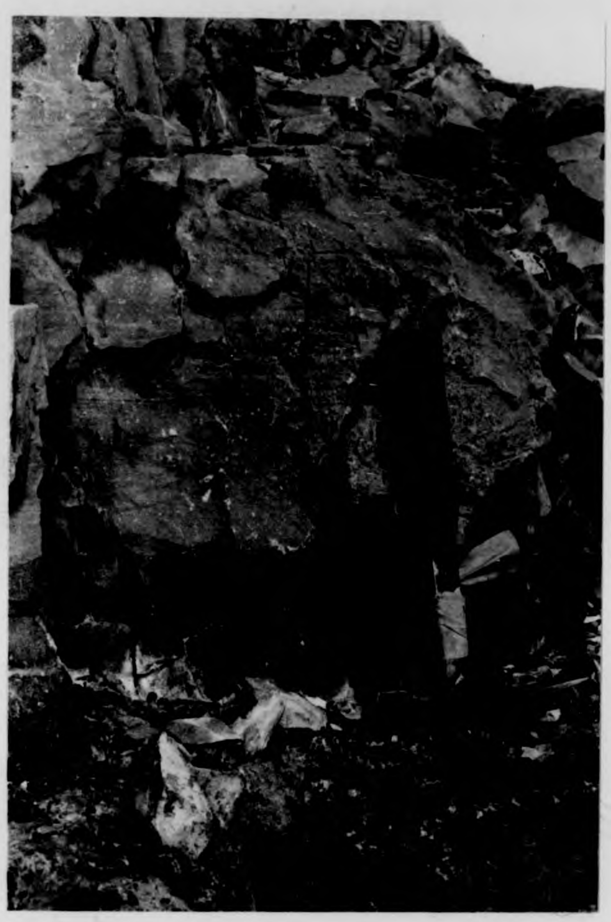

Figure 6.75. Pale dolomite bed, overlying the graded top of an 8m breccia bed. Note the sharp, scoured base, the structureless lower division and the parallel-laminated upper division. Aftenstjernesø Formation, locality 4, west Peary Land.

Figure 6.75. Pale dolomite bed, overlying the graded top of an 8m breccia bed. Note the sharp, scoured base, the structureless lower division and the parallel-laminated upper division. Aftenstjernesø Formation, locality 4, west Peary Land.

flow label (e.g. McIlreath 1977). Indeed, Hampton (1975) suggested that "most real debris flows are probably combination debris flow-grain flows" and Pierson (1981) described a modern clast-rich debris flow in which frictional forces between clasts were determined to be an important clast-support mechanism, commonly exceeding the combined effects of buoyancy and matrix strength. To resolve this problem, Lowe (1979, 1982) redefined debris flow to describe all plastic flows ranging from cohesive debris flow (or mudflow), in which grains are entirely supported by the cohesive matrix, to grain flow in which dispersive pressure provides grain support. Cohesive debris flow and grain flow form the end members in a spectrum of natural plastic flows, in which matrix strength, buoyancy, dispersive pressure and even turbulence (see Enos 1977) may contribute to clast support (Lowe 1982).

Clast-supported fabrics are typical of the carbonate breccia beds described here and dispersive pressure probably played a significant clast-supporting role during flow (Ineson 1980). Thus, they are interpreted as the deposits of submarine debris flows, *sensu* Lowe (1979) i.e. flows transitional between 'true' cohesive flows and density modified grain flows.

Debris flow deposits typically have flat, non-erosive bases and irregular, hummocky tops. Large outsized clasts are commonly rafted passively in the upper levels of the flow, buoyed up by the clast-rich slurry (Rodine & Johnson 1976). Johnson (1970) compared the flow of such debris to that of other laminar flows, such as the flow of ice or lava. Where such flows traverse an irregular surface or encounter an obstruction, the irregularity is rarely reproduced on the upper surface of the flow and deposition from the flow results in a smoothing out of topographic irregularities (e.g. Fig. 6.58). The lenticular, convex-upward profile of some beds (Fig. 6.56) and the irregular hummocky surfaces testify to the cohesive strength of the debris. Abrupt 'snouts' are typical of the margins of subaerial debris flow deposits (Johnson 1970) but are rarely recorded from inferred submarine deposits (see, however, Padget *et al.* 1977). In this study, breccia beds wedge out gradually and no reliable examples of steep margins were recorded; this may reflect a lower viscosity in the submarine environment resulting from the ample opportunity for mixing and dilution by seawater.

Clast fabrics are typically random in debris flow deposits (Middleton & Hampton 1973, Nardin *et al.* 1979) but bedding-parallel fabrics have been recorded (Lindsay 1966) and are considered to be indicative of laminar flow. Enos (1977) suggested that although much of the load in a debris flow may be transported as a rigid plug above a basal zone of laminar flow, the boundaries of the plug are likely to migrate during flow producing a parallel fabric throughout the resulting deposit (see also Hampton 1975).

The occurrence of coarse-tail grading in about 25% of the breccia beds indicates that, in these flows, clasts were able to move relative to one another within the flow (Walker 1965). In most of these beds, the grading is restricted to the upper portion and reflects a loss of competence in the upper levels of the flow and consequent downward settling of the coarse clast fraction. Surlyk (1978) attributed partial grading in conglomerates to the downward migration of the rigid plug prior to freezing of the debris flow. The upper graded interval was envisaged as the zone of shear that developed above the rigid plug; Naylor (1980) developed a similar model based on shear weakening of the fine-grained matrix at the flow boundaries. Alternatively, the loss of competence may have resulted simply from matrix dilution due to mixing with seawater at the flow surface. The graded zone commonly shows a horizontal clast fabric and a weak parallel stratification suggesting that flow remained laminar and that partial grading did not result from a flow transformation such as the development of turbulence (see Fisher 1983).

The rare beds showing continuous grading, however, reflect more mature flows that allowed extensive vertical and lateral segregation of clasts of differing size (Surlyk 1978). Parallel clast fabrics and outsized slabs within the upper levels of these beds suggest laminar flow conditions and significant cohesive strength. However, basal erosional contacts and well-developed normal grading are suggestive of turbulent flow conditions. Following Lowe (1982) these beds probably represent cohesive flows that were turbulent at flow peak. As the flow declined and turbulence was dampened the graded basal interval was deposited by suspension settling; laminar flow conditions were established and the upper levels of the bed with outsized clasts were deposited by cohesive freezing.

The grainstone caps are in sharp contrast to the underlying breccias, even in dolomitized sequences, and clearly reflect a different depositional process; the positive correlation between cap and breccia bed thickness, however, indicates a genetic relationship. The high degree of sorting, well-developed grading and sharp, erosional bases suggest deposition from waning, turbulent flows; beds showing grading, parallel lamination and ripple cross-lamination are favourably compared with classical ABC turbidites (Bouma 1962). Hampton (1972) demonstrated experimentally that sediment stripping at the nose and upper surface of a subaqueous debris flow can result in an accompanying turbulent current (the surface flow transformation of Fisher 1983). Krause & Oldershaw (1979) used this observation to explain the occurrence of turbidite caps on carbonate mass-flow breccias in the Cambrian of the Mackenzie Mountains, north-west Canada. Following these workers, the grainstone caps are interpreted as the deposits of turbidity currents that developed in association with and in response to submarine debris flows (Ineson 1980).

It is useful, at this point, to consider the evidence of flow evolution. Fig. 6.54 shows the distribution of and lateral variation within a single, well-exposed breccia bed. Independent evidence (basal drag folds) indicates flow towards the NNW, and the south to north variation reflects the proximal to distal evolution of a single gravity flow. In southern exposures, the disorganized breccia bed contains large, partially disaggregated slump-folded rafts and the transport mechanism may have been transitional between debris flow and slumping (*cf.* Cook 1979). The succeeding grainstone bed has a gradational base, is commonly structureless and is laterally impersistent, occurring only in depressions on the irregular breccia surface. Northwards, the bed shows better sorting of the coarse clast fraction and develops partial grading and a parallel clast fabric. The grainstone cap is laterally persistent and commonly displays the Bouma ABC divisions. This south to north transition reflects increasing maturity of the sediment gravity flow with flow distance and compares well with the model for downslope variation in carbonate breccia beds proposed by Krause & Oldershaw (1979) based on the resedimented conglomerate facies models of Walker (1975).

Comparison between the lithology of breccia clasts and that of *in situ* carbonate facies indicates that most of the detritus originated within the outer shelf-slope environment. The dominant tabular, nodular lime mudstone, wackestone and packstone clasts (and their dolomitized equivalents) are closely comparable to rocks assigned to the unstable shelf and upper slope assemblages. Slump scars, folds and slump-breccia beds in the upper slope assemblage reflect sediment instability in this environment and suggest that debris flows commonly originated as slumps or slides (*cf.* Cook 1979). The presence of slabs of partially disaggregated thin-bedded carbonate and nodular clasts in these beds indicates that the dominant clast size and morphology was mainly inherited from the bedding style and differentially lithified nature of the source material (*cf.* Hopkins 1977).

The pale grainstone clasts are lithologically identical to the cross-bedded, ooid-dominated grainstones of the platform margin association (7.1.2). Their incorporation in mass flows dominated by clasts derived from outer shelf-slope environments implies a multiple transport path or composite flow mechanism. Crevello & Schlager (1980) described a modern carbonate debris flow deposit from the Bahamas, that included clasts of platform and slope origin; they suggested derivation by retrogressive slumping across the upper slope-platform margin boundary. In this study, the platform margin-slope transition is characterized by chaotic foreslope breccias composed wholly of platform edge facies. Remobilization of such detritus together with intercalated *in situ* upper slope carbonates would result in polymictic mass flow deposits as described above.

The composite breccia beds offer further evidence of complex, sequential failure at the slope-platform margin transition. In the example depicted in Fig. 6.72, the lower zone is composed wholly of tabular, slope-derived clasts, whereas the upper zone mainly comprises pale grainstone clasts, derived ultimately from the shallow-water platform margin; the grainstone cap drapes both phases and nowhere separates the two. This arrangement indicates that the two breccia zones were essentially deposited from the same mass flow and yet the contrasting clast populations reflect different source regions i.e. the composite structure did not develop purely from flow separation (*cf.* Aalto 1972). Following the work of Hendry (1973; see also Surlyk 1978) these composite beds are interpreted to be the result of retrogressive slumping - successive pulses or surges within the mass flow resulted from progressive upslope sediment failure (*cf.* Hubert 1977).

## 6.2 B1. Environmental Interpretation

### 6.2.1 General

The association of Lithofacies 1-9 defines an open marine environment, predominantly below wave base. Background sedimentation of lime and siliciclastic mud from suspension and low-density turbidity currents was periodically interrupted by deposition from slumps, slides and sediment gravity flows (turbidity currents and debris flows). Comparable ancient successions are generally referred to deep-water settings such as carbonate slope and basin environments (e.g. McIlreath & James 1978; Read 1980; Pfeil & Read 1980 and papers in Cook & Enos 1977), and present-day analogues have been documented off modern carbonate banks (Mullins & Neumann 1979; Crevello & Schlager 1980).

The occurrence of gravity-displaced and redeposited carbonate detritus obviously indicates proximity to an unstable slope, but does not necessitate appreciable slopes at the site of deposition. Indeed, in modern examples, most remobilized carbonate bypasses the slope and is deposited in basinal environments (Crevello & Schlager 1980). Unequivocal evidence of *in situ* instability is needed to distinguish carbonates deposited on an appreciable depositional slope from those deposited in a gravitationally stable environment within depositional range of an unstable slope. In this study, features indicative of *in situ* sediment instability are slump folds involving minimal lateral translation ("rooted" folds), intraformational truncation surfaces (slump-slide scars, see 6.2.2) and small-scale downslope creep structures - pull-aparts, normal microfaults, boudinage, interstratal breccias and ruck folds. The latter small-scale structures are widespread and proved the most useful indicators of syndepositional slope instability.

Studies of modern deltas and continental slopes have shown that mass wastage can occur on slopes with very low gradients (e.g Lewis 1971; Embley 1976; Dingle 1977). Coleman & Prior (1978) described slides off the Mississippi delta on open slopes as low as $0.2^{\circ}$ and Embley (1976) documented mass flows that originated on slopes of $1.5^{\circ}$ and flowed over slopes with gradients as low as $0.1^{\circ}$. Evidently, sedimentation rate and sediment bulk properties are equally as important as slope gradient in determining sediment stability (Moore 1961; Nardin *et al.* 1980; Keller *et al.* 1980). Quantitative discussion of gradients is superfluous, in any event, as no reliable method was found for estimating depositional slopes within the outer shelf associations. The asymptotic transition from foreslope deposits with depositional dips of $5\text{-}25^{\circ}$ into the outer shelf rocks (Figs. 3.47, 3.51 & 7.9) suggests that slopes on the outer shelf are unlikely to have been greater than a few degrees. As demonstrated in modern marine settings and ancient successions such gradients are sufficient to promote sediment failure and mass flow.

Significantly, however, evidence of sediment instability and mass transport is not distributed evenly through the outer shelf-slope association, either laterally or vertically within a single section. The bulk sediment properties and sedimentation rates probably did not vary significantly and the irregular distribution of these features is taken to reflect a real change in environmental conditions both in time and space.

Hence, Association B is subdivided into three assemblages (Table 6.1, Fig. 6.76) based on (i) recurrent grouping of facies (Fig. 6.76), (ii) the relative abundance of structures reflecting sediment instability and (iii) the proportion of coarse-grained sediment gravity flow deposits relative to fine-grained, mud-grade hemipelagic or low-density gravity flow deposits. These assemblages are (a) Upper slope, (b) Stable shelf and (c) Unstable shelf-slope.

The lateral and vertical succession of these assemblages is discussed in Chapter 8, in relation to the coeval shallow-water deposits but a brief introduction is useful here. Fig. 6.77 shows schematically the relationships between the four sediment associations (A-D) and their constituent assemblages in the J.P. Koch Fjord area. The upper slope assemblage forms part of the transition between the outer and inner shelf environments and consequently is a strongly diachronous unit, associated with the northward prograding platform margin. In contrast, within the available biostratigraphical zonation of this succession, the stable shelf and unstable shelf-slope associations are apparently isochronous

| | Facies present | Ratio of fine grained facies (LF. 1-7) to coarse redeposited facies (LF. 8, 9) | Breccia bed thickness | Platform margin clasts in breccias | Structures indicative of gravitational instability | Depositional Processes | Environment |
|---|---|---|---|---|---|---|---|
| UPPER SLOPE | 5. Thin-bedded skeletal carbonates (90%)<br>9. Carbonate breccia beds (8%)<br>14. Carbonate breccia beds ( 2%) | 12:1 | Range 0.5 - 4.75m<br>Commonly 0.5 - 2m<br>Mean 1.64m | Rare (occurring in less than 5% of beds) | Common slump scars, slump folds, microfaults, boudinage and interstratal-creep brecciation. | Deposition from suspension, tidal and wave-induced currents and mass flows | A gravitationally unstable environment at depths near normal wave base in aerated, well-lit waters. |
| STABLE SHELF | 3. Argillaceous lime mudstones (62%)<br>1. Bituminous laminated carbonates (24%)<br>2. Dark bioturbated dolomites (8%)<br>9. Carbonate breccia beds (4%)<br>5. Thin-bedded skeletal carbonate<br>6. Phosphoritic, glauconitic skeletal carbonate 2%<br>8. Graded carbonate | 21:1 | Range 0.2 - 6m<br>Commonly 0.2 - 1m<br>Mean 1.27m | Absent | Rare small scale slump folds. | Deposition mainly from suspension and dilute sediment gravity flows. Rare deposition from small scale mass flows and bottom currents. | A stable marine environment, mainly below wave base. Circulation generally poor. |
| UNSTABLE SHELF-SLOPE | 9. Carbonate breccia beds (43%)<br>4. Platy nodular carbonates (28%)<br>8. Graded carbonates (14%)<br>1. Bituminous laminated carbonates (12%)<br>7. Irregular nodular carbonates (3%) | 0.8:1 | Range 0.5 - 45m<br>Commonly 1 - 15m<br>Mean 8.55m | Present, (occurring in 21% of beds) | Common boudinage, pull-aparts, inter-stratal creep breccias and small-scale slump folds | Deposition from varied sediment gravity flows and suspension. | A poorly oxygenated or anoxic marine environment below wave base. Gravitationally unstable. |

TABLE 6.1 Summary of the distinguishing features of the upper slope, stable shelf and unstable shelf-slope assemblages

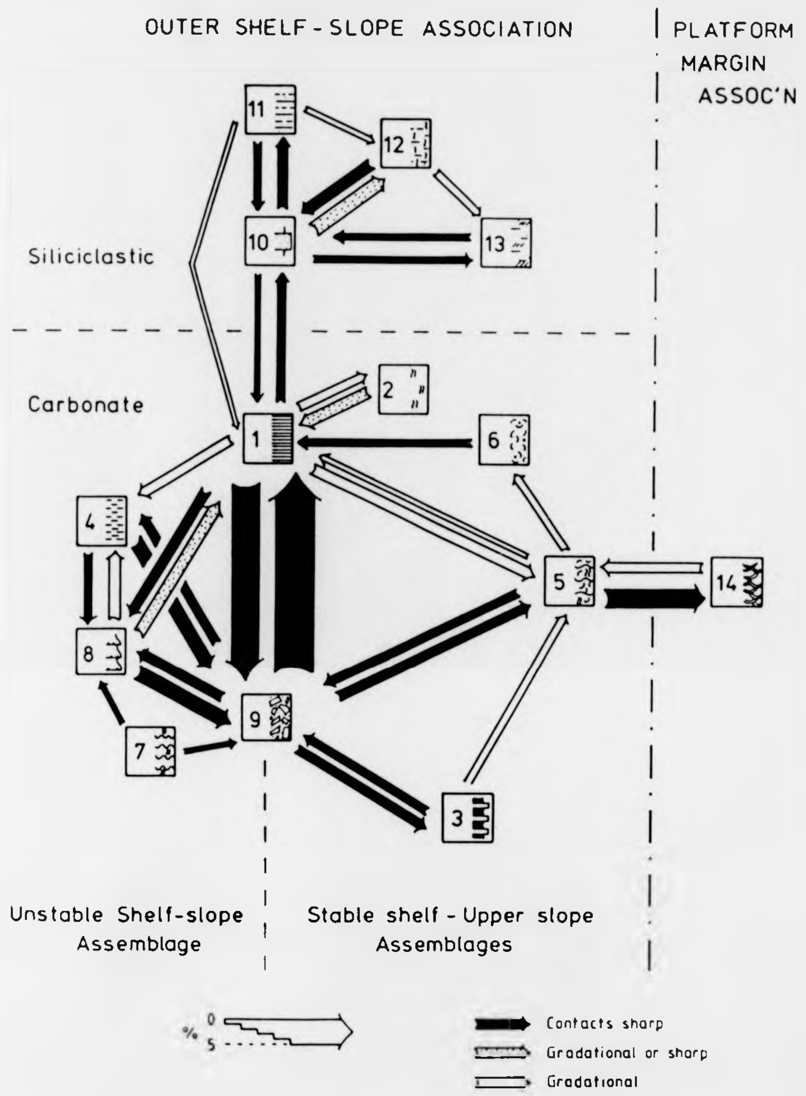


Figure 6.76. Schematic representation of the vertical facies transitions in the outer shelf-slope association based on systematic counting of the number of transitions and nature of contacts between the thirteen lithofacies in all measured sections (see Surlyk 1978 for discussion of method). Transitions shown form greater than 1% of the total number of transitions observed; arrow width indicates the % of all transitions. Note (a) Lithofacies 1 and 9 are the dominant members of the association and occur with most other lithofacies; (b) the carbonates fall into two groups (the unstable shelf assemblage and stable shelf-upper slope assemblages) with Lithofacies 1 and 9 in common. Note that upward transitions from the stable shelf-upper slope assemblages to the platform margin association are common, whereas transitions from the unstable shelf assemblage to the platform margin association are not observed. The transition from outer shelf to platform margin typically involves Lithofacies 5.

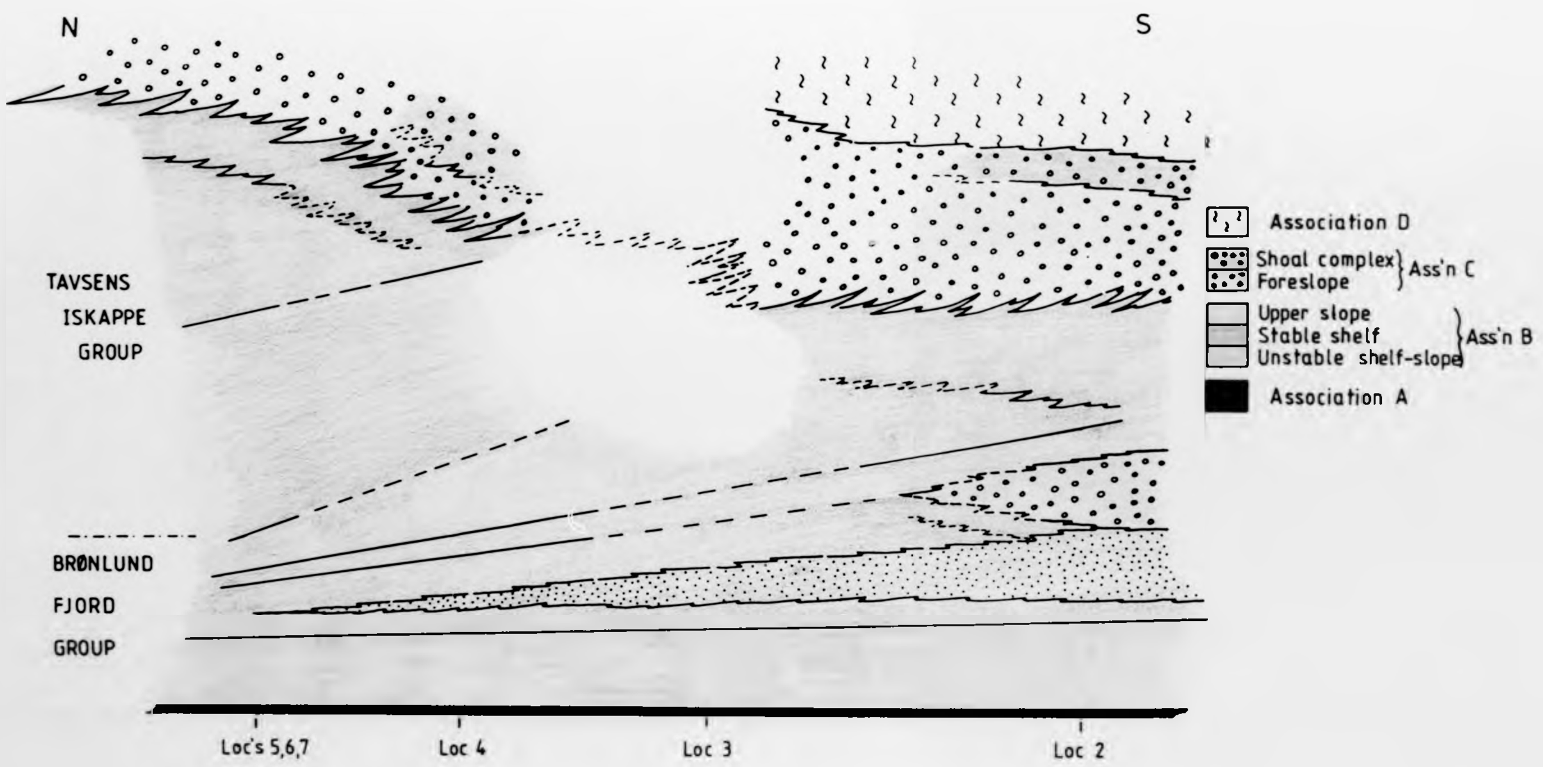


Figure 6.77. The vertical and lateral relationships between Associations A, B, C and D and their component assemblages in the north-south transect between J.P. Koch Fjord and Henson Gletscher.

and form the basis for the lithostratigraphic subdivision of the outer shelf rocks (Fig. 3.2; Ineson & Peel 1980).

6.2.2 Upper slope assemblage

This assemblage is characterized by thin, wavy-bedded skeletal carbonates (Lithofacies 5) interbedded locally with carbonate breccia beds (Lithofacies 9). A typical section is provided by the Ekspedition Bræ and Fimbuldal Formations at Koch Væg (Fig. 6.78). It is widely represented in both stratigraphic groups and forms units up to 95m thick. It commonly succeeds and northwards passes laterally into rocks of the stable shelf assemblage and is overlain by and interdigitates towards the south with light-coloured, thick-bedded strata assigned to the platform margin association (Figs 6.77 & 6.78). The carbonates of this assemblage commonly show slump folds, pull-aparts, microfaults, boudinage and discontinuous thin breccia horizons. In places, the thin bedding is interrupted by concave-upward truncation surfaces (Fig. 6.78). The best-exposed of these (Fig. 6.79) is a smooth, gently curving surface that intersects a thickness of about 2.5m of strata. The truncation plane has a maximum discordance of 20$^{o}$; the angle decreases rapidly down section to become parallel with the underlying, undisturbed beds. The surface is draped by dark, thin-bedded dolomites.

Similar structures in Silurian rocks in Ireland were interpreted as scars formed by rotational slumping (Laird 1968; see also McCabe 1978); comparable features on a larger scale have been reported from deep-water carbonate successions (Wilson 1969; Davies 1977). Truncation structures in the Permian of Texas, however, were interpreted as erosional channels cut by high-energy tractional currents (see Davies 1977). A slump-

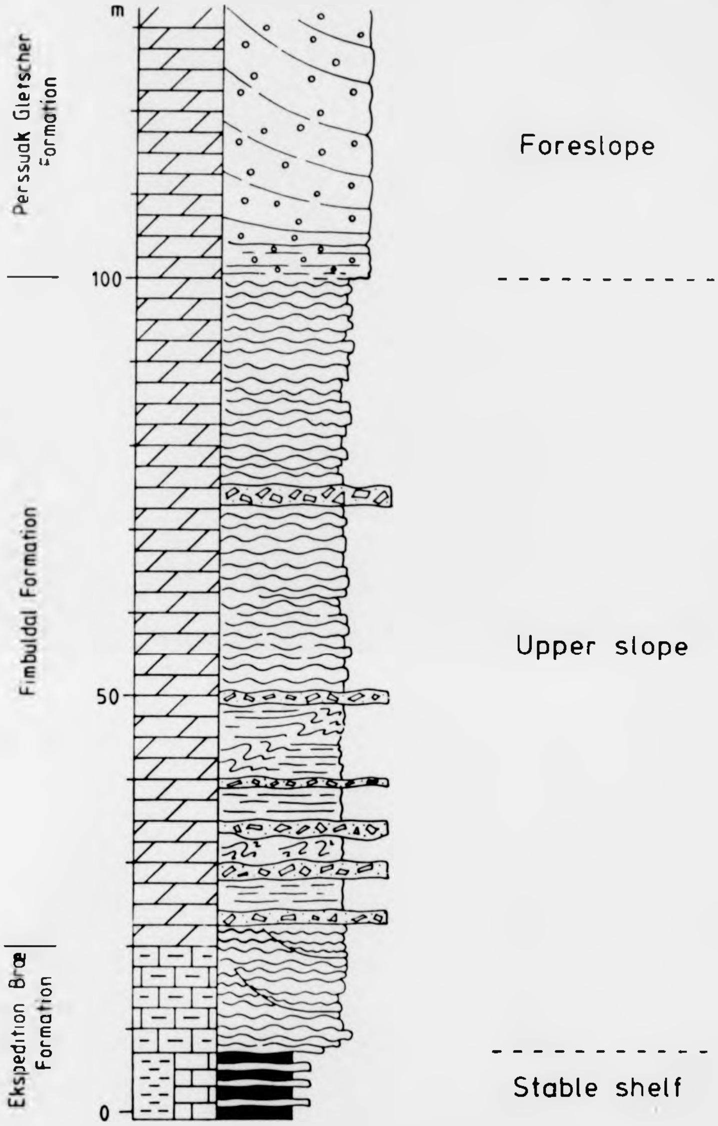


Figure 6.78. Generalized section showing the vertical transition from the stable outer shelf assemblage (lower Ekspedition Bræ Formation) through the upper slope assemblage (upper Ekspedition Bræ and Fimbuldal Formations) to the foreslope assemblage of the platform margin association (Perssuak Gletscher Formation). South Koch Væg, locality 2, west Peary Land.

Figure 6.79. Slump scar (arrowed) draped by dark laminated dolomites.
Erlandsen Land Formation, locality 13, central Peary Land.

Figure 6.79. Slump scar (arrowed) draped by dark laminated dolomites.
Erlandsen Land Formation, locality 13, central Peary Land.

-scar origin is suggested here by (a) the absence of U-shaped, channel-like profiles, (b) the smooth, gently curving nature of the truncation planes, resembling listric surfaces produced by sediment failure, and (c) by the fine-grained drape and the absence of coarse-grained lags or fill deposits.

Carbonate breccia beds in this assemblage range from 0.5 to 5m in thickness and are typically laterally discontinuous with irregular bounding surfaces. Basal contacts are particularly irregular, with up to several metres relief, and locally show the curved listric form of the slump-scar surfaces described above (Figs 6.58 and 6.79). Fig. 6.80 shows one such bed with an irregular base and subplanar top, composed of contorted, partially disaggregated slabs of thin wavy-bedded lime wackestone, lithologically identical to the enveloping *in situ* carbonates. These features suggest locally-derived mass flows that were transitional in character between slumps or slides and debris flows (Cook & Taylor 1977; Cook 1979).

Interpretation

The wavy-bedded skeletal carbonates indicate deposition in a well-oxygenated, open marine environment, at or beneath wave base (see Lithofacies 5). Deposition on a slope is suggested by the slump-scars, folds and abundant downslope creep structures. Vertical and lateral facies relationships (Fig. 6.77) suggest an upper slope environment, transitional between the high-energy, shallow-water platform margin and the deeper, calm bottom waters of the outer shelf. Brady & Koepnick (1979) proposed a similar environmental setting for closely comparable skeletal carbonates in the Middle Cambrian succession of Utah.

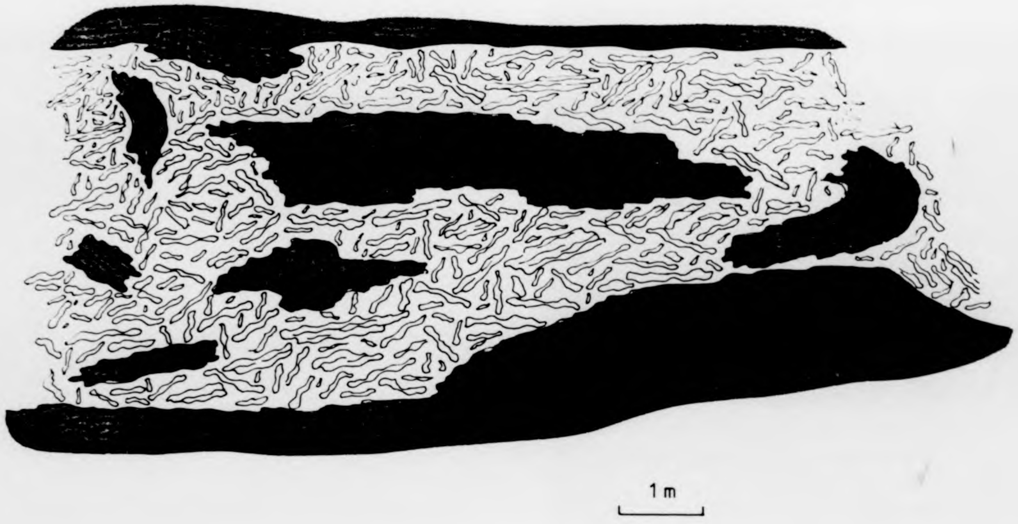


Figure 6.80. Sketch of a limestone breccia bed (LF.9) in the Ekspedition Bræ Formation in Løndal (locality 10, west Peary Land). Drawn from field sketch and photographs.

### 6.2.3 Stable shelf assemblage

This assemblage is characterized by thick, monotonous sequences of thin-bedded, dark grey, argillaceous lime mudstones and bituminous dolomites (Lithofacies 1-3) randomly interbedded with rare graded lime grainstones (Lithofacies 8) and thin carbonate breccia beds (Lithofacies 9). The Ekspedition Bræ, Holm Dal and Erlandsen Land Formations (Figs 3.25, 3.42 & 3.60) are typical representatives of the assemblage which also includes the Henson Gletscher and Sæterdal Formations (Figs. 3.16 & 3.25); the siliciclastic sediments of the latter two formations are described below (6.3).

The assemblage forms dark, shaly, recessive-weathering intervals (20 - 105m thick) sandwiched between the more prominent rocks of the unstable shelf assemblage (e.g. Figs 3.5 & 3.6). Rocks of the stable assemblage succeed those of the unstable assemblage with a sharp, planar, or irregular contact whereas upward transitions from stable shelf to unstable shelf-slope, and from stable shelf to upper slope are gradational (Figs 3.25 & 6.78). Uniform, even,parallel bedding is typical (e.g. Figs 3.44 & 3.63) and evidence of *in situ* instability is uncommon, being restricted to rare small-scale slump folds.

Coarse-grained redeposited carbonates form a minor component of the assemblage (Table 6.1). Breccia beds rarely exceed 2m in thickness and are generally limited in lateral extent. They consist of tabular, irregular clasts of lime mudstone and peloidal, skeletal wackestone or packstone - facies represented within the outer shelf-slope association. Clasts of platform margin origin are very rare.

These lime-mud dominated sequences are locally interrupted by thin intervals (0.1 - 2m thick) of burrowed, skeletal wackestones and glauconitic skeletal packstones and grainstones (Lithofacies 5, 6), often associated with phosphatic detritus and phosphorite-impregnated hardgrounds. In the Henson Gletscher Formation in Løndal, these rocks display two coarsening-upward cycles (Fig. 6.81A). Laminated bituminous dolomites or lime mudstones (Lithofacies 1) at the base grade up through burrowed, shelly lime wackestones (Lithofacies 5) into thinly interbedded, locally cross-bedded, skeletal glauconitic packstones and grainstones (Lithofacies 6). Cycle tops are sharp and are overlain by parallel-laminated lime mudstones. At Ekspedition Bræ, north-west of Løndal (Fig. 1.1), the cycles are abbreviated (Fig. 6.81B); skeletal packstones and grainstones are not developed.

Interpretation

This assemblage records deposition in a marine environment, mainly beneath wave base. Circulation and oxygenation of bottom waters was inefficient and anaerobic or dysaerobic conditions generally prevailed. Deposition was predominantly from suspension and from low-density, muddy turbidity currents; coarse sediment gravity flows were rare and localized events. The scarcity of gravitational deformation structures in comparison to the other two assemblages suggests a stable environment with low depositional gradients. The occurrence of gravity flow deposits within the assemblage, however, indicates proximity to an unstable slope; derivation from the upper slope is suggested by the dominant clast types within breccia beds.

The thin skeletal, glauconitic and phosphoritic intervals record episodes of starvation and reworking of outer shelf sediments in association with enhanced organic productivity. The shelly coarsening-upward sequences represent shallowing or 'shoaling' events. Initially,

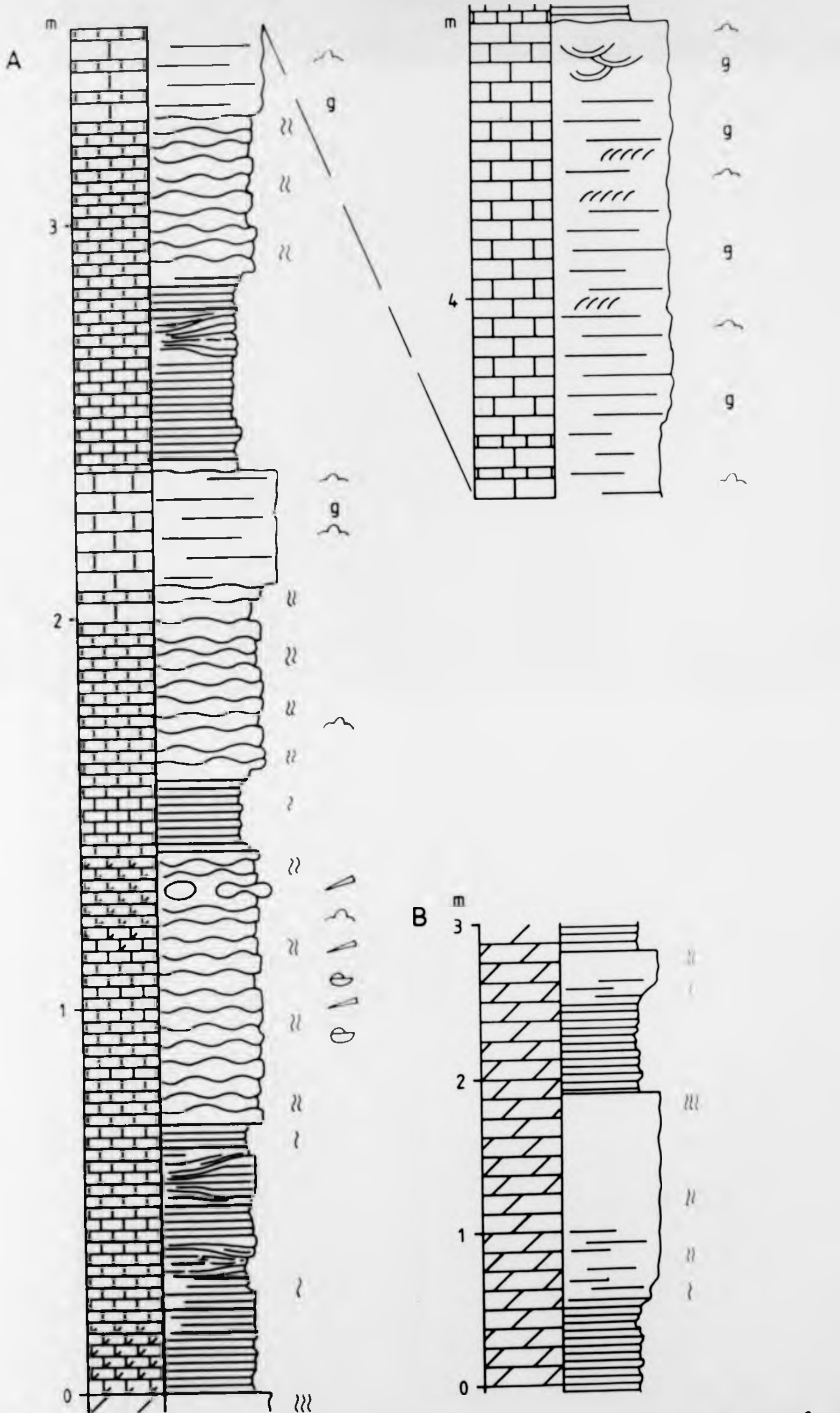


Figure 6.81. A. Detailed section of skeletal limestones near the base of the Henson Gletscher Formation in Løndal (locality 10, west Peary Land). Two coarsening-upward sequences are illustrated. B. Detailed section of dolomites near the base of the Henson Gletscher Formation at its type section (locality 1, east Freuchen Land) showing cyclic alternation of bioturbated and laminated carbonate; burrowed intervals have gradational bases and sharp tops.

increased circulation and oxygenation of bottom waters below wave base led to the establishment of a prolific infauna and benthic shelly fauna. With progressive shallowing, shelly muds became subject to winnowing and reworking, initially by storm waves and ultimately by fair weather processes as the sediment surface accreted to wave base. The abbreviated cycles in west Peary Land probably reflect a deeper-water situation. Skeletal glauconitic carbonates are a characteristic feature of the lower beds of the Henson Gletscher and Sæterdal Formations along the length of Wandel Dal, but individual shelly units are impersistent laterally. The best-developed coarsening-upward cycles probably formed on local swales or 'highs' on an undulating shelf floor. Specht & Brenner (1979) described comparable skeletal glauconitic carbonates within a regressive sequence of Upper Jurassic offshore mudstones. They attributed their development to storm-wave winnowing of fossiliferous lime muds on topographic highs in the Late Jurassic sea. Similar facies were reported by Markello & Read (1981) from inferred deep ramp environments (mainly sub-wave base) in the Cambrian of south-west Virginia. The cyclicity displayed by these late Lower Cambrian rocks probably reflects the irregular, episodic nature of shelf subsidence at that time.

This assemblage is comparable to the deep-water or basinal carbonates of Wilson (1969, 1975); numerous examples of similar facies have been described from the geological record (e.g. Bissell & Barker 1977; Davies 1977; Brady & Koepnick 1979). 'Basinal' is a term that is generally used in a relative sense to describe a deeper water environment marginal to shallow-water carbonate environments. As stressed by Brady & Koepnick (1979), the implication of an oceanic basin is rarely intended; many such carbonate basins developed on continental shelves by differential subsidence (e.g. Aitken 1978). In this study, the terms 'basin' and 'basinal' are avoided to prevent confusion on a regional scale with the coeval North Greenland trough (see Fig. 2.5; Friderichsen *et al.* 1982)

The assemblage is superficially similar to the deep ramp facies of Read (1980), Markello & Read (1981, 1982). Indeed, in their overview of the Early Palaeozoic shelf of eastern North Greenland, Hurst & Surlyk (1983) referred the outer shelf rocks of this study to a deep ramp setting, by analogy with the work of Read and his co-workers. However, the presence of mass flow deposits and the existence of a coeval carbonate platform (Fig. 6.77) conflict with the ramp model (*sensu* Ahr 1973); this assemblage is interpreted here as representing deposition in a stable, outer shelf environment.

### 6.2.4 Unstable shelf-slope assemblage

The unstable shelf-slope assemblage is represented by the Aftenstjernesø, Sydpasset and Fimbuldal Formations and the lower beds of the Løndal Formation (Figs 3.9, 3.17B, 3.38 + 3.64). It is characterized by cliff - forming units (20 - 175m thick) consisting of carbonate breccia beds (Lithofacies 9) and graded carbonates (Lithofacies 8) interbedded with nodular and laminated, fine-grained carbonates (Lithofacies 1,4,7). Carbonate breccia beds and turbidites often form over half of the succession. Breccia beds are up to 45m thick and are laterally persistent, some beds covering an area of over 350km$^2$. Fine-grained, slope-derived clasts are dominant but breccias in this assemblage commonly contain clasts of platform margin origin, which range in size from a few millimetres across to blocks of house-sized proportions. Composite breccia beds only occur in this assemblage.

Carbonate turbidites occur both as isolated beds within fine-grained carbonate successions and in turbidite-dominated sequences such as the Aftenstjernesø Formation (Fig. 6.43) where they form up to 70% of the formation. Siliciclastic turbidite successions are commonly interpreted in terms of the submarine fan model (Walker & Mutti 1973; Walker 1978) whereas carbonate submarine fans are only rarely reported from the geological record (Evans & Kendall 1977; Wright & Wilson 1984). As discussed by James & Mountjoy (1983) there is a significant difference between the sediment dispersal patterns of deep-water carbonate and siliciclastic environments. Deposition in deep clastic seas is dependent ultimately on sediment derived from terrestrial sources and introduced to the deep-water environment mainly via major submarine canyons, which act as point sediment sources. Redeposited carbonate sediment is derived primarily from the platform margin and upper slope which together form a linear sediment source and an apron of resedimented detritus is developed rather than isolated, major fans (Schlager & Chermak 1979; McIlreath 1977).

Carbonate turbidites form a major part of the Aftenstjernesø Formation from J.P. Koch Fjord to Independence Fjord, roughly parallel to depositional strike (8.2); no evidence of fan development was recognized. A weak thinning- and fining- upward trend in this formation in the J.P. Koch Fjord area probably records a gradual reduction in sediment supply. At Øvre Midsommersø, dolomitized carbonate turbidites in the upper half of the Aftenstjernesø Formation show pale cream weathering colours, contain relict ooids and possess an oomoldic porosity.

Although preservation is poor, it is clear that these beds contained a significant proportion of coated grains derived from a high-energy shallow-water environment, in contrast to the lime mud-dominated grains (intraclasts, peloids) that are typical of these rocks elsewhere. This lateral compositional variation along depositional strike supports the view that the Aftenstjernesø Formation turbidites were derived from the length of the carbonate slope or platform margin and formed an apron of resedimented carbonate.

The fine-grained, thin-bedded intervals of this assemblage are dominated by platy nodular carbonates (Lithofacies 4), displaying abundant evidence of gravitational instability. Pull-aparts, buckles, discontinuous thin brecciated levels, irregular distorted bedding and ruck folds attest to interstratal sliding within differentially lithified sediment; downslope movement is also indicated by boudinage and small-scale slump folds in laminated lime mudstones and thin-bedded carbonate turbidites. Many sections through this assemblage show a cyclic arrangement of these syn-sedimentary deformation structures. Individual cycles, as illustrated by the Sydpasset Formation (Figs 3.17B & 6.26), display a marked upward increase in the intensity of deformation; cycles are capped by a single breccia bed or an amalgamated stack of breccia beds. The Fimbuldal Formation in Holm Dal consists of two such cycles (Fig. 3.38); the upper one is capped by a 40m thick carbonate breccia bed.

<u>Interpretation</u>

Accumulation of parallel-laminated lime muds (now represented by Lithofacies 1 & 4) indicates deposition in a tranquil marine environment, below wave base. The carbonate sediment is commonly bituminous, *in situ* shelly benthic faunas are absent and bioturbation is uncommon suggesting that bottom waters were poorly oxygenated or anoxic. Abundant evidence of downslope creep, intrastratal sliding and slumping indicates a gravitationally unstable environment with a significant depositional gradient. Furthermore, the lateral persistence of these units suggests that instability was widespread over the outer shelf during the accumulation of this assemblage. A steep, unstable platform-slope break is suggested by the inclusion of house-sized platform margin blocks in mass flow deposits. Composite mass flow deposits, incorporating platform margin detritus, record retrogressive sediment failure in upper slope and platform margin environments.

This assemblage of facies is similar to inferred carbonate slope deposits described by Pfeil & Read (1980), Read (1980), Brady & Koepnick 1979, Cook & Taylor (1977) and many other workers (see papers in Cook & Enos (1977) and references in Cook & Mullins 1983).

The cycles showing an upward increase in the abundance and intensity of synsedimentary deformation structures, often in association with a parallel increase in abundance, thickness and grain size of mass flow deposits, suggest a progressive decline in the stability of the outer shelf. This suggestion is expanded in Chapter 8.

environment, below wave base. The carbonate sediment is commonly bituminous, *in situ* shelly benthic faunas are absent and bioturbation is uncommon suggesting that bottom waters were poorly oxygenated or anoxic. Abundant evidence of downslope creep, intrastratal sliding and slumping indicates a gravitationally unstable environment with a significant depositional gradient. Furthermore, the lateral persistence of these units suggests that instability was widespread over the outer shelf during the accumulation of this assemblage. A steep, unstable platform-slope break is suggested by the inclusion of house-sized platform margin blocks in mass flow deposits. Composite mass flow deposits, incorporating platform margin detritus, record retrogressive sediment failure in upper slope and platform margin environments.

This assemblage of facies is similar to inferred carbonate slope deposits described by Pfeil & Read (1980), Read (1980), Brady & Koepnick 1979, Cook & Taylor (1977) and many other workers (see papers in Cook & Enos (1977) and references in Cook & Mullins 1983).

The cycles showing an upward increase in the abundance and intensity of synsedimentary deformation structures, often in association with a parallel increase in abundance, thickness and grain size of mass flow deposits, suggest a progressive decline in the stability of the outer shelf. This suggestion is expanded in Chapter 8.

6.3 B2. Clastics

Terrigenous sediment in the outer shelf-slope association is mainly restricted to argillaceous partings and interbeds within carbonate -dominated successions (see Lithofacies 3). However, in the Henson Gletscher and Sæterdal Formations, siliciclastic rocks form a distinctive pale cream - dark grey striped interval, up to 124m thick, sandwiched between dark, thin-bedded carbonates (Figs 3.5 & 6.82). This clastic unit is prominent in the Henson Gletscher area (Fig. 3.17B) but thins northwards from 66m at Koch Væg to less than 2m in Gustav Holm Dal (Fig. 6.83). East from Henson Gletscher, it is persistent for 120km and is well developed in Sæterdal where it dominates the Sæterdal Formation (Fig. 3.25B). It thins eastward from Sæterdal and pinches out about 12km east of the type section (Fig. 3.28). The clastic unit is not recognized on the southern and north-eastern flanks of Frysefjeld (Fig. 3.28) where coeval rocks are massive light-coloured dolomites of the platform margin association (see Chapter 7) which are locally cut by shallow channels filled with terrigenous sand (Lithofacies 17). This clastic wedge is mainly of late Early Cambrian age but may be diachronous from south to north (3.3.3.2).

Sub-association B2 is subdivided into four lithofacies.

6.3.1 Lithofacies 10; Sheet sandstones

These beds typically weather pale yellow, cream or white, in sharp contrast to interbedded dark siltstones or bituminous carbonates (Fig. 6.82). They are well-sorted, very fine- to fine-grained sub-arkosic silty sandstones. Two subfacies are recognized:- 10a. massive sheet sandstones and 10b. stratified sandstones. The former dominate

6.3 B2. Clastics

Terrigenous sediment in the outer shelf-slope association is mainly restricted to argillaceous partings and interbeds within carbonate -dominated successions (see Lithofacies 3). However, in the Henson Gletscher and Sæterdal Formations, siliciclastic rocks form a distinctive pale cream - dark grey striped interval, up to 124m thick, sandwiched between dark, thin-bedded carbonates (Figs 3.5 & 6.82). This clastic unit is prominent in the Henson Gletscher area (Fig. 3.17B) but thins northwards from 66m at Koch Væg to less than 2m in Gustav Holm Dal (Fig. 6.83). East from Henson Gletscher, it is persistent for 120km and is well developed in Sæterdal where it dominates the Sæterdal Formation (Fig. 3.25B). It thins eastward from Sæterdal and pinches out about 12km east of the type section (Fig. 3.28). The clastic unit is not recognized on the southern and north-eastern flanks of Frysefjeld (Fig. 3.28) where coeval rocks are massive light-coloured dolomites of the platform margin association (see Chapter 7) which are locally cut by shallow channels filled with terrigenous sand (Lithofacies 17). This clastic wedge is mainly of late Early Cambrian age but may be diachronous from south to north (3.3.3.2).

Sub-association B2 is subdivided into four lithofacies.

6.3.1 Lithofacies 10; Sheet sandstones

These beds typically weather pale yellow, cream or white, in sharp contrast to interbedded dark siltstones or bituminous carbonates (Fig. 6.82). They are well-sorted, very fine- to fine-grained sub-arkosic silty sandstones. Two subfacies are recognized:- 10a. massive sheet sandstones and 10b. stratified sandstones. The former dominate

Figure 6.82. Sæterdal Formation (S) on the north side of Sæterdal. Sand-dominated intervals form the lower half of the formation overlain by a dark mudstone-dominated succession. Note the rapid lateral wedging of the main sand-dominated packet (base and top arrowed).

Figure 6.84. Structureless fine-grained sandstone beds (LF.10a) with laminated dark siltstone intercalations (LF.11). Note sharp, planar boundaries. Henson Gletscher Formation, locality 2, west Peary Land.


Figure 6.82. Sæterdal Formation (S) on the north side of Sæterdal. Sand-dominated intervals form the lower half of the formation over-lain by a dark mudstone-dominated succession. Note the rapid lateral wedging of the main sand-dominated packet (base and top arrowed).

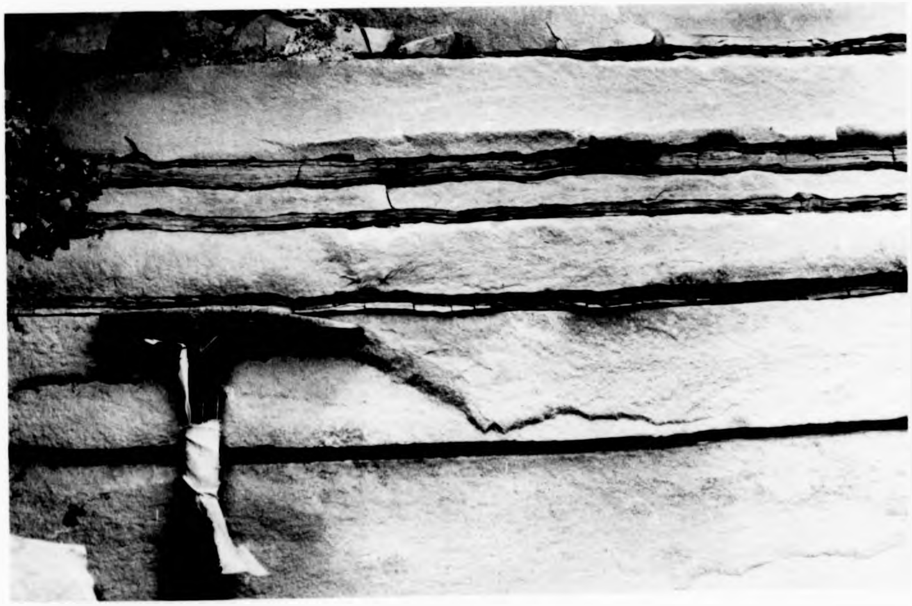

Figure 6.84. Structureless fine-grained sandstone beds (LF.10a) with laminated dark siltstone intercalations (LF.11). Note sharp, planar boundaries. Henson Gletscher Formation, locality 2, west Peary Land.

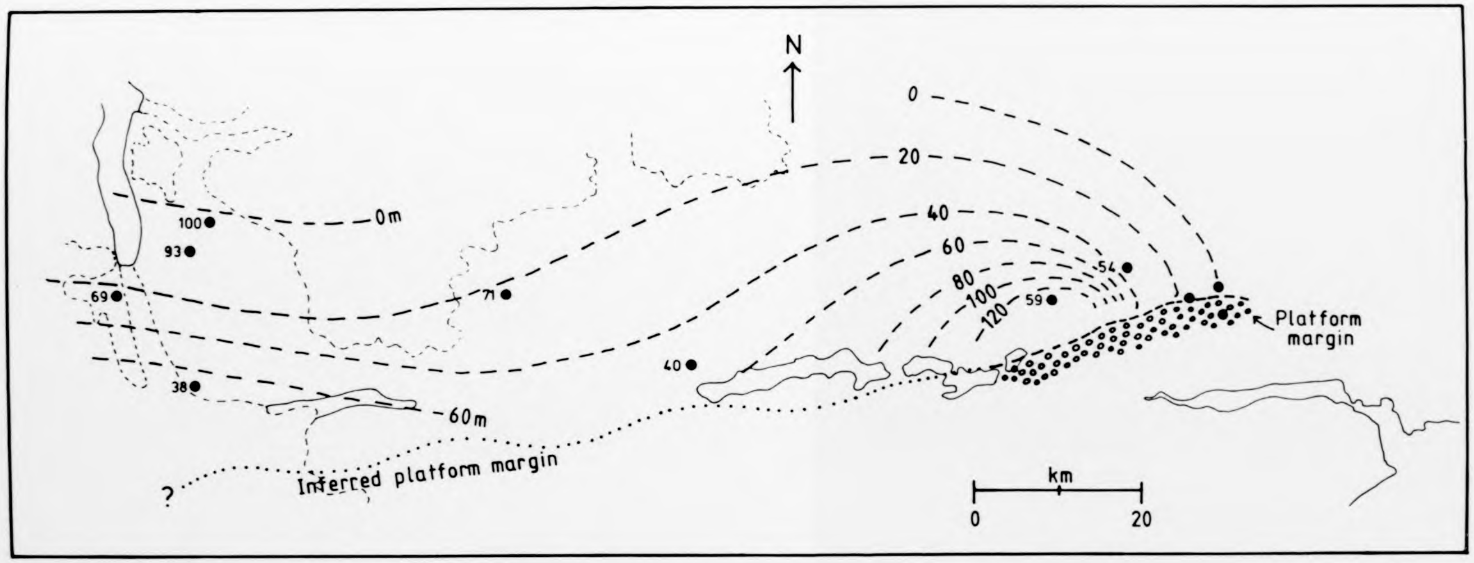


Figure 6.83. Isopach map of the siliciclastic interval within the Henson Gletscher and Sæterdal Formations. Contour interval is 20m; spots represent position of measured sections. Numbers at section localities are the percentage of the succession composed of sheet sandstone beds at that locality.

in the two detailed measured sections (92% of 167 beds) but stratified sandstones are dominant in some sections (e.g. Ekspedition Bræ, Fig. 3.16A).

10a. Massive sheet sandstones

Bed thicknesses range from 0.01 - 4m; 75% of beds are 0.03 - 0.3m thick. Parallel-sided, laterally persistent beds are typical and bed bases are sharp and planar (Figs 3.30 & 6.84) with rare scours, flames and load structures (Fig. 6.84). Beds amalgamate locally. Upper boundaries are commonly bioturbated and hence gradational but in non-burrowed intervals they are sharp and predominantly planar (Fig. 6.84). Some bed tops show rapid grading over a few millimetres into silty sandstone or siltstone and a few beds show gentle convex-upward hummocks with a relief of a few centimetres on their upper surfaces.

Grading is rare; where present,weak normal coarse-tail grading is defined by dispersed siltstone intraclasts. Many beds containing intraclasts or bioclasts are ungraded, however, and the clasts are either oriented randomly or define a weak parallel stratification. A few beds contain outsized siltstone blocks up to 0.2m across, which tend to be subparallel to bedding and can occur at any level in the bed.

Structureless, massive beds characterize the sub-facies, but 9% of measured beds show a diffuse, poorly defined lamination, subparallel to bedding. Locally, this stratification is defined by a scatter of fine pebble-sized intraclasts or bioclasts but commonly it is evident only on weathered surfaces, although probably reflecting a subtle grain size variation. Convolute lamination and sheet dewatering structures occur in a few beds.

10b. Stratified sheet sandstones

Although forming less than 10% of the facies in the detailed logs (Figs 6.85 & 6.86), these beds are critical to the interpretation of the facies as a whole. Beds are commonly 0.1 - 0.4m thick (mean 0.3m) with a maximum range of 0.05 - 1m; beds over 0.5m may represent unrecognized amalgamated beds.

They are mainly parallel-sided with sharp, planar or gently undulating erosional bases. Upper boundaries may be sharp and planar or burrowed; rarely, stratified sandstones show reworked, rippled tops. A few beds possess a structureless normally graded or ungraded lower interval that passes upwards into parallel-laminated fine-grained silty sandstone (Fig. 6.87).

These beds typically display parallel or low-angle cross-stratification. Where well-developed, the laminae are 1 - 10mm thick and are defined by an alternation of dark and light weathering very fine- to fine-grained sandstone (Fig. 6.88); dark laminae are micaceous and less well sorted. Although some beds show parallel lamination throughout, it is common to observe a vertical or lateral transition within a single bed from cross-stratification to parallel lamination and vice versa.

The cross-stratification is essentially a low-angle scour-and-fill structure. Undulating internal erosion surfaces are draped by low-angle (< $15^{o}$) curved cross-laminae that commonly thicken into scours and thin over mounds, thus passing gradationally upwards into parallel lamination (Fig. 6.89a). Sets range from 0.03 - 0.2m in thickness,

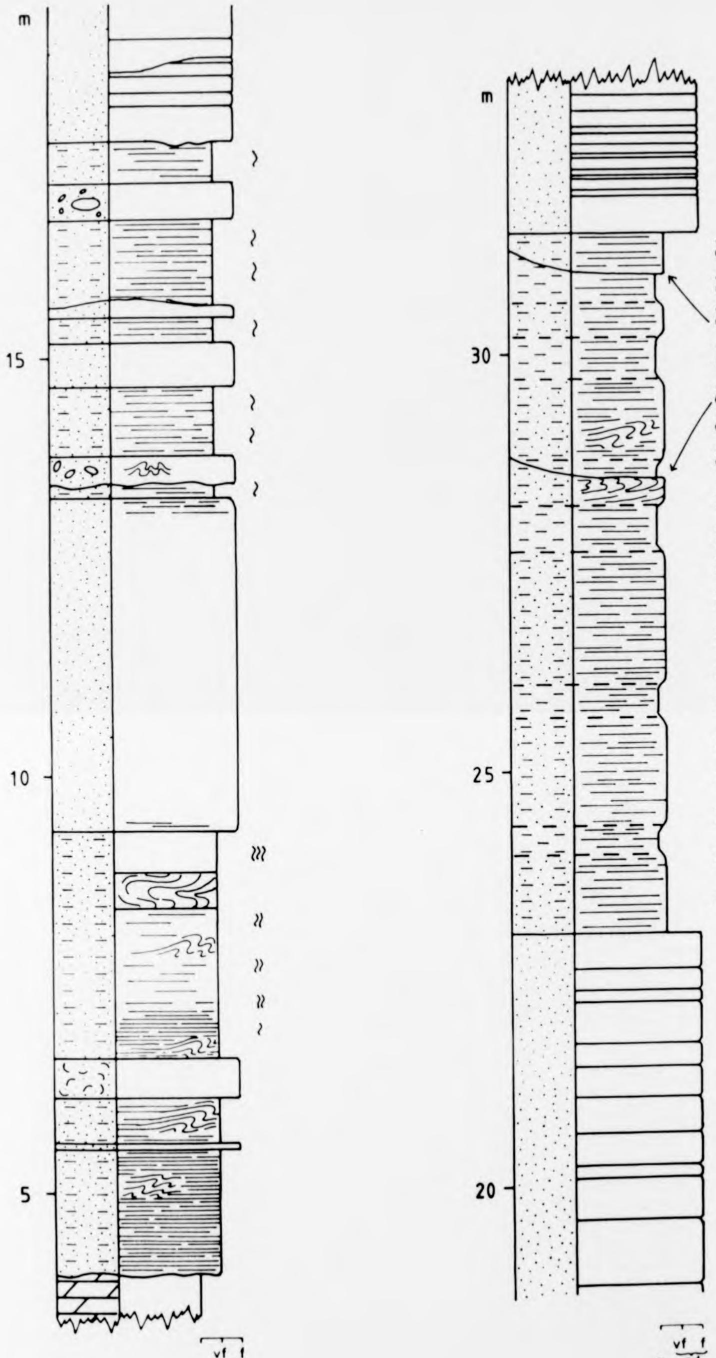


Figure 6.85. Detailed section through the clastic interval of the Henson Gletscher Formation on the north side of Øvre Midsommersø (locality 12, central Peary Land). Scale gives height above the base of the formation.

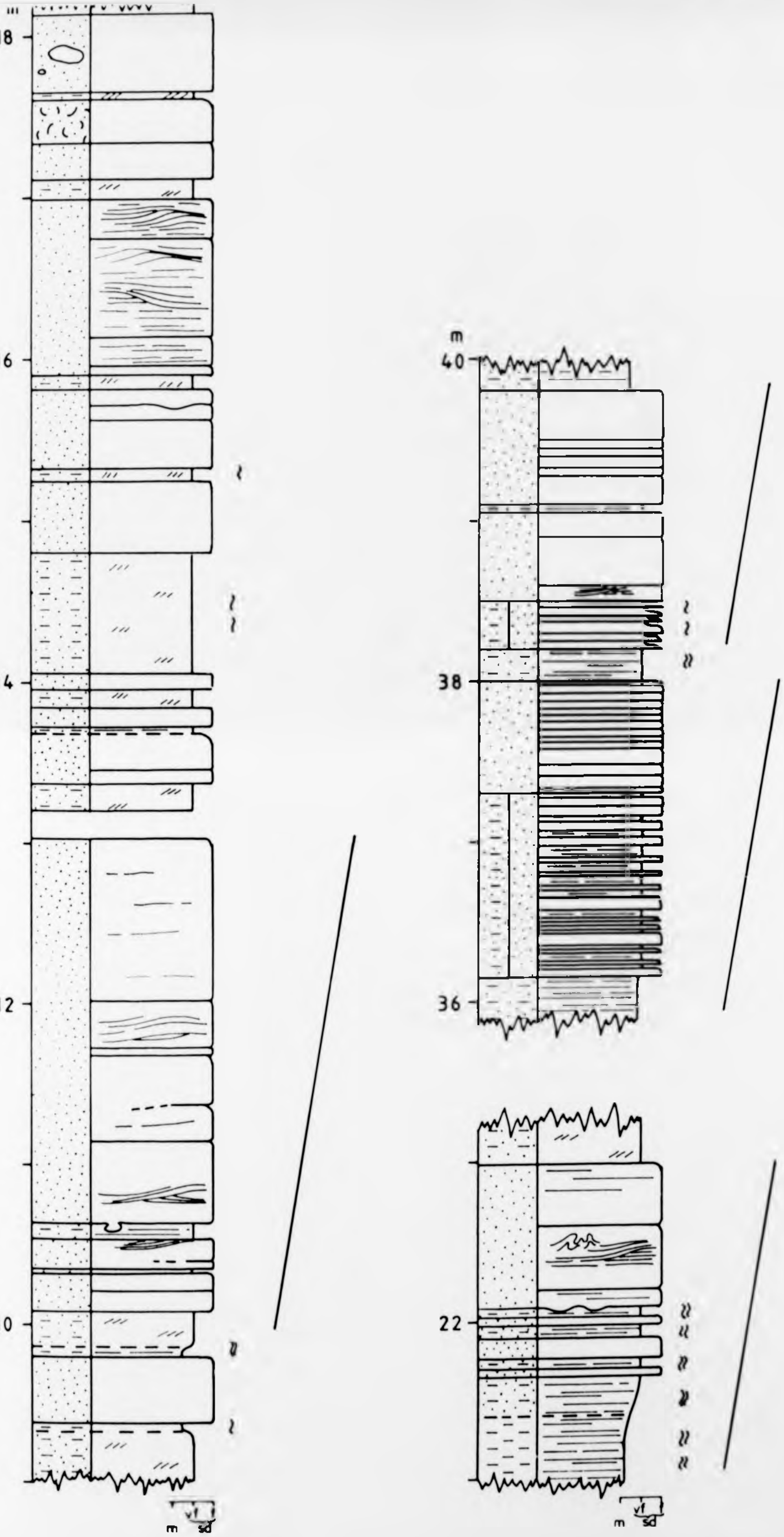


Figure 6.86. Detailed sction of the Sæ terdal Formation in Paralleldal (locality 15, central Peary Land). Scale gives height above base of formation. Sloping lines mark weak thickening-upward and/or coarsening-upward cycles.

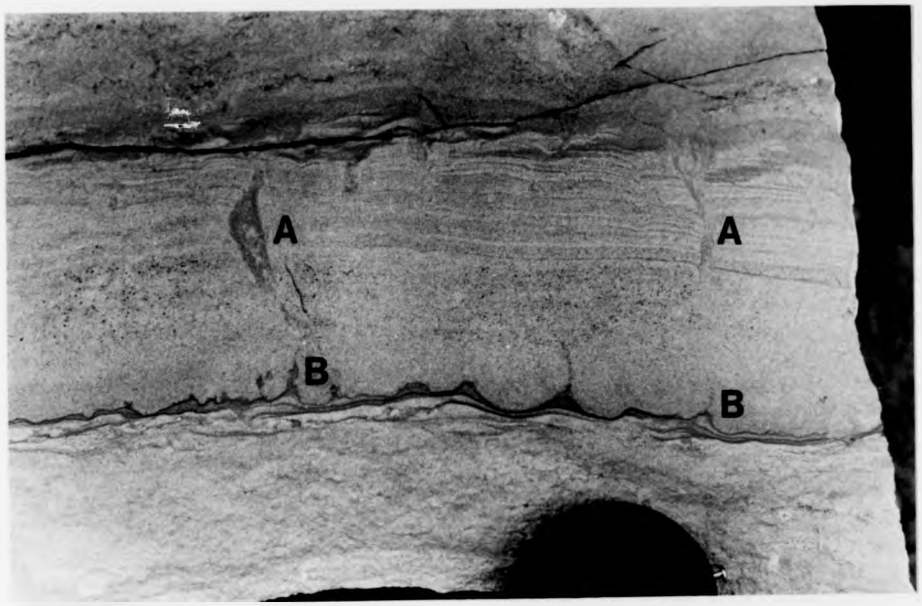


Figure 6.87. Sharp-based, graded sandstone bed (LF.10) with a basal structureless division and a parallel-laminated upper division. Note the spatial relationship between vertical dewatering structures (A) and basal loading (B). Sæterdal Formation, locality 14.

Figure 6.88. Parallel-stratified, fine-grained sandstone (LF.10b); sharp bed base at hammer head. Note the regular alternation of dark and light laminae, well illustrated in the basal 10cm. Henson Gletscher Formation, locality 1, east Freuchen Land.

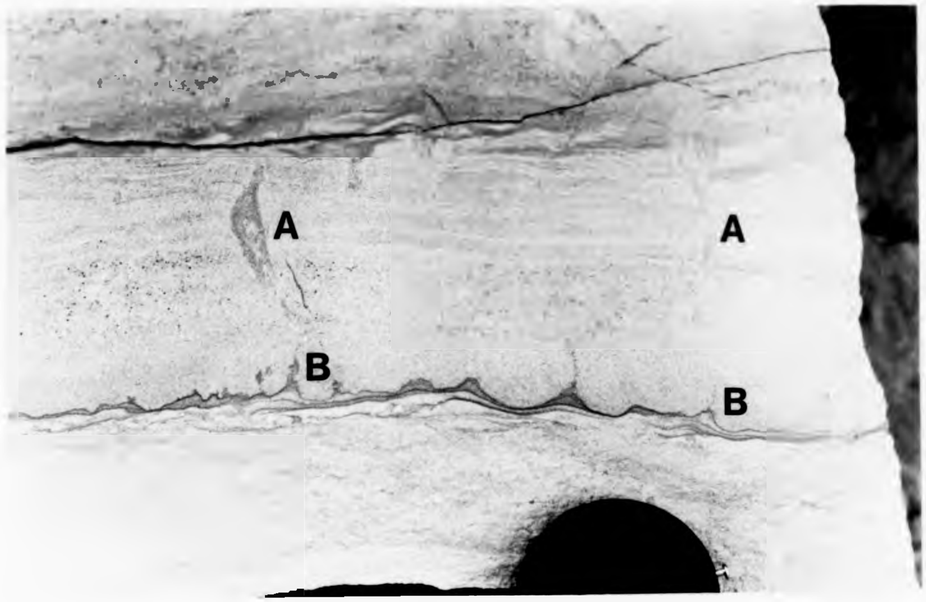


Figure 6.87. Sharp-based, graded sandstone bed (LF.10) with a basal structureless division and a parallel-laminated upper division. Note the spatial relationship between vertical dewatering structures (A) and basal loading (B). Sæterdal Formation, locality 14.

Figure 6.88. Parallel-stratified, fine-grained sandstone (LF.10b); sharp bed base at hammer head. Note the regular alternation of dark and light laminae, well illustrated in the basal 10cm. Henson Gletscher Formation, locality 1, east Freuchen Land.

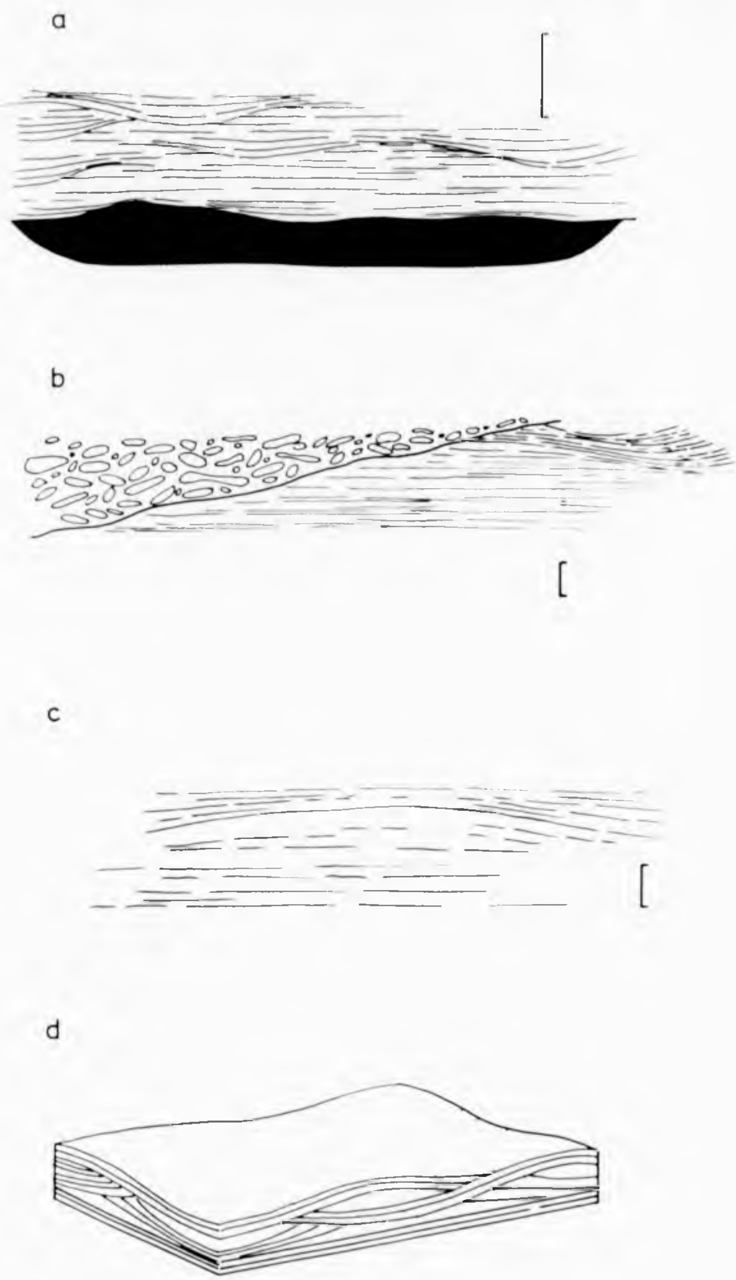


Figure 6.89. Lithofacies 10b. Scale bar = 0.2m.
a. Sketch from photograph and field sketch of sheet sandstone bed showing low-angle cross-stratification associated with hummocky internal erosion surfaces. Henson Gletscher Formation, locality 1, east Freuchen Land.
b. Fine-grained sandstone showing low-angle climbing cross-stratification cut out laterally by pebble-lined scour. Henson Gletscher Formation, locality 10, west Peary Land. Drawn from photograph and field sketch.
c. Vaguely-defined dome-like bedform, draped by succeeding laminae. Henson Gletscher Formation, locality 1, east Freuchen Land. Drawn from photograph.
d. Block diagram showing the main features of hummocky cross-stratification (after Harms *et al.* 1975).

and have a shallow trough-shaped profile in two dimensions. No reliable trough axes are observed, however, and the cross-bedding apparently results from draping and infilling of an irregular, hummocky scoured surface. A few beds show climbing cross-stratification (Fig. 6.89b) that suggests rapid deposition of sand, in association with lateral migration of a low-angle bedform. Rarely, laminae describe gentle convex-upward dome-like structures with a relief of a few centimetres and a width of 0.5 - 1m (Fig. 6.89c).

Interpretation

These beds are intercalated with fine-grained muddy sediments and typically have sharp, erosional bases and sharp or burrowed tops. This suggests episodic sand supply by relatively high energy, sand-laden currents into an environment characterized by the slow accumulation of fine-grained sediment from suspension or weak bottom currents (see Lithofacies 11 - 13).

10a. Massive sheet sandstones

The lack of diagnostic structures in this sub-facies renders it open to a range of possible interpretations. It has been suggested that similar structureless sandstones could result from slow continuous sedimentation from turbulent suspension (Kuenen & Menard 1952; Enos 1969). The occurrence of floating outsized clasts, scoured bases and bed amalgamation, however, precludes such an interpretation for the majority of these beds, although this process may have been responsible for some of the thin-bedded (0.01 - 0.05m), flat-based representatives.

The typical parallel-bounded, ungraded, structureless or faintly laminated beds are reminiscent of the facies interpreted as grain flow deposits by Stauffer (1967). Theoretical studies, however, have demonstrated that true grain flow is unlikely to be an important natural process, since gradients at or near the angle of repose are necessary to maintain such grain dispersions (Lowe 1976, 1982; Middleton & Southard 1977); furthermore, true grain flow deposits are unlikely to be thicker than 0.05m (Lowe 1976).

The occurrence of fluid-escape structures invites consideration of liquified flow and fluidized flow processes. In a theoretical study, Lowe (1976) suggested that fluidization is unlikely to be an important natural flow mechanism except during the final stages of deposition from liquified flows or turbidity currents. According to Lowe, the deposits of liquified flows are generally fine-grained (coarse silt - fine sand) but may show weak normal grading. Current-formed structures are absent and evidence of late-stage hydroplastic deformation and water escape (fluidization) is abundant. It may be difficult, however, to differentiate between true liquified flow deposits and sediments that were transported by other mechanisms but which suffered late-stage or post-depositional fluidization. Furthermore, Hiscott & Middleton (1979) demonstrated that rapid subaqueous sand-laden flows are fully turbulent and thus should be regarded as turbidity currents rather than liquified flows.

The occurrence of normal grading and erosional bed bases suggests deposition from a waning, turbulent flow; the scarcity of recognizable grading in these beds is probably a function of the fine-grained well-sorted nature of the sediment, rather than the transport mechanism.

and have a shallow trough-shaped profile in two dimensions. No reliable trough axes are observed, however, and the cross-bedding apparently results from draping and infilling of an irregular, hummocky scoured surface. A few beds show climbing cross-stratification (Fig. 6.89b) that suggests rapid deposition of sand, in association with lateral migration of a low-angle bedform. Rarely, laminae describe gentle convex-upward dome-like structures with a relief of a few centimetres and a width of 0.5 - 1m (Fig. 6.89c).

Interpretation

These beds are intercalated with fine-grained muddy sediments and typically have sharp, erosional bases and sharp or burrowed tops. This suggests episodic sand supply by relatively high energy, sand-laden currents into an environment characterized by the slow accumulation of fine-grained sediment from suspension or weak bottom currents (see Lithofacies 11 - 13).

10a. Massive sheet sandstones

The lack of diagnostic structures in this sub-facies renders it open to a range of possible interpretations. It has been suggested that similar structureless sandstones could result from slow continuous sedimentation from turbulent suspension (Kuenen & Menard 1952; Enos 1969). The occurrence of floating outsized clasts, scoured bases and bed amalgamation, however, precludes such an interpretation for the majority of these beds, although this process may have been responsible for some of the thin-bedded (0.01 - 0.05m), flat-based representatives.

The typical parallel-bounded, ungraded, structureless or faintly laminated beds are reminiscent of the facies interpreted as grain flow deposits by Stauffer (1967). Theoretical studies, however, have demonstrated that true grain flow is unlikely to be an important natural process, since gradients at or near the angle of repose are necessary to maintain such grain dispersions (Lowe 1976, 1982; Middleton & Southard 1977); furthermore, true grain flow deposits are unlikely to be thicker than 0.05m (Lowe 1976).

The occurrence of fluid-escape structures invites consideration of liquified flow and fluidized flow processes. In a theoretical study, Lowe (1976) suggested that fluidization is unlikely to be an important natural flow mechanism except during the final stages of deposition from liquified flows or turbidity currents. According to Lowe, the deposits of liquified flows are generally fine-grained (coarse silt - fine sand) but may show weak normal grading. Current-formed structures are absent and evidence of late-stage hydroplastic deformation and water escape (fluidization) is abundant. It may be difficult, however, to differentiate between true liquified flow deposits and sediments that were transported by other mechanisms but which suffered late-stage or post-depositional fluidization. Furthermore, Hiscott & Middleton (1979) demonstrated that rapid subaqueous sand-laden flows are fully turbulent and thus should be regarded as turbidity currents rather than liquified flows.

The occurrence of normal grading and erosional bed bases suggests deposition from a waning, turbulent flow; the scarcity of recognizable grading in these beds is probably a function of the fine-grained well-sorted nature of the sediment, rather than the transport mechanism.

These beds clearly represent deposition from episodic, sand-laden flows that were commonly turbulent and yet rarely deposited classical turbidites. The lack of internal structure may stem partly from the restricted range of grain sizes present, but may also reflect late-stage flow transformation (e.g. Lowe 1976; Walker 1978) or post-depositional fluidization.

10b. Stratified sheet sandstones

This sub-facies is closely comparable to hummocky cross-stratified sandstones from throughout the geological record (e.g. Cant 1980; Bourgeois 1980; Dott & Bourgeois 1982; see also Allen 1982). The term hummocky cross-stratification (HCS) was introduced by Harms *et al.* (1975), although similar structures had been described by earlier workers (Campbell 1966; Goldring & Bridges 1973). A recent discussion of HCS was given by Dott & Bourgeois (1982). A diagnostic feature is the occurrence of convex-upward laminae, producing domes, hummocks or antiforms (Hunter & Clifton 1982; Fig. 6.89). Antiformal structures have a lower preservation potential than troughs or swales, however, and are often rare or absent, particularly in amalgamated successions (Dott & Bourgeois 1982). HCS generally occurs in coarse silt to fine sand-sized detritus; the stratification is commonly defined by alternating laminae that are relatively rich and poor in mica and/or organic detritus (Hunter & Clifton 1982). Draping of low-angle erosion surfaces and 'smoothing out' of the erosional topography suggests a high concentration of suspended sediment and rapid sedimentation (Hunter & Clifton 1982).

Harms *et al.* (1975) proposed that HCS forms as the results of 'strong surges of varied direction that are generated by relatively large storm waves of a rough sea'. The characteristic hummock and swale structure is considered to reflect oscillatory sheet flow at the sediment surface due to storm wave action, combined with rapid deposition from suspension (Dott & Bourgeois 1982). Bourgeois (1980) suggested that HCS is a form of parallel lamination produced at the transition between upper and lower flow regimes under conditions of oscillatory flow.

Offshore transport of concentrated sediment suspensions, produced by river floods or stormy seas, has been attributed to density currents (Hayes 1967; Hamblin & Walker 1979), ebb storm-surge currents (Swift *et al.* 1971; Brenchley *et al.* 1979) or combined-flow currents (Hunter & Clifton 1981; Swift *et al.* 1983). Hamblin & Walker (1979) proposed that sand deposited above storm wave-base would be modified by wave action, producing hummocky cross-stratified sandstones whereas beyond the range of storm-induced wave action the density currents would deposit classical graded turbidites. However, Swift *et al.* (1983) reported hummocky bedforms that were produced during storms by combined -flow currents on the inner Atlantic Shelf of North America. They demonstrated that the contribution to offshore flow exerted by density contrast and storm-surge ebb is insignificant compared with that of down-welling geostrophic storm currents. Hummocky bedforms are produced by the interaction between the mean flow and wave orbital currents; the latter may act obliquely to the mean flow direction, suppressing linear bedforms. According to Swift *et al.* (1983) sand scoured from the upper shoreface is transported obliquely offshore and deposited as the combined flow currents deccelerate.

The stratified sandstones described here are interpreted as the deposits of episodic offshore currents that were associated with storm events. Following Swift *et al.* (1983) they were probably deposited from waning combined-flow currents although the contribution to flow exerted by density contrast may have become increasingly important as the geostrophic current waned. The presence of graded, laminated beds (Fig. 6.87) and the association with massive sheet sandstones (10a) suggest that turbulent density currents were sometimes an important process. The presence of hummocky cross-stratification and the scarcity of wave-reworked beds positions these deposits between fair-weather wave base and storm wave base.

### 6.3.2 Lithofacies 11; Laminated siltstones

The grain size of this lithofacies ranges from medium silt to fine-grained sand, but it is typically represented by dolomitic sandy coarse-grained siltstone. It occurs interbedded with sheet sandstones and burrowed siltstones (Lithofacies 10,12), forming units from a few millimetres to 10m thick. The facies shows a range of weathering colours from khaki-green or brown to dark grey or black. Horizontal lamination is ubiquitous and produces a fissile shaly bedding. Bioturbation is rare and some siltstones are notably fetid. The parallel lamination is a primary structure defined by subtle compositional and grain size variation; some laminae are rich in muscovite mica flakes.

In exposures along Saeterdal and the north side of Øvre Midsommersø these rocks commonly show small-scale slump folds and draped slump scars (Fig. 6.85). In the Saeterdal Formation type section, laminated siltstones and silty sandstones beneath a major slump-mass flow deposit exhibit a weak crenulation and fracture cleavage (*cf.* Bell 1981).

Interpretation

The fine grain size, parallel lamination and absence of current-produced structures suggest deposition from suspension in a low-energy environment, below active wave-base. The scarcity of burrowing, lack of a shelly fauna and localized bituminous nature indicate a poorly oxygenated environment.

### 6.3.3 Lithofacies 12; Bioturbated siltstones

This lithofacies consists of medium- to very coarse-grained siltstones, sandy siltstones and silty, fine- to very fine-grained sandstones, forming units 0.01 - 12.5m thick. Weathering colours range from dark grey, through brown to pale yellow or cream. The degree of bioturbation varies from isolated, discrete burrows to thoroughly churned, homogenized sediment; consequently the preservation of primary sedimentary structures is variable. Parallel lamination is often recognizable (Fig. 6.90), although commonly discontinuous or wispy. Disarticulated trilobite fragments (*Kootenia sp.*) occur locally, scattered randomly through bioturbated sandy siltstones.

Recognizable ichnogenera are few. Discrete burrows are mainly oblique or horizontal and include *Planolites* (straight or gently curved, horizontal, unlined, cylindrical and unbranched). Vertical burrows are uncommon, but are present in some sand-rich intervals; funnel-shaped *Monocraterion* burrows (5 - 30mm deep x 5 - 10mm diameter) were recorded from the Henson Gletscher Formation at Ekspedition Bræ .

deposit exhibit a weak crenulation and fracture cleavage (*cf*. Bell 1981).

Interpretation

The fine grain size, parallel lamination and absence of current-produced structures suggest deposition from suspension in a low-energy environment, below active wave-base. The scarcity of burrowing, lack of a shelly fauna and localized bituminous nature indicate a poorly oxygenated environment.

### 6.3.3 Lithofacies 12; Bioturbated siltstones

This lithofacies consists of medium- to very coarse-grained siltstones, sandy siltstones and silty, fine- to very fine-grained sandstones, forming units 0.01 - 12.5m thick. Weathering colours range from dark grey, through brown to pale yellow or cream. The degree of bioturbation varies from isolated, discrete burrows to thoroughly churned, homogenized sediment; consequently the preservation of primary sedimentary structures is variable. Parallel lamination is often recognizable (Fig. 6.90), although commonly discontinuous or wispy. Disarticulated trilobite fragments (*Kootenia sp.*) occur locally, scattered randomly through bioturbated sandy siltstones.

Recognizable ichnogenera are few. Discrete burrows are mainly oblique or horizontal and include *Planolites* (straight or gently curved, horizontal, unlined, cylindrical and unbranched). Vertical burrows are uncommon, but are present in some sand-rich intervals; funnel-shaped *Monocraterion* burrows (5 - 30mm deep x 5 - 10mm diameter) were recorded from the Henson Gletscher Formation at Ekspedition Bræ.

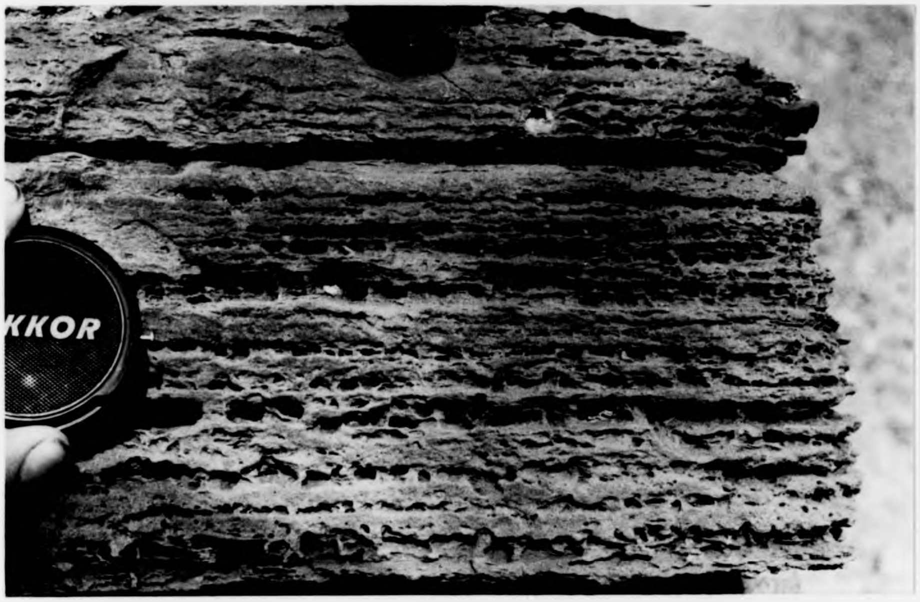


Figure 6.90. Bioturbated silty sandstone (LF.12). Henson Gletscher Formation, locality 12, central Peary Land.

Figure 6.91. Small isoclinal slump fold within bioturbated silty sandstone (LF.12). Hammer head on bedding plane for scale. Henson Gletscher Formation, locality 12, central Peary Land.

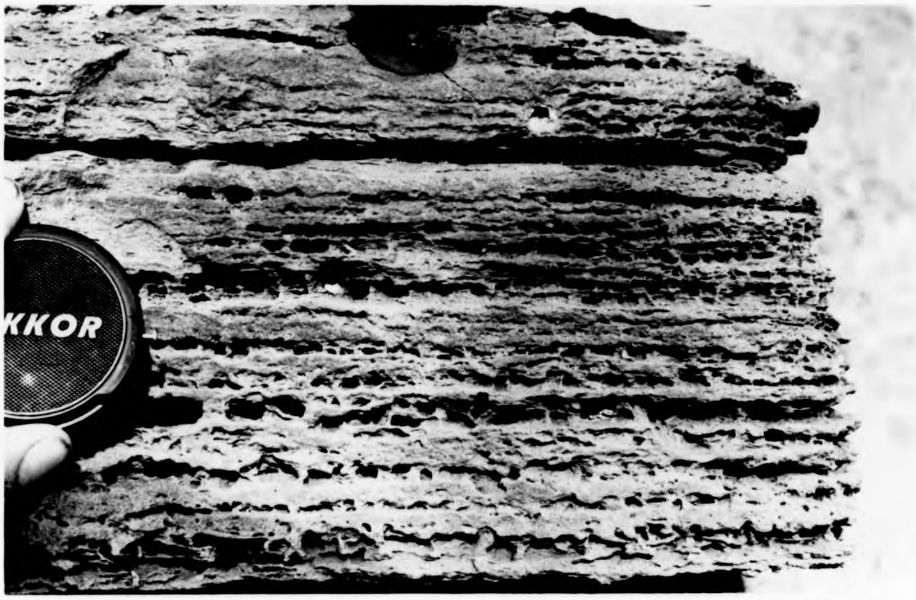


Figure 6.90. Bioturbated silty sandstone (LF.12). Henson Gletscher Formation, locality 12, central Peary Land.

Figure 6.91. Small isoclinal slump fold within bioturbated silty sandstone (LF.12). Hammer head on bedding plane for scale. Henson Gletscher Formation, locality 12, central Peary Land.

Small-scale slump folds are present at some southern localities (Fig. 6.91).

Interpretation

This lithofacies commonly grades vertically into laminated siltstones (Lithofacies 11) and where bioturbation is mild, parallel lamination is recognizable. Hence, a similar depositional mechanism is envisaged: silt, clay and fine sand settled from suspension into a low-energy marine environment below wave base. The evidence of an active burrowing infauna and rare shelly fauna indicates a greater degree of oxygenation at the sediment surface than that recorded by the well-laminated rocks. The dominance of sub-horizonatal deposit-feeding burrows also suggests a low-energy environment (Rhoads 1975), although *Planolites* traces are very common in the geological record and are generally regarded as facies-independent forms (Crimes 1970; Pickerill 1980).

### 6.3.4 Lithofacies 13. Cross-laminated sandstones

This facies forms a minor part of the clastic sequence. It is restricted to southern exposures of the Henson Gletscher and Sæterdal Formations along Wandel Dal and Sæterdal (Figs 3.16B & 3.25B). It consists of pale grey, brown or cream weathering silty, fine- to very fine-grained sandstones. They form units up to 7m thick interbedded with sheet sandstones and commonly grading vertically into bioturbated silty sandstones. These beds are characterized by wispy cross-lamination (Fig. 6.92); ripple troughs are often delineated by siltstone or silty sandstone flasers.

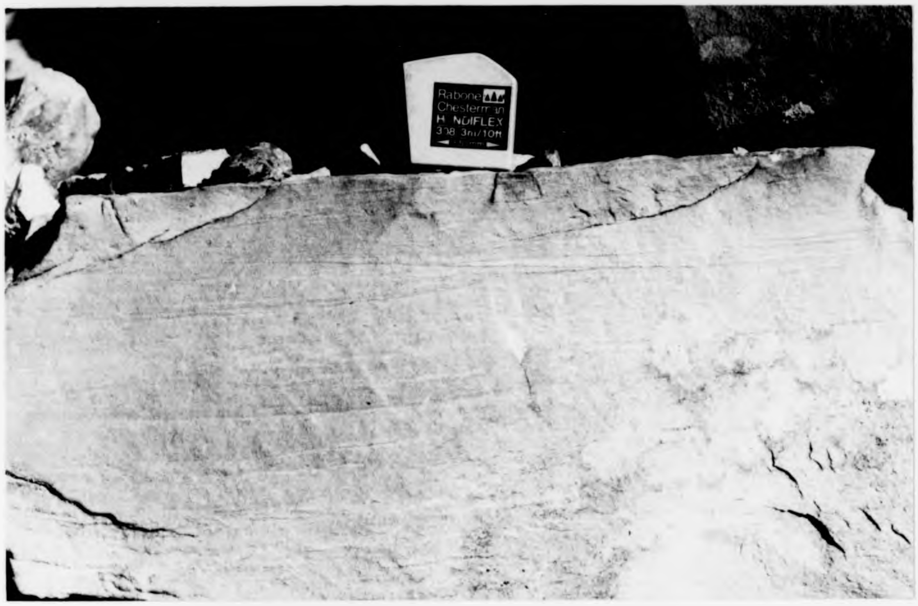


Figure 6.92. Silty fine-grained sandstone showing wispy cross-lamination defined by discontinuous darker silty laminae. Lithofacies 13, Saeterdal Formation, locality 15, central Peary Land.

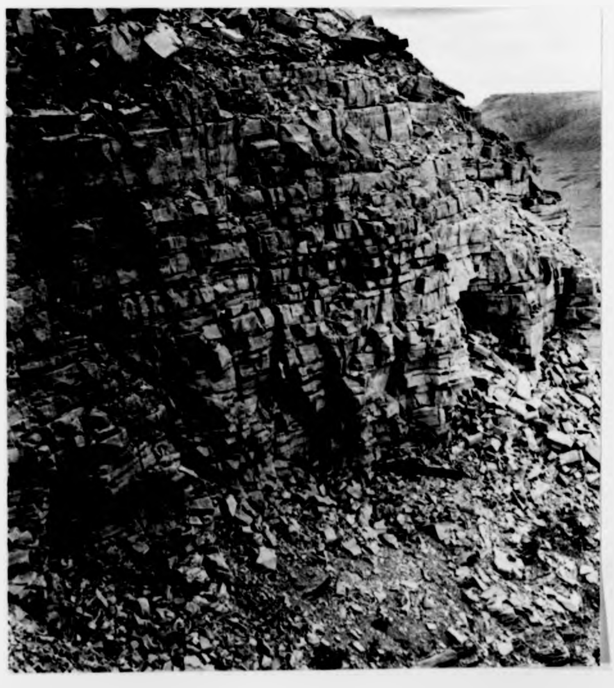

Figure 6.93. Sand-dominated packet, 14m thick (base and top arrowed). Note the lateral continuity of sheet sandstone beds (LF.13) and lack of obvious channelling. Saeterdal Formation, locality 14, central Peary Land.


Figure 6.92. Silty fine-grained sandstone showing wispy cross-lamination defined by discontinuous darker silty laminae. Lithofacies 13, Saeterdal Formation, locality 15, central Peary Land.

Figure 6.93. Sand-dominated packet, 14m thick (base and top arrowed). Note the lateral continuity of sheet sandstone beds (LF.13) and lack of obvious channelling. Saeterdal Formation, locality 14, central Peary Land.

Interpretation

This facies is rare and poorly exposed; a rigorous interpretation is not possible. The presence of silt-draped ripple troughs and cross-lamination suggests episodic reworking and entrainment of fine sediment by waves or bottom currents. Preservation of sedimentary structures is generally poor and differentiation between wave and current ripples was not possible. In view of the associated wave-influenced sheet sandstones, however, it is reasonable to infer wave reworking of sediment at or above normal wave base.

### 6.3.5 Clastic facies relationships

The clastic wedge thins towards the north suggesting derivation from the south (Fig. 6.83). Concomitant with this overall northward thinning is a marked decrease in the fine-grained facies (Lithofacies 11-13) relative to sheet sandstones (Fig. 6.83). This probably reflects the limited depositional range of silt and sand dispersed in suspension relative to high-energy, bottom-hugging currents.

Reliable palaeocurrent data is scarce in this terrigenous interval. Structureless sheet sandstones yield no data and directional structures in hummocky cross-stratified beds are rare, by the nature of the stratification (Harms *et al.* 1975). In the Paralleldal - Sæterdal area, primary current lineation and intraclast imbrication in sheet sandstone beds indicate flow towards the north-west; ripple cross-lamination indicates a similar trend (Fig. 8.2).

In exposures along Wandel Dal, from Henson Gletscher to eastern

Paralleldal (Figs 3.16B, 3.25B, 6.85 & 6.86), the clastic wedge comprises an alternation of sandstone-dominated and siltstone-dominated units, producing the characteristic striped outcrop pattern (Fig. 6.82). Sand-dominated packets are 2.5 - 15m thick and consist of sheet sandstones with thin silty sandstone and siltstone interbeds and partings (Figs 6.84 & 6.93). Intervening fine-grained units (4 - 16m thick) are dominated by silty sandstones and siltstones with localized, isolated sheet sandstone beds. In the Sæterdal area, where this differentiation is well developed, discrete sand-dominated packets have sharp boundaries and are commonly laterally persistent in east-west cliff sections although locally pinching out abruptly (Fig. 6.82). The sandstones are well-sorted and fine-grained so that fining- and/or coarsening-upward trends are very rare. Crude thickening-upward trends are recognized locally (Fig. 6.86). The relative importance of the two sheet sandstone subfacies shows no systematic variation, either laterally between sections or vertically in any one section. Detailed measured sections are few, however, and preservation of sedimentary structures is poor so that the importance of the structureless subfacies may be exaggerated.

There is a marked increase in bioturbation passing from north to south in west Peary Land, and the cross-laminated facies is restricted to southern exposures along Wandel Dal. Similarly, slump scars and slump folds only occur in sections along Wandel Dal - at Koch Væg, Øvre Midsommersø and Sæterdal.

6.4 B2 Environmental Interpretation

The clastic wedge overlies laminated, fine-grained carbonates assigned to stable shelf or upper slope assemblages; it contains trilobite fragments and locally is interbedded with fossiliferous marine limestones - an open marine environment is indicated. The distribution of facies, together with the sparse palaeocurrent data, suggest a terrigenous source region to the south or south-east and a northward deepening shelf. Evidence of slope instability and failure is limited to the southernmost exposures where the clastics are associated with upper slope carbonate facies (see 6.2.2). The clastic wedge clearly extended from the upper slope, bordering the carbonate platform, out onto the stable outer shelf (Fig. 6.77).

The interpretation is furthered by consideration of the relationship between the clastics and coeval platform margin deposits in Paralleldal. As mentioned previously, the clastics pinch out southwards across Paralleldal and are not represented on the north-eastern side of Frysefjeld (Fig. 3.28) where coeval rocks are massive platform-edge dolomites cut by shallow sand-filled channels. These channels probably represent the conduits through which land-derived clastic detritus traversed the carbonate platform-edge shoal complex. During fair weather, siliciclastic detritus was mainly confined landward of the shoal complex, with only fine-grained sediment reaching the open shelf in suspension. During storm events, however, sand-laden currents bypassed the platform margin and deposited sand sheets in upper slope and outer shelf environments. Those sandstones deposited within the range of storm waves show hummocky cross-stratification; those deposited beneath storm wave base or deposited too rapidly to allow oscillatory reworking, display features indicative of deposition from turbulent density currents. A similar relationship between density currents and storms has been proposed by Hamblin & Walker (1979).

Although local thickening may reflect centres of terrigenous supply (Fig. 6.83), the clastic wedge is persistent from J.P. Koch Fjord to Sæterdal and clearly represents a clastic apron derived from numerous local sources, rather than a few, isolated submarine fans centred on major bypass channels. Discrete sand-dominated packets probably represent individual sand lobes, however, possibly related to a single bypass channel or a complex of tidal channels. By analogy with classical submarine fan models (e.g. Mutti & Ricci-Lucchi 1972), the thickening-upward cycles within some sand packets are attributed to lobe progradation. The alternation of sand- and silt-dominated units and the abrupt upper boundaries of some sand units probably record plugging, abandonment and switching of tidal bypass channels.

No strictly comparable examples have been located in the literature, although in some respects these clastic sand lobes are similar to the carbonate sand spillover lobes that occur both landward and seaward of the Bahamian oolite banks (Ball 1967). Galloway & Brown (1973) proposed a broadly analogous model, albeit on a larger scale, for the Upper Carboniferous of central Texas where a clastic submarine fan abutted against the flanks of a carbonate platform. Clastic detritus from a high-constructive fluvio-deltaic system was transported directly to the fanhead during delta progradation or traversed the carbonate platform in channels. In the succession described here, contemporaneous platform interior facies are not preserved and the clastic source and mode of transport to the platform margin is unknown.

This clastic incursion into the outer shelf carbonates clearly

represents a major event in the evolution of the shelf, especially in view of the biostratigraphic discontinuity that roughly coincides with this unit (3.3.3.2; Peel 1982b). A similar relationship has been recognized in the Appalachian region of eastern U.S.A. where a hiatus (latest Early Cambrian to medial Middle Cambrian) coincides with a late Lower Cambrian regressive clastic sequence in nearshore, inner shelf environments (Palmer & James 1980). In deeper water, outer shelf deposits, the event (the Hawke Bay Event) is defined solely by a biostratigraphic gap spanning the Early - Middle Cambrian boundary (Palmer & James *op. cit.*).

The detailed palaeogeographic significance of this clastic incursion is not clear, but following Palmer & James (1980), it probably resulted from regression, brought about by a relative fall in sea level; in view of the regional extent of this event (the Hawke Bay Event) a eustatic mechanism is likely. Terrigenous detritus, previously restricted to nearshore environments, prograded northwards across the carbonate platform and bypassed the marginal carbonate shoal complex during storms, forming an apron of clastic sediment at the platform - outer shelf transition.

The biostratigraphic discontinuity generally occurs at the top of the clastic wedge and may have resulted from exposure of platform and upper slope environments during maximum regression. No field evidence of exposure, non-deposition or erosion was observed, however, and this suggestion is hypothetical. Exposure of inner shelf regions may also explain the presence of the hiatus in outer shelf environments, since exposure of the carbonate-producing platform would lead to

represents a major event in the evolution of the shelf, especially in view of the biostratigraphic discontinuity that roughly coincides with this unit (3.3.3.2; Peel 1982b). A similar relationship has been recognized in the Appalachian region of eastern U.S.A. where a hiatus (latest Early Cambrian to medial Middle Cambrian) coincides with a late Lower Cambrian regressive clastic sequence in nearshore, inner shelf environments (Palmer & James 1980). In deeper water, outer shelf deposits, the event (the Hawke Bay Event) is defined solely by a biostratigraphic gap spanning the Early - Middle Cambrian boundary (Palmer & James *op. cit.*).

The detailed palaeogeographic significance of this clastic incursion is not clear, but following Palmer & James (1980), it probably resulted from regression, brought about by a relative fall in sea level; in view of the regional extent of this event (the Hawke Bay Event) a eustatic mechanism is likely. Terrigenous detritus, previously restricted to nearshore environments, prograded northwards across the carbonate platform and bypassed the marginal carbonate shoal complex during storms, forming an apron of clastic sediment at the platform - outer shelf transition.

The biostratigraphic discontinuity generally occurs at the top of the clastic wedge and may have resulted from exposure of platform and upper slope environments during maximum regression. No field evidence of exposure, non-deposition or erosion was observed, however, and this suggestion is hypothetical. Exposure of inner shelf regions may also explain the presence of the hiatus in outer shelf environments, since exposure of the carbonate-producing platform would lead to

represents a major event in the evolution of the shelf, especially in view of the biostratigraphic discontinuity that roughly coincides with this unit (3.3.3.2; Peel 1982b). A similar relationship has been recognized in the Appalachian region of eastern U.S.A. where a hiatus (latest Early Cambrian to medial Middle Cambrian) coincides with a late Lower Cambrian regressive clastic sequence in nearshore, inner shelf environments (Palmer & James 1980). In deeper water, outer shelf deposits, the event (the Hawke Bay Event) is defined solely by a biostratigraphic gap spanning the Early - Middle Cambrian boundary (Palmer & James *op. cit.*).

The detailed palaeogeographic significance of this clastic incursion is not clear, but following Palmer & James (1980), it probably resulted from regression, brought about by a relative fall in sea level; in view of the regional extent of this event (the Hawke Bay Event) a eustatic mechanism is likely. Terrigenous detritus, previously restricted to nearshore environments, prograded northwards across the carbonate platform and bypassed the marginal carbonate shoal complex during storms, forming an apron of clastic sediment at the platform - outer shelf transition.

The biostratigraphic discontinuity generally occurs at the top of the clastic wedge and may have resulted from exposure of platform and upper slope environments during maximum regression. No field evidence of exposure, non-deposition or erosion was observed, however, and this suggestion is hypothetical. Exposure of inner shelf regions may also explain the presence of the hiatus in outer shelf environments, since exposure of the carbonate-producing platform would lead to

starvation and non-deposition in deep-water, outer shelf environments (*cf.* James & Mountjoy 1983).

The possibility that the clastic wedge may be diachronous in some areas and may overlie the hiatus at Ekspedition Bræ, eastern Freuchen Land (see Peel 1982b) clearly conflicts with this model; further biostratigraphical and sedimentological field work is needed to clarify the detailed history of this regressive phase. The clastics of apparent medial Middle Cambrian age at Ekspedition Bræ may record storm-induced reworking of the clastic apron during the subsequent transgression (*cf.* Swift *et al.* 1983).

# CHAPTER 7 : INNER SHELF

Inner shelf rocks form the remaining third of the Brønlund Fjord and Tavsens Iskappe Groups. In west Peary Land, these rocks are of minor importance in the Brønlund Fjord Group, but are prominent in the Tavsens Iskappe Group, particularly in the Perssuak Gletscher and Koch Væg Formations (Fig. 5.1). In central and east Peary Land, inner shelf rocks are represented in both stratigraphic groups.

Two associations are recognized.

## 7.1 Association C. Platform margin.

This is a varied group of dolomites and siliciclastic rocks that show pale weathering colours- white, pale yellow and yellow-brown. In Lower and Middle Cambrian sections (e.g. Paralleldal and Sydpasset Formations, Figs 3.21 & 3.31) the assocation consists almost exclusively of light-coloured, thick-bedded to massive dolomites whereas siliciclasic rocks form an important part of this association in the Upper Cambrian of the J.P. Koch Fjord region (Perssuak Gletscher Formation, Fig. 3.48).

Rocks of Association C overlie and pass laterally northwards into facies assigned to the outer shelf-slope association; the contact is gradational (Fig. 5.1). In many sections, rocks of Association C are overlain unconformably by the Wandel Valley Formation (e.g. Fig. 3.48) but in places they pass gradationally upwards and laterally towards the south into rocks assigned to Association D (Fig. 5.1).

Seven lithofacies are recognized in Association C.

7.1.1. Lithofacies 9; Breccia beds.

Breccia beds of this association typically form pale weathering, wedge-shaped or lenticular bodies that pinch out into adjacent outer shelf facies (see Fig. 7.21). They are up to 58m thick and are commonly over 20m thick. Bed boundaries are often poorly defined, however, and some of the thicker beds may be unrecognized multiple breccia units. Basal contacts are generally flat and non-erosive (Fig. 3.46) whereas upper boundaries may be planar or highly irregular.

Two variants are recognized:-

Dolomite breccia beds.

These beds are common in the Perssuak Gletscher, Løndal and Paralleldal Formations where they consist of medium to coarse crystalline pale-yellow or white dolomite. Nearly half of the beds contain clasts up to 2m across and a few beds contain slabs up to 20m in maximum dimension. The dominant clast population is of coarse cobble grade (0.1-0.25m) and clasts are typically angular or sub-angular. Pale dolomite slabs and blocks often show medium to thick bedding and some clasts display cross-bedding and a relict ooidal fabric; internal slump folding is present in a few blocks. Clasts are commonly poorly defined and are often barely distinguishable from the medium to coarse crystalline dolomite matrix (Fig. 3.46). Where internal structure can be seen, both clast- and matrix-supported frameworks are represented. Grading and organized clast fabrics are absent.

Dolomite-sandstone breccia beds.

Polymictic sandstone-dolomite breccias occur in the Perssuak Gletscher Formation in Holm Dal and the Hellefiskefjord Formation in north-east Peary Land (Christie & Ineson 1979). They range from breccias composed of dolomite clasts in a sandstone matrix (Figs 3.49 & 7.1) to breccias consisting of sandstone clasts in a dolomite or dolomitic sandstone matrix. Clasts are angular, equidimensional or rectangular (Fig. 7.1) and are typically 0.05-0.3m in length and 0.02-0.1m thick; some beds include slabs of sandstone up to several metres in length. The terrigenous sand component is medium- to fine-grained, well-sorted and sub- to well-rounded. Sandstone clasts are quartz arenites (up to 5% microcline feldpsar), cemented by syntaxial quartz overgrowths and sparry dolomite. Clasts sometimes show cross-bedding, parallel lamination and bioturbation, including *Monocraterion* burrows.

Beds are typically 1-2m thick; one bed of 7.5m was recorded. Lateral exposure of the Perssuak Gletscher Formation is poor in accessible terrain and the geometry of these beds is unknown. At outcrop scale, the boundaries are sharp and planar but rocks of this association typically form lenticular or wedge-shaped bodies in cliff section (Fig. 3.47).

Over 75% of these beds show normal coarse-tail grading (Figs 3.49 & 7.2). Typically the basal portion (one-third to half of the bed) is

Figure 7.1. Laminated tabular dolomite clasts in a white, medium-grained sandstone matrix. Note parallel orientation of clasts. LF. 9, Perssuak Gletscher Formation, Locality 8, west Peary Land.

Figure 7.1. Laminated tabular dolomite clasts in a white, medium-grained sandstone matrix. Note parallel orientation of clasts. LF. 9, Perssuak Gletscher Formation, Locality 8, west Peary Land.

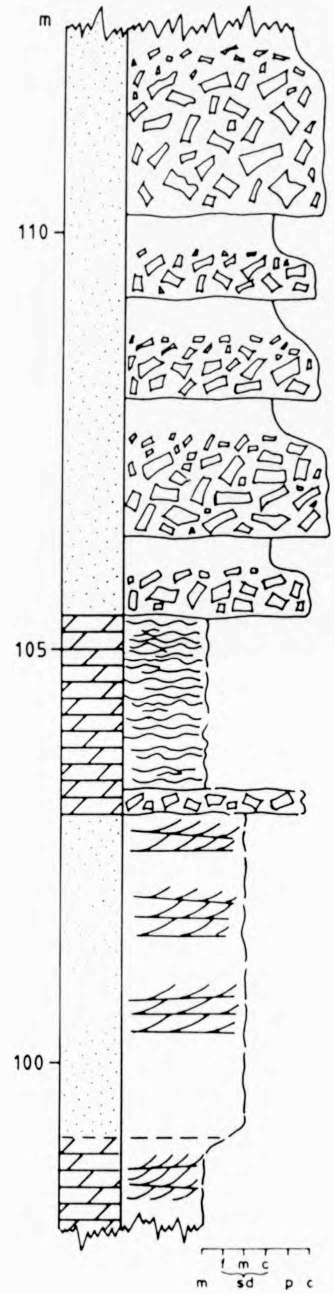


Figure 7.2. Section showing normally-graded dolomite-sandstone breccias in the Perssuak Gletscher Formation. Scale gives height above base of section. Locality 8, west Peary Land. Section measured by J.S. Peel.

ungraded and consists of clast-supported, cobble to boulder grade breccia with an interstitial sandstone matrix. Clasts become dispersed upwards to form a matrix-supported fabric and the breccia ultimately grades normally into structureless medium- to fine-grained sandstone (Figs 3.49 & 7.2). The clast-supported lower interval is generally chaotic whereas bedding-parallel clast fabrics are commonly developed within the graded, matrix-supported zone (Figs 3.49 & 7.1).

The remaining ungraded sandy breccias are clast-supported and disorganized throughout.

Interpretation.

The poor preservation of primary structures in the *dolomite breccia beds* generally precludes identification of the relative proportions of clasts to matrix, and obscures the primary nature of the matrix. The light colour of the matrix contrasts strongly with the dark-coloured, dolomitized mud-rich matrices of outer shelf breccias (see 6.1.9 and suggests a relatively mud-poor matrix. Furthermore, the pale matrix dolomite is lithologically comparable to cross-bedded ooidal dolomite blocks in these beds. The evidence is thin, but it is probable that these beds represent chaotic, poorly sorted breccias that consisted of lithified grainstone blocks in a matrix of loose, mud-poor lime sand.

Flat, non-erosive basal contacts, irregular tops, poor sorting, chaotic clast fabrics and a lack of internal stratification are recognized features of mass flow deposits (Johnson 1970; Pierson 1980). The apparent scarcity of mud-grade matrix does not preclude a mass-flow origin since a low clay content is not unusual in debris flows (Middleton & Hampton 1976; Surlyk 1978). Hopkins (1977) described similar breccia beds from the Devonian of Alberta, Canada, that consisted of nodular calcarenite clasts within a carbonate sand matrix. He suggested that they were the result of hybrid sediment gravity flows in which dispersive pressure, upward fluid migration and possibly turbulence contributed to clast support. Similar mud-poor carbonate breccias in the Cambrian of south-west Virginia, U.S.A., were interpreted as the deposits of sandy debris flows in which grain support was due to dispersive pressure and turbulence, in addition to matrix strength and the density contrast between clasts and matrix (Pfeil & Read 1980).

By analogy with these studies, the dolomite breccias of this association are interpreted as the deposits of hybrid sediment gravity flows that most closely resembled sandy debris flows (e.g. Surlyk 1978) i.e. a mechanism transitional between density-modified grain flow and cohesive debris flow (Lowe 1979, 1982). The slump-folded rafts in these beds suggest initial transport as slides or slumps followed by transformation to a plastic flow mechanism.

The *dolomite-sandstone breccia beds* show many similar features but, in addition, are commonly graded and organized. The occurrence of grading suggests that clasts were free to move relative to one another (Walker 1965); the presence of a horizontal clast fabric is indicative of a laminar flow regime (Enos 1977). Surlyk (1978) interpreted similar graded conglomerates as the deposits of sandy debris flows in which some vertical and lateral segregation had occurred. The development of a horizontal clast fabric indicates that dispersive pressure was a significant component of the system; a mechanism transitional between grain flow and cohesive debris flow is envisaged.

7.1.2. Lithofacies 14; Dolomite grainstones.

These light-coloured, yellow, orange or brown dolomites typically display a relict well-sorted grainstone fabric and parallel or cross-stratification. They occur widely in the Perssuak Gletscher, Paralleldal and Løndal Formations and are present locally in the Sydpasset Formation (Figs 3.21, 3.31 & 3.64).

Recognition of skeletal grains, peloids and intraclasts is dependant mainly on their gross external morphology, as internal structures are rarely preserved. In thin section, primary grains are defined by subtle colour variation or, less commonly, by size variation in the crystalline dolomite mosaic (Fig. 7.3). In contrast, ooidal dolomites locally show excellent preservation of the primary concentric structure (Figs 7.4, 7.5 & 7.6) particularly in partially silicified or sandy intervals. The concentric ooid cortices are well-developed; superficial ooids are not observed. Many ooids have homogeneous cores of medium to fine crystalline dolomite (Figs 7.4 & 7.5) that may represent the carbonate nuclei (peloids or skeletal grains?). Well-rounded quartz sand grains form ooid nuclei in mixed sandstone-carbonate sand intervals (Fig. 7.6). Broken 'half-moon' ooids occur in places and often show

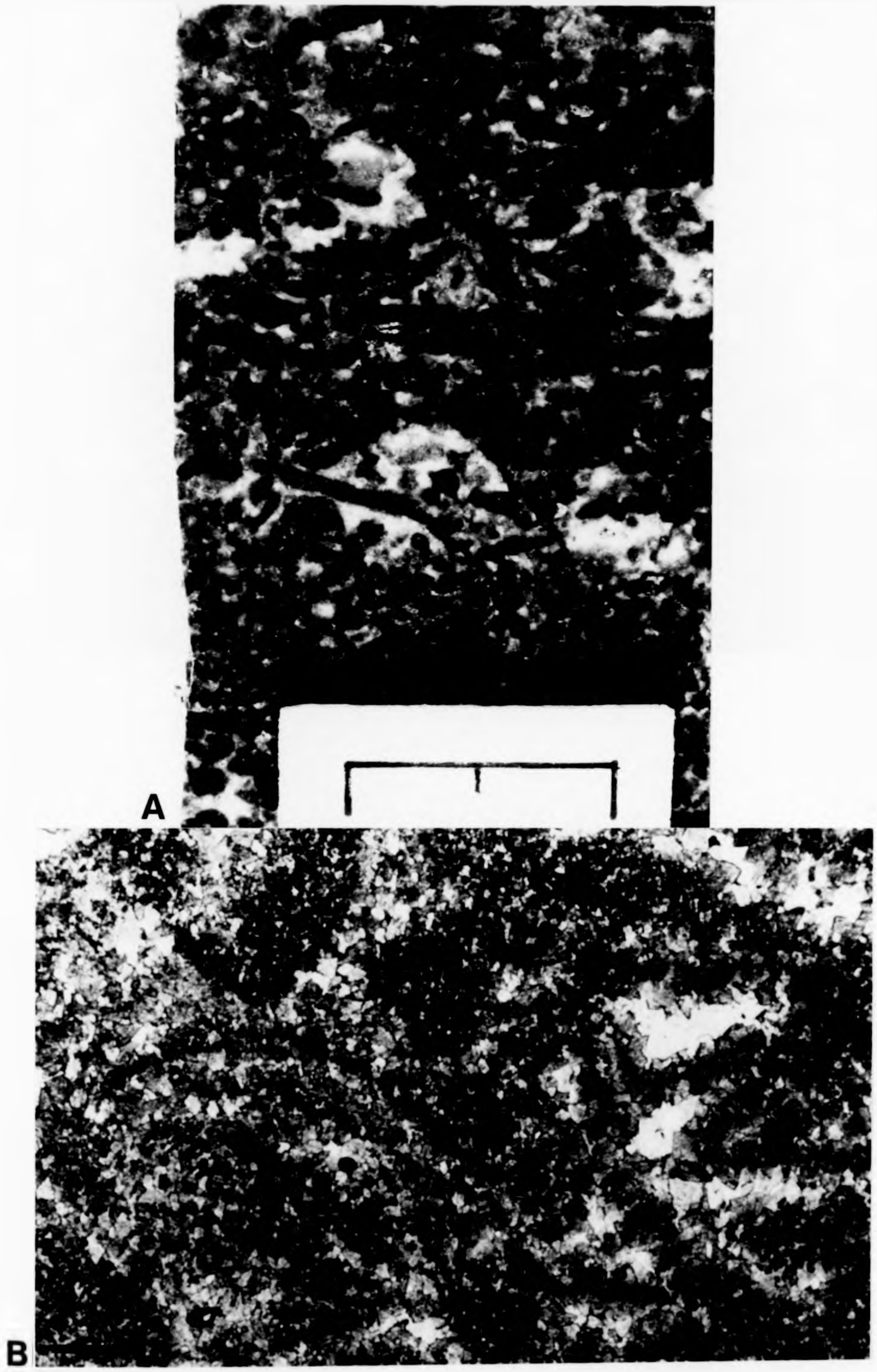


Figure 7.3. A Polished surface, cut normal to bedding,of dolomite showing a well-preserved peloidal intraclastic grainstone fabric (LF.14). Scale bar = 2cm. GGU 213421, Paralleldal Formation, locality 15, central Peary Land. B. Photomicrograph (PPL) of dolomitized skeletal, intraclastic grainstone. Scale bar = 1mm. GGU 274535, Paralleldal Formation, locality 19, central Peary Land.

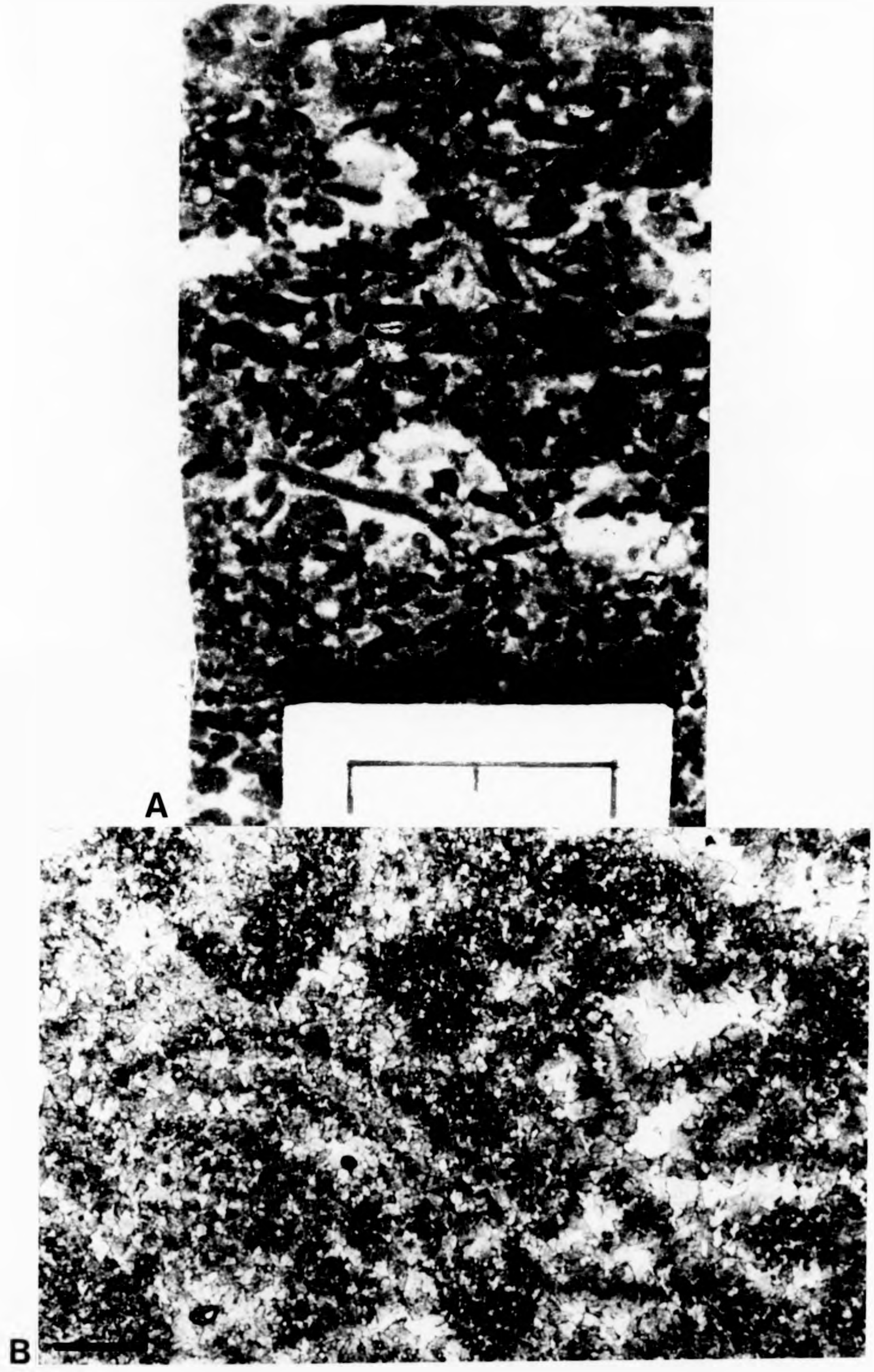

Figure 7.3. A Polished surface, cut normal to bedding, of dolomite showing a well-preserved peloidal intraclastic grainstone fabric (LF.14). Scale bar = 2cm. GGU 213421, Paralleldal Formation, locality 15, central Peary Land. B. Photomicrograph (PPL) of dolomitized skeletal, intraclastic grainstone. Scale bar = 1mm. GGU 274535, Paralleldal Formation, locality 19, central Peary Land.

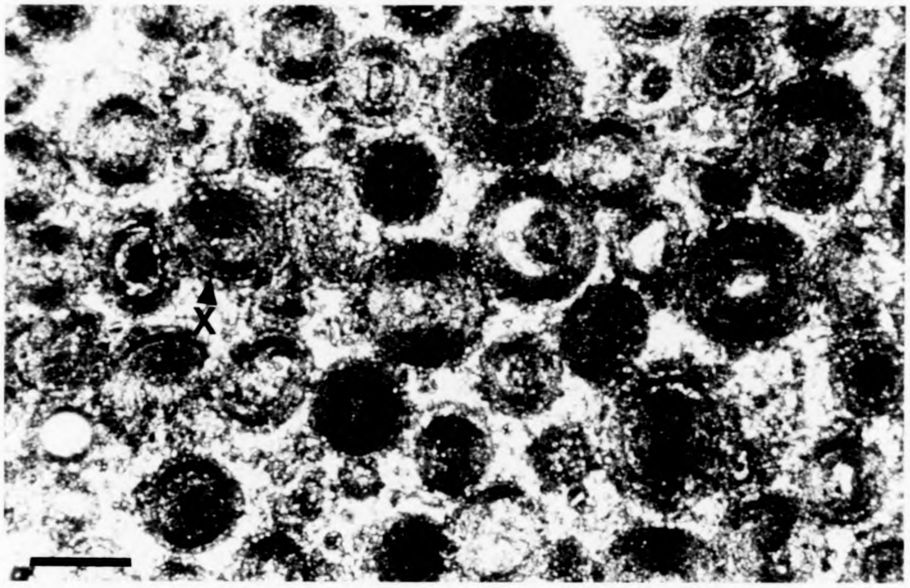


Figure 7.4. Photomicrograph (PPL) of partially silicified dolomite with a relict, well-sorted ooid grainstone fabric (LF.14). Note the secondary coatings on broken ooids (X). Scale bar = 1mm. GGU 218560, Perssuak Gletscher Formation, locality 2, west Peary Land.

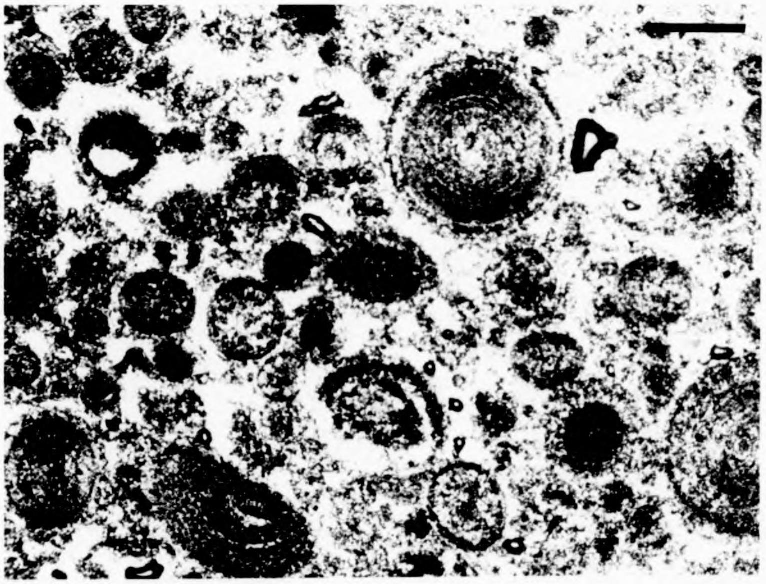

Figure 7.5. Photomicrograph (PPL) of partially silicified dolomite showing a moderately sorted ooid grainstone fabric (LF.14). Scale bar = 1mm. GGU 218559, Perssuak Gletscher Formation, locality 2, west Peary Land.

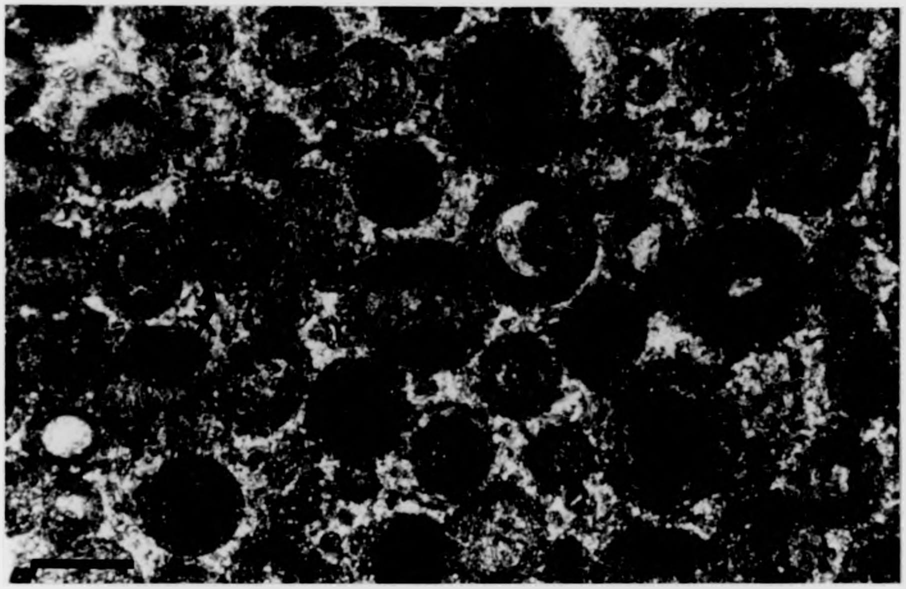

Figure 7.4. Photomicrograph (PPL) of partially silicified dolomite with a relict, well-sorted ooid grainstone fabric (LF.14). Note the secondary coatings on broken ooids (X). Scale bar = 1mm. GGU 218560, Perssuak Gletscher Formation, locality 2, west Peary Land.

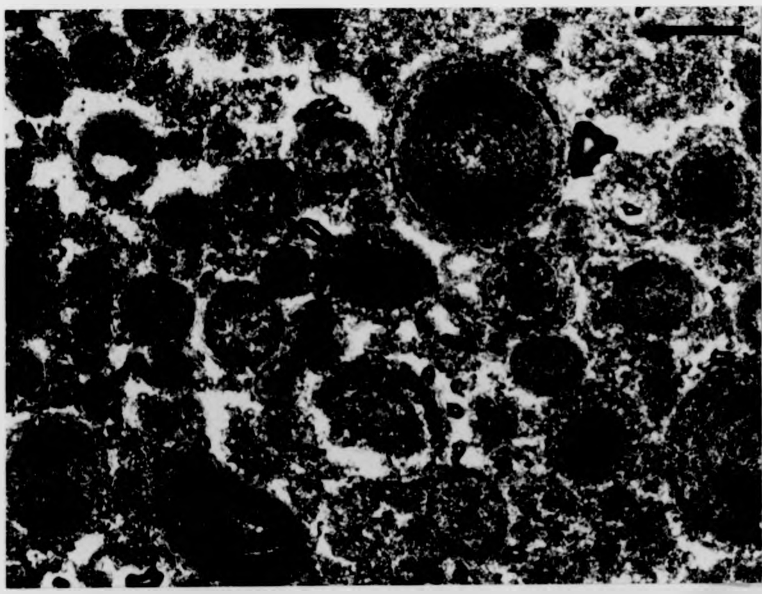

Figure 7.5. Photomicrograph (PPL) of partially silicified dolomite showing a moderately sorted ooid grainstone fabric (LF.14). Scale bar = 1mm. GGU 218559, Perssuak Gletscher Formation, locality 2, west Peary Land.

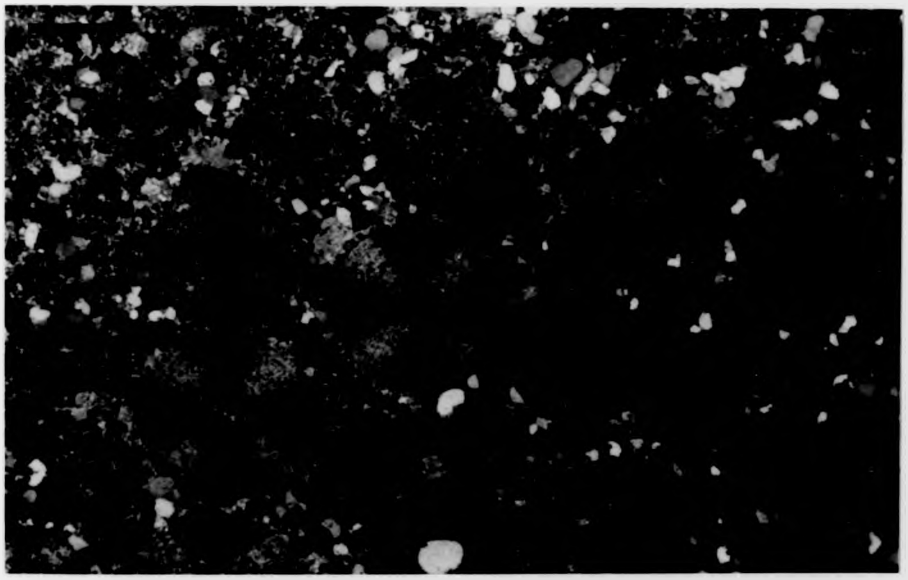

Figure 7.6. Photomicrograph (XP) of sandy dolomite with a well-preserved ooid grainstone fabric (LF.14). Note concentric ooid structure, 'pseudouniaxial' cross and occasional sand nuclei (e.g. lower centre) within ooids. Scale bar = 1mm. GGU 271221, Hellefiskefjord Formation, north-east Peary Land.

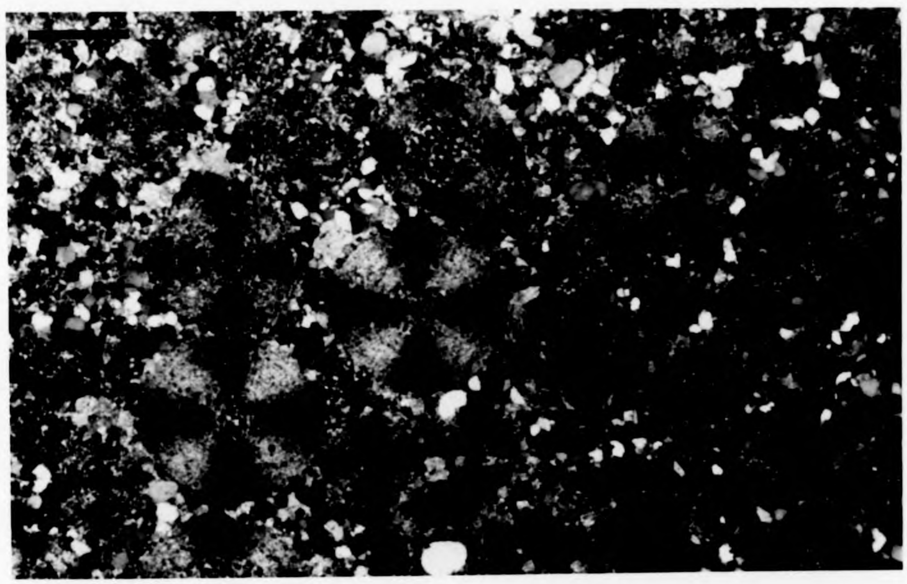

Figure 7.6. Photomicrograph (XP) of sandy dolomite with a well-preserved ooid grainstone fabric (LF.14). Note concentric ooid structure, 'pseudouniaxial' cross and occasional sand nuclei (e.g. lower centre) within ooids. Scale bar = 1mm. GGU 271221, Hellefiskefjord Formation, north-east Peary Land.

secondary growth about the ooid fragment (Fig. 7.5). Ooid cortices are composed of fine to very fine crystalline dolomite and, although radial structure is not evident in plane polarized light, the ooids commonly display a pseudo-uniaxial cross under cross-polars (Fig. 7.6). This is suggestive of a primary radial orientation of carbonate crystals (Sandberg 1983).

Two subfacies are recognized within this lithofacies:

14a. Cross-stratified grainstones.

Fabric retention is variable and rocks included in this subfacies range from dolomites showing well-preserved ooidal, peloidal, intraclastic and skeletal fabrics to medium to very coarse crystalline dolomite with no recognizable primary grains. The latter are included solely on the presence of cross-bedding which is often only recognized on favourably weathered surfaces (e.g. Fig. 3.35).

Trough cross-bedding is common and forms sets 0.1-0.5m thick (Figs 3.35 & 7.7). Tabular cross-sets occur in places and locally exceed 1.5m in thickness (Fig. 7.8). Foresets are 2-30mm thick and are generally defined by an alternation of coarser and finer detritus. In ooid grainstones, foresets commonly consist of an alternation of fine- to medium-grained and coarse- to very coarse-grained ooid sand; individual foresets are well-sorted (Fig. 7.4). Intraclastic, peloidal and skeletal grainstones are less well-sorted and often include grains ranging from very fine sand to fine pebble grade.

secondary growth about the ooid fragment (Fig. 7.5). Ooid cortices are composed of fine to very fine crystalline dolomite and, although radial structure is not evident in plane polarized light, the ooids commonly display a pseudo-uniaxial cross under cross-polars (Fig. 7.6). This is suggestive of a primary radial orientation of carbonate crystals (Sandberg 1983).

Two subfacies are recognized within this lithofacies:

14a. Cross-stratified grainstones.

Fabric retention is variable and rocks included in this subfacies range from dolomites showing well-preserved ooidal, peloidal, intraclastic and skeletal fabrics to medium to very coarse crystalline dolomite with no recognizable primary grains. The latter are included solely on the presence of cross-bedding which is often only recognized on favourably weathered surfaces (e.g. Fig. 3.35).

Trough cross-bedding is common and forms sets 0.1-0.5m thick (Figs 3.35 & 7.7). Tabular cross-sets occur in places and locally exceed 1.5m in thickness (Fig. 7.8). Foresets are 2-30mm thick and are generally defined by an alternation of coarser and finer detritus. In ooid grainstones, foresets commonly consist of an alternation of fine- to medium-grained and coarse- to very coarse-grained ooid sand; individual foresets are well-sorted (Fig. 7.4). Intraclastic, peloidal and skeletal grainstones are less well-sorted and often include grains ranging from very fine sand to fine pebble grade.

Figure 7.7. Small-scale trough cross-bedding in ooidal dolomites (LF.14a). Perssuak Gletscher Formation, locality 2, west Peary Land.

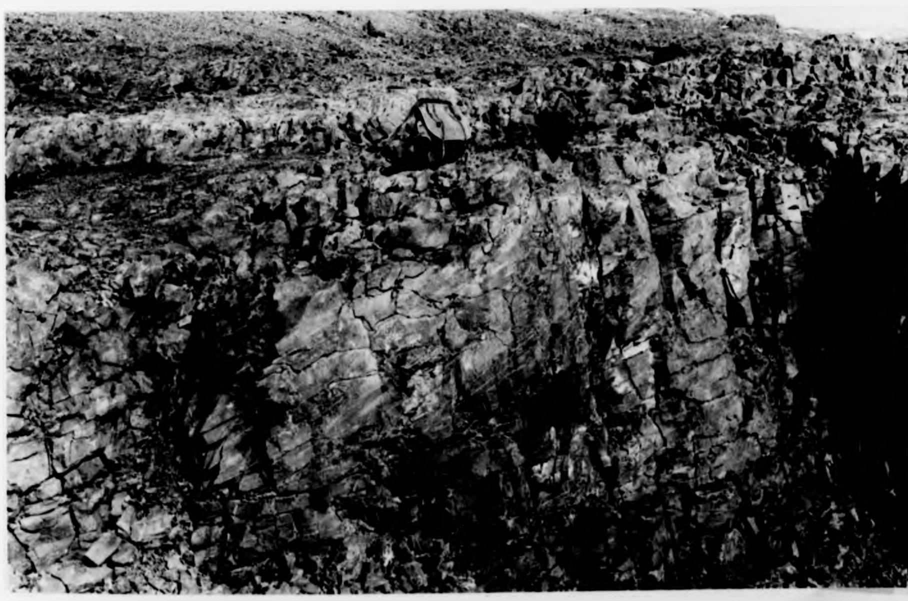

Figure 7.8. Large-scale tabular cross-bedding in skeletal dolomites; base and top of set indicated. Rucksack (upper centre) for scale. Sydpasset Formation, locality 2, west Peary Land.

Figure 7.7. Small-scale trough cross-bedding in ooidal dolomites (LF.14a). Perssuak Gletscher Formation, locality 2, west Peary Land.

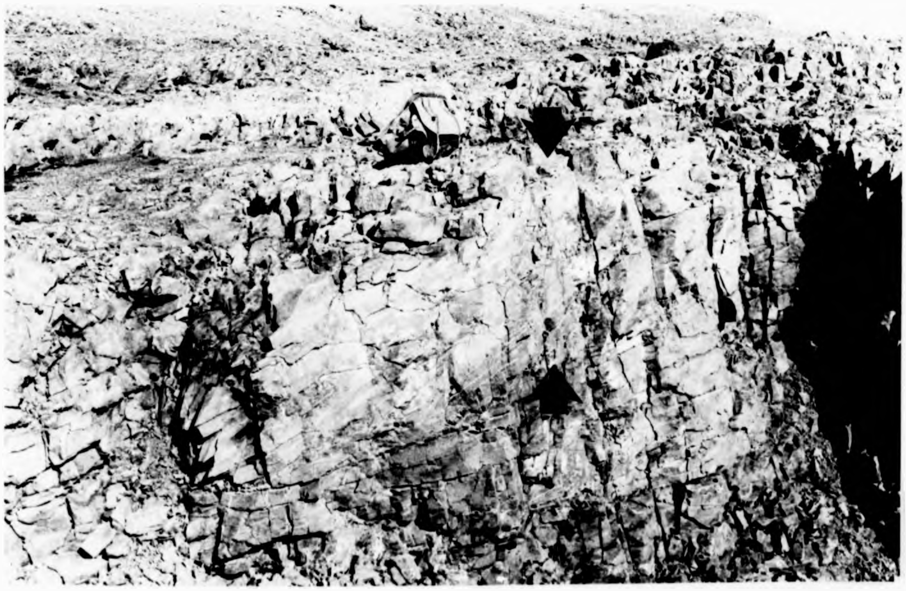

Figure 7.8. Large-scale tabular cross-bedding in skeletal dolomites; base and top of set indicated. Rucksack (upper centre) for scale. Sydpasset Formation, locality 2, west Peary Land.

14b. Parallel-stratified ooid grainstones.

This subfacies is only recognized in the Perssuak Gletscher Formation at Koch Væg (Fig. 7.9) where it occupies approximately 100m of vertical section. As with other representatives of the foreslope assemblage (see 7.2.1.1), this facies displays depositional dips towards the north. From field observations and measurements on oblique aerial photographs, the depositional dip at this locality is commonly 5-15$^{o}$, but may exceed 25$^{o}$ (Fig. 7.9). On the scale of a cliffline, these rocks form wedge-shaped bodies up to several tens of metres thick, that thin northwards and interfinger with the darker carbonates of the outer shelf-slope association (Figs 3.51 & 7.9). At outcrop scale, bedding is parallel or subparallel and beds are typically 0.02-0.2m thick (Fig. 7.10). Structureless beds predominate but some beds show a weak parallel lamination. Slumping is present locally (Fig. 7.10).

The ooid grainstones are less well-sorted than those of 14a (compare Figs 7.4 & 7.5) and consist of well-formed ooids, 0.4-1.5mm in diameter (coarse to very coarse sand grade).

Interpretation.

Although fabric retention is variable, this lithofacies is considered to represent mainly well-sorted, mud-poor carbonate sands. The relict 'ghosted' nature of allochems indicates dolomite replacement of a calcareous sediment and no evidence of early dolomite cements or primary dolomite grains is observed.

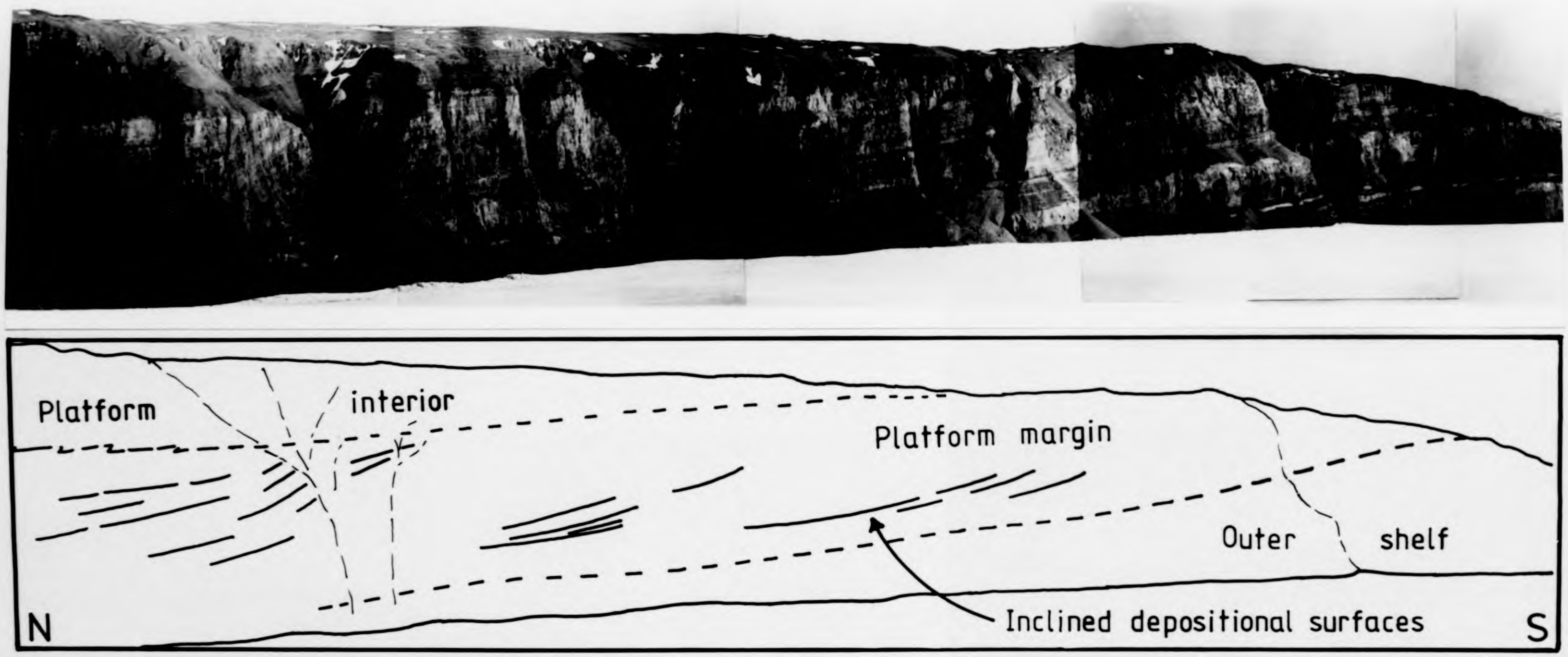


Figure 7.9. Photograph and interpretive sketch of the Tavsens Iskappe Group at the southern end of Koch Væg, viewed towards the east. Outer shelf facies (Brønlund Fjord Group and Fimbuldal Formation) are overlain by pale ooidal dolomites of the platform margin (Perssuak Gletscher Formation) showing northward-dipping depositional surfaces. These are succeeded by platform interior rocks of the Koch Væg Formation. Cliff is about 250m high.

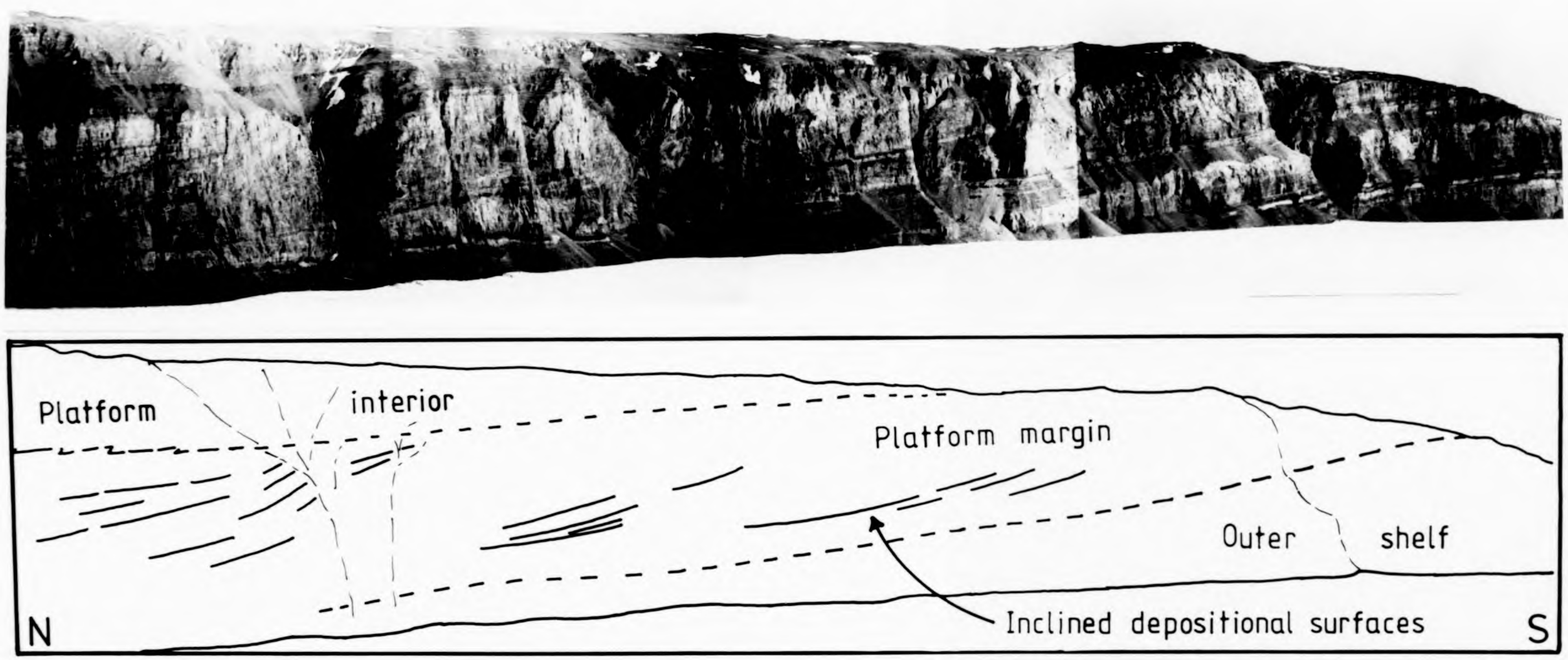


Figure 7.9. Photograph and interpretive sketch of the Tavsens Iskappe Group at the southern end of Koch Væg, viewed towards the east. Outer shelf facies (Brønlund Fjord Group and Fimbuldal Formation) are overlain by pale ooidal dolomites of the platform margin (Perssuak Gletscher Formation) showing northward-dipping depositional surfaces. These are succeeded by platform interior rocks of the Koch Væg Formation. Cliff is about 250m high.

Figure 7.10. Parallel-stratified ooidal dolomites (LF. 14b). Note the thin, parallel bedding and slump fold (arrow). Photograph taken at an oblique angle (figure gives real vertical) of a large detached block - near vertical bedding due to recent rotational landslip. Perssuak Gletscher Formation, locality 2, west Peary Land.

Figure 7.10. Parallel-stratified ooidal dolomites (IF. 14b). Note the thin, parallel bedding and slump fold (arrow). Photograph taken at an oblique angle (figure gives real vertical) of a large detached block - near vertical bedding due to recent rotational landslip. Perssuak Gletscher Formation, locality 2, west Peary Land.

Well-sorted lime sands are a common feature of modern shallow-water carbonate environments (Ball 1967; Bathurst 1971). The best-studied modern carbonate sands are those of the Bahama Banks (Ball 1967; Hine 1977; Hine & Neumann 1977; Hine *et al.* 1981) where they are typically well-developed on leeward and tide-dominated bank margins (Hine & Mullins 1983). Ooid sands occur in tide-dominated settings, particularly along open margins where tidal and storm-generated currents are unrestricted (Hine & Mullins 1983).

The environmental and geochemical conditions that favour ooid genesis have been the subject of much debate (see review by Simone 1980). In this wholly dolomitized example, fabric preservation is too poor to enter the debate concerning the primary mineralogy and fabric of the ooids (see James & Klappa 1983; Sandberg 1983). For the purposes of this interpretation it is sufficient to state that ooid growth, whether aragonite or calcite, radial or concentric, is favoured by abundant sand-sized nuclei in a turbulent, mud-free, aqueous environment, supersaturated in $CaCO_3$ (Bathurst 1971). Such optimum conditions are fulfilled in the warm, shallow, clear, turbulent waters of platform margin environments (Newell *et al.* 1960). On the Bahama Banks, the crest of ooid shoals may be awash at low tide, whereas marginal areas are covered by up to 5m of water (Ball 1967). Typically, however, ooid growth is favoured at water depths around 2m (Bathurst 1971; Hine 1977). On modern carbonate banks, peloidal and skeletal, non-coated sands generally accumulate in less energetic settings, transitional between high-energy reef or ooid shoal belts and the low energy environments of the deep shelf, slope or platform lagoon (e.g. Hine *et al.* 1981).

Ripples, megaripples and sand waves on modern carbonate sand shoals reflect active migration of sand under the influence of tides, waves and storm currents. On windward margins, bankward sand migration dominates (Hine 1977) whereas sand on leeward margins is commonly displaced offshore into deeper water (Ball 1967; Hine *et al.* 1981). Shoals are transected by channels that terminate in tidal spillover lobes on both sides of the sand shoal (Ball 1967; Hine 1977).

Hence, by analogy with modern carbonate environemts, the *cross-bedded grainstones* (14a) are interpreted as having formed and accumulated at the edge of a shallow-water carbonate platform on a linear sand belt composed of shoals, bars and tidal spillover lobes. As observed on the Bahama Banks (Ball 1967; Hine & Neumann 1977) such a transitional regime between an open sea and a shallow-water platform would experience the full force of onshore tide-, wind- or storm-induced currents. This is reflected in the well-sorted nature of the sediment, the common ooidal coatings and the cross-stratification produced by the migration of subaqueous ripples, megaripples and dunes. The occurrence of broken, recoated grains (Figs 7.4 & 7.5) and abnormally large ooids (1.5-2mm) suggests high energy conditions at the site of formation. Final deposition and burial of cross-bedded ooid sands probably occurred on the shoal flanks and on tidal spillover lobes, rather than at the high energy, mobile shoal crest where ooid growth was favoured.

Peloidal and skeletal sands were probably deposited in deeper or more protected waters where energy levels were sufficiently high to winnow, sort and periodically entrain the lime sand, but were not of sufficient magnitude or duration to promote ooid growth. In measured sections, cross-bedded, non-coated grainstones commonly succeed thin-bedded, skeletal, mud-rich carbonates of slope aspect and are overlain by ooid grainstones. This relationship suggests that the skeletal, peloidal grainstones accumulated offshore of the main shoal complex, in an environment that was transitional to the foreslope or upper slope environments.

Examples of carbonate sand complexes along fossil platform margins are numerous (e.g. Wilson 1975; Brady & Koepnick 1979; Davies 1977; Halley *et al.* 1983) particularly in stratigraphic intervals where reef-building organisms are few or diminutive (James & Mountjoy 1983).

Modern and ancient analogues of the inclined, *parallel-stratified ooid grainstone beds* (14b) are less common in the literature. Offshore dispersal of carbonate sand has been described from the western, lee-ward margin of the Bahama Banks, where peri-platform sand facies fringe the platform margin shoals to a depth of 3-400m (Mullins & Neumann 1979; Hine & Mullins 1983); slopes of 5- 20$^{o}$ are common and inferred processes include creep and grain flow. Similar peri-platform lime sands have been described off modern reef-dominated margins (Moore *et al.* 1976; Ginsberg & James 1973).

The grainstones described here form mainly structureless, ungraded thin beds that were deposited on north-facing slopes inclined at up to $30^{o}$; in many respects, they resemble grain flow deposits as described by Middleton & Hampton (1976) and Lowe (1982). True grain flows are often regarded as being unimportant in nature, since steep slopes (over $18^{o}$) are necessary to maintain the grain dispersion (Lowe 1976a). However, in this rather unique environment, depositional slopes commonly ranged from $10^{o}$ to $30^{o}$ and grain flow may have been a major transport mechanism. Indeed, in the Koch Væg cliff section (Figs 3.51 & 7.9) these rocks have the appearance of gigantic, tabular, avalanche foresets, as noted by Troelsen (1956). Similar facies were described by Pfeil and Read (1980) from the Cambrian of south-west Virginia, U.S.A. and interpreted as the deposits of a variety of mass flow mechanisms in a foreslope environment.

Hence, subfacies 14b probably records grain flow and creep processes on the sloping outer margin of a carbonate platform. Ooids from platform-edge shoals were washed offshore by tidal or storm-induced currents and cascaded down the sloping platform front to be deposited as a series of northward-dipping grainstone tongues, interdigitating with dark muddy carbonates of the outer shelf.

It is significant that this subfacies is only recognized at this one locality, where it coincides with the maximum depositional dips recorded from the Cambrian of Peary Land. It probably records a phase of enhanced platform progradation and the development of steep, rapidly accreting margin foreslopes. This may have been a local development, prograding northwards in advance of the remaining platform in a similar fashion to the sediment 'noses' prograding into the Florida Straits from the north-west corner of the Great and Little Bahama Banks (Mullins & Neumann 1979).

### 7.1.3. Lithofacies 15; Massive, archaeocyathid-bearing dolomite.

This facies is only recognized in the Lower Cambrian Paralleldal Formation in Paralleldal (Fig. 3.28, localities 18 & 19). Archaeocyathid-bearing fine to coarse crystalline dolomites occur within a pale weathering (pale-yellow-cream), poorly bedded dolomite succession in association with cross-bedded dolomites (Lithofacies 14a). Fabric preservation is patchy and the precise geometry and primary thickness of the archaeocyathid-bearing dolomites is unknown, but they occur in close vertical and lateral proximity to dolomitized ooid grainstones, and indeed are locally scoured by cross-bedded ooidal dolomites (Fig. 7.11; see also Fig. 7.19). Structureless dolomites with recognizable archaeocyathids occur sporadically throughout the upper 110m of the Paralleldal Formation at locality 18; clearly this facies formed a major component of this association during the late Early Cambrian. Bedding is weakly developed or absent in these rocks. Vague horizontal and gently inclined stratification is evident locally.

The archaeocyathids are of two basic types. Small conical skeletons, 5-30mm in diameter, have a simple septate structure (Fig. 3.34)


Figure 7.11. Sharp erosional contact (arrowed) between archaeocyathid - bearing dolomite (LF.15) and dolomitized ooid grainstones (LF.14). A: archaeocyathids. Pencil for scale. Paralleldal Formation, locality 19, central Peary Land.

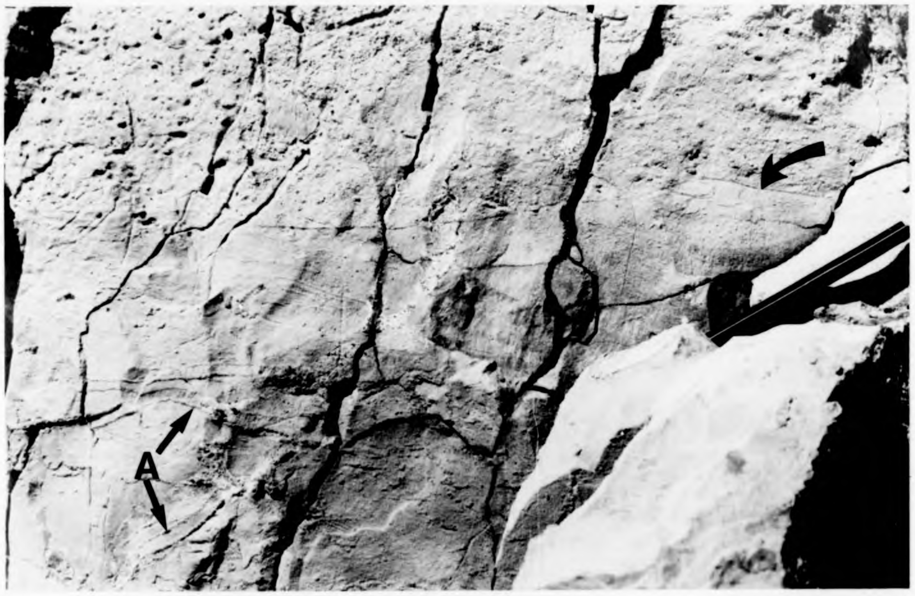


Figure 7.11. Sharp erosional contact (arrowed) between archaeocyathid - bearing dolomite (LF.15) and dolomitized ooid grainstones (LF.14). A: archaeocyathids. Pencil for scale. Paralleldal Formation, locality 19, central Peary Land.

and some specimens have a porous cellular wall structure; dissepiments are not observed. In many exposures, the former presence of these archaeocyathids is indicated by spar-lined conical vugs. Larger bowl- or vase-shaped forms with a simple septate structure (Figs 7.11 & 7.12) were recognized at a single outcrop. Debrenne (in prep; pers. comm. to J.S. Peel, 1984) reports three species of late Early Cambrian archaeocyathids from this locality.

Most archaeocyathid skeletons are complete or show *in situ* compactive fracturing; evidence of current reworking within this lithofacies is rare. Polished slabs and thin sections often reveal a relict, mottled, burrowed shelly wackestone fabric, composed of archaeocyathids and other skeletal elements (trilobite, echinoderm, *Salterella*) floating in a dolomitized lime mud matrix (Fig. 7.13).

Interpretation.

The relict depositional fabrics indicate deposition of poorly stratified, lime mud-rich skeletal wackestones or archaeocyathid floatstones that supported a benthic fauna and an active infauna. Accumulation of lime mud and the lack of abraded skeletal debris suggests a moderate to low energy environment; the open marine fauna and active infauna attest to a well-lit, oxygenated environment. In contrast, the closely associated, cross-bedded, well-sorted carbonate grainstones record deposition in shallow, turbulent waters at the carbonate platform edge (see Lithofacies 14a).

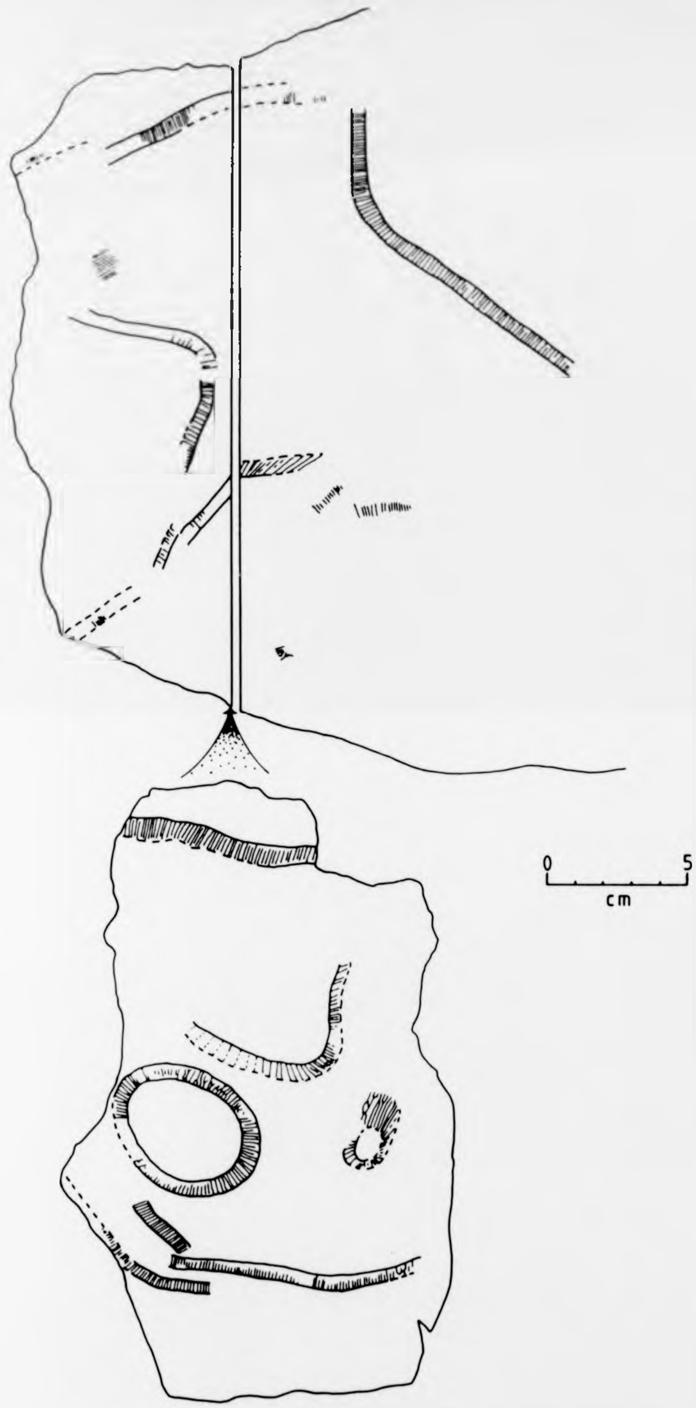


Figure 7.12. Sketch of a cut and polished block of archaeocyathid - bearing dolomite (LF.15) showing large bowl-shaped archaeocyathids. GGU 274526, Paralleldal Formation, locality 19, central Peary Land.

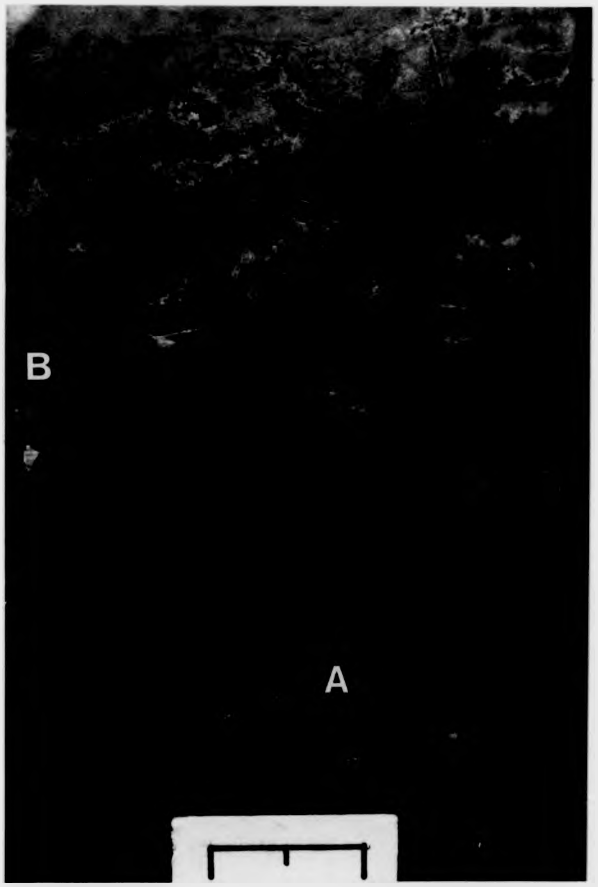


Figure 7.13. Polished slab, cut normal to bedding showing relict burrowed wackestone fabric in archaeocyathid-bearing dolomite (LF.15) A : archaeocyathid; B : inarticulate brachiopod. Scale bar = 2cm. GGU 274536, Paralleldal Formation, locality 19, central Peary Land.

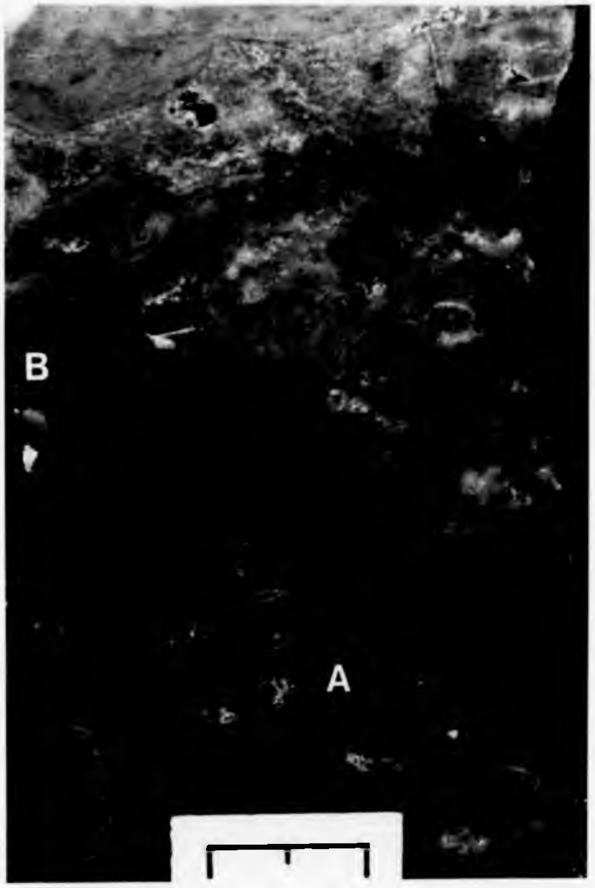


Figure 7.13. Polished slab, cut normal to bedding showing relict burrowed wackestone fabric in archaeocyathid-bearing dolomite (LF.15) A : archaeocyathid; B : inarticulate brachiopod. Scale bar = 2cm. GGU 274536, Paralleldal Formation, locality 19, central Peary Land.

Similar associations of archaeocyathid-bearing carbonates and lime grainstones have been recorded from western U.S.A. and southern Labrador (James & Kobluck 1978; Rowland 1981, 1984; James & Klappa 1983). In the Forteau Formation of southern Labrador, archaeocyathid-dominated reefal limestones occur in two contrasting depositional settings, as isolated patch reefs or as relatively thin, laterally extensive biostromes surrounded by and interstratified with skeletal and ooidal grainstones (James & Klappa 1983). A similar grainstone-biostrome association occurs in the Poleta Formation of the southern Great Basin, western U.S.A., where the biostromes may have formed wave-resistant framework reefs (Rowland 1981, 1984).

The archaeocyathid-bearing dolomites described here are poorly preserved and detailed analysis of depositional fabrics and facies relationships is impossible. However, by analogy with the examples given above, it is likely that these rocks represent archaeocyathid biostromes that formed in less energetic zones of the platform margin, probably in the lee or downslope from ooid sand shoals. The accumulation of lime mud was probably aided by the baffling effect of archaeocyathids and possibly by the binding action of algae (*cf.* James & Kobluck 1978).

### 7.1.4. Lithofacies 16; Structureless pale dolomite.

Structureless, pale cream, orange or white dolomite is a common component of this association, occurring extensively in the Løndal, Perssuak Gletscher and Paralleldal Formations (e.g. Figs 3.64 & 3.36).

These rocks are massive or show weakly defined, medium to thick bedding and are internally structureless. They comprise medium to coarse crystalline, sucrosic dolomite that typically shows no recognizable primary fabric. Rarely, small (5-20mm) curved vugs delineate the former location of possible skeletal grains; trilobite and brachiopod moulds were identified. Locally, these vugs define weak horizontal stratification.

These structureless, massive dolomites grade vertically and laterally into cross-bedded, dolomitized grainstones (Lithofacies 14), archaeocyathid-bearing dolomites (Lithofacies 15) and, less commonly, into dolomite breccias (Lithofacies 9).

Interpretation.

A confident interpretation of processes and depositional environments is precluded by the absence of diagnostic sedimentary structures and the scarcity of primary carbonate fabrics. However, these rocks commonly grade into dolomites in which depositional fabrics are preserved;clearly, the lack of structure is a diagenetic feature, resulting from dolomitization. Hence by analogy with the associated facies, these rocks are considered to represent the high-energy outer rim of a shallow-water carbonate platform. Primary carbonate sediments probably included lime grainstones, archaeocyathid biostromes (in the Early Cambrian) and foreslope breccias.

Similar thick-bedded or massive, structureless, pale carbonates are well-documented from dolomitized platform margins (e.g. the Cathedral Formation, British Columbia (McIlreath 1977); the Allen Bay Formation, Arctic Canada (Sodero & Hobson 1979)).

7.1.5. Lithofacies 17; Channelled, fine-grained sandstone.

This facies is only recognized in the Paralleldal Formation on the north-east side of Frysefjeld (Fig. 3.28, locality 17). Fine- to very fine-grained, well-sorted cream sandstones form lenticular units up to 6m thick and several tens of metres wide within pale, massive or cross-bedded dolomites (Fig. 7.14). At outcrop scale, basal contacts are sharp and may be planar or erosional. Observations of inaccessible cliff sections, however, indicate that these sand lenses occupy shallow channels, incised into massive pale dolomites of Association C (Fig. 7.14).

Channel fills may consist of a single lenticular sand bed or a multiple sequence of up to three sand lenses. The beds range from 0.4 to 3m in thickness and are mainly structureless and ungraded. In multiple channel fills, bed boundaries are sharp and locally loaded; in places the sandstone beds are intercalated with thin (5-50mm) burrowed silty sandstone beds. One fine-grained sandstone bed, 3m thick, shows faint parallel lamination near its base and low angle cross-bedding in the upper 0.5m.

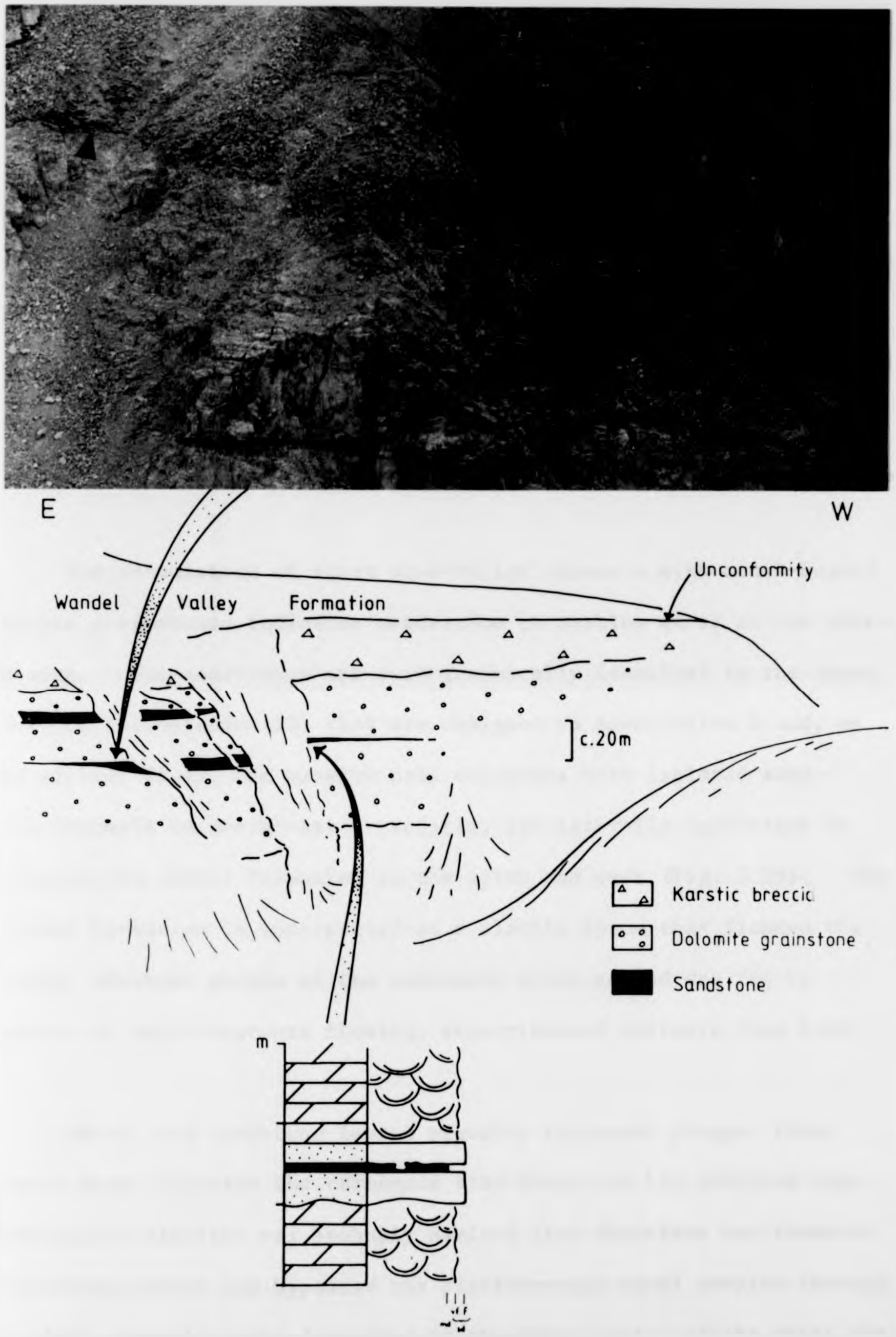


Figure 7.14. Channelled sandstones, Paralleldal Formation, north side of Frysefjeld (locality 17) central Peary Land. Photograph shows erosional channel base (arrowed) cut into pale dolomites; about 5m relief illustrated.

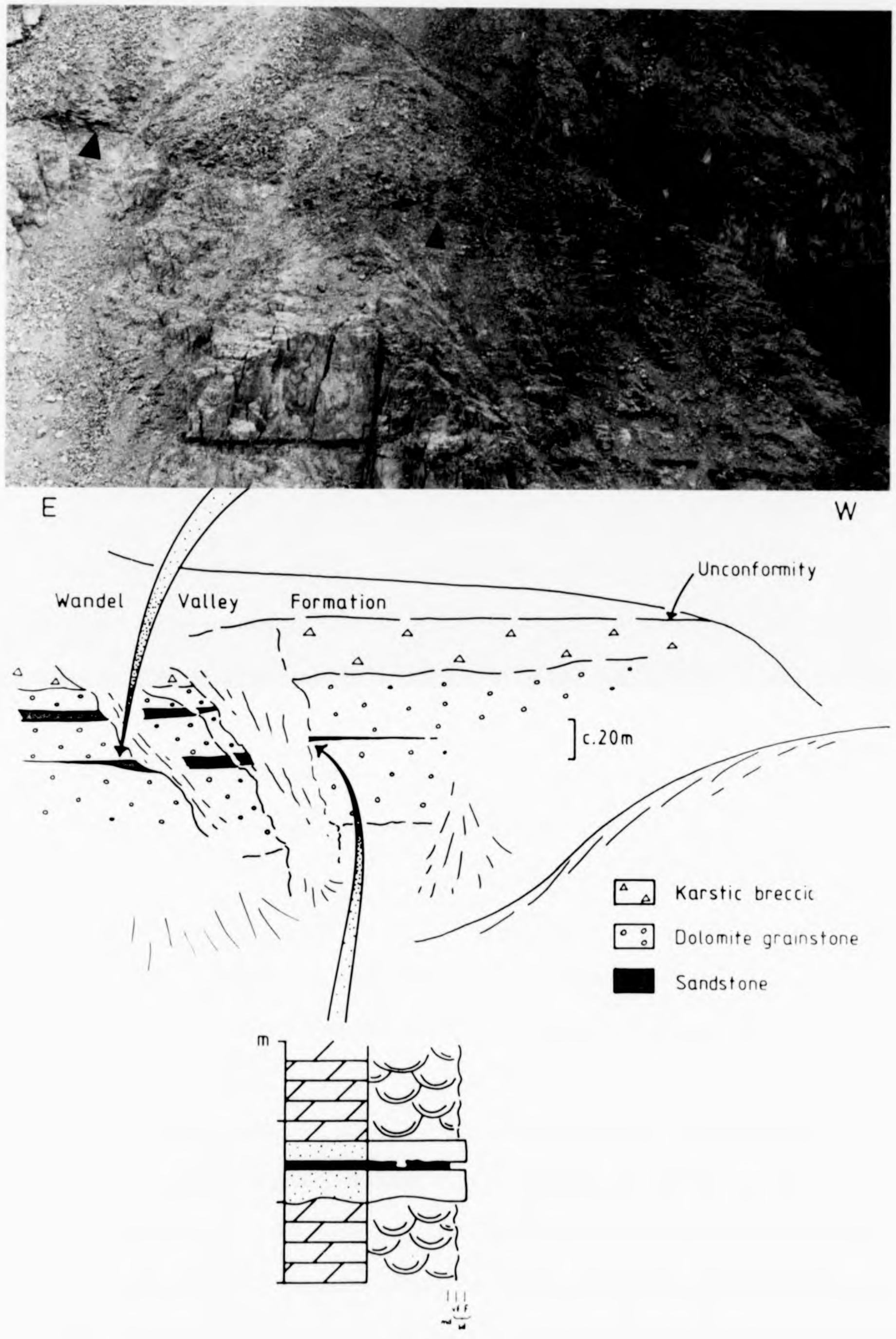


Figure 7.14. Channelled sandstones, Paralleldal Formation, north side of Frysefjeld (locality 17) central Peary Land. Photograph shows erosional channel base (arrowed) cut into pale dolomites; about 5m relief illustrated.

Interpretation.

The sharp erosive bases, abrupt planar tops and the structureless or weakly stratified nature of these beds suggest rapid deposition from episodic, high-energy currents. Together with the scarcity of cross-bedding, this suggests an episodic, storm-induced process rather than fair-weather tidal or wave processes.

The association of these sand-filled channels with cross-bedded carbonate grainstones indicates deposition in shallow water at the platform edge. The sandstones are petrographically identical to the sheet sandstones (Lithofacies 10) that are assigned to Association B and, as noted earlier (6.4), the massive pale dolomites with isolated sand-filled channels on north-east Frysefjeld, are laterally equivalent to the clastic Sæterdal Formation to the north and west (Fig. 3.28). The Sæterdal Formation is interpreted as a clastic apron that flanked the northern, offshore margin of the carbonate platform and was fed by northward or north-westward flowing, storm-induced currents (see 6.4).

Hence, the sandstone lenses probably represent plugged tidal channels that traversed the carbonate sand shoals at the platform edge. Siliciclastic detritus was probably derived from shoreface environments during storm events and bypassed the platform-edge shoal complex through such tidal channels to be deposited in the deeper water of the outer shelf.

Interpretation.

The sharp erosive bases, abrupt planar tops and the structureless or weakly stratified nature of these beds suggest rapid deposition from episodic, high-energy currents. Together with the scarcity of cross-bedding, this suggests an episodic, storm-induced process rather than fair-weather tidal or wave processes.

The association of these sand-filled channels with cross-bedded carbonate grainstones indicates deposition in shallow water at the platform edge. The sandstones are petrographically identical to the sheet sandstones (Lithofacies 10) that are assigned to Association B and, as noted earlier (6.4), the massive pale dolomites with isolated sand-filled channels on north-east Frysefjeld, are laterally equivalent to the clastic Sæterdal Formation to the north and west (Fig. 3.28). The Sæterdal Formation is interpreted as a clastic apron that flanked the northern, offshore margin of the carbonate platform and was fed by northward or north-westward flowing, storm-induced currents (see 6.4).

Hence, the sandstone lenses probably represent plugged tidal channels that traversed the carbonate sand shoals at the platform edge. Siliciclastic detritus was probably derived from shoreface environments during storm events and bypassed the platform-edge shoal complex through such tidal channels to be deposited in the deeper water of the outer shelf.

7.1.6. Lithofacies 18; Cross-bedded, medium-grained sandstones.

White or orange-brown, medium-grained, cross-beddded sandstones are recognized only within the Perssuak Gletscher Formation. As with much of the formation in west Peary Land, these rocks are either inaccessible or poorly exposed and study of Lithofacies 18 and 19 was restricted to three poorly exposed sections on the east side of Gustav Holm Dal (Fig. 3.48).

The lithofacies consists of well-sorted, well-rounded quartz-arenites forming thin (0.05m) to very thick (1m) beds. In places they contain up to 50% dolomitized ooids. They form units 1-25m thick that alternate with intervals of laminated, burrowed sandstones (Lithofacies 19) and sandy breccia beds (Lithofacies 9)(Fig. 3.48). In Gustav Holm Dal, exposure is too patchy to determine the geometry of these units, but in cliff sections along J.P. Koch Fjord and Navarana Fjord (Figs 3.47 & 7.15), individual units appear to be lenticular or wedge-shaped and truncate one another in a complex fashion. Individual beds thin towards the north, concomitant with the thinning of the sandstone wedges (Fig. 7.15).

At outcrop, these beds show small- to large-scale cross-bedding (Fig. 3.50). Simple, parallel-bounded tabular sets dominate but trough cross-bedding is present (J.S. Peel, pers. comm. 1979). Set and grain size within any one coset are generally uniform although some cosets, 2-5m thick, show an upward increase in set thickness from 0.05-0.2m at the base to 0.8-1.0m at the top.

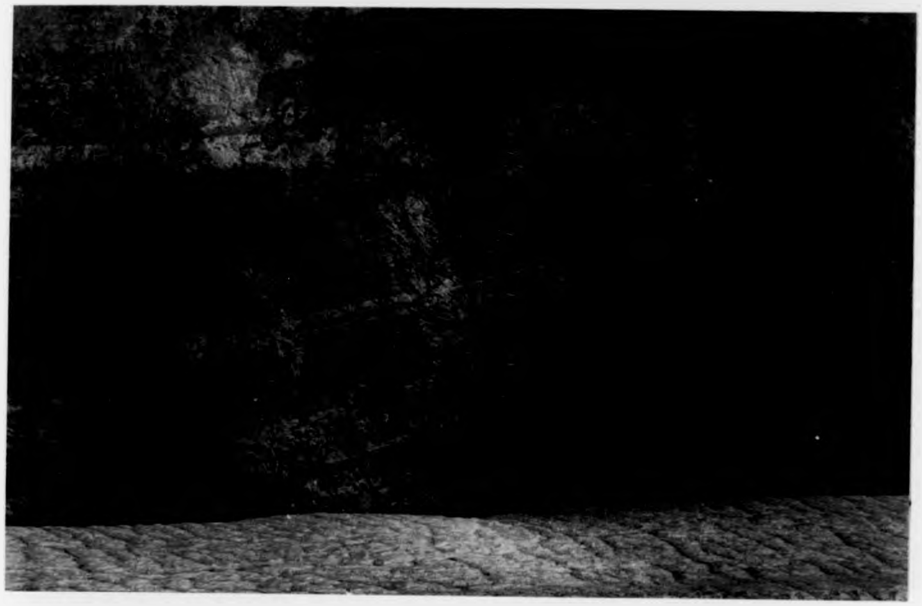

Figure 7.15. Sandstones of the Perssuak Gletscher Formation on the east side of Navarana Fjord. Note the complex, large-scale cross-stratification. Estimated vertical field of view = 50m.

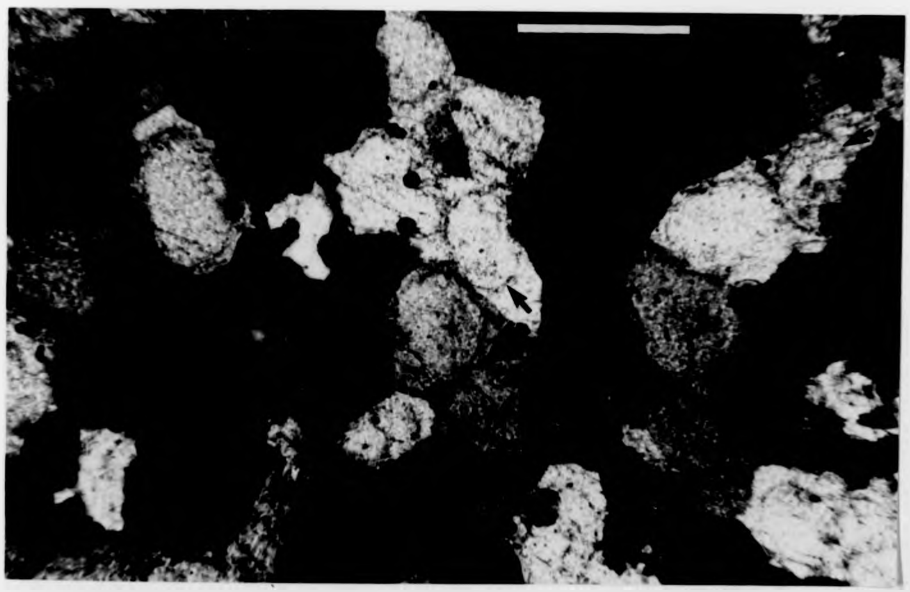

Figure 7.16. Photomicrograph (XP) of quartz arenitic sandstone (LF.18). Note well-rounded quartz grains (arrows) and syntaxial overgrowths. (Dark blebs are artifacts). Scale bar = 0.5mm. GGU 218656, Perssuak Gletscher Formation, locality 8, west Peary Land.

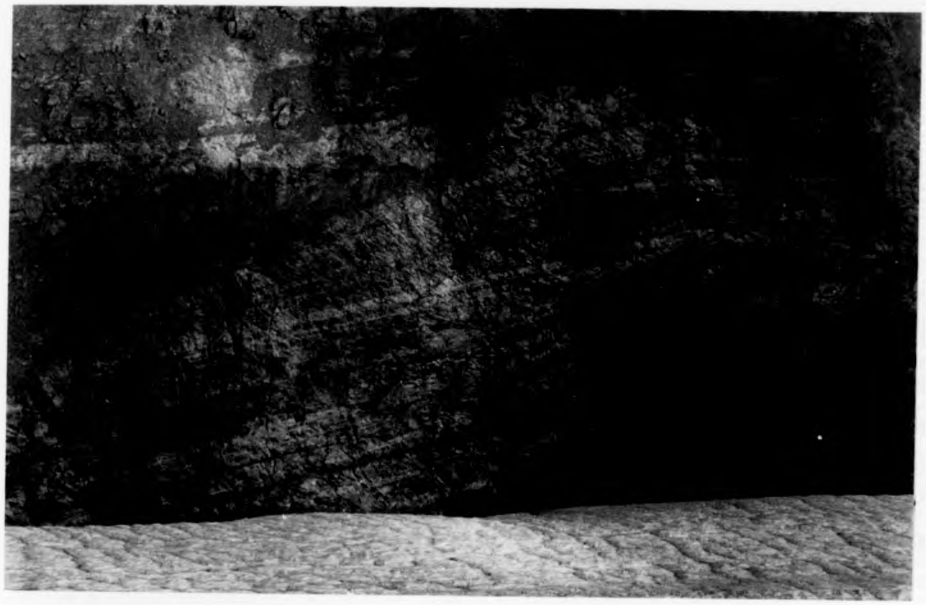

Figure 7.15. Sandstones of the Perssuak Gletscher Formation on the east side of Navarana Fjord. Note the complex, large-scale cross-stratification. Estimated vertical field of view = 50m.

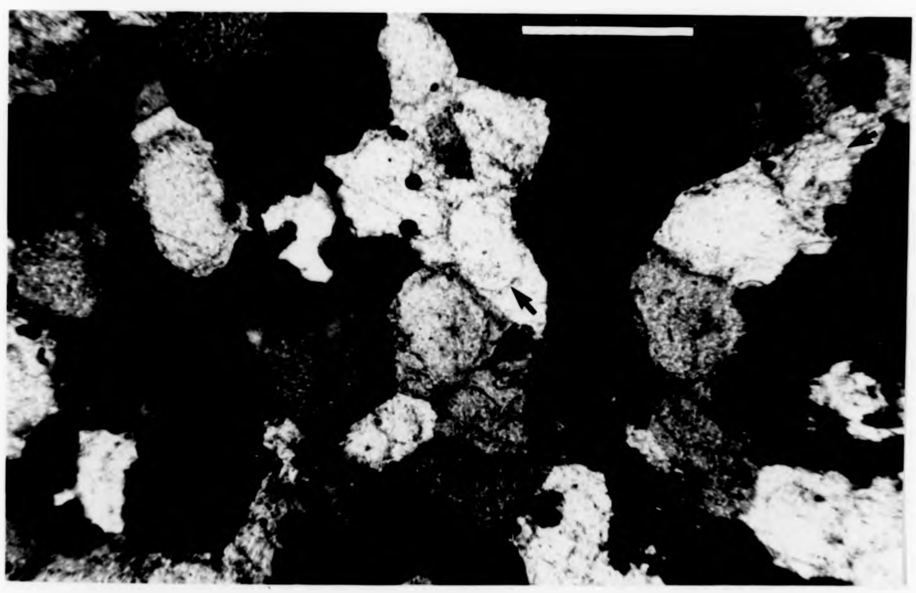

Figure 7.16. Photomicrograph (XP) of quartz arenitic sandstone (LF.18). Note well-rounded quartz grains (arrows) and syntaxial overgrowths. (Dark blebs are artifacts). Scale bar = 0.5mm. GGU 218656, Perssuak Gletscher Formation, locality 8, west Peary Land.

The limited palaeocurrent data suggest consistent northward flow (see Fig. 8.4); herringbone cross-bedding was not observed.

The sandstones are mainly cemented by syntaxial silica overgrowths (Fig. 7.16) but dolomite cements are important in some beds.

Interpretation.

A marine environment is indicated by the association with dolomitized ooid grainstones and burrowed sandstones showing a marine trace fossil assemblage (see Lithofacies 19). Furthermore, these sandstones interfinger northwards with dark carbonates that contain conodonts (Peel 1982a). The textural and mineralogical maturity of the sediment and the ubiquitous, well-developed cross-bedding suggest a high-energy, probably tide-dominated, shallow-marine environment (Johnson 1978; Levell 1980; Driese *et al.* 1981).

The cross-bedding indicates sediment entrainment by tractional currents and lateral migration of megaripples or dunes. The uniformity of grain size, set size and transport direction within any one coset suggests that individual cosets represent the deposits of a single field of megaripples (Levell 1980). The limited palaeocurrent data indicate a undirectional flow pattern and evidence of flow reversal was not observed. Although bidirectional patterns are commonly considered to be characteristic of tide-dominated sequences, unidirectional flow patterns are frequently reported from inferred tidal deposits (e.g. McCave 1973;

The limited palaeocurrent data suggest consistent northward flow (see Fig. 8.4); herringbone cross-bedding was not observed.

The sandstones are mainly cemented by syntaxial silica overgrowths (Fig. 7.16) but dolomite cements are important in some beds.

Interpretation.

A marine environment is indicated by the association with dolomitized ooid grainstones and burrowed sandstones showing a marine trace fossil assemblage (see Lithofacies 19). Furthermore, these sandstones interfinger northwards with dark carbonates that contain conodonts (Peel 1982a). The textural and mineralogical maturity of the sediment and the ubiquitous, well-developed cross-bedding suggest a high-energy, probably tide-dominated, shallow-marine environment (Johnson 1978; Levell 1980; Driese *et al.* 1981).

The cross-bedding indicates sediment entrainment by tractional currents and lateral migration of megaripples or dunes. The uniformity of grain size, set size and transport direction within any one coset suggests that individual cosets represent the deposits of a single field of megaripples (Levell 1980). The limited palaeocurrent data indicate a undirectional flow pattern and evidence of flow reversal was not observed. Although bidirectional patterns are commonly considered to be characteristic of tide-dominated sequences, unidirectional flow patterns are frequently reported from inferred tidal deposits (e.g. McCave 1973;

Anderton 1976) and reflect the dominance of either the ebb or the flood currents. Large-scale compound cross-bedding is commonly reported from ancient tidal sandstones bodies interpreted as tidal sand waves and ridges (Nio 1976; Levell 1980; Driese *et al.* 1981). Such cross-stratification was not recognized at accessible outcrop, but structures in cliff sections on the east side of Navarana Fjord (Fig. 7.15) show a gross resemblance to the large-scale compound cross-bedding figured by Johnson (1978).

Hence, on the basis of the limited data available, these mature, cross-bedded sandstones are interpreted as the result of tidal processes in a shallow marine, high-energy environment.

7.1.7. Lithofacies 19; Bioturbated laminated sandstones.

Units (0.25-5m thick) of parallel-bedded, laminated, fine- to medium-grained sandstones occur interstratified with cross-bedded sandstones and dolomite sandstone breccias in the upper half of the Perssuak Gletscher Formation in Gustav Holm Dal (Fig. 3.48). The thin bedding and lamination reflects grain size variation from very fine to medium sand; dark siltstone laminae occur locally. Laminae or thin beds range from <1mm to 30mm in thickness. Stratification is mainly horizontal (Fig. 7.17), although ripple cross-lamination is present in places.

This lithofacies is characteristically bioturbated although rarely to the point of complete obliteration of primary structures. Simple vertical burrows predominate and *Monocraterion* burrows are common

Figure 7.17. Parallel-laminated sandstones (LF.19) with abundant Monocraterion burrows. Perssuak Gletscher Formation, locality 8, west Peary Land.

Figure 7.17. Parallel-laminated sandstones (LF.19) with abundant Monocraterion burrows. Perssuak Gletscher Formation, locality 8, west Peary Land.

(Fig. 7.17). Horizontal traces are rare; unbranched, curved horizontal burrows (1-5mm wide) on one bedding plane have structureless sand fills and thin silty wall linings and are tentatively referred to *Palaeophycus*. P. Frykman and J.S. Peel (pers. comm. 1979) reported radial traces on an upper bed surface, comprising irregular grooves (5-8mm across, <40mm long) radiating from a central featureless, sub-circular field, 40-50mm across. These traces compare favourably with *Asterichnus* although this ichnogenus has previously only been reported from Cretaceous rocks (Książkiewicz 1970). Similar radial traces, albeit on a larger scale, were reported from Cambrian shallow marine clastics of Finnmark, Norway (Banks 1970).

Interpretation.

Parallel lamination in sandstones is commonly interpreted as the result of deposition from currents in the upper flow regime within the field of development of flat bedforms (Harms 1975). Such an origin is unlikely in this case; the gradational nature of most bed and laminae boundaries, the absence of primary current lineation and erosional features all argue against a high-energy depositional process. The thin parallel stratification probably resulted from deposition from suspension following the passage of intermittent currents of tidal or storm origin or, as suggested by the localized ripple cross-lamination, from the lateral migration of current ripples (*cf.* Lindholm 1982).

The scarcity of mud-grade sediment and the dominance of vertical burrows reflects a mobile shifting substrate (Rhoads 1975) that experienced frequent winnowing of fines. *Monocraterion* is characteristic of sand-dominated, shallow marine sequences (e.g. Swett *et al.* 1971; Crimes *et al.* 1977) and is commonly assigned to the *Skolithus* assemblage of Seilacher (1967), suggesting deposition in shallow neritic or littoral environments. Hallam & Swett (1966) and Crimes *et al.* (1977) suggested that *Monocraterion* burrows represent a response to slow but continuous sediment influx, allowing periodic adjustment of the level of the burrow. Thus, these traces are consistent with the interpretation of a shallow marine environment, characterized by sand deposition fron suspension or low-velocity currents, producing low, flat bedforms (*cf.* Goodwin & Anderson 1974).

## 7.2. Association C. Environment Interpretation.

### 7.2.1. Carbonates.

The carbonates of this association overlie and grade northwards into dark, fine-grained facies assigned to the outer shelf-slope association (Association B) and are overlain by or pass southwards into rocks of Association D (Fig. 5.1). In vertical section, Association C rocks occupy intervals 35-120m thick. From facies reconstructions in the Henson Gletscher, Løndal and Paralleldal areas (e.g. Fig. 5.1) it is evident that Association C rocks represent a narrow high-energy environmental belt trending approximately ENE-WSW and separating a low-energy, restricted, shallow-water environment in the south from a deeper-water, open marine outer shelf environment to the north. Such an arrangement is typical of the outer rim of carbonate platforms, as reported from modern carbonate banks (e.g. Hine & Mullins 1983) and ancient successions (e.g. Wilson 1975; Brady & Koepnick 1979). In many sections it is possible to subdivide Association C carbonates into two assemblages. Where dolomitization has resulted in complete obliteration of primary structures, subdivision is impossible and a generalized platform margin interpretation is applied.

#### 7.2.1.1. Foreslope Assemblage.

This assemblage is well represented in the Perssuak Gletscher Formation at Henson Gletscher, the Løndal Formation in Løndal and it occurs locally in the Sydpasset and Paralleldal Formations. It comprises pale, wedge-shaped debris tongues (Lithofacies 9) interbedded with dolomitized grainstones (Lithofacies 14); these rocks interfinger towards the north with dark, thin-bedded carbonates assigned to the outer shelf-slope association (Figs 3.47, 3.51 & 7.9). Characteristically, these rocks show northward dipping depositional surfaces inclined at between $5^{o}$ and $30^{o}$ (Fig. 7.9). Individual beds and packets of beds thin rapidly northwards wedging out within the darker outer shelf rocks; the pale foreslope tongues locally show a sigmoidal form and resemble large-scale tabular cross-bedding (Fig. 7.18). Along Koch Væg, where this phenomenon is superbly exposed, individual foreslope tongues have an estimated relief of over 100m; this represents the depositional relief between the accreting platform edge and the

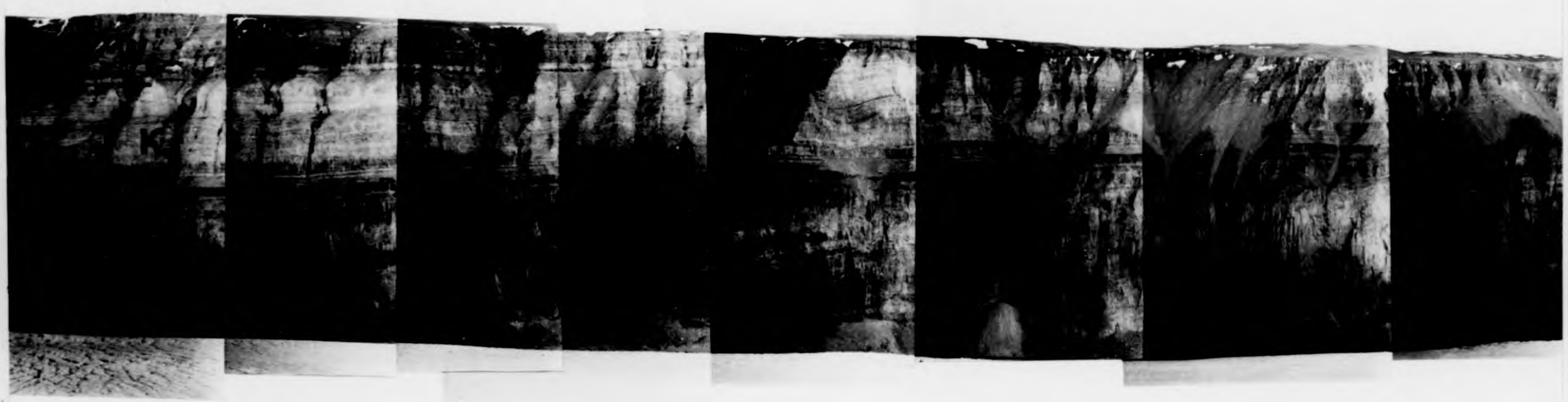

Figure 7.18. Perssuak Gletscher (P) and Koch Væg Formations (K) at Koch Væg viewed towards the east. W = Wandel Valley Formation. Note the northward-dipping inclined surfaces within the Perssuak Gletscher Formation and the interfingering of pale platform margin carbonates and dark outer shelf carbonates, producing a large-scale cross-bedded appearance.

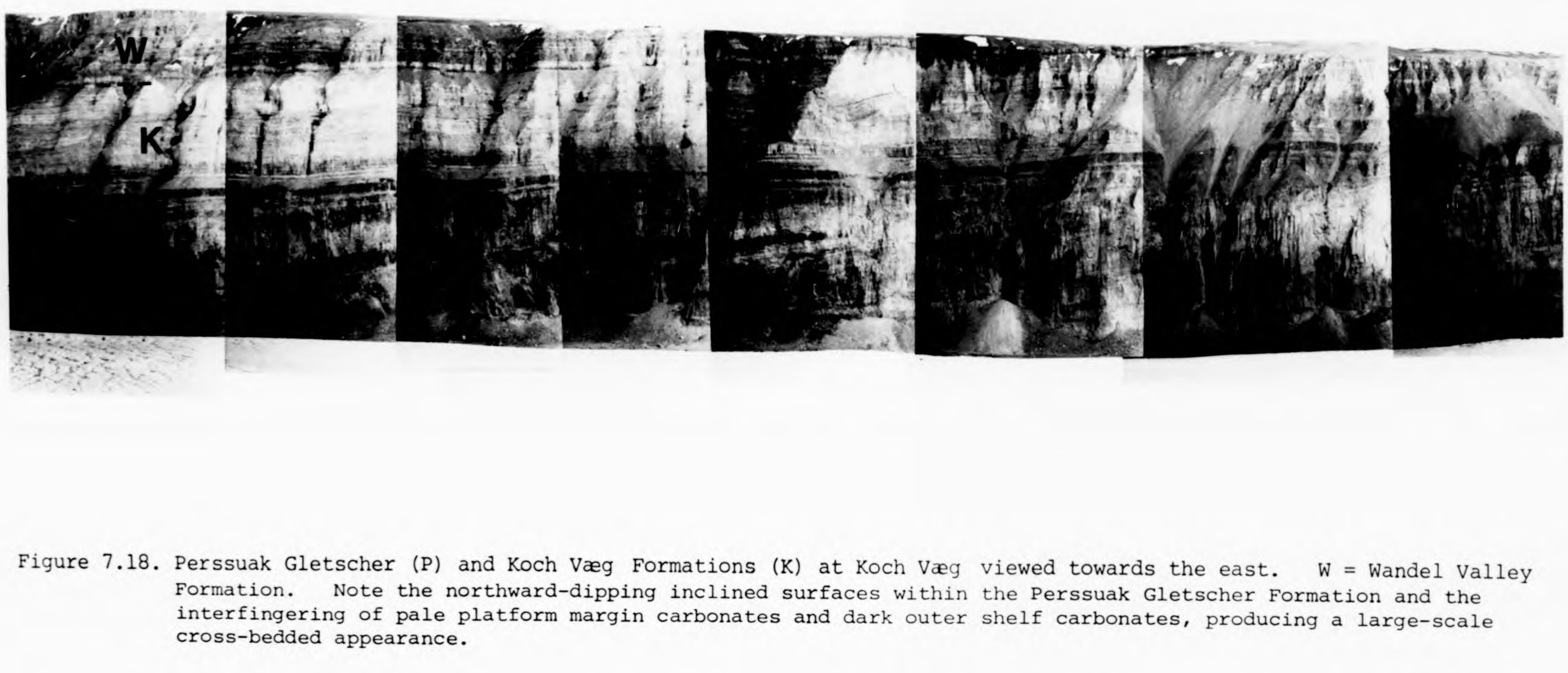


Figure 7.18. Perssuak Gletscher (P) and Koch Væg Formations (K) at Koch Væg viewed towards the east. W = Wandel Valley Formation. Note the northward-dipping inclined surfaces within the Perssuak Gletscher Formation and the interfingering of pale platform margin carbonates and dark outer shelf carbonates, producing a large-scale cross-bedded appearance.

proximal parts of the outer shelf. The sigmoidal form is most obvious where dark outer shelf rocks both underlie and onlap onto the pale foreslope tongues (Fig. 7.18). In vertical section, therefore, foreslope facies are interbedded with and ultimately succeed thin-bedded, skeletal carbonates of the upper slope; hence a precise boundary between the upper slope and foreslope assemblages is often difficult to place (e.g. Fig. 6.76).

The juxtaposition of the deposits of mass flows (debris and grain flows) with cross-bedded carbonate sands deposited from tractional bottom currents implies a gravitationally unstable environment at relatively shallow water depths, above wave base. Proximity to an ooid-dominated sand bank is indicated by the abundant ooidal detritus, both as lithified grainstone blocks in debris beds (Lithofacies 9), and as discrete grains in the inclined, parallel-stratified grainstone beds (Lithofacies 14b). Cross-bedded grainstones in this assemblage are dominated by skeletal grains, peloids and intraclasts; thin-bedded, laminated packstone units are present locally. The transition from ooid-dominated cross-bedded sands at the platform edge (see 7.2.1.2) to skeletal, intraclastic, peloidal grainstones in the foreslope assemblage reflects decrease in energy with increasing water depth (*cf.* Rees *et al.* 1976).

This assemblage thus records deposition on the sloping front of a prograding shallow-water carbonate platform, that was rimmed by lime sand shoals. It is equivalent to the peri-platform talus of McIlreath & James (1978) and the foreslope facies of Wilson (1975). Comparable rocks have been described from the Triassic of the Dolomites (Bosellini 1984) and the Cambrian of south-west Virginia, U.S.A. (Pfeil & Read 1980). The Cambrian foreslope facies reported by Pfeil & Read consist of parallel-stratified lime sands and carbonate breccia beds interbedded and interfingering laterally with thin-bedded black, shaly limestones. McIlreath (pers. comm. in Pfeil & Read 1980) observed foreslope facies in the Devonian of the Rockies that show depositional slopes of 10-15$^{o}$. Comparable light-coloured shelf foreslope carbonates were described by Davies (1977) from the Late Palaeozoic Sverdrup Basin, Arctic Canada. He reported a rapid transition from shelf edge to slope carbonates with depositional surfaces inclined at 15-50$^{o}$.

The character and degree of development of the foreslope assemblage varies considerably through the Peary Land Cambrian sequence. This subject is considered below (7.2.1.3).

7.2.1.2. Platform-edge shoal complex.

This assemblage forms much of the Perssuak Gletscher, Løndal and Paralleldal Formations and is present in the Sydpasset Formation in southern exposures along Wandel Dal. It mainly comprises light-coloured, cross-bedded dolomites composed predominately of ooids where relict grains are identifiable. The well-sorted nature of these sands, the presence of cross-bedding and the dominance of coated grains indicates a high-energy, platform-edge setting (see Lithofacies 14a). In the Lower Cambrian Paralleldal Formation, these platform-edge carbonate sands are associated with archaeocyathid-bearing massive dolomites and terrigenous sand-filled channels, which are interpreted as biostromes and storm sand-plugged tidal channels respectively.

Carbonate sand-dominated platform-edge shoal complexes are well known from modern carbonate banks (Ball 1967; Hine & Neumann 1977) and this setting is commonly inferred in studies of ancient platform carbonates (e.g. Wilson 1975; Brady & Koepnick 1979; Pfeil & Read 1980; Halley *et al.* 1983). Associated biostromal archaeocyathid-rich carbonates have been reported from a number of Lower Cambrian successions (e.g. James & Klappa 1983; Rowland 1984).

7.2.1.3. Discussion.

In recent reviews of carbonate platform development, several authors have emphasized the importance of the platform margin in dictating the evolutionary style of the platform and offshore environments (McIlreath & James 1978; Kendall & Schlager 1981; Read 1982; James & Mountjoy 1983). The platform margin (shelf-slope break of James & Mountjoy 1983) forms the optimum site for carbonate production, since it occurs in shallow, well-lit, aerated waters of normal salinity, well-supplied with nutrients and Ca $CO_3$ from the open ocean and distant from repressive, shore-bound siliciclastic detritus. Carbonate fixation may have an organic origin, yielding organic reefs and skeletal sands or may result from inorganic precipitation producing ooid sand banks and carbonate cements (James & Mountjoy 1983).

Since the shallow-water platform, and particularly the platform margin, is the source of most lime sediment deposited in slope, deep shelf and basinal settings, then in the absence of an overriding tectonic control, the nature and rate of sedimentation at the margin inevitably controls the configuration of the slope and slope-margin transition. If upward growth of the margin is rapid and vastly exceeds lateral accretion and resedimentation in foreslope-slope environments then a steep escarpment will develop, resulting in the bypass margin of McIlreath & James (1978). Conversely, if lateral accretion and carbonate dispersal into deeper water roughly matches the vertical growth rate of the platform, then the declivity of foreslope and upper slope environments will be more subdued - the depositional margin of McIlreath & James (1978). The balance between upward and lateral growth is dependant primarily on the interplay between carbonate production and the relative rate of sea level change.

To a lesser degree, the configuration of the margin is influenced by the style of sedimentation at the platform edge. Thus, reef-dominated margins commonly accrete vertically to form steep, wave-resistant escarpments, whereas carbonate sands on sand shoal-dominated margins are more readily dispersed into deeper water environments, producing a gradual transition (James & Mountjoy 1983). During the Cambrian,large metazoans capable of producing wave-resistant reef complexes were absent (James 1983) and high-energy platform margins were composed mainly of carbonate sand shoals (e.g. Brady & Koepnick 1979).

In the Peary Land Cambrian succession the platform edge was composed almost exclusively of carbonate sand banks. Archaeocyathid biostromes only occur in one restricted area in rocks of late Early Cambrian age. Despite this homogeneous sedimentation pattern at the platform edge, the nature of the transition from platform to outer shelf varies laterally and stratigraphically, reflecting the influence of progradation rates and local topography on this transition. The variation is illustrated by examples from the Paralleldal Formation (a), the Perssuak Gletscher Formation (b & c) and the Løndal Formation (d).

(a) Paralleldal Formation, Paralleldal.

The Lower Cambrian platform-outer shelf transition is exposed in a shallow re-entrant on the north side of Paralleldal (Fig. 3.28, locality 19). Dark laminated or burrowed skeletal dolomites assigned to the upper slope association are succeeded vertically and laterally towards the south by pale cross-bedded dolomites and archaeocyathid-bearing dolomites of the platform-edge assemblage (Fig. 7.19). Mass flow deposits are very rare and the foreslope assemblage is not recognized. Inclined depositional surfaces are scarce and where present are rarely greater than $5^{\circ}$. The light-coloured platform margin tongues wedge out gradually towards the north within the darker outer shelf carbonates, producing a

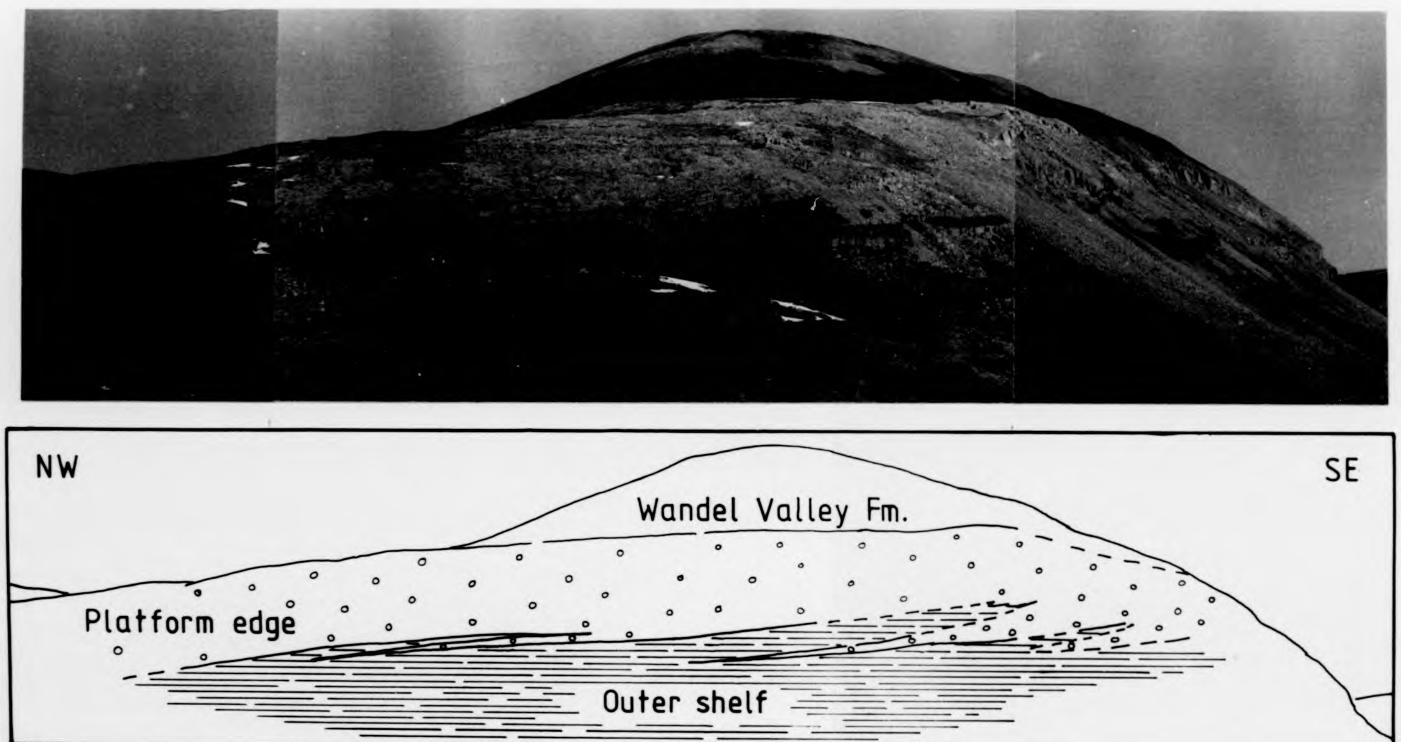


Figure 7.19. Photograph and interpretive sketch of the Paralleldal Formation at locality 19, central Peary Land.

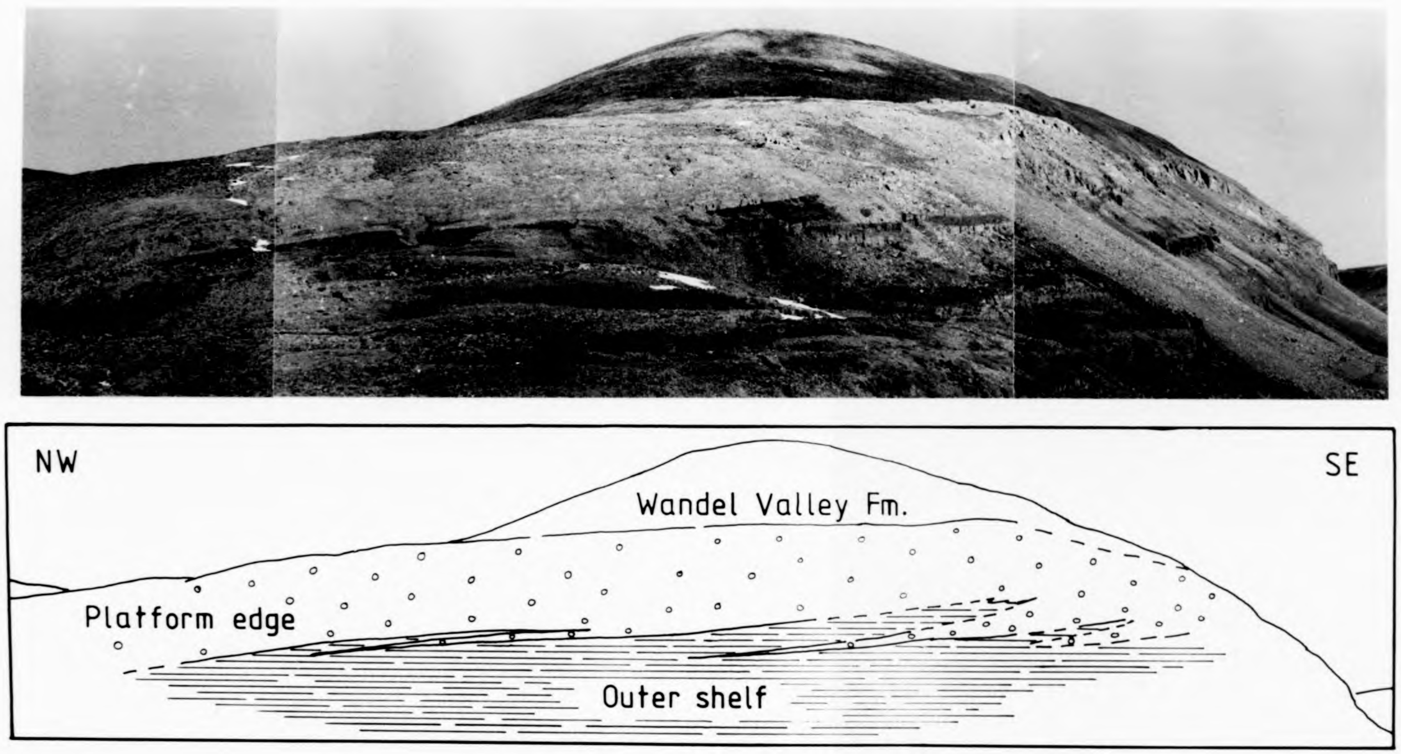


Figure 7.19. Photograph and interpretive sketch of the Paralleldal Formation at locality 19, central Peary Land.

low-angle interdigitation that reflects gradual north-westward progradation of the platform margin (Fig. 7.19).

The absence of foreslope mass flow deposits, the low depositional slopes and the gradual intercalation of the outer shelf and platform-edge facies suggest a gently sloping transition in this area during the late Early Cambrian. Ooid sand shoals, associated with archaeocyathid biostromes accumulated in moderate to high-energy shallow water at the platform edge and prograded intermittently towards the north over bioturbated skeletal sands and muds. Sedimentation rates in upper slope and outer shelf environments approximately matched accretion at the platform margin and relief was slight; consequently, foreslope facies were not developed.

It is significant that the archaeocyathid-rich biostromal carbonates only occur in this restricted area of Paralleldal and indeed this is the only record of archaeocyathids from Greenland. The absence of this facies elsewhere in Peary Land is partly due to the restricted exposure of Lower Cambrian platform margin carbonates. These rocks are well-exposed between Sæterdal and Børglum Elv, however, and yet archaeocyathids were only recognized at two localities in Paralleldal (Fig. 3.28, localities 18 & 19). This probably reflects the nature of the platform-outer shelf transition. Wave and current energy impinging on a gently sloping, gradual platform margin, as inferred for this area of Paralleldal, would be dissipated over a wider area than at an abrupt margin and would result in correspondingly lower environmental stresses. Hence the restricted occurrence of the biostromal facies probably reflects the high-energy conditions that prevailed along much of the platform margin and the scarcity of situations where energy levels were sufficiently moderated to allow the development of these sediments.

(b) Perssuak Gletscher Formation, Koch Væg.

The Perssuak Gletscher Formation in west Peary Land shows a clear subdivision into a foreslope assemblage, typified by mass flow deposits, and a platform-edge assemblage, deposited on wave-and tidal current-swept sand shoals. At the southern end of Koch Væg, the foreslope assemblage is composed almost exclusively of stratified ooid grainstones deposited by gravity flow processes on the sloping platform front (Fig. 7.20a). Depositional dips, ranging from $5^{o}$ to $25^{o}$ reflect the pronounced relief between the platform edge and the outer shelf (Fig. 7.9). Individual sloping surfaces, traced on oblique air photographs, indicate synsedimentary relief of up to 140m between the upper slope facies and the platform rim. The development and propagation of such relief suggests a gross disparity between platform margin and outer shelf sedimentation rates, and probably reflects rapid propagation of the platform margin.

This style of progradation is very similar to the 'horizontal progradation' described by Bosellini (1984, Figs 9 & 10), in which the lower boundary of the prograding platform is almost horizontal and parallel to the upper boundary. Bosellini suggested that this resulted from basinal starvation, rapid progradation or a combination of these two factors. The scarcity of mass-flow breccias in the Koch Væg section also suggests rapid progradation since lithified carbonate is unlikely conditions that prevailed along much of the platform margin and the scarcity of situations where energy levels were sufficiently moderated to allow the development of these sediments.

(b) Perssuak Gletscher Formation, Koch Væg.

The Perssuak Gletscher Formation in west Peary Land shows a clear subdivision into a foreslope assemblage, typified by mass flow deposits, and a platform-edge assemblage, deposited on wave-and tidal current-swept sand shoals. At the southern end of Koch Væg, the foreslope assemblage is composed almost exclusively of stratified ooid grainstones deposited by gravity flow processes on the sloping platform front (Fig. 7.20a). Depositional dips, ranging from $5^{\circ}$ to $25^{\circ}$ reflect the pronounced relief between the platform edge and the outer shelf (Fig. 7.9). Individual sloping surfaces, traced on oblique air photographs, indicate synsedimentary relief of up to 140m between the upper slope facies and the platform rim. The development and propagation of such relief suggests a gross disparity between platform margin and outer shelf sedimentation rates, and probably reflects rapid propagation of the platform margin.

This style of progradation is very similar to the 'horizontal progradation' described by Bosellini (1984, Figs 9 & 10), in which the lower boundary of the prograding platform is almost horizontal and parallel to the upper boundary. Bosellini suggested that this resulted from basinal starvation, rapid progradation or a combination of these two factors. The scarcity of mass-flow breccias in the Koch Væg section also suggests rapid progradation since lithified carbonate is unlikely

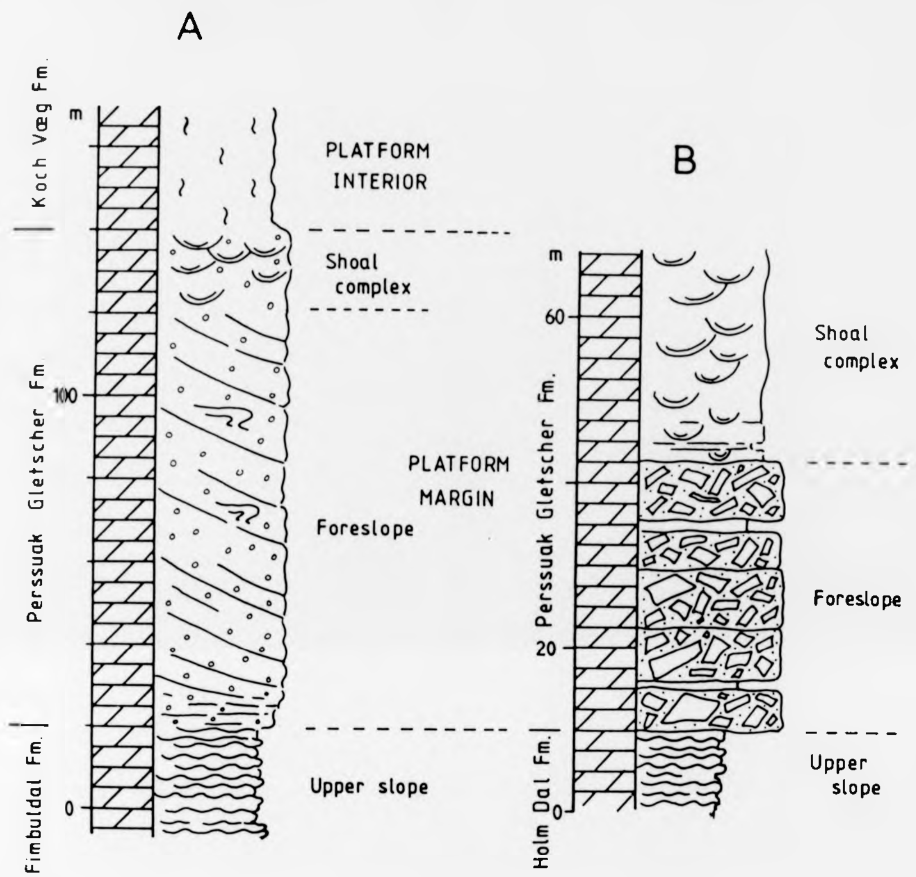


Figure 7.20. A.Generalized section showing the vertical transition from outer shelf facies to platform facies at the southern end of Koch Væ g, locality 2, west Peary Land. B. Generalized section showing the vertical transition from outer shelf to platform facies at Fimbuldal, locality 4, west Peary Land.

to be exposed in an unstable situation at the platform edge during periods of rapid lateral accretion.

(c). Perssuak Gletscher Formation, Fimbuldal.

In the Fimbuldal area, the platform-outer shelf transition in the Perssuak Gletscher Formation is dominated by chaotic mass flow breccia beds (Fig. 7.20b). In vertical section, dark thin-bedded carbonates of outer shelf aspect are overlain by and interbedded with massive, pale dolomite breccia beds. These beds contain angular blocks up to tens of metres across of pale, cross-bedded dolomitized grainstone of platform-edge aspect. In cliff sections, the mass flow deposits thin and interfinger northwards with outer shelf facies, and locally show depositional dips of up to 15$^{o}$. Passing up section, the foreslope breccias are interbedded with and ultimately replaced by cross-bedded carbonate sands of the platform edge shoal complex (Fig. 7.20b).

A foreslope assemblage composed largely of mass-flow breccias containing blocks of platform-edge carbonate is indicative firstly of an unstable platform margin, and secondly of early penecontemporaneous cementation of the shallow-water grainstones (Hopkins 1977). Breccia-dominated foreslope deposits with primary depositional dips were described by Bosellini (1984) from the Triassic of the Dolomites. He suggested that the peri-platform talus was probably eroded from the platform rim during heavy storms or detached by seismic activity; furthermore, he suggested that such a mode of platform progradation indicated exceptionally high productivity at the platform edge. The interdigitation of these mass flow deposits with the outer shelf rocks reflects the episodic nature of progradation.

(d) Løndal Formation, Løndal.

On the western slopes of Løndal, this formation displays a platform-outer shelf transition that is intermediate in character between the Perssuak Gletscher Formation and Paralleldal Formation examples. Depositional dips rarely exceed 10$^{\circ}$ and cross-bedded ooid grainstones interdigitate with wavy-bedded, burrowed dolomites of the upper slope assemblage (Fig. 7.21). Discontinuous, wedge-shaped slump units and breccia beds are present, however, and form distinctive pale tongues extending northwards in advance of the platform margin facies (Fig. 7.21). In this case, therefore, relief at the platform margin was sufficient to promote mass failure and gravity flow, and yet was not so pronounced as to preclude interdigitation of platform-edge sand shoals and upper slope skeletal muds.

7.2.2. Siliciclastics.

In Gustav Holm Dal, rocks of Late Cambrian age assigned to the Perssuak Gletscher Formation are a varied sequence of dolomite breccias, sandstone-dolomite breccias, cross-bedded sandstones and laminated, burrowed sandstones. The proportion of siliciclastic detritus increases up the section, both as discrete sandstone beds (Lithofacies 18, 19) and within mixed carbonate-sandstone breccias (Lithofacies 9; see Figs 3.48 & 7.2). The facies analysis presented above (7.1.1, 7.1.6 & 7.1.7) indicates contrasting but geographically related depositional processes.

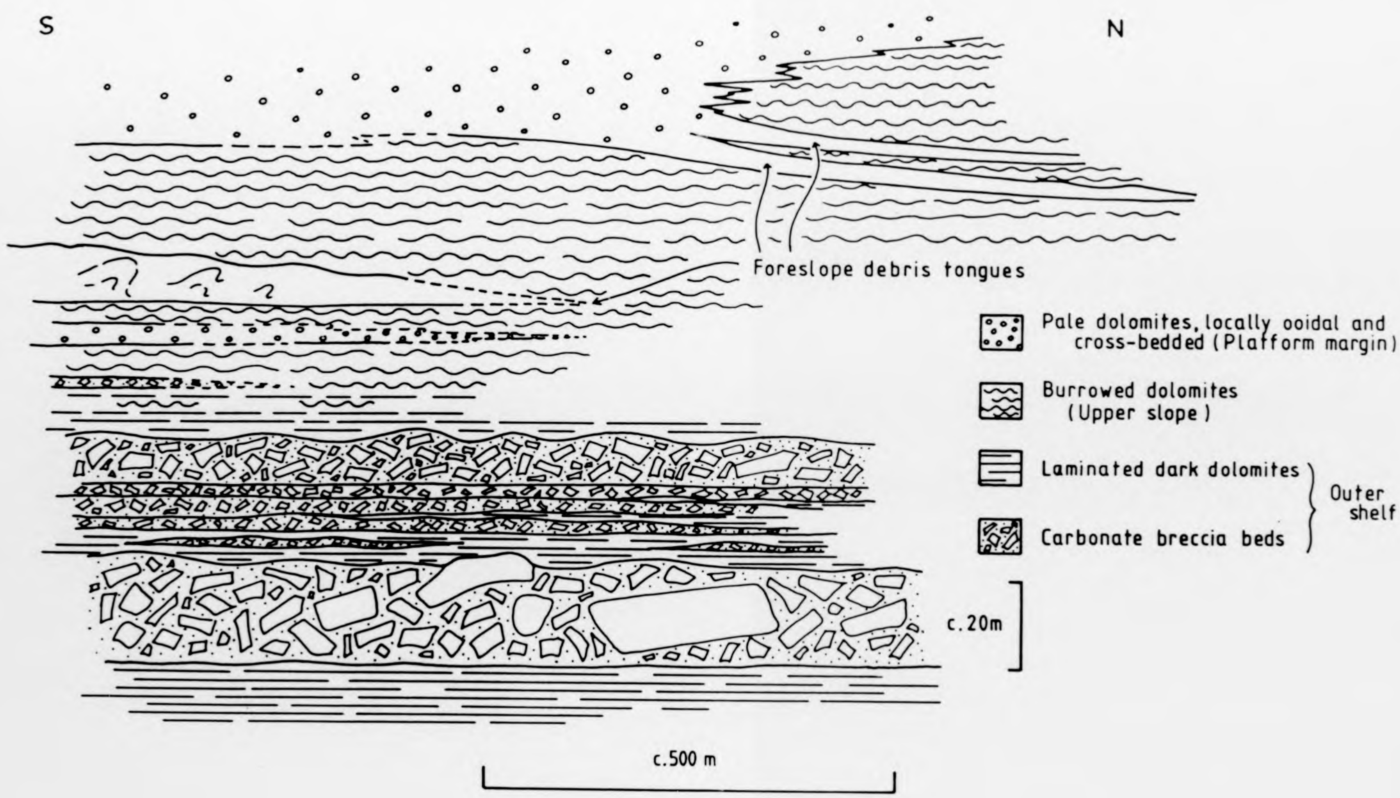


Figure 7.21. Facies relationships at the platform - outer shelf transition in the Løndal Formation on the west side of Løndal (Locality 10). Based on two correlated measured sections and observations from oblique air photographs.

The sandstone breccias and mixed sandstone-carbonate breccias are the product of mass flow processes and reflect instability at the transition from inner to outer shelf. The incorporation of angular blocks of white quartz arenite testifies to erosion or mass wastage of lithified sandstones. In contrast to this catastrophic mode of sedimentation, the laminated, burrowed and cross-bedded, well-sorted sandstones are typical products of a shallow-marine environment.

The environmental setting is not clear; at carbonate platform margins, oversteepening of slopes and mass failure may have a tectonic origin, but commonly arises purely from high carbonate productivity, rapid progradation and early cementation (James & Mountjoy 1983). On clastic marine shelves, however, mass flow processes probably reflect local tectonism rather than depositional processes. This part of the succession was not studied in detail, partly due to the patchy exposure in Gustav Holm Dal; further field work is needed to adequately interpret these rocks. Deposition occurred in shallow-water, above wave-base, at the transition from inner to outer shelf; the instability reflected by the mass flow deposits may reflect local tectonic activity or the depositional relief inherited from the preceding carbonate regime.

## 7.3. Association D. Platform Interior.

This association is typified by the Koch Væg Formation (Fig. 3.52) but is also represented locally in the Løndal, Perssuak Gletscher and Paralleldal Formations. It characteristically comprises well-bedded carbonates with subordinate clastics, showing mid-brown to pale greenish-grey weathering colours.

Five facies make up the association.

7.3.1. Lithofacies 20; Burrow-mottled dolomites.

This lithofacies is typical of the Koch Væg Formation (Fig. 3.52) and occurs in the Perssuak Gletscher Formation in Holm Dal and the Paralleldal Formation in Børglum Elv. It varies from massive, medium- to thick-bedded, fawn-brown mottled dolomites to thin, knobbly, irregular-bedded dolomites with grey-green silty mudstone partings and interbeds.

The dolomites are medium to fine crystalline and typically show an irregular vermiform burrow mottling, defined by variation in colour and crystalline grain size. Where discrete burrows are recognizable (Fig. 3.53) they are paler than the surrounding matrix, subparallel to bedding and are up to 10mm across and 0.1m in length. These straight or gently curved, cylindrical, unbranched, unlined burrows are assigned to *Planolites*. A few beds display a discontinuous wispy lamination, but bioturbation is the dominant and distinguishing feature of the lithofacies.

These rocks are largely unfossiliferous; monoplacophorans (*cf. Proplina*) and hyperstrophic onychochilacean gastropods were collected from mottled, pale grey dolomites in the upper levels of the Perssuak Gletscher Formation in Holm Dal (Ineson & Peel 1980).

Primary fabrics are rare and in thin section these rocks comprise anhedral to euhedral, medium to fine crystalline dolomites with up to 15% intercrystalline porosity. A vague pelleted structure is evident on some polished slabs.

Interpretation.

The relict pelleted structure, the lack of a recognizable grain fabric and the ubiquitous bioturbation suggests a primary mud-rich carbonate sediment.

A tranquil, subtidal environment is suggested by the inferred fine-grained nature of the sediment, the absence of current- or wave-formed structures and the lack of features indicative of emergence. The ubiquitous bioturbation reflects a well-oxygenated environment and the dominance of horizontal burrows supports the interpretation of a low-energy environment (Rhoads 1975). Although possibly a preservational feature in part, the scarcity and low diversity of the fauna in these rocks may reflect extremes in water temperature and/or salinity within a restricted, shallow-water environment (*cf.* Brady & Koepnick 1979).

Similar facies reported in the literature have been assigned to shallow subtidal, low-energy environments on shelves (Cook & Taylor 1977), platforms (Brady & Koepnick 1979; Wilson 1975) or ramps (Read 1980). Analagous burrowed pelleted lime muds have been described from low-energy zones of the Great Bahama Bank (Bathurst 1971, p 136) and the restricted lagoons of the Honduran rimmed shelf (Ginsberg & James 1974).

## 7.3.2. Lithofacies 21; Flat-pebble conglomerates.

Flat-pebble conglomerates only occur in the Koch Væg Formation at the southern end of Koch Væg (Fig. 3.52). They comprise 0.05-0.2m thick, sheet-like or lenticular beds with sharp, erosional bases and gradational, burrowed tops. The platy, discoidal, rounded or subrounded pebbles are composed of structureless or laminated, very fine crystalline dolomite. A relict pelleted fabric is present in some pebbles. Clasts are 10-60mm long and 3-15mm thick; random, horizontal and stacked, imbricated fabrics are observed. Clast-supported frameworks are typical with an interstitial matrix of medium crystalline silty, sandy dolomite containing a scatter of phosphatic skeletal fragments.

Interpretation.

Intraformational flat-pebble or "edgewise" conglomerates are common features of shallow-water carbonate successions (Wilson 1975). They are generally considered to be indicative of the intertidal-supratidal zone (Braun & Friedman 1969; James 1979; Lindholm 1980) and have been described from modern intertidal flats (Shinn *et al.* 1969). The flat-pebbles are often interpreted as the desiccated remnants of high intertidal-supratidal algal laminites or dolomite crusts that were ripped up and redeposited by storm or tidal currents (Braun & Friedmann 1969). A similar high-energy, episodic process is suggested here by the sharp, erosional bases and the presence of imbrication.

One conglomerate bed is associated with a thin desiccated stromatolitic dolomite unit, suggesting deposition in an intertidal or low supratidal environment (Fig. 3.52). Typically, however, flat-pebble conglomerate beds occur within sequences of burrowed subtidal muddy carbonates (Fig. 3.52). Jones & Dixon (1976) described thin (0.02-0.33m) intraformational conglomerate beds from the Silurian Read Bay Formation of

Arctic Canada, that are interbedded with mainly low-energy, subtidal limestones. They demonstrated that these deposits, which represent episodic high-energy events, occur in an essentially random fashion through the sequence and were probably storm-generated. Flat-pebble conglomerates of probable storm origin also occur in subtidal deposits in the Upper Nolichucky Formation, south-west Virginia (Markello & Read 1981).

In the succession described here, evidence of emergence is rare, and the flat-pebble conglomerates were mainly deposited in a shallow subtidal environment from episodic tidal or storm currents that ripped up desiccated sediment from the supratidal or high intertidal zone.

### 7.3.3. Lithofacies 22; Cross-bedded, fine-grained sandstones.

This lithofacies is recognized only in the Koch Væg Formation, at the northern end of Koch Væg (Fig. 3.52). It comprises white, sub-rounded to well-rounded, fine- to very fine-grained silty quartz arenites showing horizontal lamination and tabular cross-bedding in 0.03-0.2m sets (Fig. 7.22). Low-angle accretionary foresets are typical; herringbone cross-bedding and reactivation surfaces are present locally. Isolated vertical burrows (*Monocraterion*) are commonly truncated at erosional set boundaries (Fig. 3.54).

The lithofacies occurs in units up to 2m thick, alternating with bioturbated, mottled sandstones (Lithofacies 23) and algal-laminated

Figure 7.22. Small-scale cross-bedded, fine-grained sandstones (LF.22) of the Koch Væ g Formation, locality 3, west Peary Land.

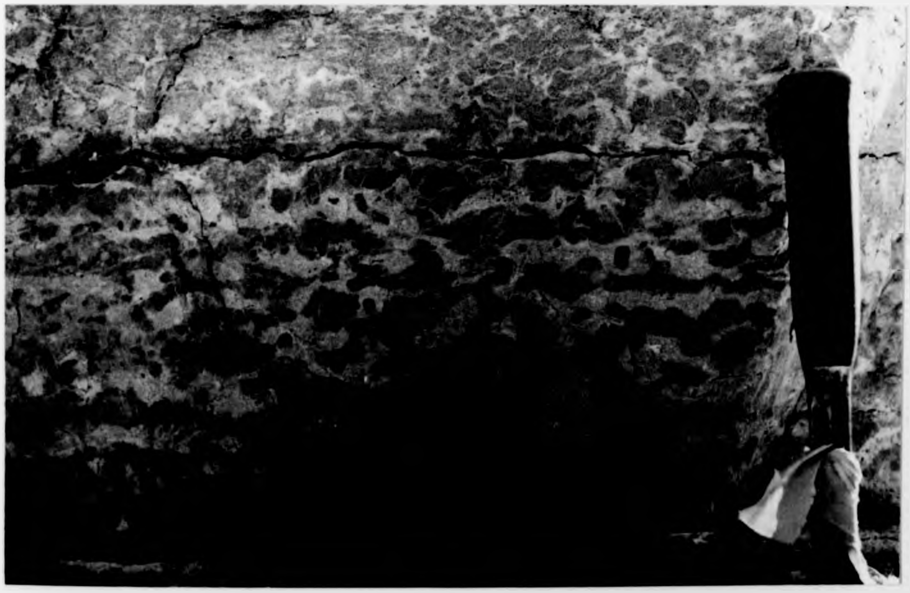

Figure 7.23. Mottled, bioturbated, fine-grained sandstone (LF.23). Koch Væ g Formation, locality 3, west Peary Land.

Figure 7.22. Small-scale cross-bedded, fine-grained sandstones (LF.22) of the Koch Væg Formation, locality 3, west Peary Land.

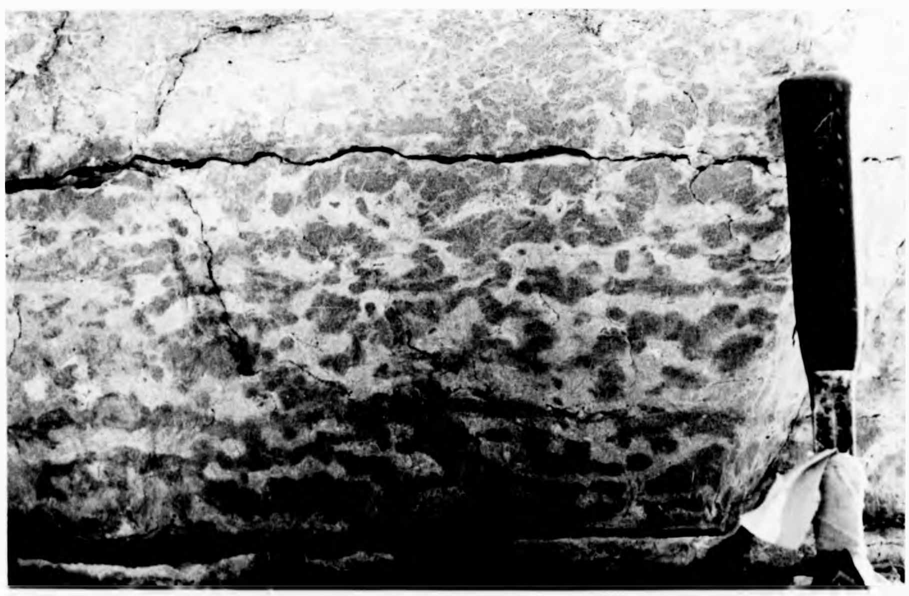

Figure 7.23. Mottled, bioturbated, fine-grained sandstone (LF.23). Koch Væg Formation, locality 3, west Peary Land.

dolomites (Lithofacies 24). The lateral extent and shape of cross-bedded units was not determined but they commonly have abrupt and locally erosional bases.

The sandstones are mainly cemented by clear, coarse crystalline dolomite; syntaxial quartz overgrowth cements are locally important.

Interpretation.

The lack of mud and the presence of cross-bedding indicates deposition from competent currents capable of winnowing out mud-grade sediment and producing ripples and megaripples. Environmental stresses were sufficiently high to deter most infaunal organisms. The presence of herring-bone cross-bedding is indicative of tidal influence (Johnson 1978) and reactivation surfaces have been reported from tide-dominated shallow-marine sands (Driese *et al.* 1981).

An intertidal or shallow subtidal environment is indicated by the association with mud-cracked algal laminites. In the intertidal zone, these sandstones may represent the fill of tidal channels traversing burrowed or algal-laminated mudflats.

7.3.4. Lithofacies 23; Bioturbated fine-grained sandstones.

These pale grey, fawn or white, fine- to very fine-grained silty sandstones are restricted to the upper beds of the Koch Væg Formation (Fig. 3.52). They are texturally identical to the cross-bedded sandstones (Lithofacies 22) and differ only in the absence of primary sedimentary structures. They exhibit a patchy mottling that, in places, delineates vague elongate sub-horizontal burrows (Fig. 7.23). Burrowed sandstone units (0.1-2m thick) are thin to medium bedded; boundaries with other facies are typically gradational.

Interpretation.

The intimate association of this facies with cross-bedded sandstones and algal laminites (Fig. 3.52) indicates a closely related depositional environment i.e. an intertidal or shallow subtidal setting. The intensive bioturbation precludes interpretation of the primary depositional processes, but is itself testament to slow sedimentation rates in a well-oxygenated environment. A mid-upper intertidal environment is envisaged, by analogy with studies of modern tidal flats (Reineck 1972) and examples from the geological record (e.g. Driese *et al.* 1981).

### 7.3.5. Lithofacies 24; Algal Dolomites.

Stromatolitic and oncolitic dolomites occur in the Koch Væg, Paralleldal and Løndal Formations. Two subfacies are recognized.

24a; Laminites.

Pale grey-green silty dolomites showing a well-developed planar, crinkly or up-domed lamination, form units 0.2-2m thick in the upper levels of the Koch Væg Formation (Fig. 3.52), interbedded with units of cross-bedded and bioturbated sandstones (Lithofacies 22 & 23). Horizontal planar lamination predominates but undulose, crinkly laminae and stromatolite domes (LLH of Logan *et al.* 1964) are developed locally (Fig. 3.55). In places, laminae are disrupted by isolated burrows and vertical, sediment-filled cracks; polygonal desiccation cracks occur on some bedding planes (Fig. 7.24).

Laminae are 0.05-2mm thick, and are defined in outcrop by a subtle colour variation - white or pale grey and grey-green. In thin section (Fig. 7.25), the lamination is defined by the crystalline grain-size and, less commonly, by the siliciclastic content. Fine crystalline (20-30μm) laminae alternate with darker, very fine crystalline dolomite; crystals in the latter range up to 50μm but are typically 5-10μm across. The pale, coarser laminae commonly have sharp planar bases but grade up into the darker, very fine crystalline dolomite laminae. Terrigenous detritus forms less than 5% of the rock; the scatter of angular-subrounded quartz silt and very fine sand commonly occurs preferentially within or upon the dark, very fine crystalline laminae.

24b. Oncolitic dolomites.

This subfacies was only recorded from a 0.5m thick bed in the Paralleldal Formation in Børglum Elv. It consists of pale cream, coarse crystalline dolomite showing a vague oncolite-intraclast-ooid grainstone fabric. In cross-section, the oncolites are oval or sub-circular, 0.4-10mm in diameter and, in places, show irregular concentric lamination.

Interpretation.

The delicate fine lamination of subfacies 24a is comparable to that produced by algal mats on modern tidal flats (e.g. Western Australia,

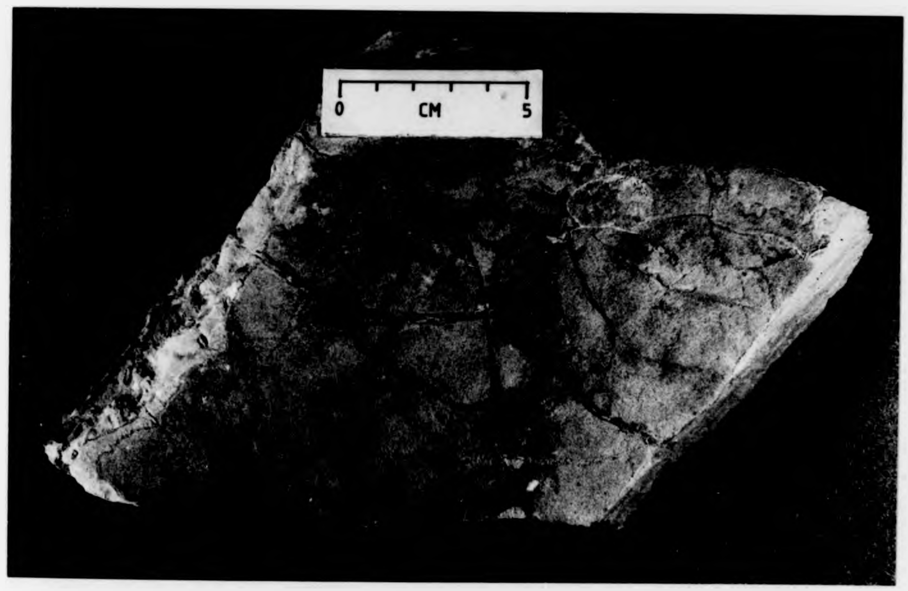


Figure 7.24. Polygonal desiccation cracks, bedding plane view. GGU 218660, Koch Væ g Formation, locality 3, west Peary Land.

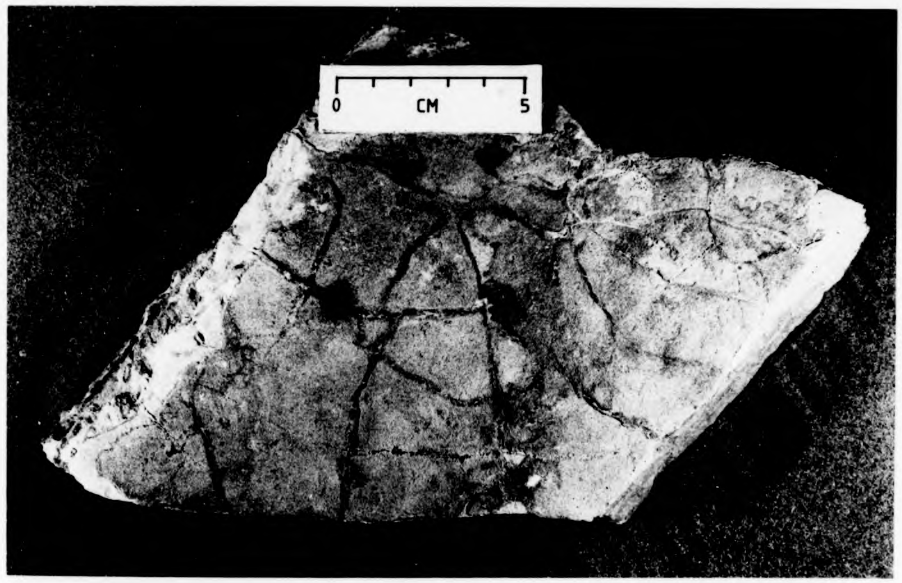


Figure 7.24. Polygonal desiccation cracks, bedding plane view. GGU 218660, Koch Væ g Formation, locality 3, west Peary Land.

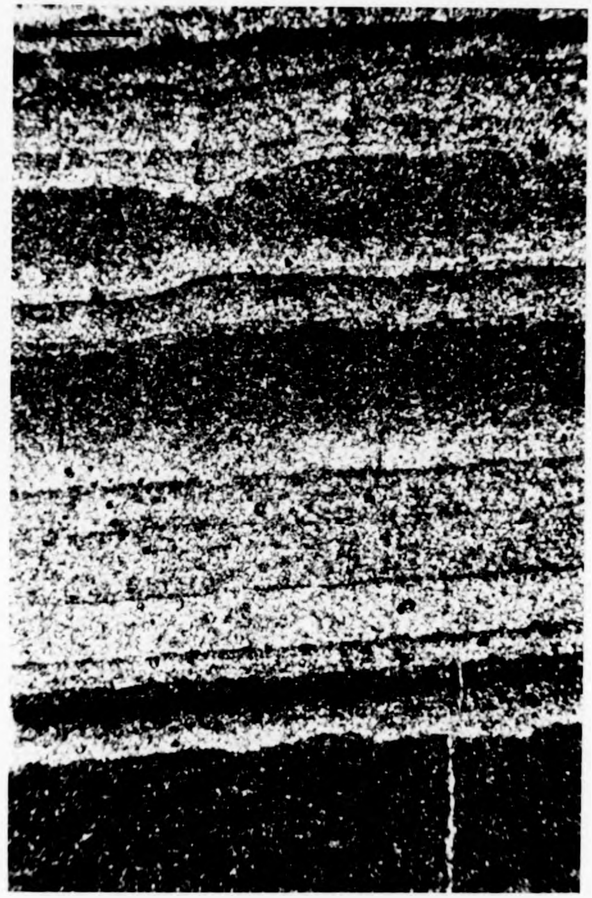

Figure 7.25. Photomicrograph (PPL) of algal-laminated dolomite (LF.24) showing alternation of pale (fine crystalline) and dark (very fine crystalline) laminae. Pale laminae have sharp bases and grade up into darker laminae. Note wavy top of lamina A, draped by overlying laminae. Scale bar = 1mm. GGU 218662, Koch Væg Formation, locality 3, west Peary Land.

Figure 7.25. Photomicrograph (PPL) of algal-laminated dolomite (LF.24) showing alternation of pale (fine crystalline) and dark (very fine crystalline) laminae. Pale laminae have sharp bases and grade up into darker laminae. Note wavy top of lamina A, draped by overlying laminae. Scale bar = 1mm. GGU 218662, Koch Væg Formation, locality 3, west Peary Land.

Logan *et al.* 1974; Persian Gulf, Kendall & Skipwith 1968). These rocks are also comparable to stratiform cryptalgal laminites described from ancient successions (Aitken 1967; James 1979). Fairchild (1980) described similar stromatolitic dolomites from the Dalradian of Scotland, in which the primary lamination is defined by the crystalline grain size, clastic content, laminar fenestrae and radial calcite. Darker, thinner, very fine crystalline laminae alternate with coarser paler laminae of detrital aspect, a textural feature present in Lithofacies 24a and common to many ancient stromatolites (Henderson 1975; Horodyski 1976). The darker, finer laminae probably represent the algal mat layer whereas the paler laminae represent detrital sediment washed over the mat surface by tides or storm currents. Angular silt grains resting upon dark algal laminae may represent wind-blown sediment that adhered to the gelatinous mat surface. An algal origin for this subfacies is supported by the localized occurrence of crinkly lamination and stromatolite domes. The spar-filled fenestrae within domal structures (Fig. 3.55) may record updoming of the sediment layers due to gas evolution beneath the sediment surface, a process described from pustular algal mats in Shark Bay, Western Australia (Davies 1970; Bathurst 1971, p. 220-1).

Although algal mats are presently typical of high intertidal and supratidal zones (Logan *et al.* 1974) they have been recorded from modern subtidal environments (Playford & Cockbain 1976). In Shark Bay, the variation in modern stromatolite forms reflects their depositional setting. Flat mats form on protected intertidal mud flats whereas club-shaped columnar forms develop on exposed headlands (Logan *et al.* 1974). The dominant planar stratiform laminites described here indicate deposition in a protected low-energy environment and the occasional desiccation features suggest a mid- to low-intertidal environment (*cf.* Ricketts 1983).

The dark laminae in these beds possess crystal dimensions similar to Recent penecontemporaneous dolomites formed by early diagenetic replacement of lime sediment in the high intertidal-supratidal zone (Illing *et al.* 1965). Similar ancient dolomicritic carbonates of inferred early diagenetic origin were described by Zenger (1972), Bose (1979) and Ricketts (1983). It is significant that throughout the whole Cambrian succession, very fine crystalline dolomites occur only in this lithofacies.

Oncolites form by accretion of algal and detrital laminae in a similar fashion to stratiform laminites but they develop around a free, mobile nucleus, thus forming spherical algal balls (SS of Logan *et al.* 1964). Hence, oncolite formation requires periodic agitation to ensure concentric growth around the nuclei. Modern oncolites are known from Florida and the Bahamas where they occur in tidal channels, shallow bays or ponds (Wilson 1975). In the Paralleldal Formation oncolites occur within well-sorted ooid-intraclast-oncolite grainstones (Lithofacies 24b) which are associated with burrow-mottled dolomites (Lithofacies 20) and cross-bedded ooid grainstones (Lithofacies 14a). They represent a transitional environment between the high-energy ooid shoals and the low-energy subtidal environment represented by the burrowed, fine-grained carbonates (*cf.* Markello & Read 1981).

7.4 Association D. Environmental Interpretation.

The association consists largely of unfossiliferous, bioturbated mudstones, reflecting deposition in a low-energy, subtidal environment with restricted circulation. Stromatolitic carbonates, locally mudcracked, indicate deposition in low energy, peritidal environments whereas cross-bedded, clastic rocks record the action of tidal currents in intertidal or shallow subtidal environments. Association D lithofacies overlie and interdigitate northwards with massive, light coloured dolomites assigned to Association C, representing the platform margin (Fig. 5.1). Association D clearly represents an inner platform setting, shoreward of the high energy margin.

Such an environmental pattern is analogous to modern rimmed shelves (Ginsburg & James 1974) and to the idealized open and restricted platform environments of Wilson (1975). Ancient analogues are well-documented (e.g. Davies 1977; Brady & Koepnick 1979; Pfeil & Read 1980).

This association is only locally preserved in the Løndal, Perssuak Gletscher and Paralleldal Formations and, where present, is commonly intercalated with cross-bedded dolomites of Association C. This suggests deposition at the transition between the high-energy margin and the quiet waters of the restricted platform or lagoon.

The Koch Væg Formation, however, is composed wholly of platform interior facies and is divisable into two distinct portions (Fig. 3.52). The lower half is well-exposed at the southern end of Koch Væg, where it overlies the grainstone-dominated platform margin carbonates of the

Perssuak Gletscher Formation. It is composed largely of unfossiliferous, burrowed silty dolomites, with thin, flat-pebble conglomerate beds, and represents a dominantly low-energy, shallow subtidal environment that experienced episodic high-energy storm currents or tidal currents. Rare mudcracked stromatolitic levels indicate that, on occasion, sedimentation outpaced subsidence resulting in local accretion into the intertidal zone. The upper beds of the formation, at the northern end of Koch Væg, comprise burrowed dolomites interbedded with cross-bedded, burrowed sandstones and algal laminites; desiccated levels occur locally. Environments ranging from shallow subtidal to mid-intertidal are indicated; bioturbated facies accumulated in shallow subtidal to low intertidal environments whilst algal laminites and cross-bedded sandstones probably reflect deposition on intertidal mudflats and in tidal channels respectively.

Thus the overall facies relationships in the Koch Væg Formation reflect a regressive sedimentation pattern, passing from the high-energy sand shoals of the underlying Perssuak Gletscher Formation through the low-energy, mainly subtidal, lagoonal deposits of the lower Koch Væg Formation into the peritidal sediments of the upper Koch Væg Formation.

# CHAPTER 8: PALAEOGEOGRAPHY AND SHELF EVOLUTION

## 8.1 Introduction

The previous three chapters are concerned principally with the inferred processes and environments of deposition and only brief mention has been made of the stratigraphic relationships between the facies associations. In this chapter the palaeogeographic evolution of the shelf (8.5) is deduced from the palaeocurrent and palaeoslope patterns (8.2) and the spatial and vertical relationships between associations (8.3). The significance of the Wandel Valley Formation basal unconformity is discussed (8.4) and the implications of the shelf history to the development of the coeval deep-water basin are considered (8.5 & 8.6).

## 8.2 Palaeocurrents and palaeoslopes

### 8.2.1 Palaeocurrents

Palaeocurrent data were obtained predominantly from rocks assigned to the platform-margin association. Much of the outer shelf succession accumulated from suspension, from dilute sediment gravity flows or from mass flows and the sediments preserve little record of the transport direction. In particular, the mass flow deposits rarely provide any indication of palaeoflow direction despite forming a large proportion of the succession. Some workers have used clast orientation in carbonate mass flow deposits to evaluate palaeoflow directions (e.g. Hubert *et al.* 1977). No reliable imbrication was observed in this study, however, and the few available palaeoflow measurements in this lithofacies were obtained from the orientation and overturning direction of drag folds in sediments underlying the mass flow deposit.

Sole marks are very rare in the carbonate turbidite lithofacies, and sedimentary structures are poorly preserved. A few measurements were obtained from cross-lamination and from imbrication within the basal graded division. Similarly, directional structures are rare in the siliciclastic succession of the Henson Gletscher and Sæterdal Formations and data are restricted to a handful of readings from the Sæterdal area.

In contrast, palaeocurrent readings are obtained readily from the dolomitized, cross-bedded carbonate grainstones of the platform margin association.

#### 8.2.1.1 Outer shelf

The few measurements obtained within carbonates of the outer shelf associations show a crude unimodal pattern (Fig. 8.1), with a mean direction towards the north-west (vector mean = $307^{o}$). Palaeocurrent data obtained from the siliciclastic interval are also few but show a similar trend (Fig. 8.2; vector mean of imbrication and cross-stratification data = $326^{o}$).

#### 8.2.1.2 Inner shelf

Platform-margin carbonates and inner shelf clastics are commonly cross-bedded and provide the most abundant and reliable

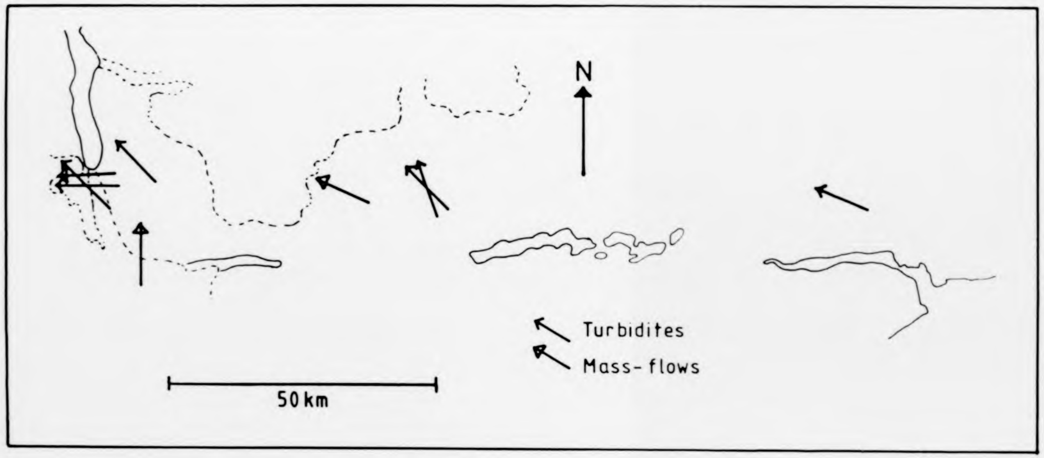


Figure 8.1. Map showing the palaeoflow data obtained from Association B (outer shelf) carbonates. Turbidite palaeocurrent directions represent single readings of flute casts, cross-stratification or pebble imbrication. Palaeoflow data for the carbonate breccia beds obtained from the axial orientation of overturned basal drag folds; each arrow represents at least 5 readings.

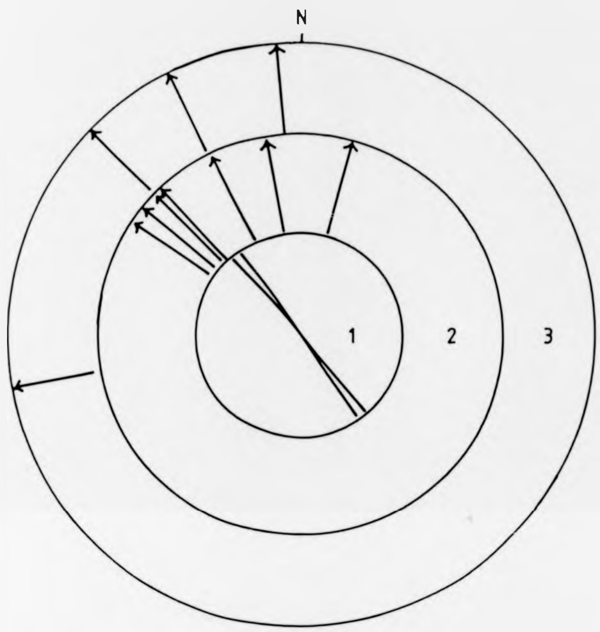


1 - Primary current lineation
2 - Imbrication / cross-bedding
3 - Ripple cross-lamination

Figure 8.2. Palaeocurrent data from the Sæterdal Formation at localities 14 and 15.

palaeocurrent data (Fig. 8.3). Most palaeocurrent roses have a broad distribution with a dominant north-westward mode; some show a subordinate mode to the south-east or east. This bimodality is particularly evident on the combined rose diagram which, if separated into two data groups, gives vector means of 322° and 106°. This asymmetric bimodal pattern probably reflects tidal processes (*cf.* Johnson 1978) with a dominant ebb (offshore) current towards the NNW. No significant lateral or stratigraphic variation is evident (Fig. 8.3).

Data from the cross-bedded sandstones of Late Cambrian age are few but display a unimodal palaeocurrent pattern (Fig. 8.4), indicating flow towards the NNW (vector mean = 342°).

### 8.2.2 Palaeoslopes

The only reliable measurements of depositional slopes were obtained from the inclined bedding within foreslope carbonates of the platform margin association. Primary dips in these beds range from 5° to 25° and show a consistent orientation, dipping towards the north or NNW (Fig. 8.5). This represents the sloping front of the platform and indicates a roughly east-west or ENE-WSW orientation of the platform edge.

Estimation of the attitude and magnitude of depositional slopes in the outer shelf environment proved more difficult. Well-exposed draped slump scars at two localities in upper slope facies indicate slopes inclined towards the north-west, as also suggested by the flow directions of mass flows and turbidity currents (Fig. 8.1).

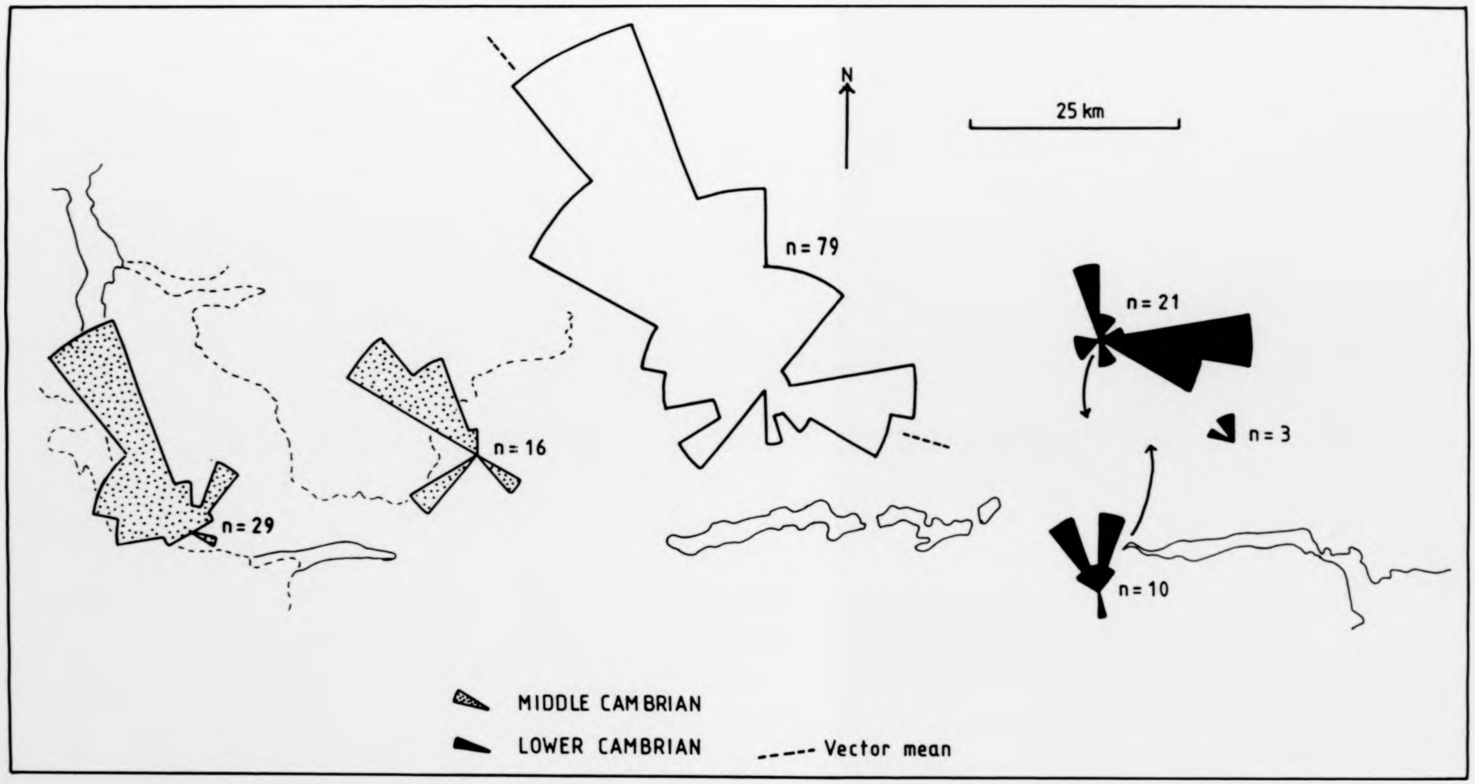


Figure 8.3. Map showing the palaeocurrents determined from cross-bedded dolomites of Association C (platform margin). The data are combined in the large rose diagram which shows an asymmetric bimodal pattern (vector means 322° and 106°).

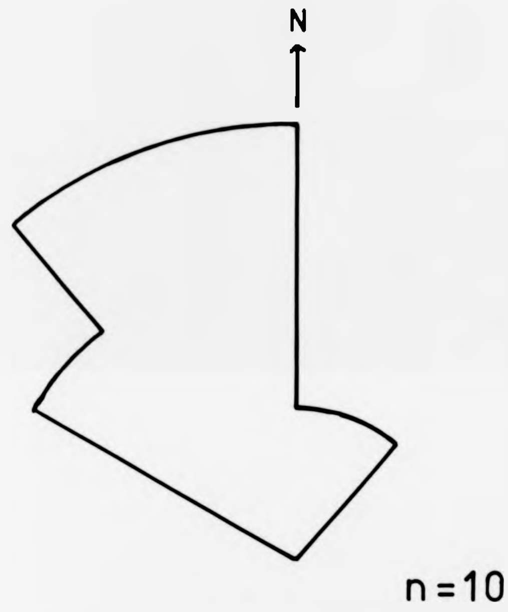


Figure 8.4. Current rose diagram for tabular cross-bedded sandstones of Late Cambrian age in west Peary Land.

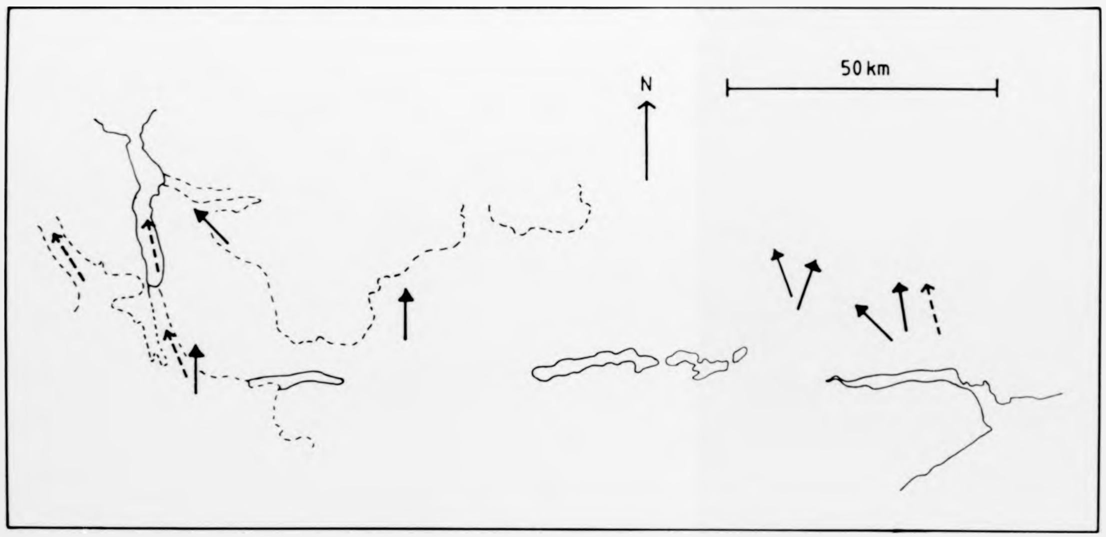


Figure 8.5. Map showing the dip direction of inclined foreslope strata. Solid arrows represent measured palaeoslopes (mean values of several readings); dashed arrows represent apparent dip direction in vertical cliff sections.

Small-scale slump folds occur locally but measurements are few and widely scattered and show no systematic orientation. Given the available data, together with the gross facies relationships (Figs 6.77 & 8.6), it is reasonable to infer a regional depositional gradient (probably < $2^{o}$) towards the north or NNW.

### 8.2.3 Summary

Despite the uneven distribution of the palaeocurrent and palaeoslope data, a broad pattern emerges. The dominant flow direction throughout the succession is towards the NNW. In view of the facies distribution, thinning directions and palaeoslope data for both platform margin and outer shelf settings, this reflects offshore dispersal of sediment, normal to ENE-WSW trending environmental belts (see Figs 6.77 & 8.22-8.25). The underlying Buen Formation records deposition on a northward-deepening marine shelf during the Early Cambrian (4.2.2). Clearly, this pattern persisted into the Middle and Late Cambrian although the facies relationships, thickness variations, palaeocurrent and palaeoslope data indicate a westerly component to this trend. Inner shelf, shallow-water lithofacies show a dispersed palaeocurrent pattern but a broadly bimodal distribution is common and probably reflects a tide-dominated regime.

## 8.3 Environmental relationships

The lateral and vertical relationships between the four associations (A-D, Chapters 5-7) indicates a large-scale, regressive cycle, involving northward progradation of shallow-water lithofacies.

8.3.1 Vertical succession of environments

In all complete vertical sections through the succession, outer shelf rocks (Associations A and B) form the lower portion and are overlain by inner shelf, shallow-water facies (Associations C and D). This pattern is present throughout southern Peary Land, despite the progressive overstep towards the east by the overlying Wandel Valley Formation (Fig. 8.6). It is clear that subsidence in west Peary Land during the Cambrian greatly exceeded that of south-eastern parts.

The glauconitic, phosphoritic carbonates of Association A form a distinctive and widespread basal unit, directly overlying the siliciclastic Buen Formation. This condensed interval represents a period of slow sedimentation and uniform environmental conditions over a wide area of the Peary Land shelf; the environment is envisaged as an incipient carbonate ramp, shelving gently towards the north or north-west.

This basal unit is overlain everywhere by carbonates and siliciclastics of the outer shelf-slope association (Association B). The transition from Association A to Association B reflects (1) the development of sufficient relief within the shelf environment to propagate mass flows and (2) the evolution of a shallow-water carbonate platform to the south of the present outcrop area. The presence of the latter is inferred from the occurrence of large slabs of cross-bedded dolomitized grainstone within mass flow deposits directly overlying the glauconitic, phosphatic ramp sediments. Evolution from a carbonate ramp to a platform-deep shelf complex may be simply a function of the normal processes of carbonate sedimentation and is commonly observed in the early stages of carbonate shelf development (Wilson 1975; Miall 1984).

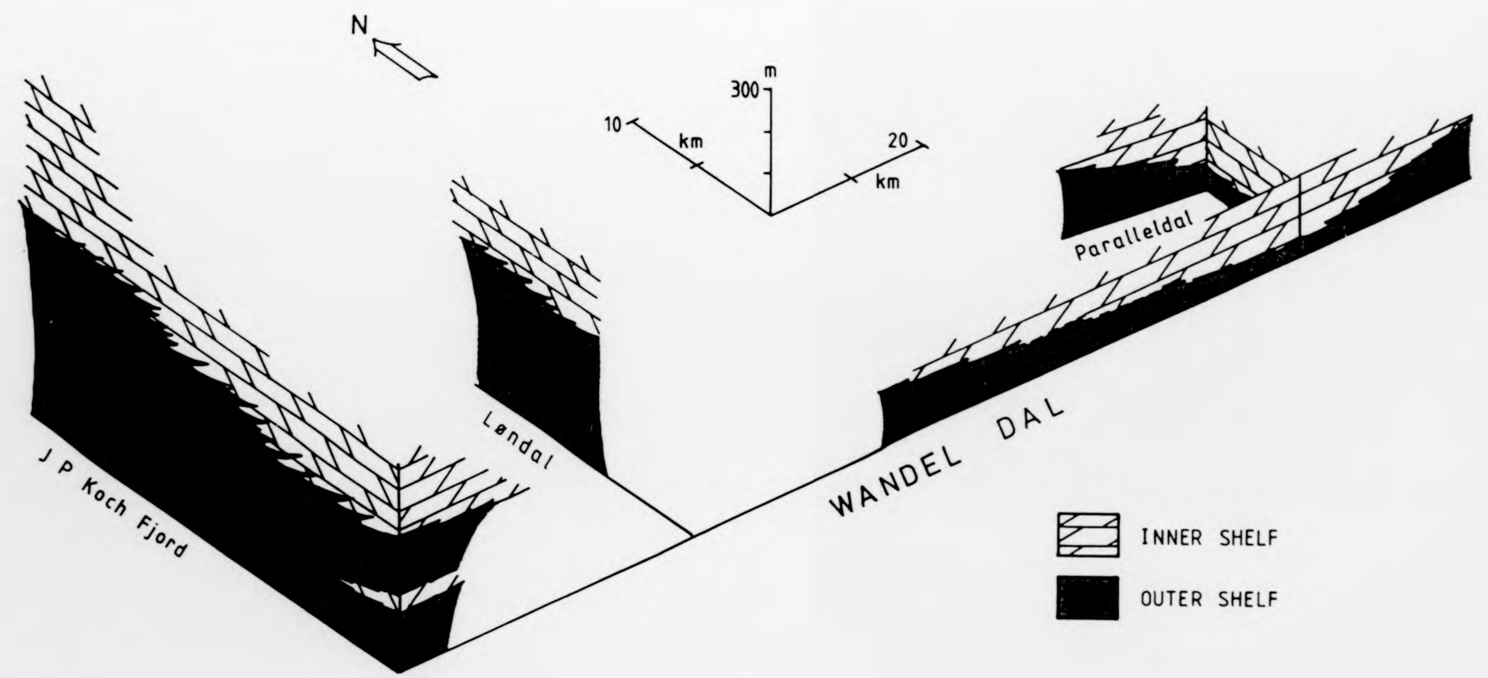


Figure 8.6. Fence diagram showing the vertical and lateral relationships between the inner and outer shelf rocks across southen Peary Land.

Shallow-water, high-energy facies of the inner ramp prograde offshore producing a flat-topped, mainly low-energy platform that grades via a steep, high-energy margin into deeper waters of the outer shelf. Continued existence of a ramp-like depositional profile is only possible so long as the relative rate of sea-level rise equals or exceeds the rate of carbonate production. Under such conditions, the high-energy zone remains fixed close to the shoreline and development of a carbonate platform is inhibited.

Rocks of the outer shelf-slope association form a large proportion of the succession, particularly in west Peary Land, but are everywhere overlain by rocks of the inner shelf (Fig. 8.6). The transition from incipient ramp (Association A) to outer shelf-slope (Association B) appears approximately isochronous, given the available biostratigraphic data. In contrast, the transition from outer shelf to inner shelf facies is strongly diachronous (Figs 8.7 & 5.1). In eastern central Peary Land, inner shelf carbonates overlie a thin (80 - 140m) outer shelf sequence that is wholly of Early Cambrian age. In west Peary Land, however, inner shelf rocks overlie a thick outer shelf succession (300 - 500m) of Early to Late Cambrian age.

The transition from outer to inner shelf is displayed in a number of vertical sections (e.g. Fig. 8.8). Typically, nodular skeletal wackestones and packstones of the outer shelf are overlain by pale-coloured, thick-bedded dolomites of the platform margin association. Foreslope breccias and stratified grainstones with inclined bedding commonly testify to a steeply sloping platform front. Where relief was more subdued, upper slope carbonates pass directly up into platform-edge

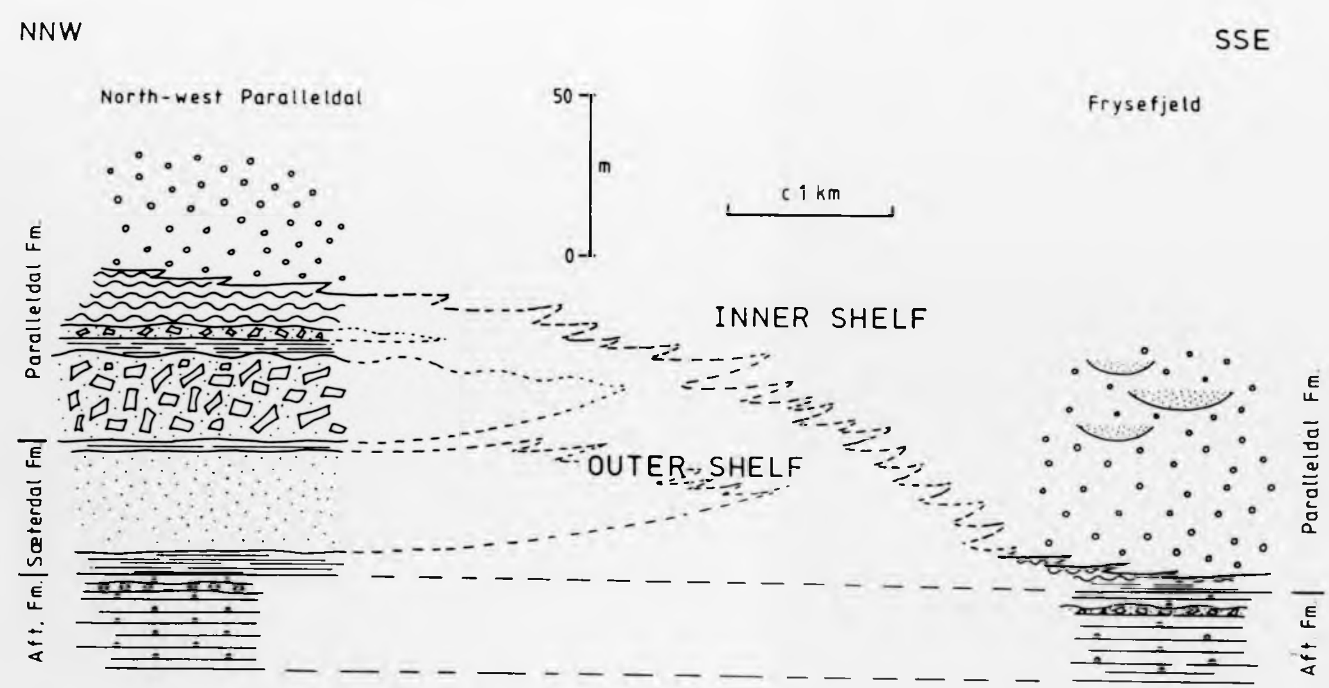


Figure 8.7. Diagram showing the relationships between Associations A, B and C, and their component assemblages, in a north-south transect between the south side of Frysefjeld and the north side of Paralleldal.

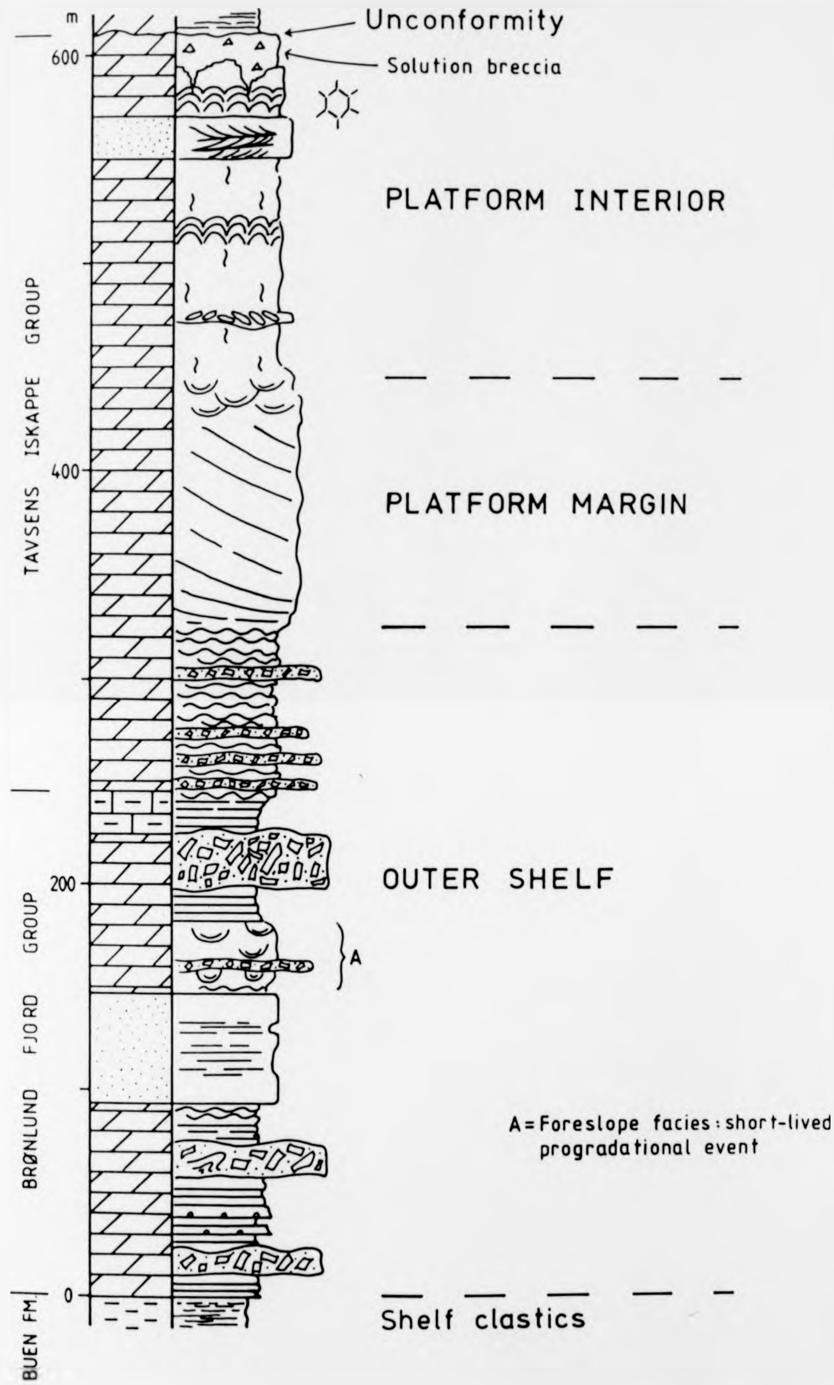


Figure 8.8. Composite, generalized section through the Brønlund Fjord and Tavsens Iskappe Groups at Koch Væg (localities 2,3), west Peary Land, showing the overall shallowing-upward, regressive sedimentation pattern.

ooidal and skeletal grainstones (e.g. Fig. 7.19).

In many sections, rocks assigned to the platform margin association form the uppermost preserved Cambrian strata and are overlain unconformably by late Lower Ordovician rocks. Around Henson Gletscher, however, platform margin rocks are succeeded by argillaceous and sandy carbonates (Association D) that were deposited in shallow subtidal to low supratidal environments in an inner platform setting. This complete vertical sequence from incipient ramp and outer shelf-slope carbonates through platform margin carbonates and into platform interior facies (Fig. 8.8) conforms to the idealized pattern of a large-scale, regressive, 'shallowing-upward' sequence (e.g. Bosellini 1984).

### 8.3.2 Lateral succession of environments

The upward transition from outer shelf to inner shelf rocks is mirrored by the lateral transition in coeval sections from inner shelf in the south to outer shelf in the north (Fig. 8.6). This is best illustrated in the J.P. Koch Fjord - Henson Gletscher region where an extensive north-south transect is exposed. Clearly, the inner-outer shelf transition is highly diachronous; the facies relationships (Fig. 5.1), palaeocurrent and palaeoslope data (8.2) indicate progradation of inner shelf facies towards the north or NNW with time. In south-east Peary Land, platform margin carbonates prograded over the outer shelf sediments during the late Early Cambrian whereas northward progradation of inner shelf facies in west Peary Land proceeded intermittently from the early Middle Cambrian to the latest Cambrian or earliest Ordovician.

The regressive, progradational pattern, summarized in Fig. 5.1, is closely comparable to the idealized 'offlap' margin of James & Mountjoy (1983). The offlap carbonate margin is characterized by a progradational regime, in which sediments of the shelf-slope break (platform margin) prograde seaward over older slope deposits, as carbonate accretion outpaces the relative sea-level rise. Excess carbonate production at the margin leads to thick accumulations of resedimented sands and conglomerates in deeper-water environments and restricted circulation or exposure of platform interior environments (James & Mountjoy 1983). Ancient analogues have been described by Davies (1977), Hileman & Mazzullo (1977) and Bosellini (1984).

### 8.3.3 Shelf stability and progradation

Within the generalized framework of overall regression a more complex picture emerges from consideration of the succession of the three outer shelf assemblages (stable shelf, unstable shelf-slope and upper slope assemblages) and their lateral relationships to the inner shelf rocks. Vertical sections through the outer shelf sediments show a rhythmic alternation of unstable and stable shelf assemblages (Fig. 8.9). In west Peary Land, where the most complete Cambrian sequence is preserved, rocks assigned to the unstable shelf assemblage form three distinct units (Aftenstjernesø, Sydpasset and Fimbuldal Formations) that alternate with units assigned to the stable assemblage (Henson Gletscher Ekspedition Bræ and Holm Dal Formations; Fig. 8.9). Within the resolution of the available biostratigraphy, these units are isochronous (Fig. 6.77).

Passing south and south-east from J.P. Koch Fjord, the outer shelf rocks are replaced laterally by inner shelf facies, due to the

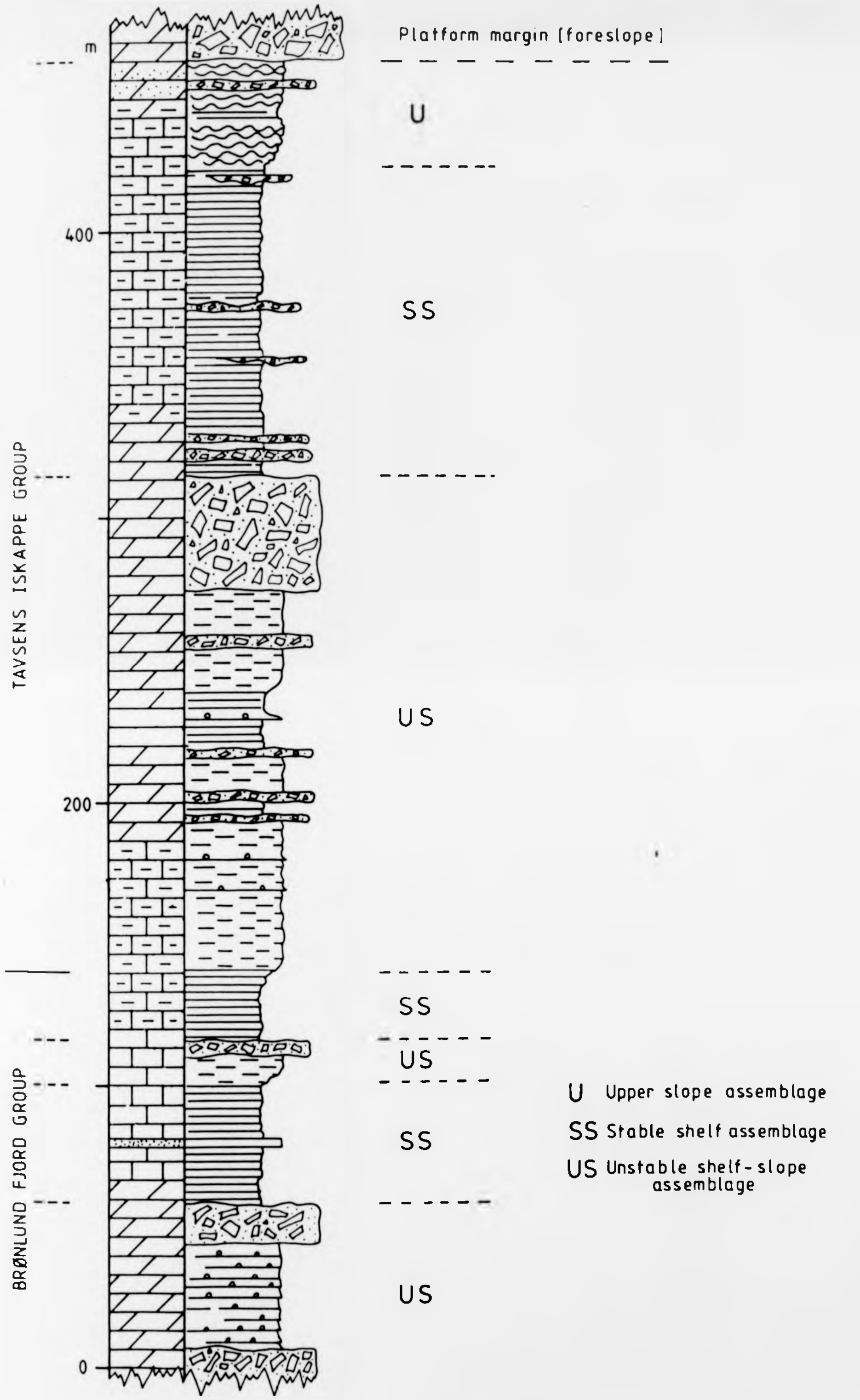


Figure 8.9. Composite, generalized section through the Brønlund Fjord and Tavsens Iskappe Groups in the Gustav Holm Dal region (localities 5-9), showing the alternation of unstable and stable assemblages within Association B.

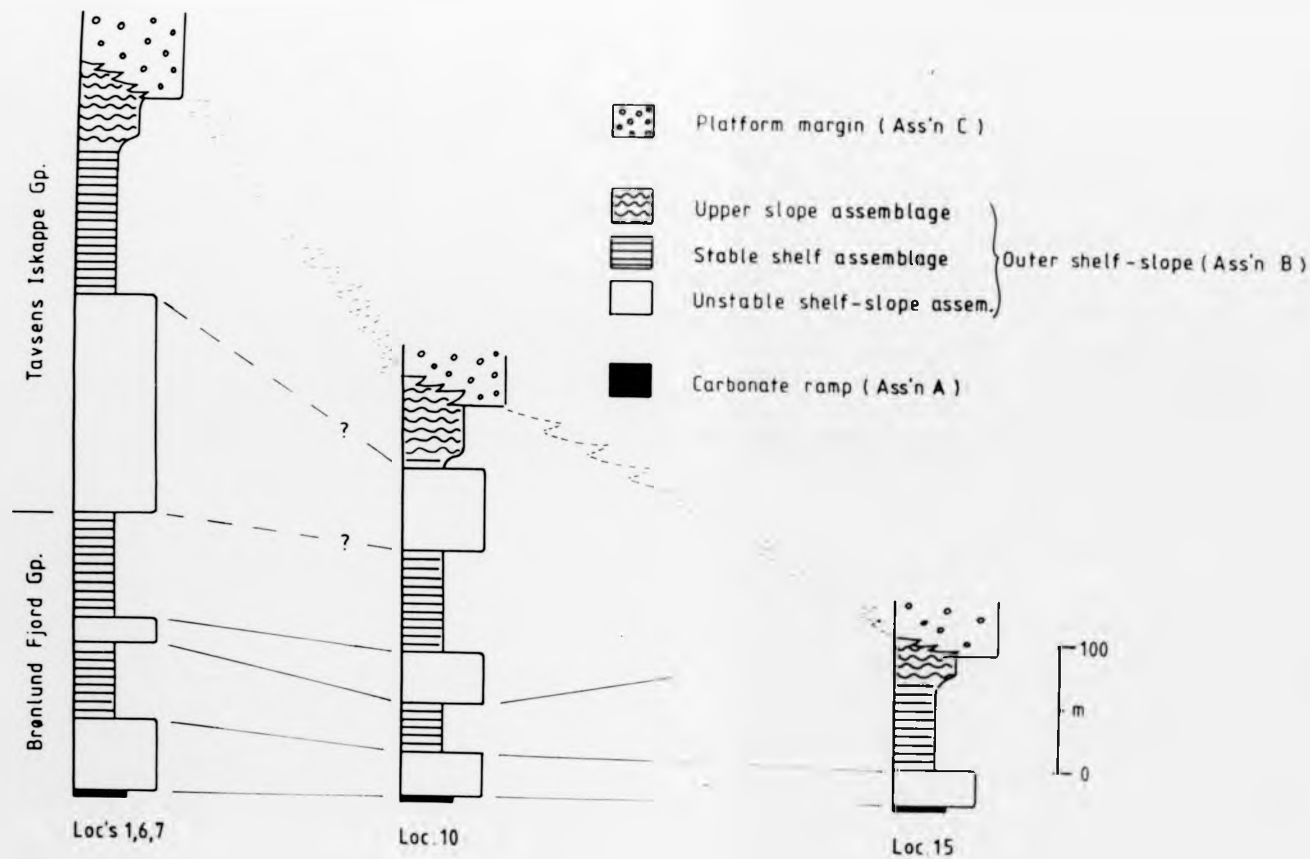


Figure 8.10. Lateral correlation of outer shelf assemblage units across southern Peary Land.

northward progradation of the shallow-water carbonate platform (Fig. 8.6). Hence, the unstable-stable shelf couplets disappear progressively towards the south-east. In Løndal, the three unstable assemblage units are recognized, although the uppermost stable shelf assemblage of the J.P. Koch Fjord section is absent (Fig. 8.10). South-east from Løndal the unstable assemblage unit of the Tavsens Iskappe Group (Fimbuldal - lower Løndal Formation) and the Sydpasset Formation unstable assemblage unit are progressively replaced by inner shelf carbonates. The Aftenstjernesø Formation forms the lowermost unstable assemblage unit which occurs throughout southern Peary Land (Fig. 8.10).

The third outer shelf assemblage, the upper slope, is transitional between the outer shelf and the platform margin and forms a strongly diachronous interval (Fig. 6.77).

Inner shelf rocks are sparsely fossiliferous and correlation between them and the richly fossiliferous outer shelf deposits is often difficult. In a few areas, however, excellent cliff exposures allow lateral correlation between measured sections and the relationship between the inner and outer shelf rocks can be traced in detail. The most complete reconstruction was possible in the J.P. Koch Fjord area, where the inner-outer shelf transition is exposed at a number of stratigraphic levels from the medial Middle Cambrian to the Upper Cambrian (Fig. 6.77). It is clear from this reconstruction that platform progradation was not a gradual, continuous process, but proceeded in an intermittent fashion. Phases of rapid northward progradation alternated with periods when the margin prograded slowly, remained stationary or retreated towards the south. The episodic nature of progradation is particularly well illustrated at the southern end of Koch Væg (Fig. 6.77).

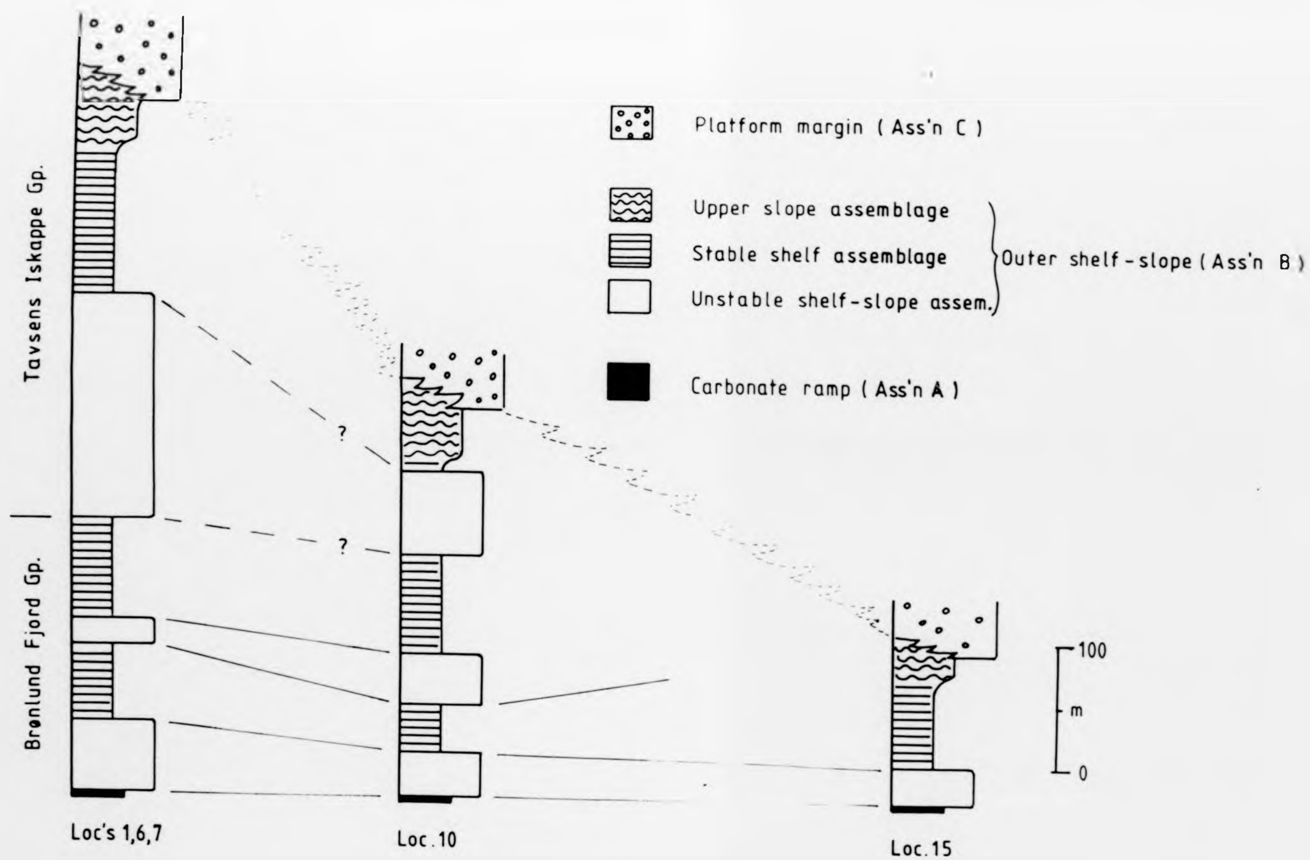


Figure 8.10. Lateral correlation of outer shelf assemblage units across southern Peary Land.

Lateral correlation between outer shelf and platform margin rocks in this area indicates that variation in the rate of platform progradation can be equated directly with the depositional characteristics of the outer shelf sediments. Phases of rapid platform progradation coincided with deposition of the stable assemblage of facies on the outer shelf. Thus the initial appearance of shallow-water facies in the medial Middle Cambrian (lower Sydpasset Formation, Koch Væg; Fig. 6.77) coincided with the accumulation of a monotonous sequence of hemipelagic lime muds on the outer shelf (upper Henson Gletscher Formation). Similarly, episodes of rapid northward progradation of inner shelf environments during the late Middle and Late Cambrian (shown by the diachronous Perssuak Gletscher Formation; Fig. 6.77) coincided with the deposition of thick sequences of argillaceous lime mudstones on the outer shelf (the stable assemblages of the Ekspedition Bræ and Holm Dal Formations).

Unstable assemblage units, however, correlate laterally with sections showing slow progradation or southwards retreat of inner shelf facies (Fig. 6.77). Thus, deposition of the unstable assemblage unit that forms the Sydpasset Formation around J.P. Koch Fjord, coincided with southward retreat of the platform in the Henson Gletscher region (Fig. 6.77). Correlation between the Fimbuldal Formation unstable unit and contemporaneous inner shelf rocks is complicated by a major fault and poor exposure at the transition. At the northern end of Koch Væg, however, platform margin dolomites (Perssuak Gletscher Formation), roughly equivalent to the Fimbuldal Formation, form a mound-like structure that is draped by, and passes laterally to the south into platform interior facies (Koch Væg Formation; Fig. 3.51). This may reflect a phase of upward growth of the margin rather than lateral accretion.

Continuous north-south exposure is rare elsewhere in southern Peary Land, but a similar relationship is demonstrable in Løndal and Paralleldal. Inner shelf sediments prograded across the Løndal outcrop area during the late Middle Cambrian and earliest Late Cambrian, the 'stable' period represented by the Holm Dal Formation to the west of Hans Tavsens Iskappe. In Paralleldal, northward progradation of inner shelf facies occurred during the latest Early Cambrian, coinciding with deposition of the stable assemblage of facies (Sæterdal, Paralleldal Formations) on the outer shelf.

This sympathetic relationship between the stability of the outer shelf and the evolutionary style of the platform implies a common controlling mechanism. As discussed earlier (7.2) the pattern of platform evolution is dependent primarily on the balance between carbonate production and relative sea-level change (Wilson 1975; Read 1982; James & Mountjoy 1983). Hence, intermittent progradation may reflect (a) variation in carbonate fixation due to intermittent nutrient and $CaCO_3$ supply or (b) episodic changes in the rate of relative sea-level rise; this may result from tectonic or eustatic mechanisms.

In this succession, the relationship between the stability of the shelf and the evolution of the platform indicates a tectonic mechanism that resulted in spatial and temporal variation in shelf subsidence.

During periods of slow regional subsidence, differential subsidence across the shelf was unimportant. The outer shelf was a stable depositional surface with low slopes. Sediment was deposited on the outer shelf from suspension and from low-density sediment gravity flows derived primarily from the upper slope. Carbonate production outpaced subsidence on the platform and the margin prograded northwards. Depositional slopes on the prograding margin ranged from a few degrees to over $25^{o}$, depending on local topography and the rate of progradation, relative to outer shelf sedimentation rates. A wedge of carbonate sediment accumulated on the seaward flank of the advancing carbonate platform (Fig. 8.11). Gravitational instability was restricted primarily to the surface of this carbonate apron (the upper slope assemblage) and to the foreslope of the prograding platform. Periodically, sediment accumulation on the outer shelf exceeded the relative sea-level rise, resulting in shallowing and the development of winnowed skeletal sand banks on localized topographic highs. This depositional model (Fig. 8.12) is closely comparable to the idealized offlap margin of James & Mountjoy (1983) and to several ancient sequences (e.g. Dunham 1972; Davies 1977; Brady & Koepnick 1979).

When regional subsidence rates were high, however, differential subsidence across the shelf produced an unstable depositional surface. Carbonate production on the platform was barely able or unable to keep pace with the relative sea level rise. Depending on the balance, the platform margin prograded slowly northwards, remained stationary or retreated towards the south. Gravitational instability was not restricted solely to the depositional slopes of the platform-outer shelf transition, but was widespread across the outer shelf. Vertical accretion of the platform margin probably resulted in a steep, unstable shelf-platform transition (Fig. 8.13) resembling the bypass margin of McIlreath & James (1978).

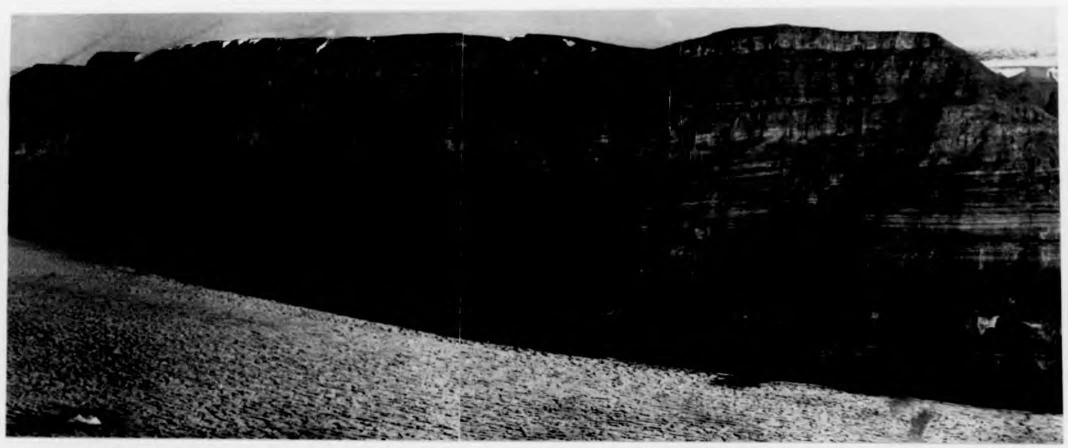

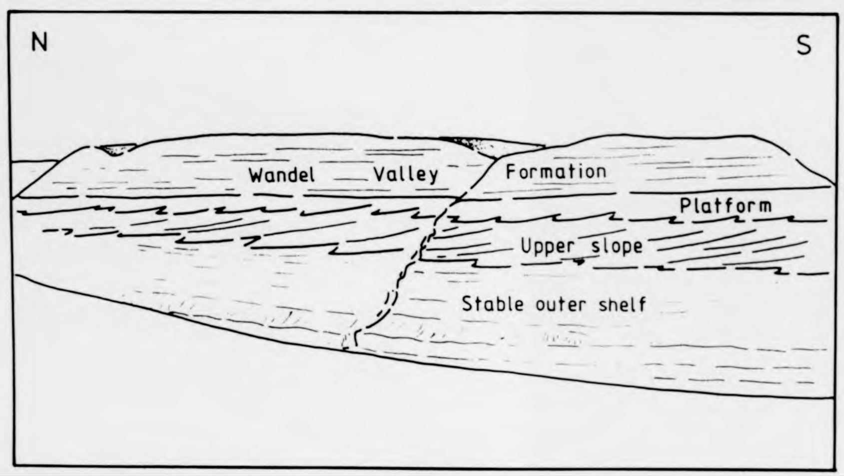


Figure 8.11. Photograph and interpretive sketch of the Tavsens Iskappe Group on the east side of J.P. Koch Fjord, viewed towards the north-east.

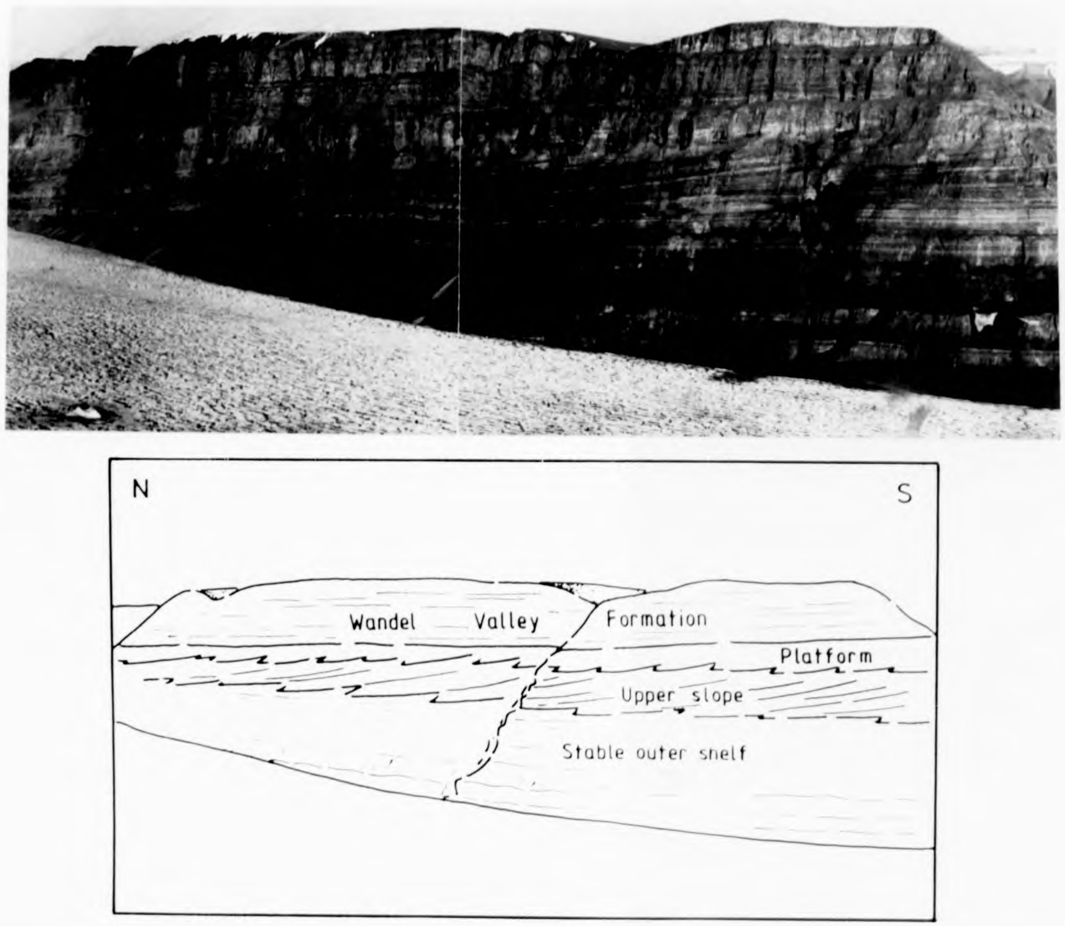


Figure 8.11. Photograph and interpretive sketch of the Tavsens Iskappe Group on the east side of J.P. Koch Fjord, viewed towards the north-east.

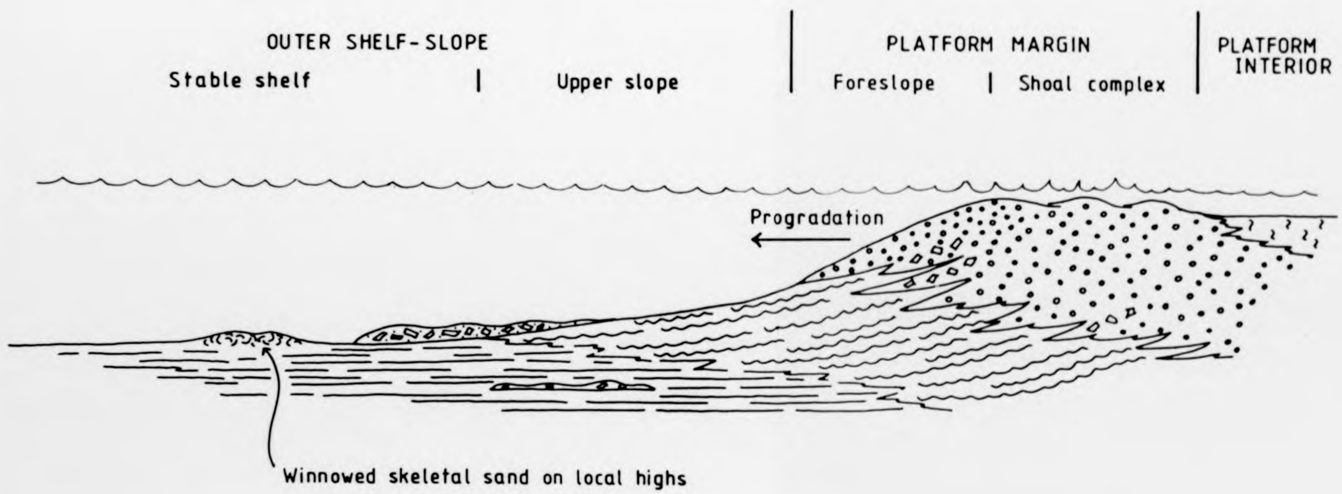


Figure 8.12. Sketch showing the inferred environmental relationships during periods of slow subsidence.

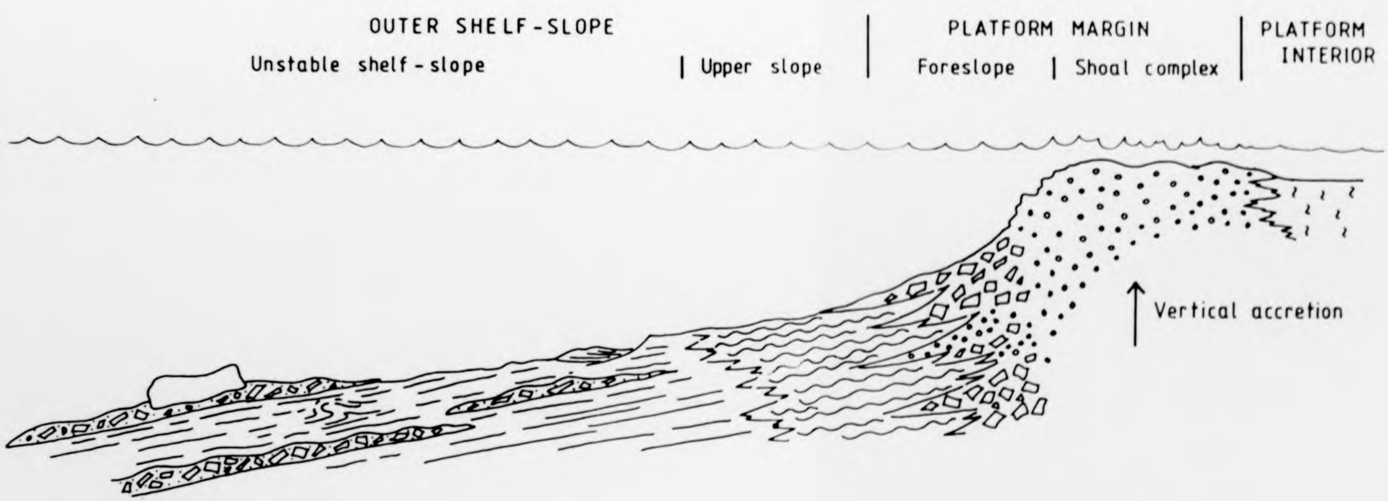


Figure 8.13. Sketch showing the inferred environmental relationships during periods of rapid, differential subsidence.

Summary

Within the framework of overall regression, the detailed facies pattern records temporal and spatial variation in shelf subsidence. Three major episodes of shelf instability are recognized. These reflect periodic warping or tilting of the shelf due to differential subsidence; seismic shocks accompanying shelf warping may have been responsible for the detachment of huge blocks of platform margin carbonate and for the mobilization of voluminous mass flows that transported this debris into deeper water. It has been noted previously that the upward transition from an unstable to a stable assemblage is typically sharp and marked by extensive mass flow deposits (Fig. 8.9). This suggests that the inferred warping of the shelf ceased relatively suddenly, possibly due to stress release along faults.

## 8.4 Wandel Valley Formation basal unconformity

### 8.4.1 Introduction

The unconformity separating the Brønlund Fjord and Tavsens Iskappe Groups from the late Lower - Middle Ordovician Wandel Valley Formation is a major feature in the shelf sequence of eastern North Greenland (Fig. 2.3) and clearly it represents an important event in the evolution of the shelf. The stratigraphic significance of the hiatus increases from west to east across southern Peary Land as the Wandel Valley Formation progressively oversteps the Cambrian strata (Fig. 3.2). It is suggested here that this south-eastward overstep is essentially a depositional feature, reflecting the Cambrian sedimentation history, and did not result from regional tilting and erosion during the early Ordovician. This suggestion is based on the regional facies variation within the Cambrian rocks, and on the detailed and large-scale character of the unconformity.

### 8.4.2 Nature of the unconformity

The unconformity is planar and parallel in most sections. Indeed, no angular discordance is evident over much of southern Peary Land, and the significance of the contact is often not obvious at outcrop. Measurable angular discordance only occurs where the Ordovician carbonates truncate primary dipping surfaces in the underlying Cambrian strata (e.g. Fig. 3.47). Rarely, in such cases, the divergence may reach 15° (Peel 1979). There is no structural evidence, therefore, for regional tilting of the shelf during the early Ordovician.

At outcrop scale, the unconformity is typically planar and sharp and often is recognized only by the lithological contrast between the Cambrian and Ordovician rocks. It is locally irregular; at the northern end of Koch Væg, the basal beds of the Wandel Valley Formation drape an irregular, hummocky surface with a relief of up to a few metres (J.S. Peel, pers. comm. 1979).

At several localities, the upper levels of the Cambrian succession are brecciated or riddled with spar-filled and/or sediment-filled fissures and vugs. Brecciated zones are particularly common in the Sæterdal - Paralleldal area where they extend as much as 70m down from the unconformity. The basal contacts of these zones are typically gradational, passing from chaotic breccia downward into fractured carbonates with extensive vug development. On the north side of Paralleldal, one such brecciated zone has a crudely lenticular shape, wedging out laterally beneath the unconformity (Fig. 8.14). The dolomite and rare sandstone clasts range from mm-sized, angular chips to blocks several tens of metres across. In places, clasts have a thin coating of pale green clay.

In central southern Peary Land, vugs and fissures are common in the upper 30 - 50m of the Cambrian succession and locally occur as much as 140m below the unconformity. The vugs are typically planar, and may be horizontal or oblique, following bedding or cross-stratification. Irregular-shaped vugs and vertical fissures are present. The sub-horizontal forms range from less than 10mm to 0.3m in thickness and are up to 1m long. Vugs are often concentrated at particular levels, where they may form as much as 60% of the rock. Typically, they are occluded by internal sediment and/or sparry dolomite cement with a relict fibrous habit (Figs 8.15 & 8.16). Internal sediment consists of fine crystalline dolomite and shows horizontal, geopetal layering; several phases of cavity fill are often present (Fig. 8.15). Later generations of vug-fill locally intrude and envelop fractured, partially brecciated older generations of internal sediment. At a few localities, the vugs are lined with fibrous crystalline dolomite fringes up to 0.1m thick. These often show internal banding (bands 0.1 - 10mm thick), reflecting successive phases of crystal growth (Fig. 8.16). The cement fringes are often thicker on the roof of the cavity than at the cavity floor; individual bands commonly thicken and become more numerous towards the centre of the cavity roof (Fig. 8.16). Some vugs display an alternation of fibrous cement and geopetal internal sediment. Open cavities occur only rarely.

At locality 14, in Sæterdal, carbonate-filled vugs are

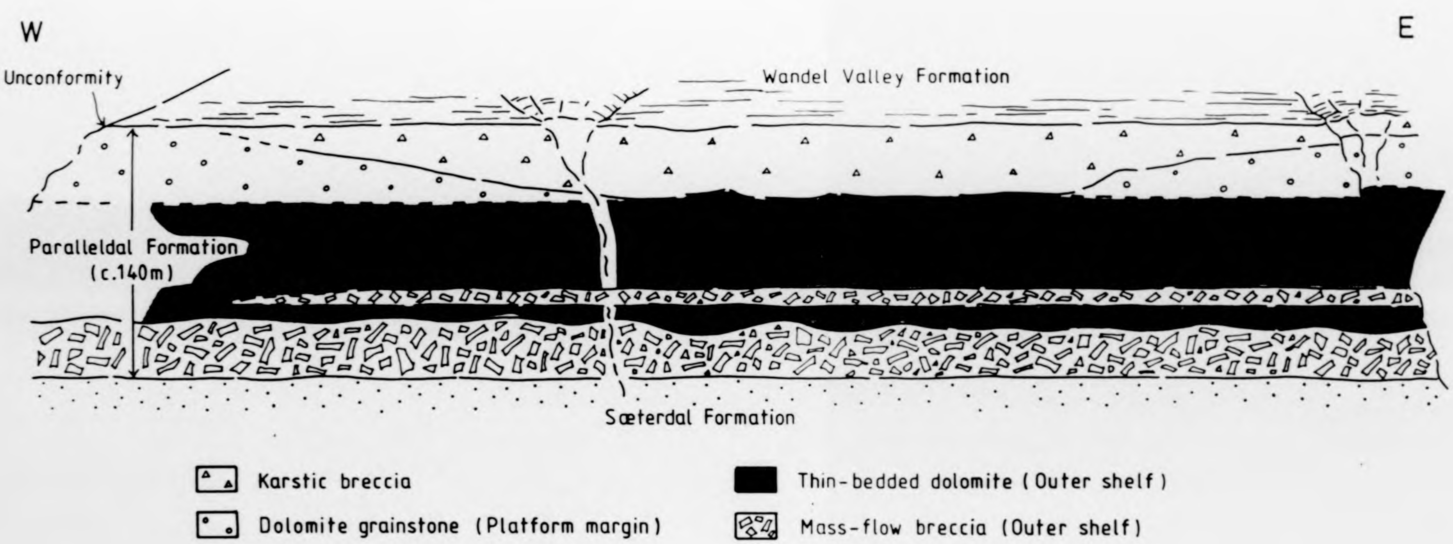


Figure 8.14. Sketch showing the distribution of karstic breccias beneath the sub-Wandel Valley Formation unconformity on the north side of Paralleldal. Drawn from field sketches.

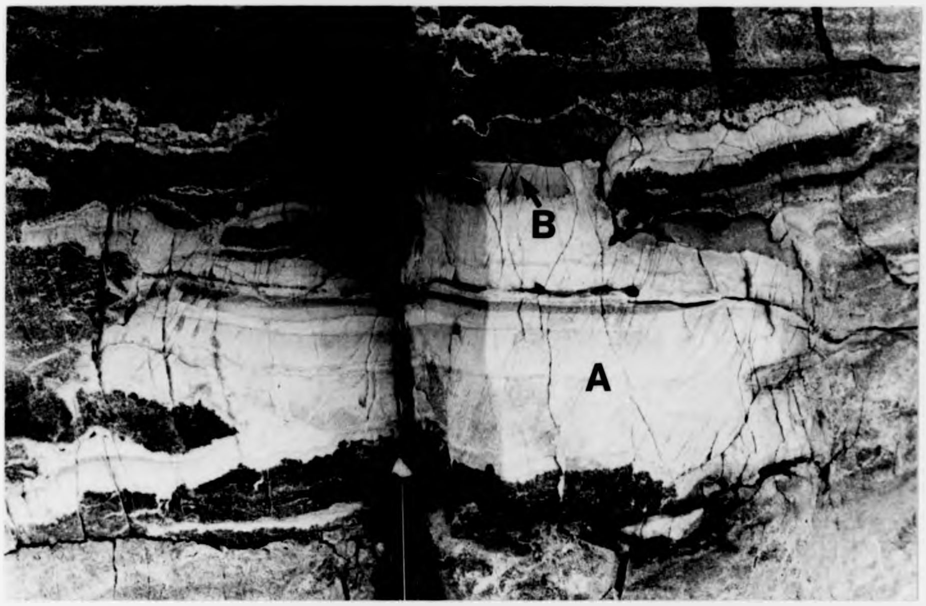


Figure 8.15. Solution vugs within skeletal dolomite (LF.5) with geopetal internal sediment showing several distinct generations of vug fill (e.g. pale sediment (A), mid-grey sediment (B) and dark grey sediment (C)). Sydpasset Formation, locality 12, central Peary Land.

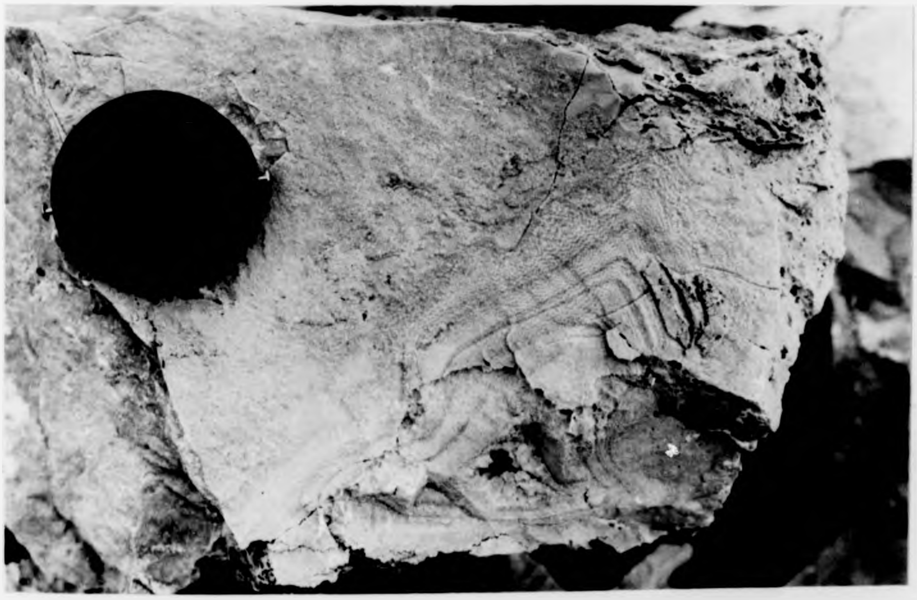

Figure 8.16. Solution vug lined with dolomitized fibrous cement. Note the thickening of individual bands from the margin to the centre of the cavity roof. Paralleldal Formation, locality 19, central Peary Land.

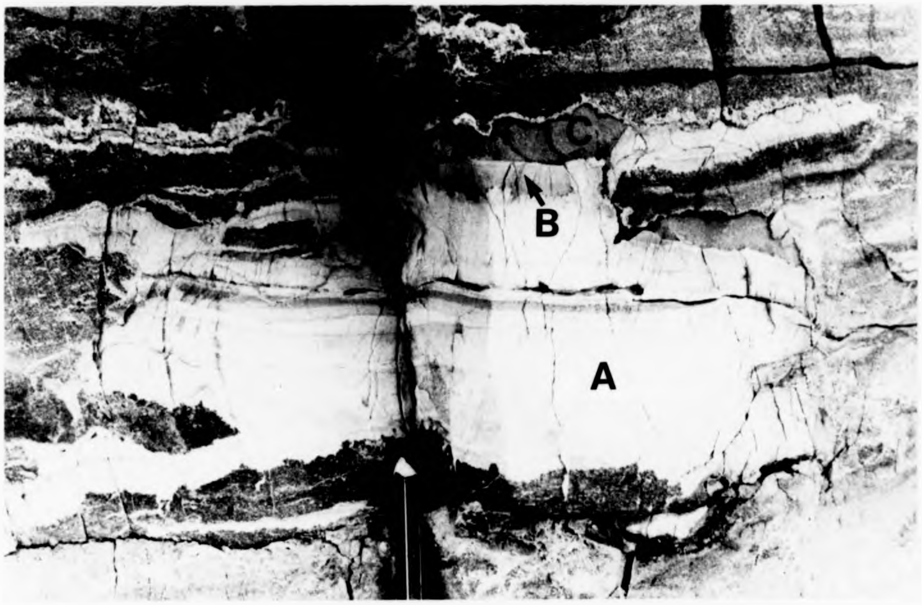


Figure 8.15. Solution vugs within skeletal dolomite (LF.5) with geopetal internal sediment showing several distinct generations of vug fill (e.g. pale sediment (A), mid-grey sediment (B) and dark grey sediment (C)). Sydpasset Formation, locality 12, central Peary Land.

Figure 8.16. Solution vug lined with dolomitized fibrous cement. Note the thickening of individual bands from the margin to the centre of the cavity roof. Paralleldal Formation, locality 19, central Peary Land.

themselves cut by fractures filled with dolomitic quartz sandstone (Fig. 8.17). Similar white sandstone-filled fissures transect dolomites of the Aftenstjernesø Formation at Buen (loc. 20). (Fig. 8.18).

The close association between the unconformity and these discordant vugs, fissures and breccias suggests that they formed as a result of solution processes at the exposed carbonate surface. An upward transition is commonly observed, passing from isolated solution vugs to chaotic brecciation incorporating both the host rock and early generations of internal sediment (Fig. 8.19). Brecciation clearly resulted from sub-surface solution which initially produced a network of sub-horizontal vugs and vertical fissures. Where leaching was localized, the host rocks were capable of supporting the cavities and the vugs were occluded by successive generations of cement and internal sediment. More extensive solution lead to collapse and the formation of solution breccias.

Such features are well documented from unconformities that developed during subaerial exposure of carbonate terrains (Esteban & Klappa 1983). Kyle (1983) described a 5m thick brecciated zone at a mid-Devonian disconformity, associated with a green clay residue that also lined and filled fractures and vugs beneath the rubble zone. Unconformities of this type may be marked by up to 100m of solution breccia (Martinez del Olmo & Esteban 1983) and are commonly associated with vadose cements, internal sediments and green-stained solution residues (Dunham & Olsen 1980; Esteban & Klappa 1983; Kyle 1983). The dolomitized cement fringes described here, are strikingly similar to flowstone or dripstone cements figured by Estaban & Klappa (1983) and


Figure 8.17. Solution vugs or solution-enlarged fractures filled with pale carbonate internal sediment (P) cut by fractures with a dark dolomite quartz sandstone fill (Q). Paralleldal Formation, locality 14, central Peary Land.


Figure 8.17. Solution vugs or solution-enlarged fractures filled with pale carbonate internal sediment (P) cut by fractures with a dark dolomite quartz sandstone fill (Q). Paralleldal Formation, locality 14, central Peary Land.

Figure 8.18. Subvertical fractures with a white quartzitic sandstone fill. Aftenstjernesø Formation, locality 20, central Peary Land.

Figure 8.18. Subvertical fractures with a white quartzitic sandstone fill.
Aftenstjernesø Formation, locality 20, central Peary Land.

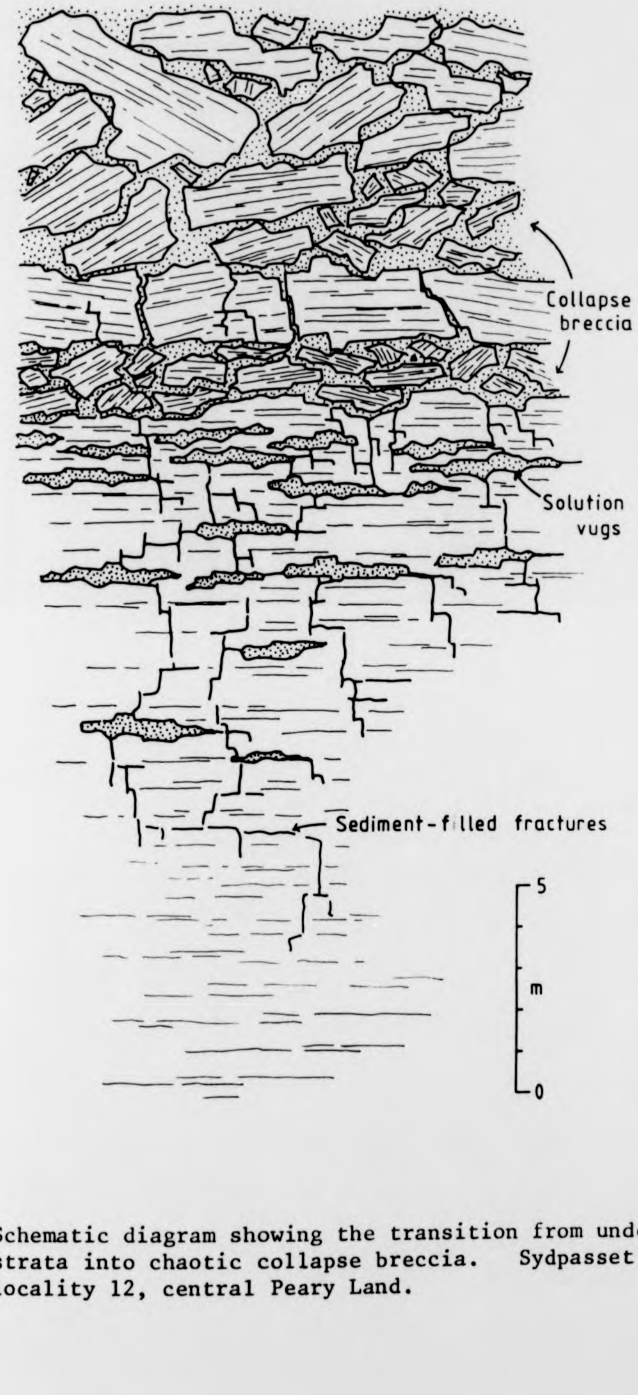


Figure 8.19. Schematic diagram showing the transition from undeformed strata into chaotic collapse breccia. Sydpasset Formation, locality 12, central Peary Land.

Bechstadt & Dohler-Hirner (1983), and by analogy are considered to represent vadose carbonate cements.

In the Paralleldal area, breccias and solution cavities with dripstone cements are abundant in the upper 50m of the Cambrian succession; this suggests emergence to at least 50m above sea-level in this area.

The evidence of repeated solution, internal sedimentation, vadose cementation, fracturing and collapse indicates a complex history of karstic processes, reflecting protracted subaerial exposure. Significantly, the most extensive record of these processes is preserved in south-east Peary Land, where the hiatus shows its maximum development.

### 8.4.3 Facies distribution and the unconformity

The regressive sedimentation pattern described earlier (8.3) is demonstrable throughout the outcrop area, despite the progressive south-eastward overstep by the Wandel Valley Formation (Fig. 8.6). This relationship implies a link between the evolution of the shelf during the Cambrian and the development of the unconformity, a conclusion also reached by Hurst & Surlyk (1983). Thus, the lateral variation in thickness and stratigraphic extent of the Cambrian strata is not the result of post-Cambrian tilting and erosion, but is essentially a primary, depositional feature, reflecting differential shelf subsidence during the Cambrian.

### 8.4.4 Discussion

In Peary Land, the unconformity resulted primarily from non-deposition due to regression and progressive exposure of the shelf during the Middle and Late Cambrian. It is clear, however, from the local angular discordance and the evidence of karstic solution that the unconformity plane represents a level of extensive chemical weathering and minor erosion. South-east from Peary Land the Wandel Valley Formation progressively oversteps the Lower Cambrian Buen and Portfjeld Formations and rests on Late Proterozoic rocks in Kronprins Christian Land (Fig. 2.3). Clearly the unconformity must represent a significant erosional feature in this area.

The occurrence of well-rounded, well-sorted quartz sand in fissures in central Peary Land probably records aeolian or fluvial transport of clastic detritus over the exposed shelf during the Middle or Late Cambrian. These rare fissure-fills are the only record of sand migration over the emergent carbonate platform; they may be related to the marine quartz-rich sandstones of the Hellefiskefjord or Perssuak Gletscher Formations.

Hurst & Surlyk (1983; Surlyk & Hurst 1983, 1984) proposed a relationship between the development of this unconformity on the shelf and the deposition of a thick succession of carbonate and chert conglomerates and turbiditic sandstones (the Amundsen Land Group) in the North Greenland trough. The basal strata of the Amundsen Land Group are of late Early Canadian age, however, and the redeposited conglomerates are mainly equivalent to the Wandel Valley Formation of the shelf sequence (Friderichsen *et al.* 1982). This age designation is incompatible with progressive erosion and redeposition of shelf carbonates from the Middle Cambrian to the Early Ordovician. Furthermore, the hiatus resulted primarily from non-deposition accompanying progressive exposure of the shelf and the unconformity does not represent a level of significant erosion in southern Peary Land. Derivation of the Amundsen Land Group conglomerates from this source is unlikely.

## 8.5 Palaeogeography

The palaeogeographic evolution of the Peary Land region during the Cambrian and Early Ordovician can be described in terms of five stages. Together these define a major transgressive-regressive couplet on the shelf which is closely linked to the contemporaneous evolution of the deep-water basin to the north. Data concerning the trough succession are mainly taken from Friderichsen *et al.* (1982), Surlyk & Hurst (1984) and Soper & Higgins (1984).

### 8.5.1 Earliest Cambrian

Proterozoic basement was transgressed in the earliest Cambrian and a widespread, low-relief carbonate platform developed in the shallow marine waters (Fig. 8.20a). In south Peary Land, the basal unconformity is planar and truncates an earlier palaeotopography related to deposition of the Moraenesø Formation (Jepsen 1971; J.D. Collinson, pers. comm. 1984). In north-east Peary Land the platform carbonates (the Portfjeld Formation) drape an irregular dissected surface. Clearly, a significant period of erosion preceded marine transgression in the earliest Cambrian. The lateral thickness variation shown by the Portfjeld Formation indicates a northward increase in subsidence, but carbonate production equalled or exceeded the subsidence rate and a shallow-water environment was maintained over the whole shelf. Indeed, minor diastems are present in southern Peary Land, reflecting local emergence, due to regression and/or a relative

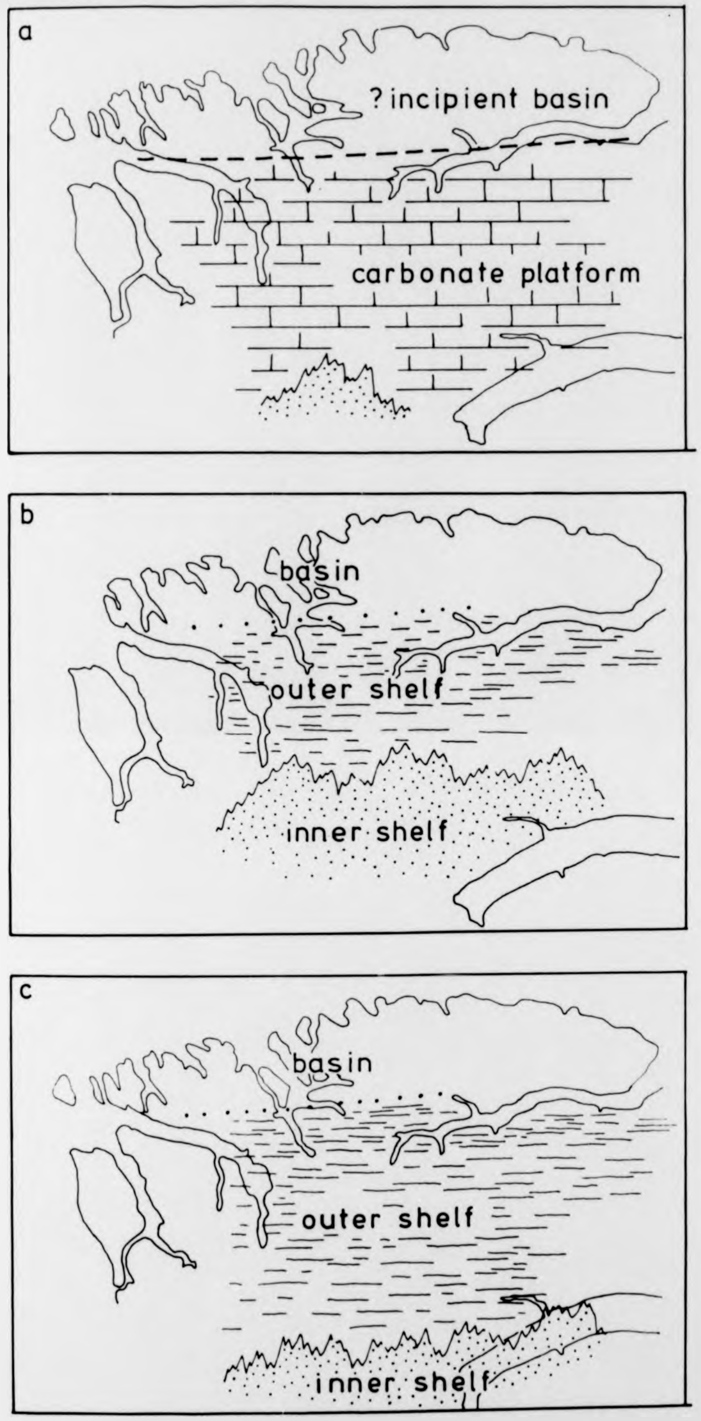


Figure 8.20. a. Palaeogeography of the Peary Land region during the earliest Cambrian (Portfjeld Formation) b. Palaeogeography of the Peary Land region during the ? middle Early Cambrian (lower Buen Formation). c. Palaeogeography of the Peary Land region during the middle-late Early Cambrian (upper Buen Formation).

drop in sea-level.

The transition from shelf carbonates into equivalent strata of the North Greenland basin is not observed and correlation between these two settings is still uncertain at this stratigraphic level. It would appear, however, that the carbonate-rich Paradisfjeld Group is the deep-water equivalent of the Portfjeld Formation, at least in part (Friderichsen *et al.* 1982). The carbonate platform represented by the Portfjeld Formation extended northwards at least as far as Depotbugt in north-east Peary Land, the mouth of Navarana Fjord in Freuchen Land (J.S. Peel, pers. comm. 1984) and the north coast of Wulff Land (Peel 1982b). The trough was restricted in areal extent at this time and was probably in an early stage of development (Surlyk & Hurst 1984). The nature of the shelf-basin transition is not clear, although Hurst & Surlyk (1983) proposed a gradual ramp-like margin. Redeposited carbonate conglomerates are common in the Paradisfjeld Group in north-east Peary Land (Hurst & Surlyk 1983) and in Nansen Land (Friderichsen & Bengaard 1984), suggesting an unstable platform margin.

### 8.5.2 Mid-late Early Cambrian

The transition from carbonate to siliciclastic sedimentation on the shelf probably records uplift and rejuvenation of the craton and consequent swamping of the carbonate platform by terrigenous sediment. Facies variations and palaeocurrent data within the Buen Formation indicate a low-relief shelf that deepened towards the north-west (Fig. 8.20b). A gradual relative rise in sea level is indicated by the vertical succession of facies (Fig. 8.20b,c).

The probable basinal equivalent of the Buen Formation is the Polkorridoren Group, a sequence of turbiditic sandstones and mudstones with subordinate carbonate conglomerates and slide blocks (Friderichsen *et al.* 1982; Frierichsen & Bengaard 1984). The uppermost unit in the group is the Frigg Fjord mudstones, a succession of thin-bedded mudstones and sandstones that crops out in southern Johannes V Jensen Land, south of the main outcrop of the turbiditic sand-rich Polkorridoren Group. Surlyk & Hurst (1984) correlated this mudstone-rich interval with the upper Buen Formation and proposed that the shelf-basin transition was gradational, passing from the deep shelf (Buen Formation) through a bypass slope (Frigg Fjord mudstones) into the deep-water basin (Polkorridoren Group north of the Harder Fjord Fault zone). They suggested that the slope boundaries were controlled by the Harder Fjord Fault zone and the postulated Navarana Fjord Fault. However, the Buen Formation is clearly recognizable at the mouth of Navarana Fjord, north of the inferred Navarana Fjord Fault, together with the underlying and overlying Portfjeld and Aftenstjernesø Formations (Soper & Higgins 1984). Neither the Navarana Fjord Fault nor the Harder Fjord Fault zone were significant syndepositional structural features during the Early Cambrian (J.S. Peel, pers. comm. 1984; Soper & Higgins 1984). West of Peary Land, a gradual transition is demonstrable between the deep shelf deposits of the Buen Formation in northern Freuchen Land and the turbiditic siliciclastics of the Polkorridoren Group in central Nansen Land (Friderichsen & Bengaard 1984; Soper & Higgins 1984). The northward-deepening shelf probably graded imperceptibly into the deep-water basin without a discrete shelf-slope break. Turbidity currents, perhaps initiated by storms on the shelf, locally bypassed the deep shelf in channels (Friderichsen & Bengaard 1984).

### 8.5.3 Late Early Cambrian

The transition from siliciclastic to carbonate sedimentation in the late Early Cambrian was marked by deposition of a distinctive phosphorite-glauconite-carbonate assemblage. This condensed interval at the base of the Brønlund Fjord Group occurs throughout Peary Land and a similar transitional facies occurs in western North Greenland at the boundary between the clastic Humboldt Formation and the carbonate Kastrup Elv Formation (Henriksen & Peel 1976). It probably records a eustatic sea-level rise, causing drowning of the shelf and suppression of terrigenous distributory systems. Facies variation within this unit in Peary Land indicates a stable, northward-deepening shelf (Fig. 8.21) that resembled the gently-shelving carbonate ramp of Ahr (1973).

The northern limit of this carbonate ramp cannot be accurately placed, but the clastic-carbonate transition has been recorded as far north as northern Wulff Land and southern Nansen Land (Soper & Higgins 1984). Farther north in Nansen Land, the carbonates are replaced by dark cherty mudstones. The gradual shelf-basin transition of the previous clastic phase was probably still present. Shelf drowning and silciclastic starvation led to a condensed carbonate sequence on the shelf and starved, anoxic sediments in the deep-water basin.

### 8.5.4 Late Early Cambrian - Early Ordovician

This stage in the shelf evolution, represented by the Brønlund Fjord and Tavsens Iskappe Groups, forms the regressive part of the couplet following the progressive deepening of the marine shelf in the preceding three stages. Intermittent northward progradation of shallow-water

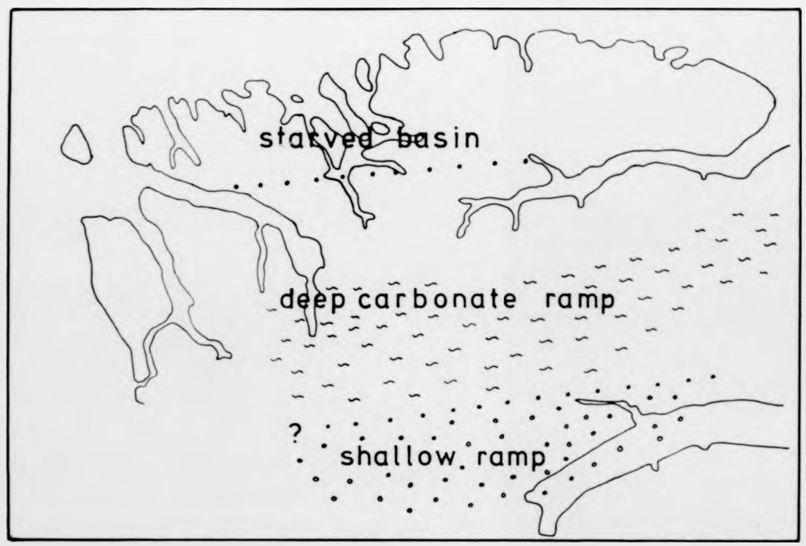


Figure 8.21. Palaeogeography of the Peary Land region during the late Early Cambrian (basal Brønlund Fjord Group).

sediments (Figs 8.22 & 8.27) resulted in progressive exposure of the inner shelf and development of a major hiatus. In south-east and central Peary Land this hiatus accounts for the Middle and Late Cambrian and much of the Early Ordovician. In west Peary Land, subsidence was more pronounced and a thick, near-complete Cambrian sequence is preserved.

Platform carbonates of late Early Cambrian age are only preserved in south-eastern outcrops, but evidence from mass flow deposits indicates that this environment persisted across southern Peary Land, south of the present outcrop area (Fig. 8.22). A shallow-water platform sequence of Cambrian age in the Wulff Land - Warming Land region to the south-west (the Blue Cliffs Group; Peel 1980a; Peel & Wright 1984) may represent the continuation of this platform.

In the latest Early Cambrian, shallow-water facies prograded rapidly northwards, possibly due to a fall in sea-level. Terrigenous detritus prograded across the inferred platform and bypassed the platform-edge shoal complex forming an apron of coalescing sand lobes at the transition from platform margin to outer shelf. The detailed palaeogeography of this transition during the late Early Cambrian is depicted schematically in Fig. 8.23, based on the cliff sections of Paralleldal and Sæterdal. The platform edge was a complex of ooid shoals and archaeocyathid biostromes, dissected locally by tidal channels. This shallow-water, high-energy environment passed offshore via a marked break in slope into the deeper water of the outer shelf, where sedimentation was dominated by deposition from suspension and from sediment gravity flows. Storm-induced currents swept terrigenous sediment offshore, utilizing tidal channels to bypass the ooid shoals and producing

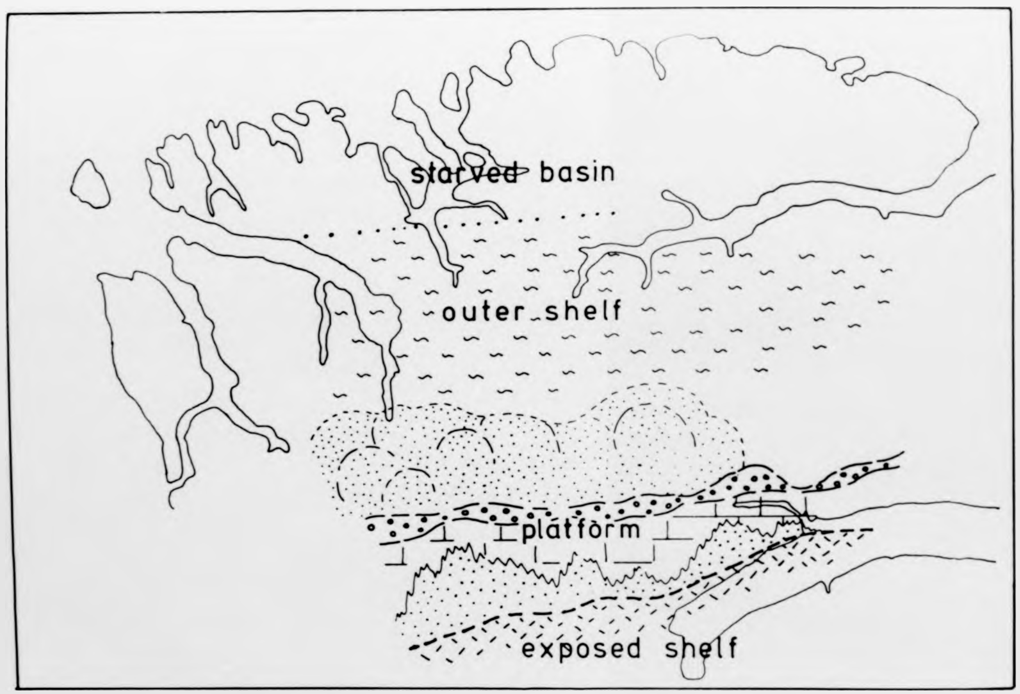


Figure 8.22. Palaeogeography of the Peary Land region during the latest Early Cambrian (lower Brønlund Fjord Group).

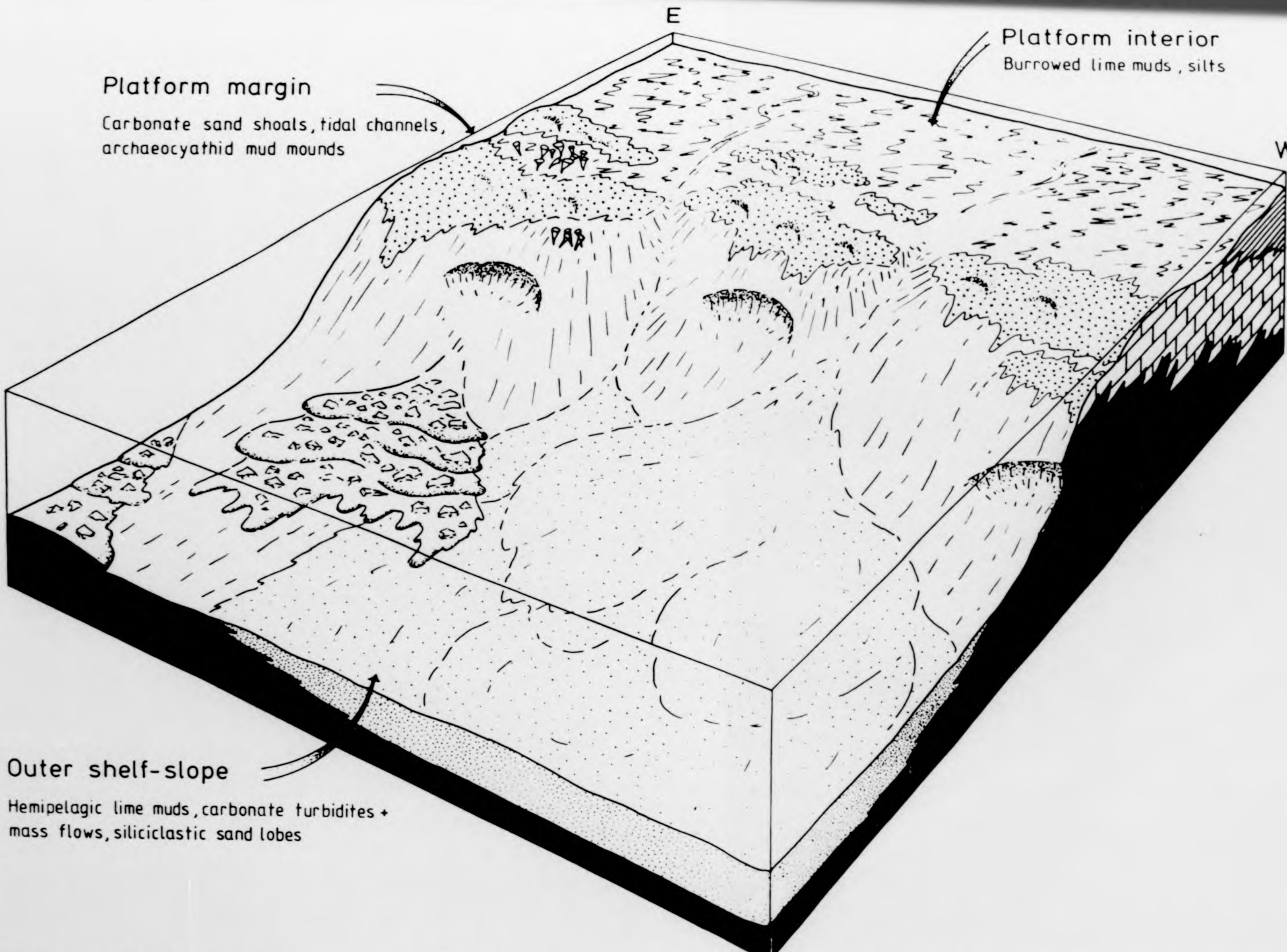


Figure 8.23. Block diagram showing the depositional model proposed for the Paralleldal - Sæterdal region during the **latest Early** Cambrian.

a siliciclastic apron at the outer shelf-platform transition.

A biostratigraphical discontinuity coincides roughly with the siliciclastic incursion into outer shelf environments in the latest Early Cambrian. The significance of this hiatus is not fully understood but it has been correlated with the Hawke Bay Event (Peel 1982b), a regressive event of probable eustatic origin described from the eastern seaboard of North America (Palmer & James 1980). A minor sea-level fall may have resulted in widespread exposure of the platform and carbonate starvation in offshore environments. The precise nature and location of this hiatus requires further field investigation.

During the medial Middle Cambrian, sedimentation on the Peary Land shelf was restricted to western and northern parts. In south-east Peary Land there is no record of sedimentation from the late Early Cambrian to the late Early Ordovician and it is probable that this area was emergent for much of this time. During the Middle and Late Cambrian, inner shelf environments migrated intermittently northwards and the carbonate shelf was progressively exposed (Figs 8.24 & 8.25).

In latest Cambrian and possibly early Ordovician times, the carbonate-dominated regime was replaced by terrigenous sedimentation in shallow shelf and upper slope environments (Fig. 8.26). This clastic influx represents the final regressive phase in the Cambrian cycle, perhaps precipitated by a relative sea-level fall resulting in northward progradation of craton-derived siliciclastic sediment.

Contemporaneous basinal rocks in the North Greenland trough sequence of Johannes V Jensen Land are the Cambrian Volvedal Group and

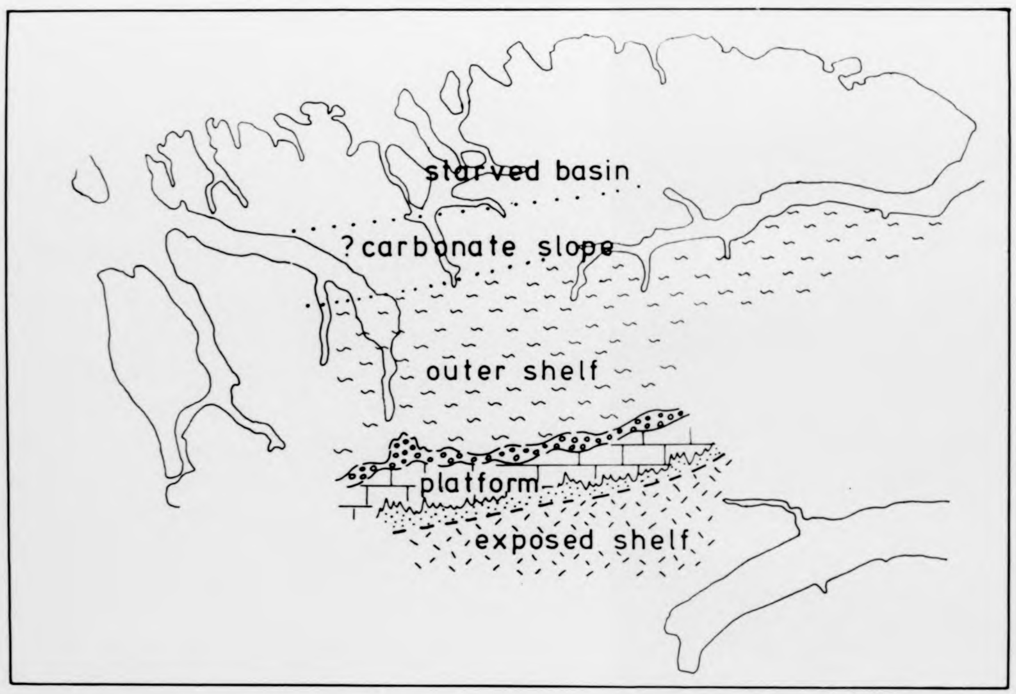


Figure 8.24. Palaeogeography of the Peary Land region during the medial Middle Cambrian (upper Brønlund Fjord Group).

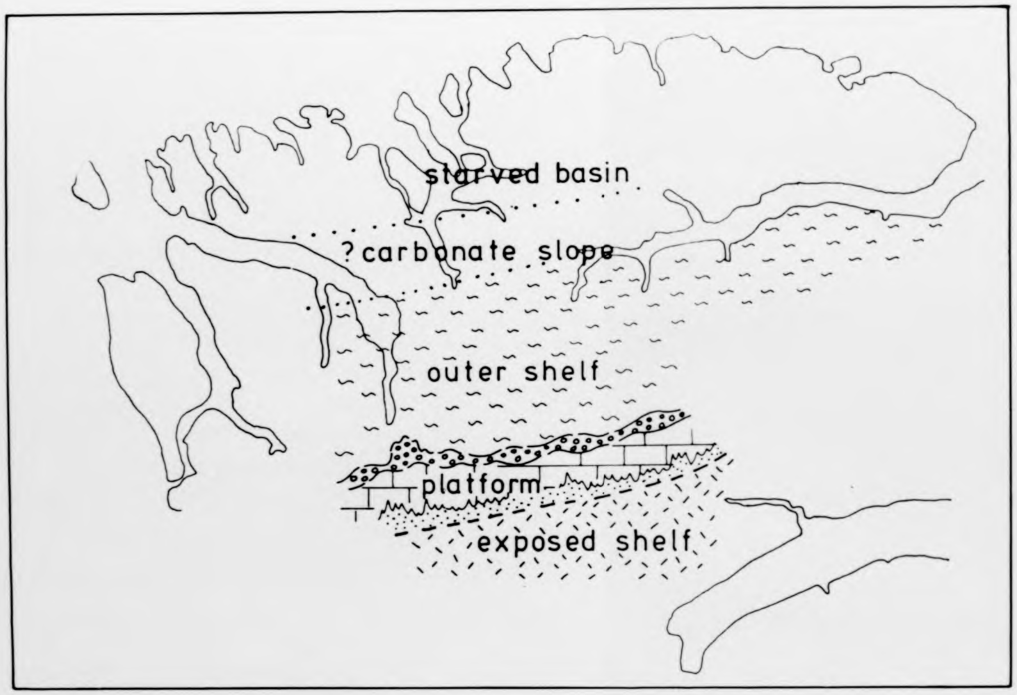


Figure 8.24. Palaeogeography of the Peary Land region during the medial Middle Cambrian (upper Brønlund Fjord Group).

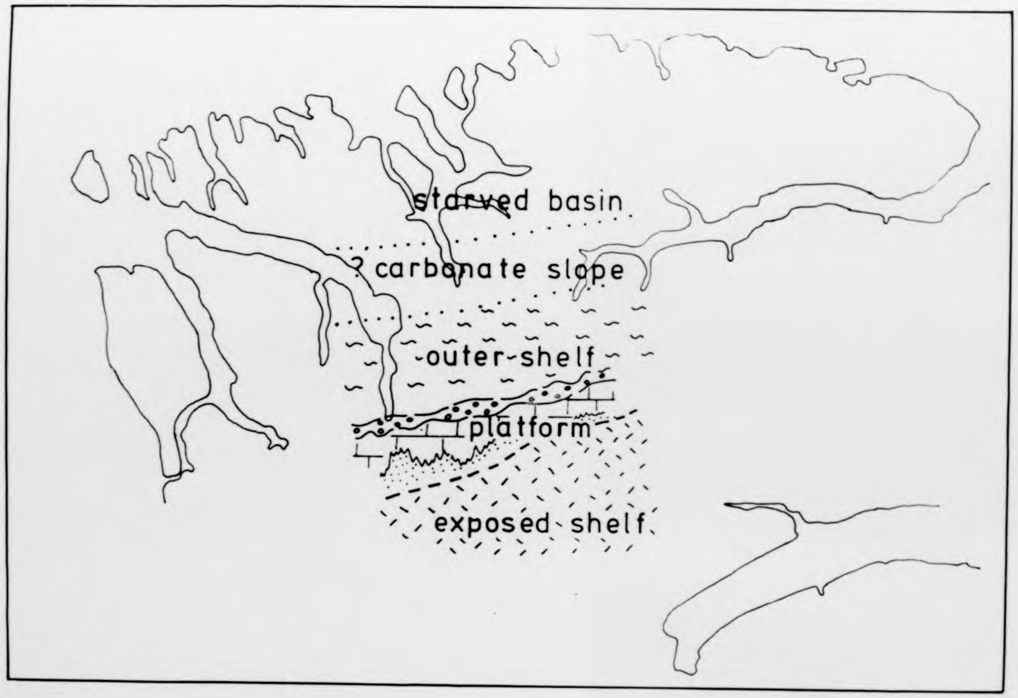


Figure 8.25. Palaeogeography of the Peary Land region during the late Middle to early Late Cambrian (lower Tavsens Iskappe Group).

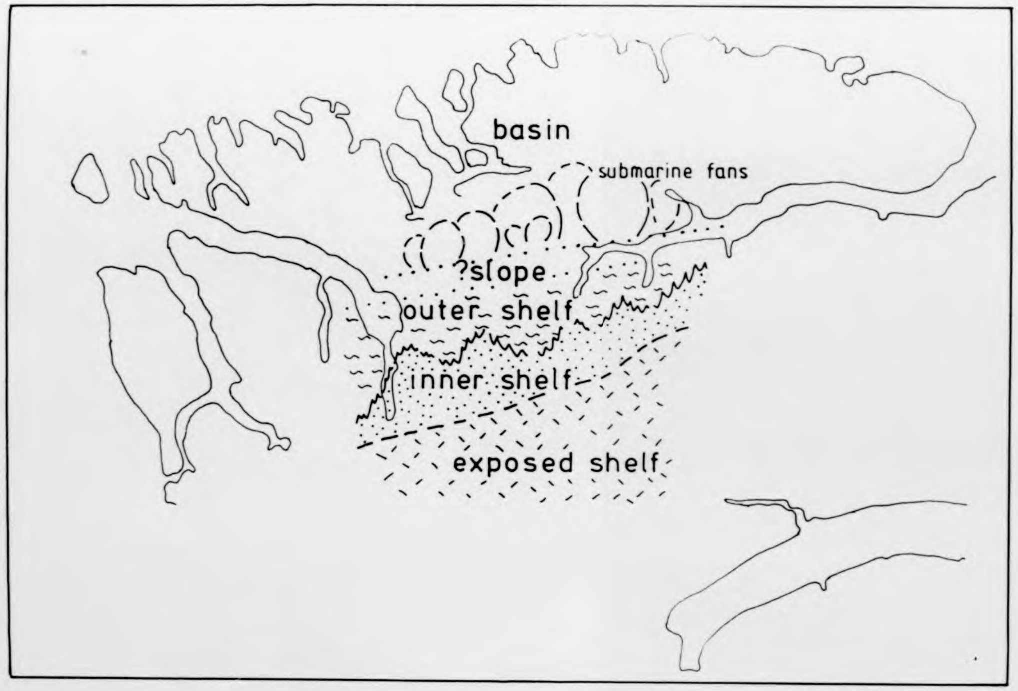


Figure 8.26. Palaeogeography of the Peary Land region during the Late Cambrian (upper Tavsens Iskappe Group).

the lower beds of the Ordovician Amundsen Land Group (Friderichsen *et al.* 1982; Surlyk & Hurst 1984). The Volvedal Group shows two distinct portions (Fig. 2.5). The lower fine-grained interval (?Lower - Middle Cambrian) consists of dark cherty mudstones with subordinate thin-bedded siliciclastic turbidites and carbonate mass-flow conglomerates. The upper portion of the group (?Middle Cambrian - earliest Ordovician) is sand-dominated and represents deposition on southerly-derived submarine fans. These sand bodies thin and pinch out northwards into fine-grained basin plain facies (Surlyk & Hurst 1983, 1984). The Amundsen Land Group consists mainly of dark cherts and mudstones with subordinate thin-bedded sandstones and localized thick developments of carbonate and chert redeposited conglomerates (Friderichsen *et al.* 1982). Surlyk & Hurst (1983, 1984) proposed that the Amundsen Land Group records a phase of basin starvation that persisted through most of the Ordovician period.

The transition from shelf to deep-water basin is not observed directly in eastern North Greenland; Hurst & Surlyk (1983) inferred a distally steepened ramp margin or an incipient escarpment, controlled by the Navarana Fjord Fault. Work in central North Greenland, however, has demonstrated the persistence of Lower Cambrian shelf rocks (Portfjeld, Buen and Aftenstjernesø Formations) to the north of the postulated Navarana Fjord Fault (Soper & Higgins 1984). Furthermore, Soper & Higgins have shown that the Cambro - Ordovician shelf-basin transition is represented by a carbonate-chert slope sequence that can be traced from J.P. Koch Fjord in the east to Nyeboe Land in the west and is equivalent to the Hazen Formation of Ellesmere Island, Arctic Canada. This slope sequence grades upwards and northwards into basinal cherts and mudstones. Clearly then, to the west of Peary Land, the gradual shelf-basin transition of the Early Cambrian evolved into a broad carbonate slope that passed northwards into a poorly oxygenated, deep-water basin. The position of the slope is apparently unrelated to any major tectonic lineament. A similar arrangement may have existed in the Peary Land region during the Middle Cambrian (Fig. 8.27), although the possibility of lateral variation in the nature of the shelf-basin boundary cannot be discounted.

Between the late Middle Cambrian and the Early Ordovician the shelf was progressively exposed whilst the basin became increasingly isolated, sediment-starved and stagnant. This contrasting sedimentation pattern suggests increasing differentiation between shelf and basin and implies narrowing and steepening of the transition zone. A similar trend is observed in northern Wulff Land and Nansen Land where slope carbonates grade up into basinal facies (Soper & Higgins 1984), reflecting a southward shift in the shelf-basin boundary in the Early Ordovician.

The southerly-derived submarine fan sandstones of the Volvedal Group are restricted to the eastern outcrop of the trough succession (Soper & Higgins 1984) and were probably related to the incursion of terrigenous sand onto the Peary Land shelf in the Late Cambrian.

## 8.5.5 Late Early Ordovician

Carbonate shelf sedimentation resumed in the late Early Ordovician following a regional marine transgression over eastern North Greenland; marine platform carbonates of this age are recognized throughout North Greenland and probably extended south-east as far as central East Greenland. The Wandel Valley Formation of eastern North Greenland

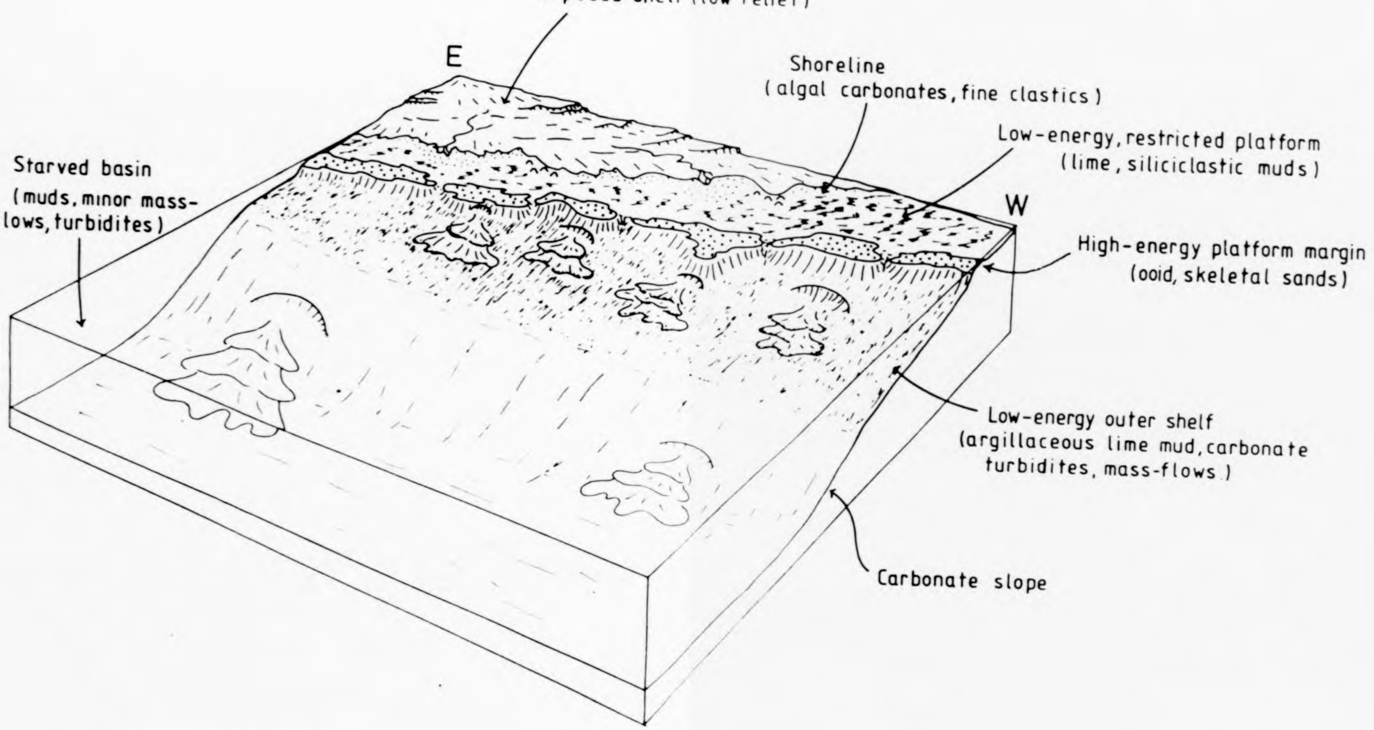


Figure 8.27. Block diagram showing a possible reconstruction of the shelf-to-basin transition during the Middle Cambrian (modified after Surlyk & Hurst 1983, Fig 4).

is a uniform carbonate sequence recording blanket sedimentation in shallow subtidal and intertidal environments on a low-relief, low-energy shelf (Fig. 8.28). This widespread transgression in the late Early Ordovician probably resulted from a eustatic sea-level rise (*cf.* Barnes 1982); evidence of a transgressive event is also seen in western North Greenland where poorly fossiliferous, evaporitic Lower Ordovician carbonates are overlain by the Nunatami Formation limestones yielding rich late Early Ordovician marine faunas (Peel & Yochelson 1979; Peel 1982b).

Equivalent basinal strata in Johannes V Jensen Land are assigned to the Amundsen Land Group (Lower Ordovician - Lower Silurian; Friderichsen *et al.* 1982). This is a succession of dark cherts and mudstones with local developments of carbonate and chert conglomerates which thicken towards the south. In its northernmost outcrops (inner J.P. Koch Fjord, G.B. Schley Fjord) the Wandel Valley Formation is of shallow-water aspect, suggesting a rapid transition into the starved basin represented by the Amundsen Land Group. The mass-flow carbonate conglomerates in the latter group also suggest a relatively abrupt boundary between the shelf and the basin.

## 8.6 Discussion

The palaeogeographic evolution of the Cambrian shelf suggested by this study (see 8.5) has a bearing on the progressive development of the contemporaneous deep-water basin across northern Greenland (see Friderichsen *et al.* 1982; Surlyk & Hurst 1984; Soper & Higgins 1984).

### Early basin development

In the earliest Cambrian, a sea-level rise resulted in a wide-

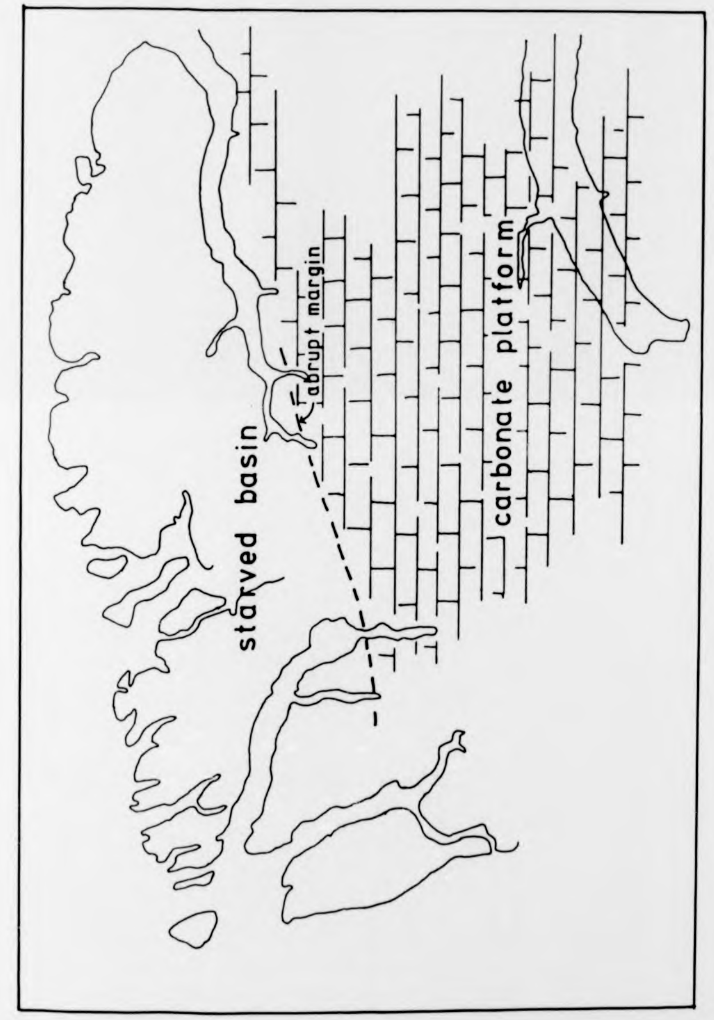


*Figure 8.28. Palaeogeography of the Peary Land region during the late Early Ordovician.*

spread marine transgression and in the development of an extensive shallow-water carbonate platform, represented by the Portfjeld Formation. The rise in sea-level on the shelf may have been partly due to eustatic change but was primarily the result of regional shelf subsidence in response to downwarping and early basin development in northernmost Greenland (Fig. 8.29).

Regional subsidence and basin expansion

The progressive deepening of the marine shelf recorded by the Lower Cambrian Buen Formation mirrors the deepening and areal expansion of the basin. The shelf-to-basin transition was gradational and the sedimentation pattern suggests simple differential subsidence between the basin and the craton to the south (Fig. 8.29).

Shelf-basin differentiation

In the latter part of the Early Cambrian, an episode of slow sedimentation on the shelf is thought to record a regional transgression of probable eustatic origin. Subsequent carbonate-dominated sedimentation, represented by the Brønlund Fjord and Tavsens Iskappe Groups, records the progressive differentiation of shelf and basin. During the late Early and Middle Cambrian, the shelf-to-basin transition was a broad carbonate slope; phases of shelf instability record episodic warping or tilting of the shelf, probably in response to periods of rapid basin subsidence. The regressive sedimentation pattern shown by Middle and Upper Cambrian shelf strata contrasts markedly with the uniform, starved, stagnant conditions indicated by the basin sediments; this reflects the increasing importance of differential subsidence between shelf and basin. Subsequently, in the latest Cambrian or

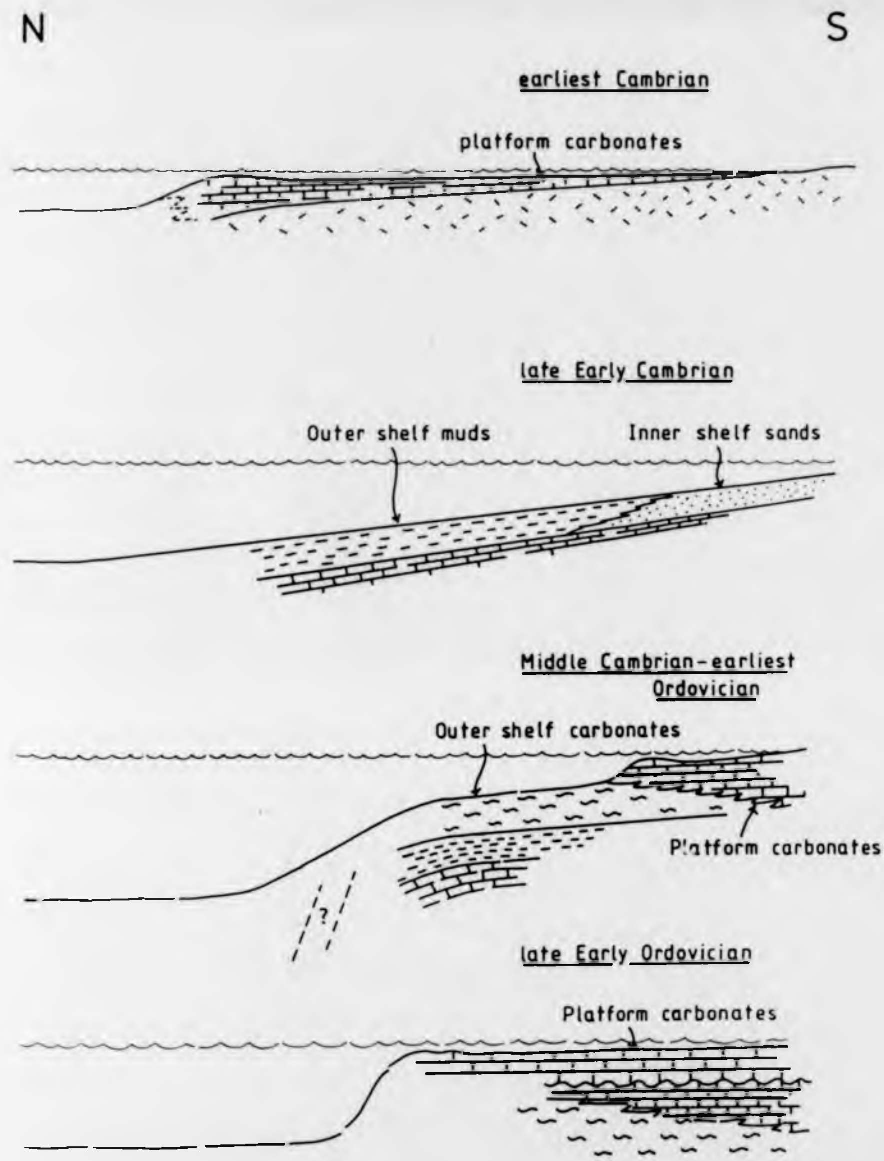


Figure 8.29. Schematic representation of basin and shelf evolution in the Peary Land region during the Cambrian and early Ordovician.

earliest Ordovician, this trend probably resulted in the development of a well-defined shelf margin (Fig. 8.29).

## Tectonic control of sedimentation

It has been suggested that syndepositional faulting in northern Greenland during the Early Palaeozoic was instrumental in controlling basin development and accommodating differential subsidence between shelf and basin. Surlyk & Hurst (1984; Hurst & Surlyk 1983) developed a model for basin development that relies heavily on the interpretation of two postulated syndepositional fault systems, the Harder Fjord Fault Zone and the Navarana Fjord Fault. It has yet to be proved, however, that either of these lineaments formed fault scarps during the Early Palaeozoic, and the significance of these structural lineaments has been disputed (e.g. Higgins *et al.* 1981; Soper & Higgins 1984). Recent work to the west and north-west of Peary Land has demonstrated that neither of these lineaments were influential during the Early Cambrian (Soper & Higgins 1984). In Navarana Fjord, shelf carbonates of uppermost Ordovician and Silurian age terminate at an abrupt scarp and pass northwards into basinal rocks; this scarp forms the east-west lineament referred to as the Navarana Fjord Fault (Surlyk & Hurst 1984). The shelf margin clearly showed significant topographic relief in this area during the Late Ordovician and Early Silurian (up to several hundreds of metres; Hurst 1984) and yet there is no evidence of fault displacement across this feature within Upper Ordovician and Silurian strata (J.S. Peel. pers. comm. 1984). The escarpment was apparently maintained by a combination of vertical carbonate accretion and differential subsidence between shelf and basin (Hurst 1984). The differential subsidence pattern across this lineament, however, implies vertical displacement at depth and probably reflects a deep-seated basement fault or fault zone.

It is likely that the relief at the Late Ordovician to Silurian shelf margin was partly an inherited feature and, as also suggested by Hurst (1984), probably reflects the marked differentiation of shelf and basin in the Late Cambrian and Early Ordovician. Given the contrasting depositional regimes between the shallow-water or exposed Late Cambrian shelf and the deep-water, sediment-starved, stagnant basin, the presence of an abrupt, possibly faulted, basin margin at this time is most probable. The position of this margin is poorly constrained by the present Upper Cambrian outcrop, but subsequent Ordovician and Silurian sedimentation patterns point towards the line of the Navarana Fjord escarpment. Indirect evidence of syndepositional tectonism during the Cambrian is found within the Brønlund Fjord and Tavsens Iskappe Groups. The rhythmic alternation of unstable and stable assemblages within outer shelf rocks suggests progressive warping of the shelf, followed by a relatively sudden reversion to stable shelf conditions, perhaps reflecting stress release along faults.

In reviewing the evolution of the Early Palaeozoic shelf and basin in eastern North Greenland, Hurst & Surlyk (1983; Surlyk & Hurst 1984) suggested that shelf instability and differential subsidence during the Cambrian resulted from shelf tilting. They proposed that this represented an early Caledonian tectonic event, a tectonic bulge that was related to subduction at the eastern margin of Iapetus Ocean. However, the thickness variations, facies relationships, palaeocurrents and palaeoslope data in the Cambrian strata (8.2 & 8.3) indicate a northward-deepening shelf, rather than westward as would be expected from tilting related solely to tectonism along the north-south trending margin bordering the Iapetus Ocean. Furthermore, it is evident from palaeogeographic reconstructions in this study (8.5) that events on the Cambrian shelf were intimately related to the contemporaneous development of the North Greenland basin.

On a regional scale, however, the eastern margin of North Greenland was uplifted relative to central and west North Greenland during the Cambrian. In central and west North Greenland the Cambro-Ordovician shelf sequence is apparently uninterrupted (Peel 1982b) suggesting continuous shelf subsidence. In eastern North Greenland, however, a major discontinuity separates Cambrian or older rocks from Ordovician platform carbonates (Fig. 2.3) and it is clear that the southern and eastern parts of the shelf in this area were emergent for much of the Cambrian period. The regional tectonic significance of this event is unknown but, whatever the cause, its effects were clearly lost by the late Early Ordovician when the shelf zone of eastern North Greenland was the site of a vast, low-relief, shallow-water carbonate platform that extended south into East Greenland and west into western North Greenland.

In summary, the Brønlund Fjord and Tavsens Iskappe Groups of Peary Land record a period of unstable shelf sedimentation caused by the interaction of the actively subsiding North Greenland basin and the stable craton to the south and south-east.

ACKNOWLEDGEMENTS

This research was undertaken at Department of Geology, University of Keele during the tenure of a NERC-CASE studentship which is gratefully acknowledged. I am indebted to the Geological Survey of Greenland (GGU), Copenhagen for the opportunity to work in North Greenland and for permission to submit this thesis. In particular, I am grateful for the help and guidance given by Dr. John S. Peel throughout this project and for the superb logistic support orchestrated by Dr. Niels Henriksen.

I thank Dr. Philip Lane and Dr. John Collinson for supervision and encouragement in the field, at Keele University and during the protracted writing-up period. For help in the field, I thank Peter Frykman, Howard Armstrong, Alan Thomas and, in particular, Bob Christie who patiently guided me through my first Arctic season.

I acknowledge the use of drafting, photographic and library facilities at Keele University, GGU, University of Cambridge and British Antarctic Survey. I am grateful to Tom Harland, Peter Frykman, David Macdonald, Jane Francis, Alan Meneilly and Alistair Crame for discussion and constructive criticism of various thesis drafts.

Finally, I would like to thank Margaret Harrison, Mary Askham, Heather Thomson and Karen Whitley for typing this thesis.

## REFERENCES


1. AALTO, K.R. (1972) Flysch pebble conglomerate of the Cap-des-Rosiers Formation (Ordovician), Gaspé Peninsula, Quebec. *J. Sedim. Petrol.* 42, 922-926.

2. AHR, W.M. (1973) The carbonate ramp: an alternative to the shelf model. *Trans. Gulf Coast Assoc. Geol. Soc.*, 23, 221-225.

3. AITKEN, J.D. (1967) Classification and environmental significance of cryptalgal limestones and dolomites, with illustrations from the Cambrian and Ordovician of southwestern Alberta. *J. Sedim. Petrol.*, 37, 1163-1178.

4. AITKEN, J.D. (1978) Revised models for depositional grand cycles, Cambrian of the southern Rocky Mountains, Canada. *Bull. Can. Petrol. Geol.*, 26, 515-542.

5. ALLEN, J.R.L. (1970) The sequence of sedimentary structures in turbidites with special reference to dunes. *Scott. J. Geol.*, 6, 146-161.

6. ALLEN, J.R.L. (1982) *Sedimentary structures: their character and physical basis. Volume II*, pp. 663. Developments in Sedimentology 30B, Elsevier, Amsterdam.

7. ANDERTON, R. (1976) Tidal shelf sedimentation: an example from the Scottish Dalradian. *Sedimentology*, 23, 429-458.

8. ANDERTON, R., BRIDGES, P.W., LEEDER, M.R. & SELLWOOD, B.W. (1979) *A Dynamic Stratigraphy of the British Isles*, pp. 301, George Allen & Unwin, London.

9. ARMSTRONG, H.A. & LANE, P.D. (1981) The un-named Silurian(?) dolomite formation, Børglum Elv, central Peary Land. *Rapp. Grønlands geol. Unders.*, 55, 10-14.

10. BALDWIN, C.T. (1977) The stratigraphy and facies associations of trace fossils in some Cambrian and Ordovician rocks of north western Spain. In: *Trace Fossils 2* (Ed. by T.P. Crimes & J.C. Harper), pp. 9-40. *Geol. J. Spec. Issue*, 9.

11. BALL, M.M. (1967) Carbonate sand bodies of Florida and the Bahamas. *J. sedim. Petrol.*, 37, 556-591.

12. BANKS, N.L. (1970) Trace fossils from the late Precambrian and Lower Cambrian of Finnmark, Norway. In: *Trace fossils* (Ed. by T.P. Crimes & J.C. Harper) pp. 19-34. *Geol J. Spec. Issue*, 3.

13. BARNES, C.R. (1982) Lower Ordovician eustatic events in Canada. *Paleont. Contr. Univ. Oslo.*, 280, 6.

14. BATHURST, R.G.C. (1971) *Carbonate sediments and their diagenesis. Developments in Sedimentology*, 12, pp. 620. Elsevier, Amsterdam.

15. BATTEN, D.J., BROWN, P.E., DAWES, P.R., HIGGINS, A.K. ESKE KOCH, B., PARSONS, I. & SOPERS, N.J. (1981) Peralkaline volcanicity on the Eurasia Basin margin. *Nature*, 294, 150-152.

16. BATURIN, G.N. (1982) *Phosphorites on the sea floor: origin, composition and distribution*, pp. 343. Elsevier, Amsterdam.

17. BATURIN, G.N., KOCHENOV, A.V. & PETELIN, V.P. (1970) Phosphorite formation on the shelf of S.W. Africa. *Lith. and Min. Res.*, 3, 266-276.

18. BECHSTADT, T. & DOHLER-HIRNER, B. (1983) Lead-Zinc Deposits of Bleiberg-Kreuth. In: *Carbonate Depositional Environments*. (Ed. by P.A. Scholle, D.G. Bebout & C.H. Moore) *Mem. Am. Ass. Petrol. Geol.*, 33, 55-63.

19. BELL, C.M. (1981) Soft-sediment deformation of sandstone related to the Dwyka glaciation in South Africa. *Sedimentology*, 28, 321-329.

20. BENTOR, Y.K. (1980) Phosphorites - the unsolved problems. In: *Marine Phosphorites* (Ed. by Y.K. Bentor) pp. 3-18. *Spec. publ. Soc. econ. Paleont. Miner.*, 29, Tulsa.

21. BERG, R.R. (1975) Depositional environment of Upper Cretaceous Sussex Sandstone, House Creek Field, Wyoming. *Bull. Am. Ass. Petrol. Geol.* 59, 2099-2110.

22. BORNHOLD, B.D. & PILKEY, O.H. (1971) Bioclastic turbidite sedimentation in Columbus Basin, Bahamas. *Bull. geol. Soc. Am.*, 82, 1341-1354.

23. BOSE, P.K. (1979) Penecontemporaneous dolomitization in the Precambrian Bhander Limestone, Rajasthan, India- a petrographic attestation. *Geol. Rdsch.*, 68, 680-695.

24. BOSELLINI, A. (1984) Progradation geometries of carbonate platforms: examples from the Triassic of the Dolomites, northern Italy. *Sedimentology*, 31, 1-24.

25. BOUMA, A.H. (1962) *Sedimentology of some flysch deposits: A graphic approach to facies interpretation*, pp. 168. Elsevier, Amsterdam.

26. BOURGEOIS, J. (1980) A transgressive shelf sequence exhibiting hummocky stratification: The Cape Sebastian sandstone (Upper Cretaceous) southwestern Oregon. *J. sedim. Petrol.*, 50, 681-702.

27. BOWMAN, M.B.J. (1979) The depositional environments of a limestone unit from the San Emiliano Formation (Namurian/Westphalian), Cantabrian Mts., NW Spain. *Sedim. Geol.*, 24, 25-43.

28. BRADY, M.J. & KOEPNICK, R.B. (1979) A Middle Cambrian platform-to-basin transition, House Range, west central Utah. *Brigham Young Univ. Geol. Stud.*, 26, 1-7.

29. BRAUN, M. & FRIEDMAN, G.M. (1969) Carbonate lithofacies and environments of the Tribes Hill Formation (Lower Ordovician) of the Mohawk Valley, New York. *J. sedim. Petrol.*, 39, 113-135.

30. BRENCHLEY, P.J. & NEWALL, G. (1982) Storm-influenced inner-shelf sand lobes in the Caradoc (Ordovician) of Shropshire, England. *J. sedim. Petrol.*, 52, 1257-1269.

31. BRENCHLEY, P.J., NEWALL, G. & STANISTREET, I.G. (1979) A storm surge origin for sandstone beds in an epicontinental platform sequence, Ordovician, Norway. *Sedim. Geol.*, 22, 185-217.

32. BRENNER, R.L. & DAVIES, D.K. (1974) Oxfordian sedimentation in Western Interior United States. *Bull. Am. Ass. Petrol. Geol.*, 58, 407-428.

33. BROMLEY, R.G. (1965) *Studies in the lithology and conditions of sedimentation of the Chalk Rock and comparable horizons.* Ph.D. Thesis, University of London, pp. 355. (Unpublished).

34. BROMLEY, R.G. (1967) Marine phosphorites as depth indicators. *Mar. Geol.*, 5, 503-509.

35. BROWN, P.E. & PARSONS, I. (1981) The Kap Washington Group volcanics. *Rapp. Grønlands geol. Unders.*, 106, 65-68.

36. BURNETT, W.C., VEEH, H.H. & SOUTAT, A. (1980) U-series, oceanographic and sedimentary evidence in support of Recent formation of phosphate nodules off Peru. In: *Marine Phosphorites* (Ed. by Y.K. Bentor) pp. 61-71. *Spec. Publ. Soc. econ. Paleont. Miner.*, 29, Tulsa.

37. BYERS, C.W. (1977) Biofacies patterns in euxinic basins: a general model. In: *Deep-Water Carbonate Environments* (Ed. by H.E. Cook & P. Enos), pp. 5-17. *Spec. Publ. Soc. econ. Paleont Miner.*, 25, Tulsa.

38. CAMPELL, C.V. (1966) Truncated wave-ripple laminae. *J. sedim. Petrol.*, 36, 825-828.

39. CANT, D.J. (1980) Storm-dominated shallow marine sediments of the Arisaig Group (Silurian-Devonian) of Nova Scotia. *Can. J. Earth Sci.*, 17, 120-131.

40. CHRISTIE, R.L. & INESON, J.R. (1979) Precambrian-Silurian geology of the G.B. Schley Fjord region, eastern Peary Land, North Greenland. *Rapp. Grønlands geol. Unders.* 88, 63-71.

41. CHRISTIE, R.L. & PEEL, J.S. (1977) Cambrian-Silurian stratigraphy of Børglum Elv, eastern North Greenland. *Rapp. Grønlands geol. Unders.*, 82, 1-48.

42. CLEMMENSEN, L.B. (1979) Notes on the palaeogeographical setting of the Eocambrian tillite-bearing sequence of southern Peary Land, North Greenland. *Rapp. Grønlands geol. Unders.*, 88, 15-22.

43. CLIFTON, H.E. (1973) Pebble segregation and bed lenticularity in wave-worked versus alluvial gravel. *Sedimentology*, 20, 173-188.

44. COLEMAN, J.M. & PRIOR, D.B. (1978) Contemporary gravity tectonics-an everyday catastrophe? (abs.) *Bull. Am. Ass. Petrol. Geol.*, 62, 505.

45. COLLINSON, J.D. (1969) The sedimentology of the Grinslow Shales and the Kinderscout Grit: a deltaic complex in the Namurian of northern England. *J. sedim. Petrol.*, 39, 194-221.

46. COLLINSON, J.D. (1979) The Proterozoic sandstones between Heilprin Land and Mylius-Erichsen Land, eastern North Greenland. *Rapp. Grønlands geol. Unders.*, 88, 5-10.

47. COLLINSON, J.D. (1980) Stratigraphy of the Independence Fjord Group (Proterozoic) of eastern North Greenland. *Rapp. Grønlands geol. Unders.*, 99, 7-23.

48. COLLINSON, J.D. (1983) Sedimentology of unconformities within a fluvio-lacustrine sequence; Middle Proterozoic of eastern North Greenland. *Sedim. Geol.*, 34, 145-166.

49. COOK, H.E. (1979) Ancient continental slope sequences and their value in understanding modern slope development. In: *Geology of Continental Slopes.* (Ed. by L.J. Doyle & O.H. Pilkey), pp. 287-305. *Spec. Publ. Soc. econ. Paleont. Miner.*, 27, Tulsa.

50. COOK, H.E. & ENOS, P. (Eds.)(1977) *Deep-Water Carbonate Environments*, pp. 336. *Spec. Publ. Soc. econ. Petrol. Miner.*, 25, Tulsa.

51. COOK, H.E., MCDANIELS, P.M., MOUNTJOY, E.W., & PRAY, L.C. (1972) Allochthonous carbonate debris flows at Devonian bank ("reef") margins, ALberta, Canada. *Bull. Can. Petrol. Geol.*, 20, 439-497.

52. COOK, H.E. & MULLINS, H.T. (1983) Basin margin environment. In: *Carbonate Depositional Environments* (Ed. by P.A. Scholle, D.G. Bebout & C.H. Moore) pp. 539-617. *Mem. Am. Ass. Petrol. Geol.*, 33, Tulsa.

53. COOK, H.E. & TAYLOR, M.E. (1977) Comparison of continental slope and shelf environments in the Upper Cambrian and lowest Ordovician of Nevada. In: *Deep-Water Carbonate Environments.* (Ed. by H.E. Cook & P. Enos), pp. 51-81. *Spec. Publ. Soc. econ. Paleont. Miner.*, 25, Tulsa.

54. COWIE, J.W. (1961) The Lower Paleozoic geology of Greenland. In: *Geology of the Arctic* (Ed. by G. O. Rasch), pp. 160-169. Toronto University Press, Toronto.

55. COWIE, J.W. (1971) The Cambrian of the North American Arctic regions. In: *Cambrian of the New World* (Ed. by C.H. Holland), pp. 325-383. Interscience, London.

56. CREVELLO, P.D. & SCHLAGER, W. (1980) Carbonate debris sheets and turbidites, Exuma Sound, Bahamas. *J. sedim. Petrol.*, 50, 1121-1148.

57. CRIMES, T.P. (1970) The significance of trace fossils in sedimentology, stratigraphy and palaeoecology with examples from Lower Palaeozoic strata. In: *Trace fossils* (Ed. by T.P. Crimes & J.C. Harper), pp. 101-126. *Geol. J. Spec. Issue*, 3.

58. CRIMES, T.P., LEGG, I., MARCOS, A. & ARBOLEYA, M. (1977) ? Late Precambrian - low Lower Cambrian trace fossils from Spain. In; *Trace fossils 2* (Ed. by T.P. Crimes & J.C. Harper) pp. 91-138. *Geol. J. Spec. Issue*, 9.

59. DAVIES, D.K. (1968) Carbonate turbidites, Gulf of Mexico. *J. sedim. Petrol.*, 38, 1100-1109.

60. DAVIES, G.R. (1970) Algal-laminated sediments, Gladstone embayment, Shark Bay, Western Australia. *Mem. Am. Ass. Petrol. Geol.*, 13, 169-205.

61. DAVIES, G.R. (1977) Turbidites, debris sheets, and truncation structures in Upper Paleozoic deep-water carbonates of the Sverdrup Basin, Arctic Archipelago. In: *Deep-Water Carbonate Environments* (Ed. by H.E. Cook & P. Enos), pp. 221-247. *Spec. Publ. Soc. econ. Paleont. Miner.*, 25, Tulsa.

62. DAWES, P.R. (1971) The North Greenland fold belt and environs. *Bull. geol. Soc. Denmark*, 20, 197-239.

63. DAWES, P.R. (1976a) Precambrian to Tertiary of northern Greenland. In: *Geology of Greenland* (Ed. by A. Escher and W.S. Watt), pp. 248-303. Geological Survey of Greenland, Copenhagen.

64. DAWES, P.R. (1976b) Reconnaissance of Eocambrian and Lower Palaeozoic strata in south-western Peary Land, North Greenland. *Rapp. Grønlands geol. Unders.* 80, 9-14.

65. DAWES, P.R. & HALLER, J. (1979) Historical aspects in the geological investigation of northern Greenland. Part 1: New maps and photographs from the 2nd Thule Expedition 1916-1918 and the Bicentenary Jubilee Expedition 1920-1923. *Meddr Grønland,* 200(4), pp. 38.

66. DAWES, P.R. & PEEL, J.S. (1981) The northern margin of Greenland from Baffin Bay to the Greenland Sea. In: *The Ocean Basins and Margins,* vol.5 (Ed. by A.E.M. Nairn, M. Churkin Jr. & F.G. Stehli), pp. 201-264. Plenum, New York.

67. DAWES, P.R. & SOPER, N.J. (1973) Pre-Quaternary history of north Greenland. In: *Arctic Geology* (Ed. by M.G. Pitcher), *Mem. Am. Ass. Petrol. Geol.,* 19, 117-134.

68. DICKSON, J.A.D. (1965) A modified staining technique for carbonates in thin section. *Nature,* 205, 587.

69. DICKSON, J.A.D. & BARBER, C. (1976) Petrography, chemistry and origin of early diagenetic concretions in the Lower Carboniferous of the Isle of Man. *Sedimentology,* 23, 189-211.

70. DINGLE, R.V. (1977) The anatomy of a large submarine slide on a sheared continental margin (SE Africa). *J. geol. Soc. Lond.,* 134, 293-310.

71. DOTT Jr., R.H. (1964) Wacke, graywacke and matrix - what approach to immature sandstone classification? *J. sedim. Petrol.,* 34, 625-632.

72. DOTT Jr., R.H. & BOURGEOIS, J. (1982) Hummocky stratification: significance of its variable bedding sequences. *Bull. geol. Soc. Am.,* 93, 663-680.

73. DRIESE, S.G., BYERS, C.W. & DOTT, R.H. Jr. (1981) Tidal deposition in the basal Upper Cambrian Mt Simon Formation in Wisconsin. *J. sedim. Petrol.,* 51, 367-381.

74. DUNHAM, J.B. & OLSON, E.R. (1980) Shallow subsurface dolomitization of subtidally deposited carbonate sediments in the Hanson Creek Formation (Ordovician-Silurian) of central Nevada. In: *Concepts and Models of Dolomitization* (Ed. by D.H. Zenger, J.B. Dunham & R.L. Ethington) pp. 139-161. *Spec. Publ. Soc. econ. Paleont. Miner.,* 28, Tulsa.

75. DUNHAM, R.J. (1962) Classification of carbonate rocks according to depositional texture. In: *Classification of Carbonate Rocks* (Ed. by W.E. Ham), pp. 108-121. *Mem. Am. Ass. Petrol. Geol.,* 1. Tulsa.

76. DUNHAM, R.J. (1972) *Capitan Reef - New Mexico and Texas: Facts and questions to aid interpretation and group discussion*, pp. 267. *Spec. Publ. Soc. econ. Paleont. Miner. Permian Basin Sec.*, 72-14.

77. EKDALE, A.A. (1977) Abyssal trace fossils in worldwide Deep Sea Drilling Project cores. In: *Trace Fossils 2* (Ed. by T.P. Crimes & J.C. Harper), pp. 163-182. *Geol. J. Spec. Issue*, 9.

78. EMBLEY, R.W. (1976) New evidence for occurrence of debris flow deposits in the deep sea. *Geology*, 4, 371-374.

79. EMBRY, A.F. & KLOVAN, J.E. (1971) A Late Devonian reef tract on northeastern Banks Island, Northwest Territories. *Bull. Can. Petrol. Geol.*, 19, 730-781.

80. ENOS, P. (1969) Anatomy of a flysch. *J. sedim. Petrol.*, 39, 680-723.

81. ENOS, P. (1977) Flow regimes in debris flow. *Sedimentology*, 24, 133-142.

82. ESTEBAN, M. & KLAPPA, C.F. (1983) Subaerial Exposure Environment. In: *Carbonate Depositional Environments* (Ed. by P.A. Scholle, D.G. Bebout & C.H. Moore) *Mem. Am. Ass. Petrol. Geol.*, 33, 1-54.

83. EVANS, I & KENDALL, C.G. St.C. (1977) An interpretation of the depositional setting of some deep-water Jurassic carbonates of the central High Atlas Mountains, Morocco. In: *Deep-Water Carbonate Environments* (Ed. by H.E. Cook & P. Enos) pp. 249-261. *Spec. Publ. Soc. econ. Paleont. Miner.*, 25, Tulsa.

84. FAIRCHILD, I.J. (1980) Sedimentation and origin of a late Precambrian 'Dolomite' from Scotland. *J. sedim. Petrol.*, 50, 423-446.

85. FISHER, R.V. (1983) Flow transformations in sediment gravity flows. *Geology*, 11, 273-274.

86. FOLK, R.L. (1965) Some aspects of recrystallization in ancient limestones. In: *Dolomitization and limestone diagenesis: A symposium* (Ed. by L.C. Pray & R.C. Murray), pp 14-48. *Spec. Publ. Soc. econ. Paleont. Miner.*, 15, Tulsa.

87. FOLK, R.L. & PITTMAN, J.A. (1971) Length-slow chalcedony: a new testament for vanished evaporites. *J. sedim. Geol.*, 41, 1045-1058.

88. FRAKES, L.A. (1979) *Climates through Geologic Time.* pp. 310. Elsevier, Amsterdam.

89. FRIDERICHSEN, J.D. & BENGAARD, H.J. (1984) Lithostratigraphy and structures of Cambrian rocks in Nansen Land. Geological Survey of Greenland internal report. (Unpublished).

90. FRIDERICHSEN, J.D., HIGGINS, A.K., HURST, J.M., PEDERSON, S.A.S., SOPER, N.J. & SURLYK, F. (1982) Lithostratigraphic framework of the upper Proterozoic and Lower Palaeozoic deep-water clastic deposits of North Greenland. *Rapp. Grønlands geol. Unders.*, 107, pp. 19.

91. FRYKMAN, P. (1980) A sedimentological investigation of the carbonates at the base of the Brønlund Fjord Group (Early-Middle Cambrian), Peary Land, eastern North Greenland. *Rapp. Grønlands geol. Unders.*, 99, 51-55.

92. FRYKMAN , P. (1981) Om kondensation og hardgrounds i overgangen fra klastiske sedimenter til carbonater i det Nordgrønland ske Nedre Kambrium. University of Copenhagen, Speciale. (Unpublished).

93. FÜRSICH, F.T. (1973) *Thalassinoides* and the origin of nodular limestone in the Corallian Beds (Upper Jurassic) of southern England. *Neues. Jahrb. Geol. Palaeontol. Monatsh.* 136-156.

94. GALLOWAY, W.E. & BROWN, L.F. Jr. (1973) Depositional systems and shelf-slope relations on cratonic basin margin, Uppermost Pennsylvanian of north-central Texas. *Bull. Am. Ass. Petrol. Geol.*, 57, 1185-1218.

95. GARRISON, R.E. & FISCHER, A.G. (1969) Deep-water limestones and radiolarites of the Alpine Jurassic. In: *Depositional Environments in Carbonate Rocks* (Ed. by G.M. Friedman), pp. 20-56. *Spec. Publ. Soc. econ. Paleont. Miner.*, 14, Tulsa.

96. GARRISON, R.E. & KENNEDY, W.J. (1977) Origin of solution seams and flaser structure in Upper Cretaceous chalks of southern England. *Sedim. Geol.*, 19, 107-137.

97. GEE, D.G. & STURT, B.A. (Eds.)(In press) *The Caledonide Orogen-Scandinavia and related areas.* Wiley & Sons, New York.

98. GINSBURG, R.N. & JAMES, N.P. (1973) British Honduras by submarine. *Geotimes*, 18, 23-24.

99. GINSBURG, R.N. & JAMES, N.P. (1974) Holocene carbonate sediments of continental shelves. In: *The Geology of Continental Margins* (Ed. by C.A. Burk & C.L. Drake), pp. 137-155. Springer-Verlag, Berlin.

100. GINSBURG, R.N. & JAMES, N.P. (1976) Submarine botryoidal aragonite in Holocene reef limestones, Belize. *Geology*, 4, 431-436.

101. GOLDRING, R. & BRIDGES, P. (1973) Sublittoral sheet sandstones. *J. sedim. Petrol.*, 43, 736-747.

102. GOLDSTEIN, A.G. & COLLINS, E.W. (1984) Deformation of Permian strata overlying a zone of salt dissolution and collapse in the Texas Panhandle. *Geology*, 12, 314-317.

103. GOODWIN, P.W. & ANDERSON, E.J. (1974) Associated physical and biogenic structures in environmental subdivision of a Cambrian tidal sand body. *J. Geol.*, 82, 779-794.

104. GRESSLY, A. (1838) Observations géologiques sur le Jura Soleurois. *Neue Denkschr. allg. schweiz, Ges. ges. Naturw.*, 2, 1-112.

105. HÅKANSSON, E. (1979) Carboniferous to Tertiary development of the Wandel Sea Basin, eastern North Greenland. *Rapp. Grønlands geol. Unders.*, 88, 73-83.

105. HÅKANSSON, E., HEIBBERG, C & STEMMERIK, L. (1981) The Wandel Sea Basin from Holm Land to Lockwood Ø, eastern North Greenland. *Rapp. Grønlands geol. Unders.*, 106, 47-63.

106. HALLAM, A. & SWETT, K. (1966) Trace fossils from the Lower Cambrian Pipe Rock of the north-west Highlands. *Scott. J. Geol.*, 2, 101-106.

107. HALLEY, R.B., HARRIS, P.M. & HINE, A.C. (1983) Bank margin environment. In: *Carbonate Depositional Environments* (Ed. by P.A. Scholle, D.G. Debout & C.H. Moore) pp. 463-506. *Mem. Am. Ass. Petrol. Geol.*, 33, Tulsa.

108. HAMBLIN, D.P. & WALKER, R.G. (1979) Storm-dominated shallow-marine deposits: The Fernie-Kootenay (Jurassic) transition. *Can. J. Earth Sci.*, 26, 1673-1689.

109. HAMPTON, M.A. (1972) The role of subaqueous debris flow in generating turbidity currents. *J. sedim. Petrol.*, 42, 775-793.

110. HAMPTON, M.A. (1975) Competence of fine-grained debris flows. *J. sedim. Petrol.*, 45, 834-844.

111. HÄNTZCHEL, W. (1975) Trace fossils and problematica In: *Treatise on invertebrate paleontology, Part W, Miscellanea.* (Ed. by C. Teichert) pp. W1-W296. Geol. Soc. Am. (and University of Kansas Press), Boulder, Colorado.

112. HARMS, J.C. (1975) Stratification produced by migrating bedforms. In: *Depositional Environments as Interpreted from Primary Sedimentary Structures and Stratification Sequences*, pp. 45-61. *Soc. econ. Paleont. Miner.*, *Short Course* 2, Dallas.

113. HARMS, J.C., SOUTHARD, J., SPEARING, D.R. & WALKER, R.G. (1975) *Depositional Environments as Interpreted from Primary Sedimentary Structures and Stratification Sequences. Lecture Notes: Soc. econ. Paleont. Miner.*, *Short Course* 2, Dallas, pp. 161.

114. HARRIS, A.L., HOLLAND, C.H. & LEAKE, B.E. (Eds). (1979) *The Caledonides of the British Isles - Reviewed. Spec. Publ. geol. Soc. Lond.*, 8, pp. 768.

115. HAYES, M.O. (1967) Hurricanes as geological agents: case studies of Hurricanes Carla, 1961, and Cindy, 1963. *Rep. Invest. Bur. econ. Geol.*, Austin, Texas, 61, 54.

116. HEDBERG, H.D. (Ed.)(1979) *International Stratigraphic Guide: a guide to stratigraphic classification, terminology and procedure*, pp. 200. Wiley, New York.

117. HENDERSON, J.B. (1975) Archaean stromatolites in the Northern Slave Province, Northwest Territories, Canada. *Can. J. Earth Sci.*, 12, 1619-1630.

118. HENDRY, H.E. (1972) Breccias deposited by mass flow in the Breccia Nappe of the French pre-Alps. *Sedimentology*, 18, 277-292.

119. HENRIKSEN, N & PEEL, J.S. (1976) Cambrian - Early Ordovician stratigraphy in south -western Washington Land, western North Greenland. *Rapp. Grønlands geol. Unders.*, 80, 17-23.

120. HIGGINS, A.K., FRIDERICHSEN, J.D. & SOPER, N.J. (1981) The North Greenland fold belt between central Johannes V. Jensen Land and eastern Nansen Land. *Rapp. Grønlands geol. Unders.*, 106, 35-45.

121. HIGGINS, A.K., MAYR, U. & SOPER, N.J. (1982) Fold belts and metamorphic zones of northern Ellesmere Island and North Greenland. In: *Nares Strait and the drift of Greenland a conflict in plate tectonics* (Ed. by P.R. Dawes & J.W. Kerr), pp. 159-166. *Meddr. Grønland, Geoscience*, 8.

122. HILEMAN, M.E. & MAZZULLO, S.J. (Eds.)(1977) *Upper Guadalupian Facies Permian Reef Complex, Guadalupe Mountains, New Mexico and West Texas*, pp. 508. *Spec. Publ. Soc. econ. Paleont. Miner. Permian Basin Sec.*, 77-16.

123. HILL, D. (1972) Archaeocyatha. In: *Treatise on invertebrate paleontology, Part E (revised)*. (Ed. by C. Teichert), pp. 158. Geol. Soc. Am. (and University of Kansas Press), Boulder, Colorado.

124. HINE, A.C. (1977) Lily Bank, Bahamas: History of an active oolite sand shoal. *J. sedim. Petrol.*, 47, 1554-1581.

125. HINE, A.C. & MULLINS, H.T. (1983) Modern carbonate shelf-slope breaks. In: *The Shelfbreak - Critical Interface on Continental Margins* (Ed. by D.J. Stanley & G.T. Moore), pp. 169-188. *Spec. Publ. Soc. econ. Paleont. Miner.*, 33, Tulsa.

126. HINE, A.C. & NEUMANN, A.C. (1977) Shallow carbonate-bank-margin growth and structure, Little Bahama Bank, Bahamas. *Bull. Am. Ass. Petrol. Geol.*, 61, 376-406.

127. HINE, A.C., WILBER, R.J. & NEUMANN, A.C. (1981) Carbonate sand bodies along contrasting shallow bank margins facing open seaways in northern Bahamas. *Bull. Am. Ass. Petrol. Geol.*, 65, 261-290.

128. HISCOTT, R.N. & MIDDLETON, G.V. (1979) Depositional mechanics of thick-bedded sandstones at the base of a submarine slope, Tourelle Formation (Lower Ordovician), Quebec, Canada. In: *Geology of Continental Slopes* (Ed. by L.J. Doyle & O.H. Pilkey), pp. 307-326. *Spec. Publ. Soc. econ. Paleont. Miner.*, 27, Tulsa.

129. HOPKINS, J.C. (1977) Production of foreslope breccia by differential submarine cementation and downslope displacement of carbonate sands, Miette and Ancient Wall Buildups, Devonian, Canada. In: *Deep-Water Carbonate Environments* (Ed. by H.E. Cook & P. Enos), pp. 155-170. *Spec. Publ. Soc. econ. Paleont. Miner.*, 25, Tulsa.

130. HORODYSKI, R.J. (1975) Stromatolites of the Lower Missoula Group (Middle Proterozoic), Belt Supergroup, Glacier National Park, Montana. *Precamb. Res.*, 2, 215-264.

131. HUBERT, J.F. (1966) Modification of the model for internal structures in graded beds to include a dune division. *Nature*, 211, 614.

132. HUBERT, J.F., SUCHECKI, R.K. & CALLAHAN, R.K.M. (1977) The Cow Head Breccia: sedimentology of the Cambro - Ordovician continental margin, Newfoundland. In: *Deep-Water Carbonate Environments* (Ed. by H.E. Cook & P. Enos), pp. 125-154 *Spec. Publ. Soc. econ. Paleont. Miner.*, 25, Tulsa.

133. HUNTER, R.E. & CLIFTON, H.E. (1982) Cyclic deposits and hummocky cross-stratification of probable storm origin in Upper Cretaceous rocks of the Cape Sebastian area, southwestern Oregon. *J. sedim. Petrol.*, 52, 127-143.

134. HURST, J.M. (1980) Silurian stratigraphy and facies distribution in Washington Land and western Hall Land, North Greenland. *Bull. Grønlands geol. Unders.*, 138, pp. 95.

135. HURST, J.M. (1981) Platform edge and slope relationships: Silurian of Washington Land, North Greenland and comparison to Arctic Canada. *Bull. Canad. Petrol. Geol.*, 29, 408-419.

136. HURST, J.M. (1984) Upper Ordovician and Silurian carbonate shelf stratigraphy, facies and evolution, eastern North Greenland. *Bull. Grønlands geol. Unders.*, 148, pp. 73.

137. HURST, J.M. & MCKERROW, W.S. (1981) The Caledonian nappes of eastern North Greenland. *Nature*, 290, 772-774.

138. HURST, J.M., MCKERROW, W.S., SOPER, N.J. & SURLYK, F. (1983) The relationship between Caledonian nappe tectonics and Silurian turbidite deposition in North Greenland. *J. Geol. Soc. Lond.*, 140, 123-132.

139. HURST, J.M. & PEEL, J.S. (1979) Late Proterozoic (?) to Silurian stratigraphy of southern Wulff Land, North Greenland. *Rapp. Grønlands geol. Unders.*, 91, 37-56.

140. HURST, J.M. & SURLYK, F.S. (1980) Notes on the Lower Palaeozoic clastic sediments of North Greenland. *Rapp. Grønlands geol. Unders.*, 99, 73-78.

141. HURST, J.M. & SURLYK, F. (1982) Stratigraphy of the Silurian turbidite sequence of North Greenland. *Bull. Grønlands geol. Unders.*, 145, pp. 121.

142. HURST, J.M. & SURLYK, F. (1983) Initiation, evolution and destruction of an Early Palaeozoic carbonate shelf, eastern North Greenland. *J. Geol.*, 91, 671-691.

143. ILLING, L.V., WELLS, A.J. & TAYLOR, J.C. (1965) Penecontemporary dolomite in the Persian Gulf. In: *Dolomitization and Limestone Diagenesis - a Symposium* (Ed. by L.C. Pray & R.C. Murray), pp. 89-111. *Spec. Publ. Soc. econ. Paleont. Miner.*, 13, Tulsa.

144. INESON, J.R. (1980) Carbonate debris flows in the Cambrian of south-west Peary Land, eastern North Greenland. *Rapp. Grønlands geol. Unders.*, 99, 33-42.

145. INESON, J.R. & PEEL, J.S. (1980) Cambrian stratigraphy in Peary Land, eastern North Greenland. *Rapp. Grønlands geol. Unders.*, 99, 33-42.

146. JAMES, N.P., (1979) Facies models 10. Shallowing-upward sequences in carbonates. In: *Facies Models* (Ed. by R.G. Walker), pp. 109-120. *Geosci. Can. Reprint Ser.*, 1.

147. JAMES, N.P. (1983) Reef Environment. In: *Carbonate Depositional Environments* (Ed. by P.A. Scholle, D.G. Bebout & C.H. Moore) pp. 345-440. *Mem. Am. Ass. Petrol. Geol.*, 33, Tulsa.

148. JAMES, N.P. & GINSBURG, R.N. (1979) *The seaward margin of Belize Barrier and Atoll Reefs.* pp. 191. *Spec. Publ. int. Ass. Sediment.*, 3.

149. JAMES, N.P. & KLAPPA, C.F. (1983) Petrogenesis of Early Cambrian reef limestones, Labrador, Canada. *J. sedim. Petrol.*, 53, 1051-1096.

150. JAMES, N.P. & KOBLUCK, D.R. (1978) Lower Cambrian patch reefs and associated sediments: southern Labrador, Canada. *Sedimentology*, 25, 1-35.

151. JAMES, N.P. & MOUNTJOY, E.W. (1983) The shelf-slope break in fossil carbonate platforms: an overview. In: *The Shelf-break: Critical Interface on Continental Margins.* (Ed. by D.J. Stanley & G.T. Moore), pp. 189-206. *Spec. Publ. Soc. econ. Paleont. Miner.*, 33, Tulsa.

152. JARVIS, I. (1980) The initiation of phosphatic chalk sedimentation - the Senonian (Cretaceous) of the Anglo-Paris basin. In: *Marine phosphorites* (Ed. by Y.K. Bentor) pp. 167-192. *Spec. Publ. Soc. econ. Paleont. Miner.*, 29, Tulsa.

153. JENKYNS, H.C. (1974) Origin of red nodular limestones (Ammonitico Rosso, Knollenkalke) in the Mediterraneon Jurassic: a diagenetic model. In: *Pelagic Sediments: on Land and under the sea.* (Ed. by K.J. Hsü & H.C. Jenkyns), pp. 249-271. *Spec. Publ. int. Ass. Sediment.*, 1.

154. JEPSEN, H.F. (1966) Intrusive rocks of the Midsommersø area, southern Peary Land, and their stratigraphical position. *Rapp. Grønlands geol. Unders.*, 11, 8-10.

155. JEPSEN, H.F. (1969) Preliminary report on the stratigraphy of the Precambrian and Eocambrian sediments in the Jørgen Brønlund Fjord - Midsommersø area, southern Peary Land. *Rapp. Grønlands geol. Unders.* 19, 11-14.

156. JEPSEN, H.F. (1971) The Precambrian, Eocambrian and early Palaeozoic stratigraphy of the Jørgen Brønlund Fjord area, Peary Land, North Greenland. *Bull. Grønlands geol. Unders.*, 96, 1-42.

157. JEPSEN, H.F. (1984) Investigations in Late Proterozoic to Silurian sediments in Wulff Land. Geological Survey of Greenland internal report. (Unpublished).

158. JEPSEN, H.F. & KALSBEEK, F. (1981) Non-existence of the Carolinidian orogeny in the Prinsesse Caroline - Mathilde Alper of Kronprins Christian Land, eastern North Greenland. *Rapp. Grønlands geol. Unders.*, 106, 7-14.

159. JEPSEN, H.F., KALSBEEK, F. & SUTHREN, R.J. (1980) The Zig-Zag Dal Basalt Formation, North Greenland. *Rapp. Grønlands geol. Unders.*, 99, 25-32.

160. JEPSEN, H.F., & SUTHREN, R.J. (1979) The Zig-Zag Dal Basalt, North Greenland. Geological Survey of Greenland internal report. (Unpublished).

161. JOHNSON, A.M. (1970) *Physical Processes in Geology*, pp. 577. Freeman, Cooper & Co., San Francisco.

162. JOHNSON, H.D. (1978) Shallow Siliciclastic Seas. In: *Sedimentary Environments and Facies* (Ed. by H.G. Reading), pp. 207-258. Blackwell Scientific, Oxford.

163. JONES, B. & DIXON, O.A. (1976) Storm deposits in the Read Bay Formation (Upper Silurian), Somerset Island, Arctic Canada (an application of Markov chain analysis). *J. sedim. Petrol.*, 46, 393-401.

164. JONES, B., OLDERSHAW, A.E. & NARBONNE, G.M. (1979) Nature and origin of rubbly limestones in the Upper Silurian Read Bay Formation of Arctic Canada. *Sedim. Geol.*, 24, 227-252.

165. JOPLING, A.V. & WALKER, R.G. (1968) Morphology and origin of ripple-drift cross-lamination, with examples from the Pleistocene of Massachusetts. *J. sedim. Petrol.*, 38, 971-984.

166. KAZAKOV, A.V. (1937) The phosphorite facies and the genesis of phosphorites. In: *Geol. Investigations of Agricultural Ores. Trans. Sci. Inst. Fertilizers and Insecto-Fungicides*, 142, 95-113.

167. KEITH, B.D. & FRIEDMAN, G.M. (1977) A slope-fan-basin-plain model, Taconic sequence, New York and Vermont. *J. sedim. Petrol.*, 38, 1040-1058.

168. KELLER, G.H., LAMBERT, D.N. & BENNETT, R.H. (1979) Geotechnical properties of continental slope deposits - Cape Hatteras to Hydrographer Canyon. In: *Geology of Continental Slopes* (Ed. by L.J. Doyle & O.H. Pilkey), pp. 131-151. *Spec. Publ. Soc. econ. Paleont. Miner.*, 27, Tulsa.

169. KELTS, K. & ARTHUR, M.A. (1981) Turbidites after ten years of deep-sea drilling-wringing out the mop? In: *The Deep-Sea Drilling Project: a decade of progress.* (Ed. by J.E. Warme, R.G. Douglas & E.L. Winterer), pp. 91-127. *Spec. Publ. Soc. econ. Paleont. Miner.*, 32, Tulsa.

170. KENDALL, C.G. St. G. & SCHLAGER, W. (1981) Carbonates and relative changes in sea level. *Mar. Geol.*, 44, 181-212.

171. KENDALL, C.G. St. C. & SKIPWITH, P.A. d'E. (1968) Recent algal mats of a Persian Gulf lagoon. *J. sedim. Petrol.*, 38, 1040-1058.

172. KENDALL, C.G. St. C. & SKIPWITH, P.A. d'E. (1969) Holocene shallow-water carbonate and evaporite sediments of Khor al Bazam. Abu Dhabi, Southwest Persian Gulf. *Bull. Am. Ass. Petrol. Geol.*, 53, 841-849.

173. KENNEDY, W.J. & GARRISON, R.E. (1975a) Morphology and genesis of nodular phosphates in the Cenomanian Glauconitic Marl of south-east England. *Lethaia*, 8, 339-360.

174. KENNEDY, W.J. & GARRISON, R.E. (1975b) Morphology and genesis of nodular chalks and hardgrounds in the Upper Cretaceous of southern England. *Sedimentology*, 22, 311-386.

175. KOCH, L. (1923a) Resultaterne af Jubilaeumsezpeditionen Nord om Grønland i 1921. *Naturens Verden* 1923, 49-74.

176. KOCH, L. (1923b) Preliminary report upon the geology of Peary Land, Arctic Greenland. *Am. J. Sci.* 5, 189-199.

177. KOCH, L. (1929) Stratigraphy of Greenland. *Meddr Grønland* 73, 205-320.

178. KOCH. L. (1935) Geologie von Grönland. In: *Geologie der Erde* (Ed. by E. Krenkel), pp. 159. Gebrüder Borntrager, Berlin.

179. KRAUSE, F.F. & OLDERSHAW, A.E. (1979) Submarine carbonate breccia beds - a depositional model for two-layer, sediment gravity flows from the Sekwi Formation (Lower Cambrian), Mackenzie Mountains, Northwest Territories, Canada. *Can. J. Earth Sci.*, 16, 189-199.

180. KSIAŻKIEWICZ, M. (1970) Observations on the ichnofauna of the Polish Carpathians. In: *Trace fossils* (Ed. by T.P. Crimes & J.C. Harper) pp. 283-322. *Geol. J. Spec. Issue*, 3.

181. KUENEN, PH.H. & MENARD, H.W. (1952) Turbidity currents, graded and non-graded deposits. *J. sedim. Petrol.*, 22, 83-96.

182. KYLE, J.R. (1983) Economic aspects of Subaerial Carbonates. In: *Carbonate Depositional Environments* (Ed. by P.A. Scholle, D.G. Bebout & C.H. Moore) *Mem. Am. Ass. Petrol. Geol.*, 33, 73-92.

183. LAIRD, M.G. (1968) Rotational slumps and slump scars in Silurian rocks, western Ireland. *Sedimentology*, 10, 111-120.

184. LARSON, O. & DAWES, P.R. (1974) K/Ar and Rb/Sr age determinations on Precambrian crystalline rocks in the Inglefield Land - Inglefield Bredning region, Thule district, western North Greenland. *Rapp. Grønlands geol. Unders.*, 66, 4-8.

185. LEVELL, B.K. (1980) Evidence for currents associated with waves in Late Precambrian shelf deposits from Finnmark, North Norway. *Sedimentology*, 27, 153-166.

186. LEWIS, K.B. (1971) Slumping on a continental slope inclined at $1^{o}$-$4^{o}$. *Sedimentology*, 16, 97-110.

187. LINDHOLM, R.C. (1980) Intraclast orientation in Cambro-Ordovician limestones in western Maryland. *J. sedim. Petrol.*, 50, 1205-1212.

188. LINDHOLM, R.C. (1982) Flat stratification: two ancient examples. *J. sedim. Petrol.*, 52, 227-231.

189. LINDSAY, J.F. (1966) Carboniferous subaqueous mass-movements in the Manning - Macleay Basin, Kempsey, New South Wales. *J. sedim. Petrol.*, 36, 719-732.

190. LOGAN, B.W., HOFFMAN, P. & GEBELEIN, C.F. (1974) Algal mats, cryptalgal fabrics and structures, Hamelin Pool, Western Australia. *Mem. Am. Ass. Petrol. Geol.*, 22, 140-194.

191. LOGAN, B.W., REZAK, R. & GINSBURG, R.N. (1964) Classification and environmental significance of algal stromatolites. *J. Geol.*, 72, 68-83.

192. LOHMAN, K.C. (1976) Lower Dresbachian (Upper Cambrian) platform to deep-shelf transition in Eastern Nevada and Western Utah: an evaluation through lithologic cycle correlation: *Salt Lake City, Brigham Young Univ. Studies.*, 23, 111-132.

193. LOWE, D.R. (1976a) Grain flow and grain flow deposits. *J. sedim. Petrol.*, 46, 188-199.

194. LOWE, D.R. (1976b) Subaqueous liquefied and fluidized sediment flows and their deposits. *Sedimentology*, 23, 285-308.

195. LOWE, D.R. (1979) Sediment gravity flows: their classification and some problems of application to natural flows and deposits. In: *Geology of Continental Slopes* (Ed. by L.J. Doyle & O.H. Pilkey) pp. 75-82. *Spec. Publ. Soc. econ. Paleont. Miner.*, 27, Tulsa.

196. LOWE, D.R. (1982) Sediment gravity flows: II. Depositional models with special reference to the deposits of high-density turbidity currents. *J. sedim. Petrol.*, 52, 279-297.

197. MABILLARD, J.E. (1980) Silurian carbonate mounds of south-east Peary Land, eastern North Greenland. *Rapp. Grønlands geol. Unders.*, 88, 51-54.

198. MARKELLO, J.R. & READ, J.F. (1981) Carbonate ramp-to-deeper shale shelf transitions of an Upper Cambrian intrashelf basin, Nolichucky Formation, Southwest Virginia Appalachians. *Sedimentology*, 28, 573-597.

199. MARKELLO, J.R. & READ, J.F. (1982) Upper Cambrian intrashelf basin, Nolichucky Formation, Southwest Virginia Appalachians. *Bull. Am. Ass. Petrol. Geol.*, 66, 860-878.

200. MARTINEZ DEL OLMO, W. & ESTEBAN, M. (1983) Paleokarst Development. In: *Carbonate Depositional Environments* (Ed. by P.A. Scholle, D.G. Bebout & C.H. Moore) *Mem. Am. Ass. Petrol. Geol.*, 33, 93-95.

201. McCABE, P.J. (1978) The Kinderscoutian delta (Carboniferous) of northern England: a slope influenced by density currents. In: *Sedimentation in Submarine Canyons, Fans and Trenches* (Ed. by D.J. Stanley & G. Kelling), pp. 116-126. Dowden, Hutchinson & Ross, Stroudsburg.

202. McCAVE, I.N. (1973) The sedimentology of a transgression: Portland Point and Cooksburg Members (Middle Devonian), New York State. *J. sedim. Petrol.*, 43, 484-504.

203. McILREATH, I.A. (1977) Accumulation of a Middle Cambrian, deep-water limestone debris apron adjacent to a vertical submarine escarpment, southern Rocky Mountains, Canada. In: *Deep-water Carbonate Environments* (Ed. by H.E. Cook & P. Enos), pp. 113-124. *Spec. Publ. Soc. econ. Paleont. Miner.*, 25, Tulsa.

204. McILREATH, I.A. & JAMES, N.P. (1978) Facies models - 13. Carbonate slopes. *Geosci. Can.*, 5, 189-199.

205. McRAE, S.G. (1972) Glauconite. *Earth Sci. Rev.*, 8, 397-440.

206. MEYERS, W.J. (1977) Chertification in the Mississipian Lake Valley Formation, Sacramento Mountains, New Mexico. *Sedimentology*, 24, 75-105.

207. MIALL, A.D. (1984) *Principles of Sedimentary Basin Analysis*, pp. 490. Springer-Verlag, New York.

208. MIDDLETON, G.V. & HAMPTON, M.A. (1973) Sediment gravity flows: mechanics of flow and deposition. In: Turbidites and Deep-water Sedimentation (Ed. by L.J. Doyle & O.H. Pilkey), pp. 1-38. *Soc. econ. Paleont. Miner., Pacific Sect., Short Course Lecture Notes.*, Anaheim.

209. MIDDLETON, G.V. & HAMPTON, M.A. (1976) Subaqueous sediment transport and deposition by sediment gravity flows. In: *Marine Sediment Transport and Environmental Management* (Ed. by D.J. Stanley & D.J.P. Swift), pp. 197-218. John Wiley, New York.

210. MIDDLETON, G.V. & SOUTHARD, J.B. (1977) *Mechanics of sediment movement.* Soc. econ. Paleont. Miner. Short Course 3, Lecture Notes, pp. 250.

211. MOORE, C.H.Jr., GRAHAM, E.A. & LAND, L.S. (1976) Sediment transport and dispersal across the deep fore-reef and island slope (-55m to 305m), Discovery Bay, Jamaica. *J. sedim. Petrol.*, 46, 174-187.

212. MOORE, D.G. (1961) Submarine slumps. *J. sedim. Petrol.*, 31, 343-357.

213. MOUNTJOY, E.W., COOK, H.E., PRAY, L.C. & McDANIEL, P.N. (1972) Allochthonous carbonate debris flows - worldwide indicators of reef complexes, banks or shelf margins. *24th Int. geol. Congr.*, Montreal, Sect. 6, 172-189.

214. MULLINS, H.T. & NEUMANN, A.C. (1979) Deep carbonate bank margin structure and sedimentation in the northern Bahamas. In: *Geology of Continental Slopes* (Ed. by L.J. Doyle & O.H. Pilkey), pp. 165-192. *Spec. Publ. Soc. econ. Paleont. Miner.*, 27, Tulsa.

215. MULLINS, H.T., NEUMANN, A.C., WILBER, R.J. & BOARDMAN, M.R. (1980) Nodular carbonate sediment on Bahamian slopes: possible precursors to nodular limestones. *J. sedim. Petrol.*, 50, 117-131.

216. MÜLLER, J. & FABRICUS, F. (1974) Magnesian-calcite nodules in the Ionian deep sea: an actualistic model for the formation of some nodular limestones. In: *Pelagic Sediments: on Land and under the Sea* (Ed. by K.J. Hsü & H.C. Jenkyns), pp. 249-271. *Spec. Publ. int. Ass. Sediment.*, 1.

217. MUTTI, E. & RICCI LUCCHI, F. (1972) Le torbiditi dell'Appennino settentrionale: introduzione all'analisi di facies. *Mem. Soc. geol. Ital.*, 11, 161-199.

218. NARDIN, T.R., HEIN, F.J., GORSLINE, D.S. & EDWARDS, B.D. (1979) A review of mass movement processes, sediment and acoustic characteristics and contrasts in slope and base-of-slope systems versus canyon-fan-basin floor systems. In: *Geology of Continental Slopes* (Ed. by L.J. Doyle & O.H. Pilkey), pp. 61-73. *Spec. Publ. Soc. econ. Paleont. Miner.*, 27, Tulsa.

219. NAYLOR, M.A. (1980) The origin of inverse grading in muddy debris flow deposits - a review. *J. sedim. Petrol.*, 50, 1111-1116.

220. NELSON, C.H. (1982) Modern shallow-water graded sand layers from storm surges, Bering Shelf: a mimic of Bouma sequences and turbidite systems. *J. sedim. Petrol.*, 52, 537-545.

221. NEUMANN, A.C. & LAND, L.S. (1975) Lime mud deposition and calcareous algae in the Bight of Abaco, Bahamas. *J. sedim. Petrol.*, 45, 763-768.

222. NEWELL, N.D., PURDY, E.G. & IMBRIE, J. (1960) Bahamian oolitic sand. *J. Geol.*, 68, 481-497.

223. NIO, S.D. (1976) Marine transgressions as a factor in the formation of sand wave complexes. *Geol. Mijnb.*, 55, 18-40.

224. NOBLE, J.P.A. & HOWELLS, K.D.M. (1974) Early marine lithification of the nodular limestones in the Silurian of New Brunswick. *Sedimentology*, 21, 597-609.

225. O'CONNOR, B. (1979) The Portfjeld Formation (?Early Cambrian) of eastern North Greenland. *Rapp. Grønlands geol. Unders.*, 88, 23-28.

226. ODIN, G.S. & LETOLLE, R. (1980) Glauconitization and Phosphatization environments: a tentative comparison. In: *Marine Phosphorites* (Ed. by Y.K. Bentor), pp. 227-237. *Spec. Publ. Soc. econ. Paleont. Miner.*, 29, Tulsa.

227. OLDERSHAW, A.E. & SCOFFIN, T.P. (1967) The source of ferroan and non-ferroan calcite cements in the Halkin and Wenlock Limestones. *Geol. J.*, 5, 309-320.

228. PADGETT, G., EHRLICH, R. & MOODY, M. (1977) Submarine debris flow deposits in an extensional setting - Upper Devonian of western Morocco. *J. sedim. Petrol.*, 47, 811-818.

229. PALMER, A.R. (1979) Report on examination of Cambrian faunas from Peary Land. Geological Survey of Greenland internal report. (Unpublished).

230. PALMER, A.R. & JAMES, N.P. (1980) The Hawke Bay Event: a circum-Iapetus regression near the lower Middle Cambrian boundary. In: *The Caledonides in the U.S.A.* (Ed. by D.R. Wones), pp. 15-18. Mem. Virginia Polytechnic Instit. & State Univ., Blacksburg.

231. PALMER, A.R. & PEEL, J.S. (1979) New Cambrian faunas from Peary Land, eastern North Greenland. *Rapp. Grønlands geol. Unders.*, 91, 29-36.

232. PEDERSON, K.R. (1970) Late Precambrian microfossils from Peary Land. *Rapp. Grønlands geol. Unders.*, 28, 16-17.

233. PEEL, J.S. (1979) Cambrian - Middle Ordovician stratigraphy of the Adams Gletscher region, south-west Peary Land, North Greenland. *Rapp. Grønlands geol. Unders.*, 88, 23-39.

234. PEEL, J.S. (1980a) Cambrian and Ordovician geology of Warming land and southern Wulff Land, central North Greenland. *Rapp. Grønlands geol. Unders.*, 101, 55-60.

235. PEEL, J.S. (1980b) Early Cambrian microfossils from the Portfjeld Formation, Peary Land, eastern North Greenland. *Rapp. Grønlands geol. Unders.*, 100, 15-17.

236. PEEL, J.S. (1980c) Geological reconnaisance in the Caledonian foreland of eastern North Greenland, with comments on the Centrum Limestone. *Rapp. Grønlands geol. Unders.*, 99, 61-72.

237. PEEL, J.S. (1982a) The age of the Tavsens Iskappe Group, central North Greenland. *Rapp. Grønlands geol. Unders.*, 108, 30.

225. O'CONNOR, B. (1979) The Portfjeld Formation (?Early Cambrian) of eastern North Greenland. *Rapp. Grønlands geol. Unders.*, 88, 23-28.

226. ODIN, G.S. & LETOLLE, R. (1980) Glauconitization and Phosphatization environments: a tentative comparison. In: *Marine Phosphorites* (Ed. by Y.K. Bentor), pp. 227-237. *Spec. Publ. Soc. econ. Paleont. Miner.*, 29, Tulsa.

227. OLDERSHAW, A.E. & SCOFFIN, T.P. (1967) The source of ferroan and non-ferroan calcite cements in the Halkin and Wenlock Limestones. *Geol. J.*, 5, 309-320.

228. PADGETT, G., EHRLICH, R. & MOODY, M. (1977) Submarine debris flow deposits in an extensional setting - Upper Devonian of western Morocco. *J. sedim. Petrol.*, 47, 811-818.

229. PALMER, A.R. (1979) Report on examination of Cambrian faunas from Peary Land. Geological Survey of Greenland internal report. (Unpublished).

230. PALMER, A.R. & JAMES, N.P. (1980) The Hawke Bay Event: a circum-Iapetus regression near the lower Middle Cambrian boundary. In: *The Caledonides in the U.S.A.* (Ed. by D.R. Wones), pp. 15-18. Mem. Virginia Polytechnic Instit. & State Univ., Blacksburg.

231. PALMER, A.R. & PEEL, J.S. (1979) New Cambrian faunas from Peary Land, eastern North Greenland. *Rapp. Grønlands geol. Unders.*, 91, 29-36.

232. PEDERSON, K.R. (1970) Late Precambrian microfossils from Peary Land. *Rapp. Grønlands geol. Unders.*, 28, 16-17.

233. PEEL, J.S. (1979) Cambrian - Middle Ordovician stratigraphy of the Adams Gletscher region, south-west Peary Land, North Greenland. *Rapp. Grønlands geol. Unders.*, 88, 23-39.

234. PEEL, J.S. (1980a) Cambrian and Ordovician geology of Warming land and southern Wulff Land, central North Greenland. *Rapp. Grønlands geol. Unders.*, 101, 55-60.

235. PEEL, J.S. (1980b) Early Cambrian microfossils from the Portfjeld Formation, Peary Land, eastern North Greenland. *Rapp. Grønlands geol. Unders.*, 100, 15-17.

236. PEEL, J.S. (1980c) Geological reconnaisance in the Caledonian foreland of eastern North Greenland, with comments on the Centrum Limestone. *Rapp. Grønlands geol. Unders.*, 99, 61-72.

237. PEEL, J.S. (1982a) The age of the Tavsens Iskappe Group, central North Greenland. *Rapp. Grønlands geol. Unders.*, 108, 30.

238. PEEL, J.S. (1982b) The Lower Palaeozoic of Greenland. In: *Arctic Geology and Geophysics*, (Ed. by A.F. Embry & H.R. Balkwill) *Mem. Can. Soc. Petrol. Geol.*, 8, pp. 309-330.

239. PEEL, J.S. (In press) Cambrian - Silurian platform stratigraphy of eastern North Greenland. In: *The Caledonide Orogen - Scandinavia and related areas* (Ed. by D.G. Gee & B.A. Sturt). Wiley & Sons, New York.

240. PEEL, J.S. & CHRISTIE, R.L. (1975) Lower Palaeozoic stratigraphy of southern Peary Land, eastern North Greenland. *Rapp. Grønlands geol. Unders.*, 75, 21-25.

241. PEEL, J.S.& CHRISTIE, R.L. (1982) Cambrian - Ordovician stratigraphy, correlations around Kane Basin. In: *Nares Strait and the drift of Greenland: a conflict in plate tectonics* (Ed. by P.R. Dawes & J.W. Kerr), pp. 117-135. *Meddr Grønland, Geoscience*, 8.

242. PEEL, J.S., INESON, J.R., LANE, P.D. & ARMSTRONG, H.A. (1981) Lower Palaeozoic stratigraphy around Danmark Fjord, eastern North Greenland. *Rapp. Grønlands geol. Unders.*, 106, 21-27.

243. PEEL, J.S. & WRIGHT, S.C. (1984) Cambrian: Freuchen Land - Warming Land. Geological Survey of Greenland internal report. (Unpublished).

244. PEEL, J.S. & YOCHELSON, E.L. (1979) *Ceratopea* (Gastropoda) from Washington Land, western North Greenland. *Rapp. Grønlands geol. Unders.*, 91, 87-91.

245. PETTIJOHN, F.J. (1954) Classification of sandstones. *J. Geol.*, 62, 360-365.

246. PFEIL, R.W. & READ, J.F. (1980) Cambrian carbonate platform margin facies, Shady Dolomite, southwestern Virginia, U.S.A. *J. sedim. Petrol.*, 50, 91-116.

247. PHILLIPS, F.C. (1971) *The use of Stereographic Projection in Structural Geology (3rd Ed.)*, pp. 90. Edward Arnold, London.

248. PICKERILL, R.K. (1980) Phanerozoic flysch trace fossil diversity - observations based on an Ordovician flysch ichnofauna from the Aroostook - Matapedia Carbonate Belt of northern New Brunswick. *Can. J. Earth Sci.*, 17, 1259-1270.

249. PIERSON, T.C. (1980) Erosion and deposition by debris flows at Mt. Thomas, North Canterbury, New Zealand. *Earth Surf. Proc.*, 5, 227-247.

250. PIERSON, T.C. (1981) Dominant particle support mechanisms in debris flows at Mt. Thomas, New Zealand and implications for flow mobility. *Sedimentology*, 28, 49-60.

251. PLAYFORD, P.E. & COCKBAIN, A.E. (1976) Modern algal stromatolites at Hamelin Pool, a hypersaline barred basin in Shark Bay, Western Australia. In: *Stromatolites* (Ed. by M.R. Walter), pp. 389-412. Elsevier, Amsterdam.

252. POULSEN, V. (1974) Olenellacean trilobites from eastern North Greenland. *Bull. geol. Soc. Denmark*, 23, 79-101.

253. PRATT, B.R. (1982) Limestone response to stress: pressure solution and dolomitization - discussion and examples of compaction in carbonate sediments. *J. sedim. Petrol.*, 52, 323-328.

254. RAISWELL, R. (1971) The growth of Cambrian and Liassic concretions. *Sedimentology*, 17, 147-171.

255. RAISWELL, R. & WHITE, N.J.M. (1978) Spatial aspects of concretionary growth in the Upper Lias of northeast England. *Sedim. Geol.*, 20, 291-300.

256. READ, J.F. (1980) Carbonate ramp-to-basin transitions and foreland basin evolution, Middle Ordovician, Virginia Appalachians. *Bull. Am. Ass. Petrol. Geol.*, 80, 1575-1612.

257. READ, J.F. (1982) Carbonate platforms of passive (extensional) continental margins: Types, characteristics and evolution. *Tectonophys.*, 81, 195-212.

258. READING, H.G. (1978) Facies. In: *Sedimentary Environments and Facies* (Ed. by H.G. Reading). pp. 4-14. Blackwell Scientific, Oxford.

259. REES, M.N., BRADY, M.J. & ROWELL, A.J. (1976) Depositional environments of the Upper Cambrian Johns Wash Limestone (House Range, Utah). *J. sedim. Petrol.*, 46, 38-47.

260. REINECK, H.E. (1972) Tidal flats. In: *Recognition of Ancient Sedimentary Environments* (Ed. by J.K. Rigby & W.K. Hamblin), pp. 146-159. *Spec. Publ. Soc. econ. Paleont. Miner.*, 16, Tulsa.

261. REINHARDT, J. (1977) Cambrian off-shelf sedimentation, Central Appalachians. In: *Deep-water Carbonate Environments* (Ed. by H.E. Cook & P. Enos), pp. 83-112. *Spec. Publ. Soc. econ. Paleont. Miner.*, 25, Tulsa.

262. RHOADS, D.C. (1967) Biogenic reworking of intertidal and subtidal sediments in Barnstaple Harbor and Buzzards Bay, Massachusetts. *J. Geol.*, 75, 461-476.

263. RHOADS, D.C. (1975) The paleoecological and environmental significance of trace fossils. In: *The study of trace fossils*. (Ed. by R.W. Frey), pp. 147-159. Springer-Verlag, New York.

264. RICCI LUCCHI, F. & VALMORI, E. (1980) Basin-wide turbidites in a Miocene, over-supplied deep-sea plain: a geometrical analysis. *Sedimentology*, 27, 241-270.

265. RICKETTS, B.D. (1983) The evolution of a middle Precambrian dolostone sequence - a spectrum of dolomitization regimes. *J. sedim. Petrol.*, 53, 565-586.

266. ROBISON, R.A. (1972) Mode of life of agnostid trilobites. *24th Int. geol. Congr.*, Montreal, Sect. 7, 33-40.

267. ROBISON, R.A. (1981) Report on examination of some Middle and Late Cambrian faunas from Peary Land, North Greenland. Geological Survey of Greenland internal report. (Unpublished).

268. ROBISON, R.A. (1984) Cambrian Agnostida of North America and Greenland, Part I, Ptychagnostidae. *University of Kansas Paleontological Contributions*, Paper 109, pp. 60.

269. RODINE, J.D. &JOHNSON, A.M. (1976) The ability of debris, heavily freighted with coarse clastic material, to flow on gentle slopes. *Sedimentology*, 23, 213-234.

270. ROLLE, F. & WRANG, P. (1981) A preliminary oil geological evaluation of the Peary Land region in North Greenland. Geological Survey of Greenland internal report. (Unpublished).

271. ROWLAND, S.M. (1981) Archaeocyathid reefs of the southern Great Basin, western United States. In: *Short papers for the second international symposium on the Cambrian System* (Ed. by M.E. Taylor), pp. 193-197. U.S. Geol. Surv. Open-File Report 81-743.

272. ROWLAND, S.M. (1984) Were there framework reefs in the Cambrian? *Geology*, 12, 181-183.

273. RUSNAK, C.A. & NESTERROFF, W.D. (1964) Modern turbidites: terrigenous abyssal plain versus bioclastic basin. In: *Papers in Marine Geology* (Ed. by R.L. Miller), pp. 488-507. Macmillan and Co., New York.

274. SANDBERG, P.A. (1983) An oscillating trend in Phanerozoic non-skeletal carbonate mineralogy. *Nature*, 305, 19-22.

275. SCHLAGER, W. & CHERMAK, A. (1979) Sediment facies of platform-basin transition, Tongue of the Ocean, Bahamas. In: *Geology of Continental Slopes* (Ed. by L.J. Doyle & O.H. Pilkey), pp. 193-208. *Spec. Publ. Soc. econ. Paleont. Miner.*, 27, Tulsa.

276. SCHLAGER, W. & JAMES, N.P. (1978) Low-magnesium calcite limestones forming at the deep-sea floor, Tongue of the Ocean, Bahamas. *Sedimentology*, 25, 675-702.

277. SEILACHER, A. (1967) Bathymetry of trace fossils. *Mar. Geol.*, 5, 413-428.

278. SELLWOOD, B.W. (1978) Shallow-water Carbonate Environments. In: *Sedimentary Environments and Facies* (Ed. by H.G. Reading), pp. 259-313. Blackwell Scientific, Oxford.

279. SHINN, E.A. (1969) Submarine lithification of Holocene carbonate sediments in the Persian Gulf. *Sedimentology*, 12, 109-144.

280. SHINN, E.A., HALLEY, R.B., HUDSON, J.H. & LIDZ, B.H. (1977) Limestone compaction: an enigma. *Geology*, 5, 21-24.

281. SHINN, E.A., LLOYD, R.M. & GINSBURG, R.N. (1969) Anatomy of a modern carbonate tidal flat, Andros Island, Bahamas. *J. sedim. Petrol.*, 39, 1202-1228.

282. SIMONE, L. (1980) Ooids: a review. *Earth Sci. Rev.*, 16, 319-355.

283. SMITH, A.G., HURLEY, A.M. & BRIDEN, J.C. (1981) *Phanerozoic paleocontinental world maps*. pp. 102. Cambridge University Press, Cambridge.

284. SMITH, D.L. (1977) Transition from deep- to shallow-water carbonates, Paine Member, Lodgepole Formation, central Montana. In: *Deep-water Carbonate Environments* (Ed. by H.E. Cook & P. Enos), pp. 187-201. *Spec. Publ. Soc. econ. Paleont. Miner.*, 25, Tulsa.

285. SODERO, D.E. & HOBSON, J.R. (1979) Depositional facies of Lower Paleozoic Allen Bay carbonate rocks and contiguous shelf and basin strata, Cornwallis and Griffith Islands, Northwest Territories, Canada. *Bull. Am. Ass. Petrol. Geol.*, 63, 1059-1091.

286. SOPER, N.J. & HIGGINS, A.K. (1984) Stratigraphic and structural investigations of the Cambro-Ordovician platform margin - west Amundsen Land to north Nyeboe Land. Geological Survey of Greenland internal report. (Unpublished).

287. SOPER, N.J., HIGGINS, A.K. & FRIDERICHSEN, J.D. (1980) The North Greenland Fold belt in eastern Johannes V. Jensen Land. *Rapp. Grønlands geol. Unders.*, 99, 89-98.

288. SPEARING, D.R. (1975) Shallow marine sands. In: *Depositional Environments as Interpreted from Primary Sedimentary Structures and Stratification Sequences*, pp. 103-132. *Soc. econ. Paleont. Miner. Short Course*, 2.

289. SPECHT, R.W. & BRENNER, R.L. (1979) Storm-wave genesis of bioclastic carbonates in Upper Jurassic epicontinental mudstones, east-central Wyoming. *J. sedim. Petrol.*, 49, 1307-1322.

290. STAUFFER, P.H. (1967) Grain-flow deposits and their implications, Santa Ynez Mountains, California. *J. sedim. Petrol.*, 37, 487-508.

291. STOW, D.A.V. & SHANMUGAM, G. (1980) Sequence of structures in fine-grained turbidites: comparison of recent deep-sea and ancient flysch sediments. *Sedim. Geol.*, 25, 23-42.

292. SURLYK, F. (1978) Submarine fan sedimentation along fault scarps on tilted fault blocks (Jurassic - Cretaceous boundary, East Greenland). *Bull. Grønlands geol. Unders.*, 128, pp. 108.

293. SURLYK, F. (1982) Nares Strait and the down-current termination of the Silurian turbidite basin of North Greenland. In: *Nares Strait and the drift of Greenland: a conflict in plate tectonics* (Ed. by P.R. Dawes & J.W. Kerr), pp. 147-150. *Meddr Grønland, Geoscience*, 8.

294. SURLYK, F. & HURST, J.M. (1983) Evolution of the early Paleozoic deep-water basin of north Greenland - Aulacogen or narrow ocean? *Geology*, 11, 77-81.

295. SURLYK, F. & HURST, J.M. (1984) The evolution of the early Paleozoic deep-water basin of North Greenland. *Bull. geol. Soc. Am.*, 95, 131-154.

296. SURLYK, F., HURST, J.M. & BJERRESKOV, M. (1980) First age-diagnostic fossils from the central part of the North Greenland fold belt. *Nature*, 286, 800-803.

297. SWETT, K. & CROWDER, R.K. (1982) Primary phosphatic oolites from the Lower Cambrian of Spitzbergen. *J. sedim. Petrol.*, 52, 587-593.

298. SWETT, K., KLEIN, G. DE VRIES & SMIT, D.E. (1971) A Cambrian tidal sand body - the Eriboll Sandstone of Northwest Scotland: an ancient-recent analog. *J. Geol.*, 79, 400-415.

299. SWIFT, D.J.P., FIGUEIREDO Jr., A.G., FREELAND, G.L. & OERTEL, G.F. (1983) Hummocky cross-stratification and megaripples: a geological double standard? *J. sedim. Petrol.*, 53, 1295-1317.

300. SWIFT, D.J.P., STANLEY, D.J. & CURRAY, J.R. (1971) Relict sediments on continental shelves: a reconsideration. *J. Geol.*, 79, 322-346.

301. TEICHERT, C. (1958) Concept of Facies. *Bull. Am. Ass. Petrol. Geol.*, 42, 2718-2744.

302. THEIDE, J. & VAN ANDEL, T.H. (1977) The paleoenvironment of anaerobic sediments in the late Mesozoic South Atlantic Ocean. *Earth Planet. Sci. Letts.*, 33, 301-309.

303. THOMSON, A.F. & THOMASSON, M.R. (1969) Shallow to deep water facies development in the Dimple Limestone (Lower Pennsylvanian) Marathon region. In: *Depositional environments in carbonate rocks* (Ed. by G.M. Friedman), pp. 57-78. *Spec. Publ. Soc. econ. Paleont. Miner.*, 14, Tulsa.

304. TRETTIN, H.P. & BALKWILL, H.R. (1979) Contributions to the tectonic history of the Innuitian Province, Arctic Canada. *Can. J. Earth Sci.*, 16, 748-769.

305. TROELSEN, J.C. (1949) Contributions to the geology of the area around Jørgen Brønlund Fjord, Peary Land, North Greenland. *Meddr Grønland*, 149, 1-29.

306. TROELSEN, J.C. (1956) The Cambrian of North Greenland and Ellesmere Island. *Internatl. geol. Congr.*, *20, Mexico*, 3, 1, 71-90.

307. TUCKER, M.E. (1969) Crinoidal turbidites from the Devonian of Cornwall and their palaeogeographical significance. *Sedimentology*, 13, 281-290.

308. TUCKER, M.E. (1974) Sedimentology of Palaeozoic pelagic limestones: the Devonian Griotte (Southern France) and Cephalopodenkalk (Germany)." In: *Pelagic Sediments: on Land and under the Sea* (Ed. by K.J. Hsu and H.C. Jenkyns), pp. 71-92. *Spec. publ. int. Ass. Sediment.*, 1.

309. VANNEY, J.R. & STANLEY, D.J. (1983) Shelfbreak physiography: an overview. In: *The Shelfbreak: Critical Interface on Continental Margins* (Ed. by D.J. Stanley & G.T. Moore), pp. 1-24. *Spec. Publ. Soc. econ. Paleont. Miner.*, 33, Tulsa.

310. WALKER, R.G. (1965) The origin and significance of the internal sedimentary structures of turbidites. *Proc. Yorks. geol. Soc.*, 35, 1-32.

311. WALKER, R.G. (1975) Generalized facies models for resedimented conglomerates of turbidite association. *Bull. geol. Soc. Am.*, 86, 737-748.

312. WALKER, R.G. (1978) Deep-water sandstone facies and ancient submarine fans: Models for exploration for stratigraphic traps. *Bull. Am. Ass. Petrol. Geol.*, 62, 932-966.

313. WALKER, R.G. & MUTTI, E. (1973) Turbidite facies and facies associations. In: *Turbidites and Deep-Water Sedimentation*, pp. 119-157. Soc. econ. Paleont. Miner. Pacific Section, Short course, Anaheim.

314. WALTON, E.K. (1967) The sequence of internal structures in turbidites. *Scott. J. Geol.*, 3, 306-317.

315. WANLESS, H.R. (1979) Limestone response to stress: pressure solution and dolomitization. *J. sedim. Petrol.*, 49, 437-462.

316. WANLESS, H.R. (1982) Limestone response to stress: pressure solution and dolomitization - reply. *J. sedim. Petrol.*, 52, 328-332.

317. WAPLES, D.W. (1983) Reappraisal of anoxia and organic richness, with emphasis on Cretaceous of North Atlantic. *Bull. Am. Ass. Petrol. Geol.*, 67, 963-978.

318. WILLIAMS, L.A. (1983) Deposition of the Bear Gulch Limestone: a Carboniferous Plattenkalk from central Montana, *Sedimentology*, 30, 843-860.

319. WILSON, J.E. & JORDAN, C. (1983) Middle shelf environment. In: *Carbonate Depositional Environments* (Ed. by P.A. Scholle, D.G. Bebout & C.H. Moore), pp. 297-343. *Mem. Am. Ass. Petrol. Geol.*, 33, Tulsa.

320. WILSON, J.L. (1969) Microfacies and sedimentary structures in "deeper water" lime mudstone. In: *Depositional environments in carbonate rocks* (Ed. by G.M. Friedman), pp. 4-19. *Spec. Publ. Soc. econ. Paleont. Miner.*, 14, Tulsa.

321. WILSON, J.L. (1975) *Carbonate Facies in Geologic History*, pp. 471. Springer-Verlag, Berlin, Heidelberg, New York.

322. WOBBER, F.J. (1967) Post-depositional structures in the Lias, South Wales. *J. sedim. Petrol.*, 37, 166-174.

323. WRIGHT, V.P. & WILSON, R.C.L. (1984) A carbonate submarine-fan sequence from the Jurassic of Portugal. *J. sedim. Petrol.*, 54, 394-412.

324. YOCHELSON, E.L. & PEEL, J.S. (1975) *Ceratopea* and the correlation of the Wandel Valley Formation, eastern North Greenland. *Rapp. Grønlands geol. Unders.*, 75, 28-31.

325. YUREWICZ, D.A. (1977) Sedimentology of Mississippian basin carbonates, New Mexico and West Texas - the Rancheria Formation. In: *Deep-Water Carbonate Environments* (Ed. by H.E. Cook & P. Enos), pp. 203-219. *Spec. Publ. Soc. econ. Paleont. Miner.*, 25, Tulsa.

327. ZENGER, D.H. (1972) Significance of supratidal dolomitization in the geologic record. *Bull. geol. Soc. Am.*, 83, 1-12.